Zbornik 3. Študentske konference Mednarodne podiplomske šole Jožefa Stefana

Proceedings of 3rd Jožef Stefan International Postgraduate School Students Conference

ZBORNIK
Proceedings of
IPSSC

1. DEL
Part I.

25. maj 2011, Ljubljana, Slovenija

Zbornik 3. Študentske konference Mednarodne podiplomske šole Jožefa Stefana
(Proceedings of the 3rd Jožef Stefan International Postgraduate School Students Conference)

Uredniki:
Dejan Patelin
Aleš Tavčar
Brigita Rožič
Bogdan Pogorelc

Priprava zbornika:
Dejan Petelin

Oblikovanje naslovnice:
Ernest Vider

Založnik:
Mednarodna podiplomska šola Jožefa Stefana, Ljubljana

Tisk:
Franc Jagodic, s.p. - Jagraf

Naklada:
150 izvodov

Ljubljana, maj 2011

IPSSC organizira študentski svet Mednarodne podiplomske šole Jožefa Štefana -
(IPSSC is organized by Jožef Stefan International Postgraduate School - IPS student council)

CIP - Kataložni zapis o publikaciji
Narodna in univerzitetna knjižnica, Ljubljana

5/6(082)
378.046-021.68:001.891(497.4)(082)

MEDNARODNA podiplomska šola Jožefa Stefana. Študentska
konferenca (3 ; 2011 ; Ljubljana)
   Zbornik prispevkov = Proceedings / 3. študentska konferenca
Mednarodne podiplomske šole Jožefa Stefana = 3rd Jožef Stefan
International Postgraduate School Students Conference, 25. maj
2011, Ljubljana, Slovenija ; [organizira študentski svet Mednarodne
podiplomske šole Jožefa Stefana = organized by Jožef Stefan
International Postgraduate School - IPS student council] ; uredili,
edited by Dejan Patelin ... [et al.]. - Ljubljana : Mednarodna
podiplomska šola Jožefa Stefana, 2011

ISBN 978-961-92871-2-5

1. Petelin, Dejan 2. Mednarodna podiplomska šola Jožefa Stefana
(Ljubljana)

256081408

3. ŠTUDENTSKA KONFERENCA MEDNARODNE PODIPLOMSKE ŠOLE JOŽEFA STEFANA

3rd JOŽEF STEFAN INTERNATIONAL POSTGRADUATE SCHOOL STUDENTS CONFERENCE

Zbornik - 1. del

Proceedings - part 1

Uredili / Edited by

Dejan Petelin, Aleš Tavčar, Brigita Rožič in Bogdan Pogorelc

25. maj 2011, Ljubljana, Slovenija

Organizacijski odbor / Organising Committe

Dejan Petelin

Aleš Tavčar

Brigita Rožič

Bogdan Pogorelc

Miha Mlakar

Violeta Mirchevska

Z inovativnim raziskovanjem do izboljšanja kakovosti življenja

Po dveh do sedaj uspešno izpeljanih konferencah, ki sta pripomogli k vzpostavitvi številnih vezi med študenti Mednarodne podiplomske šole Jožefa Stefana in predstavniki iz gospodarstva, z velikim zadovoljstvom tudi letos organiziramo 3. Študentsko konferenco Mednarodne podiplomske šole Jožefa Stefana.

Še posebej v tem času, ko se tudi naše gospodarstvo sooča s številnimi problemi, je pomembno, da se krepi povezava med raziskovalci in podjetji. S skupnimi močmi, ki vključujejo tudi naša inovativna raziskovanja, bomo zagotovo ne le ohranili, temveč tudi izboljšali kakovost našega življenja.

Pomembno je poudariti, da je takšna konferenca velikega pomena in nujno potrebna. Nam študentom omogoča, da dosežke svojih raziskav in možnosti njihove uporabe v praksi, predstavimo tudi širšemu občinstvu, ne le z objavami v znanstvenih revijah. Na ta način se vzpostavijo tudi neposredni stiki med študenti in podjetji. Ta tako pridobijo informacije in direkten pristop k raziskavam in kadrom, ki bi jih utegnili zanimati, študentje pa poglobimo poznavanje razvojnih potreb in pristopov v industriji in storitvenih dejavnostih. S tem se odprejo številne možnosti za medsebojna sodelovanja in zaposlitve. V ta namen smo se letos še posebej posvetili vabljenju podjetij, ki se zavedajo pomembnosti raziskav in bodo

svoje razvojne programe in interese za povezovanje z raziskovalci ustno predstavili. Pri tem si želimo, da bi se prav vsaka predstavitev razvila v aktivno razpravo, ki bo spodbudila številne nove stike med predstavniki podjetij in raziskovalci.

V želji, da naša konferenca sledi merilom mednarodnih znanstvenih konferenc, smo korak naprej naredili tudi na področju prispevkov. Tako smo prispevke študentov razširili iz povzetkov v krajše članke, sestavljene iz strokovnega teksta in povzetka v širše razumljivem jeziku. S tem smo dvignili strokovno raven, ter hkrati približali poznavanje naših raziskav tudi širšemu občinstvu.

Vsem študentom se zahvaljujemo, da so sprejeli izziv, se nam pridružili in s tem dokazali, da se zavedajo pomembnosti in si želijo sodelovanja z gospodarstvom. Zahvala gre tudi vsem podjetjem, ki so pokazala svojo pripravljenost sodelovanja, tako s predstavijo svojega dela in razvojnih potreb kot tudi s finančno podporo. Seveda pa se moramo za vso pomoč in podporo zahvaliti celotnemu osebju na Mednarodni podiplomski šoli Jožefa Stefana z dekanom prof. dr. Robertom Blincem na čelu. Še posebej gre velika zahvala prodekanki prof. dr. Aleksandri Kornhauser Frazer, ki je vseskozi podpirala organiziranje konference ter pregledala vse prispevke, dr. Emilu Rojcu, ki nam je neposredno pomagal pri vzpostavitvi številnih kontaktov v razvojno-raziskovalnih oddelkih podjetij, ter Tadeji Samec, ki nam je pomagala prav pri vseh nalogah in težavah. Nikakor pa ne smemo pozabiti naših mentorjev. Njim gre vsa zahvala za vso njihovo pomoč in trud pri usmerjanju na naših raziskovalnih poteh.

Organizacijski odbor

Beseda predsednika MPŠ

Ekonomska in tehnološka globalizacija predstavljata sodobnemu svetu velik izziv. Tako je bila sprejeta vrsta deklaracij in sklepov, med njimi tudi dokumenti Evropske skupnosti o strategiji njenega razvoja. Vse to z namenom, da bi »zgradili najbolj kompetitivno, dinamično ter na znanju temelječo ekonomijo«. V tej smeri deluje tudi novo vzpostavljeni Evropski raziskovalni prostor – ERA, ki naj bi omogočal boljšo integracijo nacionalnih raziskav v širšem evropskem prostoru.

Sedanja svetovna gospodarska recesija sovpada z ekonomsko krizo, klimatskimi spremembami, problemi zdravja in zdrave prehrane, pomanjkanja vode, ohranitve biološke raznolikosti in še kaj bi lahko dodali. Vse to je potegnilo za seboj vrsto socialnih problemov, ki jih danes občutimo in ki predstavljajo velik družbeni izziv. Za njihovo reševanje je med drugim potrebno visoko kvalitetno podiplomsko izobraževanje vključno z vrhunskim raziskovalnim delom, kar omogoča tem raziskovalcem uspešno kariero. To pa pomeni odlične zaposlitvene možnosti pri nadaljnjem razvoju znanj in tehnoloških inovacij. To so izzivi za nove generacije, ki so upravičene do boljše prihodnosti, kot jim jo ponuja sedanjost. Dolžni smo jim omogočati, da se uspešno spopadejo z izzivi v domačem okolju, ne pa da iščejo izpolnitve svojih ambicij in eksistenčnih možnosti z »begom možganov«.

S temi razmišljanji je Institut »Jožef Stefan« (IJS), najbolj elitna slovenska raziskovalna organizacija na področju naravoslovnih in tehničnih ved, sprejel odločitev o ustanovitvi Mednarodne podiplomske šole Jožefa Stefana (MPŠ). Po večletnih prizadevanjih in s podporo uspešnih slovenskih gospodarskih podjetij je IJS leta 2004 ustanovil samostojni visokošolski zavod. Študijske usmeritve zajemajo nova področja, kot so nanotehnologije in nanoznanosti, informacijske in komunikacijske tehnologije, ekotehnologije ter s tem povezan menedžment. Da je bila ustanovitev te podiplomske šole več kot upravičena, kaže veliko zanimanje za vpis, saj je v šolskem letu 2010/2011 vpisanih 216 podiplomcev, od ustanovitve šole pa je bilo podeljeno 63 doktoratov in 26 magisterijev.

IJS in MPŠ v tesni sodelavi izkoriščata odlično raziskovalno opremo in vrhunske kadrovske potenciale ter mednarodne povezave za usposabljanje vrhunskih raziskovalnih kadrov, sposobnih prenašanja odličnega znanja, pridobljenega na temeljnih raziskavah, tudi v gospodarstvo. Tako prispevajo in bodo prispevali k pospešenemu zagonu slovenskega gospodarstva ter hitrejšemu prehodu v družbo znanja.

Znanje je vrednota, ki omogoča narodu ekonomski razvoj in obstoj. Mladi vrhunski raziskovalci pa so pogoj za uspešen gospodarski razvoj, so srce družbe znanja.

Prof. dr. Vito Turk
Predsednik MPŠ

Beseda predstavnice gospodarstva

Dr. MARTINA OBERŽAN, raziskovalka v razvoju in tehnologiji tehnične keramike v mednarodno uveljavljeni industriji ETI - Elektroelement v Izlakah, je prva med industrijci na podiplomskem študiju na MPŠ dosegla doktorat znanosti. Njena disertacija z naslovom *Visoko glinični porcelan z izboljšanimi mehanskimi in termičnimi lastnostmi* pod mentorstvom prof. dr. Marije Kosec je celo presegla sicer zelo stroge zahteve MPŠ za doktorat: njene izvirne dosežke je objavila druga svetovno najvišje rangirana znanstvena revija na tem področju, je prva avtorica patentnih prijav, njeni dosežki so neposredno obogatili proizvodnjo v ETI, skupaj z mentorico in sodelavci pa je prejela tudi najvišje državno priznanje za prenos znanja v gospodarstvo – Puhovo nagrado 2010. Njene izkušnje in predlogi so bistveni za usmerjanje mladih raziskovalcev v gospodarstvo, kar bo ključna značilnost alumni programa MPŠ. Ta naj bi tudi usmerjal vse magistre in doktorje MPŠ v delo v industriji ali učinkovito sodelovanje z njo.

Moji pogledi na doktorski študij na MPŠ

Tako kot vsi raziskovalci smo tudi industrijski raziskovalci in razvojniki izpostavljeni utemeljenim zahtevam po mednarodno primerljivi znanstveni kakovosti našega dela. Globalizacija gospodarstva pa prinaša še bistvene dodatne zahteve. Slovensko tržišče je največkrat veliko premajhno za rentabilni obseg

proizvodnje, treba se je prebiti na svetovnem trgu. Za to pa mora biti ponudba hitrejša v inovacijah, bolj kakovostna in cenovno ugodnejša od konkurentov. To pomeni tudi ostrejše ciljanje raziskav v smeri produkta ali storitve in za to potreben čas ter stroški postanejo bistveni dodatni kriteriji.
Pri takih pritiskih ostro ciljanih raziskav obstaja nevarnost, da zanemarimo širše in globlje raziskovanje ter celovito sistemsko mišljenje, kar dolgoročno povzroča veliko škodo. Zato sem že dolga leta goijila željo, da bi se na najvišji ravni strokovno izpopolnila za opravljanje svojega dela in hkrati formalno napredovala v izobrazbi. Ta želja se mi je uresničila v sklopu doktorskega študija na MPŠ, ki sem ga zaključila v letu 2009.

Ob prvih razgovorih za spodbujanje doktorskega študija s predstavniki MPŠ ob obisku v ETI se mi je zdelo, da sem prestara za vpis na doktorski študij, saj sem v tistem letu dočakala Abrahama. Danes razmišljam drugače – prav sem se odločila! Še kar nekaj let bom delala in sedaj z izpopolnjenim znanjem bolj učinkovito opravljam svoje razvojno delo in se vključujem v razvojne projekte v firmi, a tudi bolj sistemsko in širše razmišljam o novih možnostih. Predvsem pa nimam več predsodkov glede sodelovanja z raziskovalci iz različnih znanstvenih institucij, saj mi je študij na MPŠ odprl vrata v znanstveno sfero in v poznavanje njenega delovanja. Ne dvomim, da sva ob mojem doktorskem študiju pridobili obe, tako jaz, ki sem se zavzeto lotila študija in napredovala v izobrazbi, kot firma, ki je moj študij financirala. Upam tudi, da so v to vključeni raziskovalci pridobili pozitivne izkušnje za sodelovanje z industrijo.

Podiplomski študij na MPŠ, še posebej njegov izvirni način izvajanja, ki doktorski študij umesti v industrijske projekte, je zelo primeren za nas raziskovalce iz industrije. Meni je bil prav pisan na kožo, za kar gre zahvala v veliki meri moji mentorici. Na drugi strani pa sem imela tudi veliko razumevanje za moje delo v ETI. Celotni študij je bil organiziran in voden tako, da je bilo moje raziskovalno delo neposredno povezano s prenosom raziskovalnih dosežkov v redno proizvodnjo. Hkrati sem pridobila veliko širšega in specialističnega znanja s področja keramičnih materialov, ki jih izdeluje ETI – in s tem potencial za odpiranje novih perspektiv.

Študij na MPŠ mi je omogočil tudi spoznavanje raziskovalcev na IJS in njihovega dela ter poznavanje raziskovalne opreme za potrebe naše industrije. Vesela sem, da smo se preko mojega študija na MPŠ spet povezali z IJS in da se sodelovanje pri raziskavah na keramičnem področju nadaljuje. Kajti naj se raziskovalci v industriji še tako trudimo, ne zmoremo hkrati obvladovati razvojnih procesov v industriji in učinkovito zasledovati nove dosežke temeljnega raziskovanja, ki prinašajo seme novih rešitev. Po drugi strani pa raziskovalci v inštitutih sami ne morejo prodreti v razvojne programe industrije. Prepletanje naporov obeh je pomembna naloga nas vseh – in MPŠ je v ta namen odličen katalizator.

Dr. Martina Oberžan

Kazalo (Table of Contents)

Ekotehnologija (Ecotechnology)

Določanje vsebnosti steroidnih estrogenov v odpadnih vodah brez predhodne ekstrakcije vzorcev

Miha Avberšek[1,2], Bojana Žegura[3], Metka Filipič[3], Ester Heath[1,2]

[1] Odsek za znanosti o okolju, Institut Jožef Stefan, Ljubljana, Slovenija

[2] Mednarodna podiplomska šola Jožefa Stefana, Ljubljana, Slovenija

[3] Nacionalni institut za biologijo, Ljubljana, Slovenija

miha.avbersek@ijs.si

Steroidni estrogeni so organska onesnažila naravnega izvora, ki lahko z vstopom v okolje povzročijo negativne učinke v ekosistemu. Zaradi njihovih nizkih koncentracij v okolju (ng/L) potrebujemo za zaznavanje teh spojin občutljive kemijske oziroma biološke metode. Ena izmed bioloških metod je tudi in vitro ER-Calux® test, ki za zaznavanje estrogenosti uporablja celično linijo. V naši raziskavi smo s prilagoditvijo ER-Calux® testa razvili postopek, ki omogoča zaznavanje estrogenega potenciala brez prehodne ekstrakcije vzorcev. Metodo smo optimizirali na umetnih vzorcih pitne in odpadne vode, kasneje pa še na realnih vzorcih iz čistilnih naprav in rečnih vod. Rezultati ER-Calux testa brez predhodne ekstrakcije vzorcev so pokazali, da je metoda dovolj občutljiva za dokazovanje prisotnosti nizkih vrednosti estrogenega potenciala v vodnih vzorcih, kar smo potrdili tudi z realnimi vzorci. Postopek nam omogoča testiranje večjega števila vzorcev z nižjimi materialnimi stroški in krajšim časom analize.

Ključne besede: steroidni estrogeni, odpadne vode, rečne vode, ER-Calux®

1 Uvod

Steroidni estrogeni (estron (E1), 17β-estradiol (E2), estriol (E3) in 17α-etinilestradiol (EE2)) so organska onesnažila, ki so pogosto prisotna v odpadnih vodah komunalnih čistilnih naprav in v vodnem ekosistemu, kamor se te vode stekajo [1]. Čeprav so večinoma naravnega izvora, so posledice njihove prisotnosti v okolju opazne kot motnje v rasti in razvoju živih organizmov (sesalci, ribe itd.),

prav tako pa lahko vplivajo na razmnoževanje in posledično na razvoj celotne populacije [2]. Prisotnost steroidnih estrogenov v odpadnih vodah so dokazali že v mnogih študijah. Koncentracije posameznih spojin, povzete po pregledni študiji Miege in sodelavcev [3], dosegajo do 670 ng/L (mediana 69 ng/L) v dotokih čistilnih naprav in do 285 ng/L (10 ng/L) v iztokih čistilnih naprav. V rečnih vodah so koncentracije tudi pod 1 ng/L, kar je že dovolj, za povzročanje negativnih učinkov na žive organizme, ki se zaradi kronične izpostavitve le še povečujejo.

Zaradi nizkih koncentracij so za ugotavljanje prisotnosti steroidnih estrogenov v okoljskih vzorcih potrebne dolgotrajne priprave vzorcev, ekstrakcije želenih spojin ter občutljive kemijske in biološke metode zaznavanja teh spojin v vzorcih [4], [5].

Kemijske metode zaznavanja steroidnih estrogenov temeljijo na ločbi analitov s plinsko ali tekočinsko kromatografijo in detekcijo z masno spektrometrijo [4]. Analizne metode nam podajo koncentracije posameznih analitov, ne pa tudi informacije o dejanski estrogeni aktivnosti vzorca. Le-to lahko določimo z *in vivo* ali *in vitro* biološkimi testi. Biološke metode uporabljajo različne vrste organizmov, pri čemer pa so, glede na podatke iz literature, zaradi enostavnega dela, hitrosti in nižje cene, *in vitro* testi na celičnih linijah ali kvasovkah med najbolj pogosto uporabljenimi. [5]. Tako kemijske kot tudi biološke metode zahtevajo dolgotrajno pripravo in predhodno ekstrakcijo vzorca.

V naši študiji smo uporabili ER-Calux® test [6], ki z uporabo celične linije omogoča zaznavanje estrogenosti v vzorcih. Cilj raziskave je bil, z uporabo in prilagoditvijo tega testa, razviti postopek, ki bo omogočal testiranje okoljskih vzorcev, predvsem odpadnih vod, brez predhodne ekstrakcije spojin ter razvito metodo optimizirati in uporabiti na realnih vzorcih.

2 Metode in materiali

1.1 Priprava vzorcev

Za optimizacijo postopka smo uporabili vzorce pitnih vod in odpadnih vod iz komunalne čistilne naprave, ki smo jim dodali znane količine standardnih raztopin štirih steroidnih estrogenov (estron (E1), 17β-estradiol (E2), estriol (E3) in 17α-etinilestradiol (EE2)) v okoljsko relevantnih koncentracijah (0-50 ng/L). Po dodatku standardov smo vzorce 30 minut stresali, nato pa po 10 mL vsakega vzorca shranili v zamrzovalniku (T=-20 °C). Preostanek, 200 mL vzorca, smo

ekstrahirali na trdem nosilcu (SPE). Po ekstrakciji smo preiskovane spojine eluirali z etil acetatom. Vzorce odpadne vode smo zaradi prisotnosti nečistoč dodatno čistili na silikagelski koloni. Neekstrahirane vzorce in njihove ujemajoče ekstrakte smo hkrati testirali z ER-Calux® testom in primerjali rezultate.

1.2 ER-Calux® test

ER-Calux® test je *in vitro* test za zaznavanje estrogenega potenciala v vzorcih. Temelji na celični liniji T47D-EREtata-Luc, ki je posebej občutljiva za zaznavanje spojin, ki se vežejo na estrogenski receptor.

Test izvedemo tako, da celice pripravimo na plošči s 96 luknjicami, ki jih po 48 urah rasti izpostavimo vzorcem, ki jih želimo testirati. Vzorec (ekstrakt) razredčimo (1:1, 1:3, 1:10, 1:30, 1:100) in ga primešamo rastnemu mediju tako, da je koncentracija topila 0,1 %. Na isto ploščo vključimo tudi umeritveno krivuljo s standardnimi koncentracijami 17β-estradiola (0,6-30 pM), ki služijo za kasnejšo kvantifikacijo estrogenosti v vzorcu.

Za testiranje neekstrahiranih vzorcev pripravimo celice na enak način kot za ekstrahirane vzorce. Postopka se razlikujeta v načinu izpostavitve vzorca, saj v tem primeru celice izpostavimo vzorcu, ki je v razmerju 1:5 dodan rastnemu mediju. Vzorec pred uporabo steriliziramo z ANOTOP filtrom (velikost por 0,2 μm). Tudi v tem primeru vključimo umeritveno krivuljo, ki je pripravljena v testnem mediju razredčenem s PBS (1:5).

Po 24 urah izpostavitve celicam dodamo SteadyLite plus® luminiscenčni kit. Ta celice lizira in sprosti luciferazo, ki je nastala kot posledica vezave spojin na estrogenske receptorje. Luciferaza povzroči nastanek luminiscence, ki jo izmerimo z luminimetrom. Intenziteta luminiscence je sorazmerna z estrogenostjo vzorca.

3 Rezultati in diskusija

Hitro in učinkovito zaznavanje prisotnosti steroidnih estrogenov je ključno pri oceni tveganja zaradi prisotnosti teh spojin v okoljskih vzorcih. V okviru naše raziskave smo razvili postopek, s katerim lahko estrogenost vzorcev določamo brez predhodne ekstrakcije in se tako izognemo zamudni pripravi vzorcev. Po naših

podatkih smo prvi laboratorij, ki je je uspešno razvil in optimiziral tovrsten postopek.

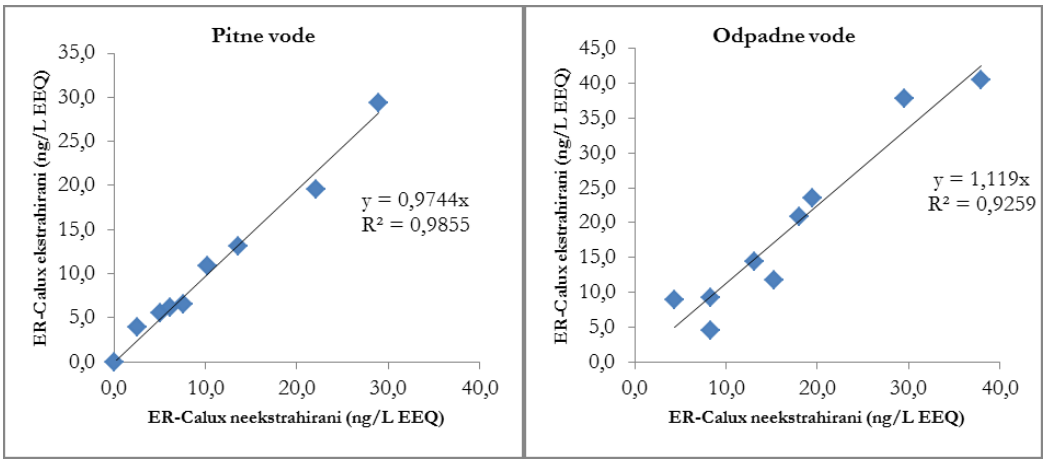

Slika 1: Primerjava rezultatov ekstrahiranih in neekstrahiranih vzorcev pitne in odpadne vode z dodanimi standardi

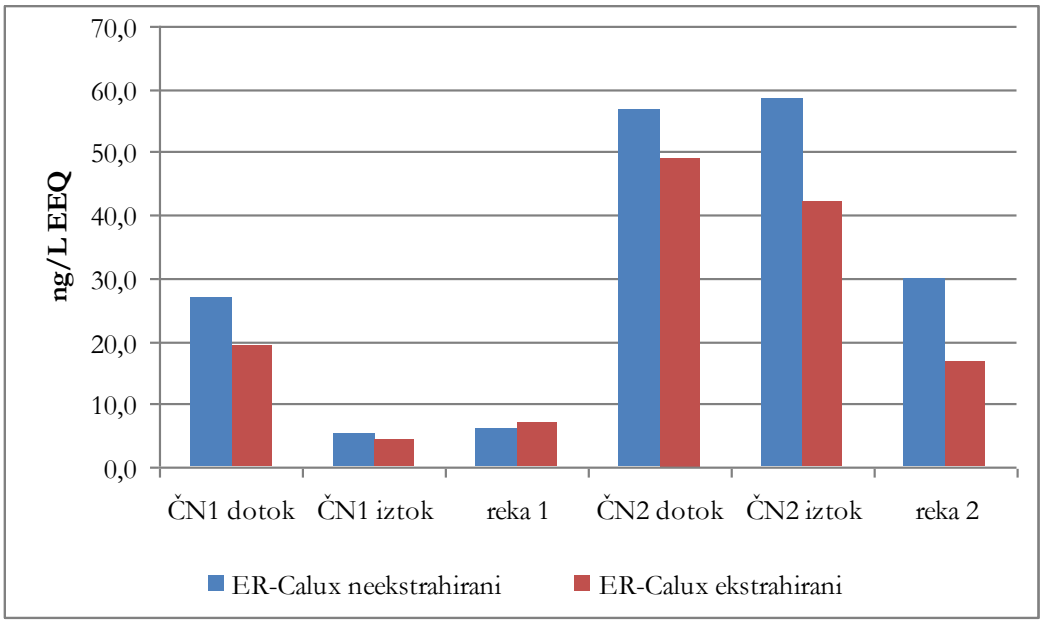

Slika 2: Primerjava rezultatov ekstrahiranih in neekstrahiranih vzorcev dotokov in iztokov z dveh komunalnih čistilnih naprav ter rek, v katere se iztoka izlivata.

Preverjanje delovanja postopka in njegovo optimizacijo smo izvedli na vzorcih pitne in odpadne vode z dodanimi znanimi količinami steroidnih estrogenov (0-50 ng/L). Rezultati (Slika 1) kažejo, da so vrednosti estradiolskih ekvivalentov (EEQ)

v ekstrahiranih in neekstrahiranih vzorcih medsebojno primerljive, saj se tako v primeru pitne, kot tudi odpadne vode, rezultati dobro ujemajo (r^2>0,90).

Pri obeh uporabljenih metodah je faktor redčenja enak, zato pri postopku brez ekstrakcije ohranimo občutljivost testa in posledično dosegamo dovolj nizke meje zaznave (LOD) in kvantifikacije (LOQ) za proučevanje prisotnosti estrogenov v okoljskih vzorcih.

Optimizirano metodo smo preizkusili na realnih rečnih in odpadnih vodah (Slika 2). Rezultati kažejo, da se določene vrednosti estrogenosti (estradiolskih ekvivalentov - EEQ) medsebojno ujemajo, kar potrjuje uporabnost metode za izvajanje presejalnih testov in nadzornih meritev.

Rezultati testiranja vzorcev brez predhodne ekstrakcije so primerljivi z običajno metodo, kjer je potrebno vzorce predhodno ekstrahirati. Prednost in uporabnost postopka je predvsem v tem, da hitreje pridemo do želenih rezultatov, kar omogoča hitre presejalne teste in izvajanje nadzornih meritev ter istočasno prihrani tudi porabljen material.

4 Literatura

[1]G. D'Ascenzo, A. Di Corcia, A. Gentili, R. Mancini, R. Mastropasqua, M. Nazzari, R. Samperi. Fate of natural estrogen conjugates in municipal sewage transport and treatment facilities. *The Science of The Total Environment*, 302: 199-209, 2003

[2]J.P. Sumpter, S. Jobling. Vitellogenesis as a biomarker for estrogenic contamination of the aquatic environment. *Environmental Health Perspectives*, 103: 173-178, 1995

[3]C. Miège, J.M. Choubert, L. Ribeiro, M. Eusèbe, M. Coquery. Fate of pharmaceuticals and personal care products in wastewater treatment plants - Conception of a database and first results. *Environmental Pollution*, 157: 1721-1726, 2009

[4]V. Gabet, C. Miège, P. Bados, M. Coquery. Analysis of estrogens in environmental matrices. *TrAC Trends in Analytical Chemistry*, 26: 1113-1131, 2007

[5]C.G. Campbell, S.E. Borglin, F.B. Green, A. Grayson, E. Wozei, W.T. Stringfellow. Biologically directed environmental monitoring, fate, and transport of estrogenic endocrine disrupting compounds in water: A review. *Chemosphere*, 65: 1265-1280, 2006

[6]J. Legler, C. van den Brink, A. Brouwer, A. Murk, P. van der Saag, A. Vethaak, B. van der Burg. Development of a stably transfected estrogen receptor-mediated luciferase reporter gene assay in the human T47D breast cancer cell line. *Toxicological Sciences*, 48: 55-66, 1999

Za širši interes

V Skupini za organsko analizo Odseka za znanosti o okolju se ukvarjamo z raziskovanjem prisotnosti organskih onesnažil (npr. zdravila in hormoni) v okoljskih vzorcih. Proučujemo njihov izvor (kje nastanejo), kroženje (kako potujejo) in vpliv na ekosistem (kakšen je njihov dejanski učinek). Zgoraj opisana študija je del širšega projekta (v sodelovanju z Nacionalnim inštitutom za biologijo), ki proučuje steroidne estrogene (hormone) in druge spojine, ki povzročajo motnje človeškega in živalskega hormonskega sistema. Steroidni estrogeni so pogosto prisotni v odpadnih vodah komunalnih čistilnih naprav in v površinskih vodah, kamor se odpadne vode iztekajo. Čeprav so naravnega izvora, njihova prisotnost v okolju povzroča negativne učinke na živih organizmih (motnje v rasti in razvoju osebkov). Cilj te študije je razviti metodo, ki bo omogočala hitro zaznavanje teh spojin v okolju in zagotavljala učinkovito proučevanje njihove (negativne) vloge v ekosistemu. Ker so koncentracije steroidnih estrogenov v vzorcih zelo majhne (ng/L) je potrebno spojine v vzorcih koncentrirati z zamudnimi postopki. V naši študiji smo uporabili ER-Calux® test, ki smo ga prilagodili tako, da omogoča neposredno testiranje vzorcev, brez predhodne obdelave, pri čemer postopek skrajšamo iz nekaj ur na nekaj minut. Hkrati ohranimo zmožnost zaznavanja dovolj nizkih koncentracij, ki so običajne v okoljskih vzorcih. Ta test omogoča izvedbo hitrih presejalnih testov in posledično hitrejšo in cenejšo oceno tveganja, ki ga povzročajo estroidni estrogeni v okolju.

Oxygen breathing manipulations for enhancing erythropoietin production

Tadej Debevec[1, 2], **Igor B. Mekjavic**[1]

[1] Department of Automation, Bicybernetics and Robotics, Jozef Stefan Institute, Ljubljana, Slovenia

[2] Jozef Stefan International Postgraduate School, Ljubljana, Slovenia

tadej.debevec@ijs.si

SUPERVISOR: Prof. Igor B. Mekjavic

Abstract. Manipulations of oxygen content in inspired air are commonly used to enhance erythropoiesis. Recently, relative changes in tissue oxygenation above hypoxic level, using hyperoxic breathing, have also been shown to stimulate erythropoietin EPO concentration. This study investigated plasma EPO levels [EPO] in eighteen subjects before, between and after 1 h of pure oxygen and 1 hour of hypoxic air mixture breathing (IHH group), or 2 h of placebo normoxic breathing (CON group). The samples were also taken 3, 5, 8, 24, 32 and 48 hours after the exposure. No significant differences were observed in [EPO] concentration between groups following the intervention. There were significant changes within groups at 8 and 32 h in the CON and at 32 h only in the IHH group. The tested protocol of hyperoxic-hypoxic air mixture breathing did not induce [EPO] production stimulation above normal variation and cannot be recommended for erythropoiesis augmentation.

Keywords: Hyperoxia, Hypoxia, Erythropoiesis

1 Introduction

Different hypoxic training modalities are nowadays used extensively both in sports and clinical applications [1]. It is well established that sufficiently long and strong hypoxic exposure can induce beneficial hematological adaptations [2] and subsequent performance enhancements through blood oxygen capacity augmentation [3]. This adaptation is especially important for endurance athletes, providing them with competitive advantage. Its importance is also clearly emphasized with a broad use of illegal recombinant Erythropoietin (EPO) and other simulating EPO agents in elite sport [4]. Enhanced erythropoiesis is also sought after as an important factor when employing pre-acclimatization protocol

before altitude expeditions, as well as to subsequently improve performance at altitude and reduce the risk of altitude related medical problems.

The key role player in this physiological adaptation is glycosolated hormone EPO, as its escalated blood concentration intensifies the red bone marrow progenitor cell activity in producing red blood cells [5]. While renal tissue hypoxia is an established trigger of *de novo* erythropoietin (EPO) production, it has recently been suggested that EPO synthesis may be stimulated also by relative hypoxia, induced by an acute exposure to hyperoxia followed by a return to normoxia [6]. This phenomenon has been termed the "normobaric oxygen paradox" since it seems to appear independently of absolute tissue hypoxia. We hypothesized that successive and acute combination of hyperoxic and hypoxic gas breathing would increase EPO plasma levels [EPO]. In particular, a relative change induced by normobaric oxygen breathing and subsequent hypoxic air breathing could lead to the same or even superior increases in [EPO] concentration, compared to hyperoxia breathing alone. Accordingly, the purpose of this study was to evaluate whether such relative hypoxia, induced by acute and successive exposures to hyperoxia and hypoxia, can stimulate EPO synthesis.

2 Procedures

[EPO] was measured in ten healthy males before, in the middle, and after a 2 hr hyperoxic/hypoxic (IHH) protocol comprising breathing oxygen (F_iO_2=1.0) for 60 minutes, followed by breathing a hypoxic mixture (F_iO_2=0.15) for 60 minutes. Values were compared with those obtained during the trial in which eight matched subjects breathed a normoxic air mixture for 2 hrs (CON). Thereafter, blood samples were taken 3, 5, 8, 24, 32 and 48 hours after the cessation of IHH and Normoxic exposures. All blood samples were immediately stored in BD Vacutainer (K2E, Becton Dickinson, New Jersey, USA) and centrifuged (10 min - 3000 rpm). The obtained plasma was instantly frozen to -80°C and stored for further analysis. The [EPO] concentration was determined in 100 µl of plasma using sandwich enzyme-linked immunoassay (Quantikine IVD EPO ELISA, R&D Systems, Minneapolis, USA). The quantification of the optical density was performed on a microplate reader Quant (Bio-Tek instruments, Winooski, USA) set at 450 nm and

corrected at 600 nm. All samples were assayed two times, whereas only one microplate was used for each subject samples in order to avoid the possible variability between the plates.

3 Results

The absolute [EPO] levels were not significantly different between groups at neither sampling period (Figure 1). There were significant differences in [EPO] concentration within groups at different time periods. In particular, the [EPO] was significantly increased 8 and 32 hrs after the exposure in the control group and only after 32 hrs in the experimental group.

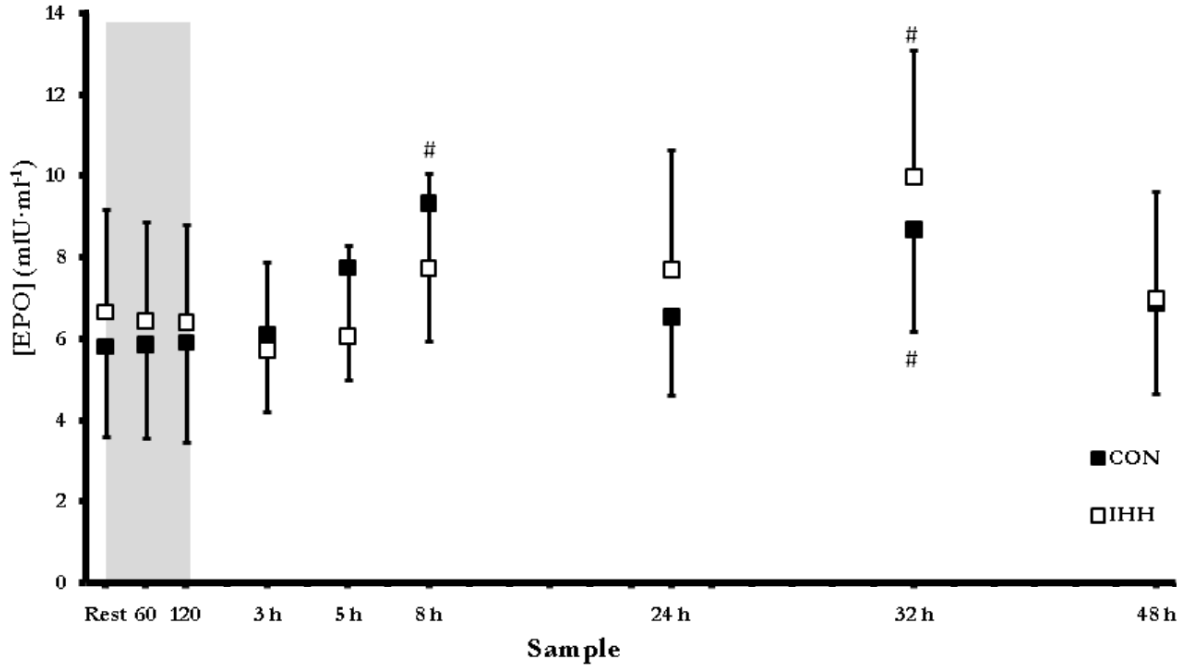

Figure 1: Changes in absolute EPO levels in both groups during the protocol (* significant difference from rest; $P < 0.05$)

Relative Δ[EPO] levels were significantly lower in the IHH group compared to CON 5 and 8 hours following exposure (Figure 2).

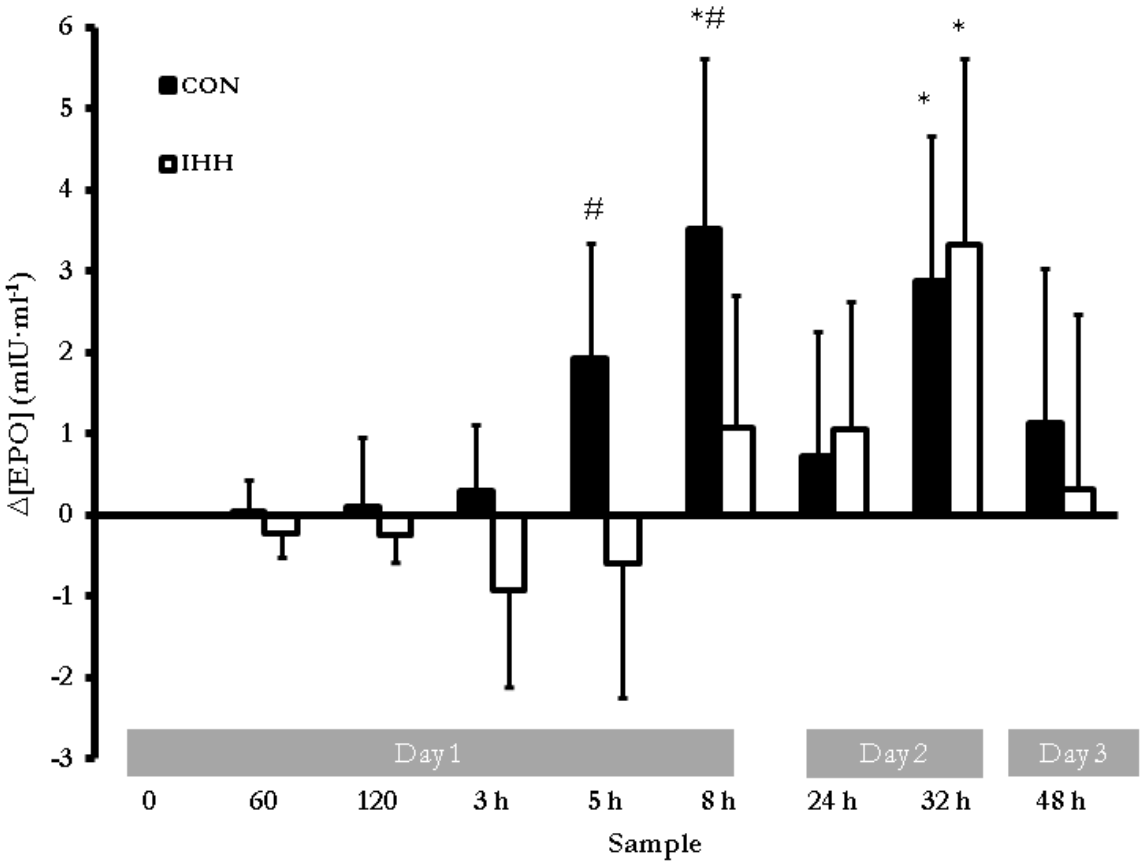

Figure 2: Changes in relative EPO levels (ΔEPO) in both groups during the protocol (* sig. diff. from rest, # sig. diff. between groups; $P < 0.05$)

4 Discussion

Successive and acute periods of breathing hyperoxic and hypoxic gas mixtures had no effect on [EPO], which in both the IHH and Normoxia seems to follow a circadian rhythm. In contrast to other studies showing increases in absolute EPO concentration following short duration hyperoxic [6] or hypoxic breathing [7], our results showed no significant changes compared to a placebo control within 48 hours following exposure cessation. Although some significant changes were observed within groups these are probably attributable to the natural circadian EPO fluctuations [8]. Furthermore, the relative [EPO] changes showed that the tested protocol induced significantly lower [EPO] synthesis within the first 8 hours following IHH exposure, suggesting that EPO synthesis was suppressed following the IHH. The results of the current study show that a combination of short-term hyperoxic and hypoxic breathing does not augment the [EPO] *de novo* synthesis, thus, our findings do not support the existence of the "normobaric oxygen

paradox". The validity of our observation is fortified by the study design, incorporating a matched control group undergoing a single-blind placebo protocol.

Although the tested protocol did not induce increases in EPO production, the aim of inducing beneficial changes following short period breathing of hypoxic/hyperoxic is indeed intriguing. Induction of changes in the shortest possible time is motivated by different possible applications necessitating fast results. Briefly, athletes aim at increasing the oxygen carrying capacity of the blood (among the main factors affecting the high oxygen flux) with as little distribution to their normal daily routine as possible. Furthermore, military personnel can be deployed to high altitude areas in the short time period, requiring a fast and effective pre-acclimatization, if one wishes them to operate optimally. Besides this, clinical applications could also benefit from an efficient protocol providing increases in EPO concentration. If both short term hypoxia and hyperoxia would provide benefits that would prove helpful in the treatment of different anemia types associated with chronic diseases and overcoming anemia's arising from pre-operative blood donations, as already suggested by Burk [9].

References:

[1]Levine, B.D. and J. Stray-Gundersen, Point: positive effects of intermittent hypoxia (live high:train low) *J Appl Physiol*, 99(5): 2053-5, 2005

[2]Erslev, A.J., Clinical erythrokinetics: a critical review. *Blood Rev*, 11(3): 160-7, 1997

[3]Lamon, S., Robinson N. and Saugy M., Procedures for monitoring recombinant erythropoietin and analogs in doping. *Endocrinol Metab Clin North Am*, 39(1): 141-54, 2010

[4]Elliott, S., Erythropoiesis-stimulating agents and other methods to enhance oxygen transport. *Br J Pharmacol*, 154(3): 529-41, 2008

[5]Jelkmann, W., Erythropoietin: structure, control of production, and function. *Physiol Rev*, 72(2): 449-89, 1992

[6]Balestra, C., Germonpre P., Poortmans J.R. and Marroni A., Serum erythropoietin levels in healthy humans after a short period of normobaric and hyperbaric oxygen breathing: the "normobaric oxygen paradox". *J Appl Physiol*, 100(2): 512-8, 2006

[7]Eckardt, K.U., Boutellier U., Kurtz A., Schopen M., Koller E.A. and Bauer C., Rate of erythropoietin formation in humans in response to acute hypobaric hypoxia. *J Appl Physiol*, 66(4): 1785-8, 1989

[8]Klausen, T., Dela F., Hippe E. and Galbo H., Diurnal variations of serum erythropoietin in trained and untrained subjects. *Eur J Appl Physiol Occup Physiol*, 67(6): 545-8, 1993

[9]Burk, R., Oxygen breathing may be a cheaper and safer alternative to exogenous erythropoietin (EPO). Med Hypotheses, 69(6): 1200-4, 2007

For wider interest

This paper presents one of a series of studies investigating the physiological consequences of manipulating oxygen partial pressure in the inspired air. The studies conducted during the course of my PhD training mainly dealt with the effects of simulated altitude exposure or training in simulated altitude on subsequent sports performance. Hypoxia (lower oxygen levels) or hyperoxia (higher oxygen levels) are nowadays extensively used in sports and medicine to enhance human performance and alleviate or treat respiratory and haematological medical disorders, respectively. The main aims of the studies were to investigate the effects of short protocols employing intermittent or chronic hypoxia on selected physiological indexes that could prove beneficial for sports and medical use. Our findings have shown that some benefits (e.g. certain adaptation to hypoxic environment, enhancement of performance at altitude) can be expected following short intermittent hypoxic protocols, but a certain threshold has to be surpassed if the beneficial adaptations are to be expected. The physiologically applied nature of the described work does not exclude the possible applicability of our work to industry. Moreover, even if our studies are manly oriented to investigate the selected human physiological mechanism and effect, their possible applications cover a range of clinical, health and sports related fields. The investigated protocols, if proved efficient, could be applied to hospital environments and health or sports related practices with the involvement of industrial partners concerned in medical equipment production and development. In particular, the studies directed by prof. Igor B. Mekjavic have already led to a fruitful collaboration with a foreign industrial partner that is now becoming one of the main European producers of altitude training simulation systems and facilities (b-Cat, The Netherlands).

Plasma sterilization as a key for cleaning delicate materials

Kristina Eleršič[1,2], **Miran Mozetič**[1*]

[1] Department of F4, Jožef Stefan Institute, Ljubljana, Slovenia

[2] Jožef Stefan International Postgraduate School, Ljubljana, Slovenia

kristina.elersic@ijs.si

Abstract. Sterilization of delicate materials by oxygen plasma represents an interesting task for plasma scientists. We are presenting an environmental friendly method to clean the surface of materials. The degradation steps are followed by Atomic Force Microscopy (AFM). The bacterial capsule is removed in about 15 s. Once the capsule is removed, degradation of the cell wall occurs causing bacterial death leaving clean and sterile surface of the material.

Keywords: Oxygen plasma, sterilization, bacteria

1 Introduction

Outbreaks of diseases resulting from infection by pathogenic microorganisms like *E.coli,* greatly disrupt daily life and constitute significant health problem. The materials and components should therefore be sterilized occasionally. Steam, heat, UV and chemical sterilization seems not to be sufficient techniques to fight against microorganisms. Another solution is to destroy microorganisms with physical methods.

By definition, sterilization is the process by which living organisms are removed or killed to the extent that they are no longer detectable in standard culture media in which they previously have been found to proliferate. According to this definition, both the process used to achieve sterility and the methods testing for it are equally important [1-5].

Since a lot of materials (such as polymers) are not stable in autoclave and chemicals are highly dangerous for the environment, we have to find new solutions for sterilization. The basic idea behind plasma sterilization is to destroy bacteria either by oxidizing (or etching) them, or by heating them with recombination of oxygen atoms on their surface. The basic mechanisms involved in the plasma inactivation

of microorganisms are where plasma particles interact with bacterial constituents through destruction of bacterial DNA (by UV radiation), etching of organic materials (by charged particles as well as neutral plasma radicals), and drilling holes into the bacterial cell wall (by ion bombardment) [3].

Many parameters have influence on sterilization. Different discharges or gases can be used for special applications [6-9]. Here we present oxygen plasma using RF discharge.

2 Experimental

To investigate the effects of the plasma on the morphology of bacterial cells, atomic force microscopy (AFM) was used to inspect cells for physical damage following exposure to the oxygen atoms. AFM images were made in a semi-contact mode. Control and plasma-treated suspensions of bacteria were investigated in detail.

For the experiments we used bacteria E. coli strain ATCC 25922. It was grown at 37 °C on LB plates for 24 hours. Cells were then resuspended in sterile water. The number of cells was adjusted to approximately 108 cfu (colony forming unite). Before exposure to plasma, we deposited bacteria solution on activated silica wafer substrate and then treated them with plasma for different periods of time (5 s, 10 s, 15 s, 30 s, 45 s, 60 s, 120 s and 240 s). Some representative AFM images are presented in Figure 1. Picture A shows bacteria without treatment. Some bacteria moving shifts like fimbriae are very well seen. Pictures B and C are presenting treated bacteria after treatment with highly reactive oxygen plasma.

The plasma reactor used to treat the bacteria was powered by an inductively coupled radiofrequency generator operating at 27.12 MHz. Its output power was set at 200 W. The system was pumped with a two stage rotary pump with a maximum pumping speed of 16 m^3/h. commercially available oxygen was leaked into the system at room temperature through a needle valve. Oxygen pressure in the reactor was kept at 75 Pa.

A

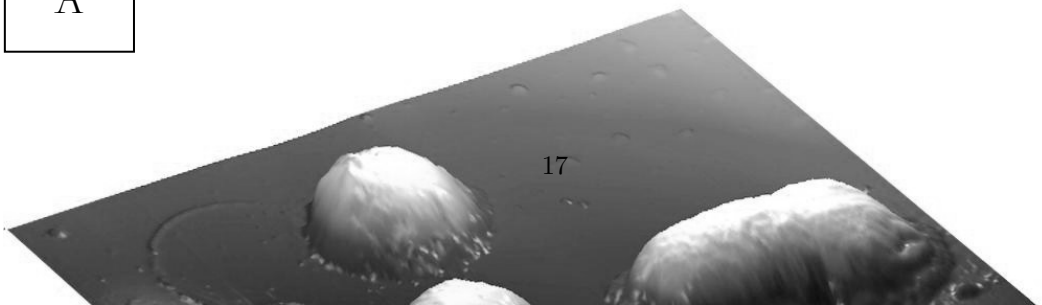

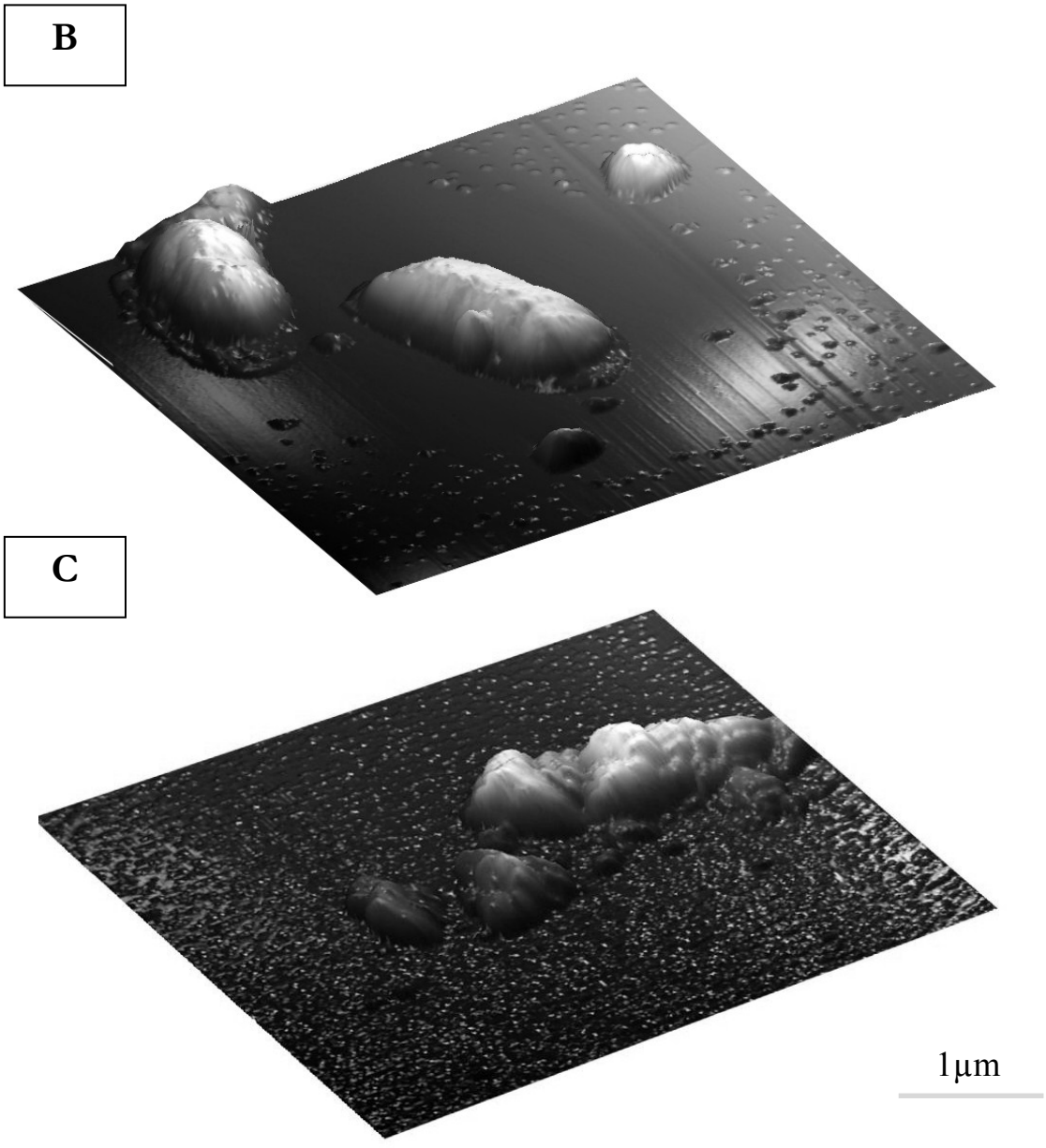

Figure 1: AFM images of bacteria; A - reference, B – plasma treatment for 10 s and C – plasma treatment for 120 s.

3 Results

The cell envelope of the Gram-negative *E. coli* is multilayered with two membranes, an inner cytoplasm membrane (~8 nm thick) and an outer lip polysaccharide membrane (also ~8 nm thick) enclosing a very thin (~2 nm) layer of murein embedded in a gel-like periplasm layer of thickness ~14 nm. While the entire envelope is about 30 nm thick, it is this very thin murein layer (consisting of sugars cross-linked by amino acids) that provides the strength and rigidity of the bacterium [10-13]. Since bacteria have more then one protective coating, there are several steps during degradation. At the beginning of the treatment, cell appendage pili and fimbriae are etched which are very well seen on figure 1 A. They are on the surface of bacteria and are used for motility and gen conjugation between pairs of bacteria. Next step is degradation of murein protective part (it consists of sugars cross-linked by amino acids). It took approximately 10 s in plasma to decompose this protective layer (Figure 1 B). Bacterial death accrue after approximately 120 s. Plasma can have biocidal effect from their reactive species and does not leave any residue on the material.

Although different types of bacteria exhibit different resistance to plasma treatment it is clear that all sorts of bacteria as well as their spores can be destroyed using plasma with suitable parameters [14]. In order to avoid (or at least minimize) the degradation of substrates, it is advisable to use plasma with optimized parameters. Plasma should be energetic enough to assure rapid degradation of bacteria, but also mild enough to preserve the original properties of the substrates.

4 Conclusions

The observation on which we focus here is the structural damage suffered by the Gram-negative bacteria (*E. coli*) when exposed to oxygen plasma. Their outer membrane appears to be massively disrupted leading to the release of their cytoplasm to the surrounding medium and degraded during prolonged treatment.

Most of the available disinfectants are aggressive or very toxic to the surfaces of materials. Using highly reactive oxygen plasma with variable parameters and different gases can improve surface properties in many procedures where sterile environment plays an important role.

References:

[1] M. Moisan , J. Barbeau, S. Moreau, J. Pelletier, M. Tabrizian, L'H. Yahia, Low-temperature sterilization using gas plasmas: a review of the experiments and an analysis of the inactivation mechanisms, *Int. J. Pharm.* 226 (2001), 1-2

[2] I. A. Soloshenko, V. V. Tsiolko, V. A. Khomich, A. I. Shchedrin, A. V. Ryabtsev, V. Y. Bazhenov, I. L. Mikhno, Sterilization of medical products in low-pressure glow discharges, *Plasma Phys. Reports* 26 (2000) 792-800

[3] B. J. Park, K Takatori, M. H. Lee, D. W. Han, Y. I. Woo, H. J. Son, J. K. Kim, K. H. Chung, S. O. Hyun, J. C. Park, Escherichia coli sterilization and lipopolysaccharide inactivation using microwave-induced argon plasma at atmospheric pressure, *Surf. Coat. Technol.* 201 (2007), 5738-5741

[4] G. Fridman, A. D. Brooks, M. Balasubramanian, A. Fridman, A. Gutsol, V. N. Vasilets, H. Ayan, G. Friedman, Comparison of direct and indirect effects of non-thermal atmospheric-pressure plasma on bacteria*, Plasma Process. Polym.* 4 (2007), 370-375

[5] S. Moreau, M. Moisan, M. Tabrizian, J. Barbeau, J. Pelletier, A. Ricard, L'H. Yahia, Using the flowing afterglow of a plasma to inactivate Bacillus subtilis spores: Influence of the operating conditions*, J. Appl. Phys.* 88 (2000), 1166-1174

[6] O. Kylian, F. Rossi, Sterilization and decontamination of medical instruments by low-pressure plasma discharges: application of $Ar/O_2/N_2$ ternary mixture, *J. Phys. D Appl. Phys.* 42 (2009), 085207

[7] A. Ricard, M. Moisan, S. Moreau, Determination, through titration with NO, of the concentration of oxygen atoms in the flowing afterglow of $Ar\text{-}O_2$ and $N_2\text{-}O_2$ plasmas used for sterilization purposes*, J. Phys. D Appl. Phys.* 34 (2001) 1203-1212

[8] S. Lerouge, M.R. Wertheimer, R. Marchand, M. Tabrizian, L. H. Yahia, Effect of gas composition on spore mortality and etching during low-pressure plasma sterilization, *J. Biomed. Mater. Res.* 51 (2000), 128-135

[9] K. Stapelmann, O. Kylian, B. Denis, F. Rossi, On the application of inductively coupled plasma discharges sustained in $Ar/O_2/N_2$ ternary mixture for sterilization and decontamination of medical instruments*, J. Phys. D Appl. Phys.* 41 (2008), 192005

[10] U. Cvelbar, D. Vujošević, Z. Vratnica, M. Mozetič, The influence of substrate material on bacteria sterilization in an oxygen plasma glow discharge*, J. Phys. D Appl. Phys.* 39 (2006), 3487-3493

[11] D. Vujošević, M. Mozetič, U. Cvelbar, N. Krstulović, S. Milošević, Optical emission spectroscopy characterization of oxygen plasma during degradation of Escherichia coli, *J. Appl. Physic.* 101 (2007), 103305-1-103305-7

[12] C. Canal, F. Gaboriau, S. Villeger, U. Cvelbar, A. Ricard, Studies on antibacterial dressings obtained by fluorinated post-discharge plasma, *Int. J. Pharm.* 367 (2009), 155-161

[13] Z. Vratnica, D. Vujošević, U. Cvelbar, M. Mozetič, Degradation of bacteria by weakly ionized highly dissociated redio-frequency oxygen plasma*, IEEE Trans. Plasma Sci.* 36 (2008) 1300-1301

[14] A. Drenik, U. Cvelbar, A. Vesel, M. Mozetič, Weakly ionized oxygen plasma*, Inf. MIDEM* 35 (2005), 85-91

[15] C. Thomas, K. Kelly-Wintenberg and J. Reece Roth; An Overview of Research Using the One Atmosphere Uniform Glow Discharge Plasma (OAUGDP) for Sterilization of Surfaces and Materials*; IEEE transactions on plasma science*, 2000; vol.28, no. 1

[16] M. Laroussi, D .A. Mendis and M. Rosenberg; Plasma interaction with microbes; *New Journal of Physics* 5 (2003) 41.1-41.10

[17] Y. Sun; Y. Qiu; A. Nie; Xudong Wang; Experimental Research on Inactivation of Bacteria by Using Dielectric Barrier Discharge; Plasma Science, *IEEE Trans. Plasma Science* 2007 ; 35:1496 – 1500

For wider interest

Applying sterile material in many applications can have several difficulties; one of these is unstable material which can be damaged during the sterilization processes, for example melted in autoclave. For this reason, developers are trying to make sterile surfaces by making simple and environmental friendly processes of sterilization. One of very promising methods is plasma treatment of surfaces. We are trying to use weakly ionised plasma which has a low temperature and has specially adapted properties. In our experimental work, we sterilize materials, which are usually destroyed during normal disinfection processes such as polymers and polymer composites. Using plasma in the procedure can create clean surfaces and help reusing materials which will be a huge step for the environment. Investigation also includes degradation steps of bacteria *Escherichia coli*. This bacterium is one of the most investigated bacteria in biochemistry and also plays important role in infections due to many pathogens from their strain. By applying reactive plasma we can destroy bacteria and remove dust on the surface but leave the material almost intact.

Čiste premogovne tehnologije in projekt CoGasOUT

Jerneja Lazar [1,2], Simon Zavšek [1,2], Sergej Jamnikar [1,2], Janja Žula [1], Gregor Uranjek [1,2], Ludvik Golob [1]

[1] Premogovnik Velenje d.d., Partizanska 78, Velenje

[2] Mednarodna podiplomska šola Jožefa Stefana - MPŠ

jerneja.lazar@rlv.si

Mentor: Prof. dr. Sevket Durucan, gostujoči profesor MPŠ – Imperial College London

So-mentor: Dr. Simon Zavšek

Povzetek: Pomen premoga kot vira energije se v zadnjih letih ponovno povečuje. Prednosti pred drugimi energenti lahko iščemo v razvoju novih, ekološko bolj prijaznih tehnologij uporabe premoga, tako imenovanih čistih premogovnih tehnologij (ang: Clean Coal Technologies). Zato smo se na Premogovniku Velenje odločili ustanoviti projektno skupino Čiste premogovne tehnologije za tri projektne naloge: razplinjevanje lignitnega sloja; zajem, transport in shranjevanje CO_2 in na podzemno uplinjanje premoga. Julija 2010 se je začelo v okviru prve projektne naloge razplinjevanje lignitnega sloja z izvajanjem mednarodnega projekta CoGasOUT (Razvoj novih tehnologij za napoved in preprečevanje izbruhov plinov ter nenadzorovanih emisij v premogovnikih z debelimi in/ali strmimi sloji premoga). Na pričetku trajanja projekta je bil izpeljan program geotehničnih in plinskih meritev ter raziskav v jamskem okolju, obdelani so bili pridobljeni podatki ter povezani z dogodki, ko je zaradi odkopavanja prihajalo do povečanih volumnov premogovega plina.

Ključne besede: čiste premogovne tehnologije, projekt CoGasOUT, razplinjevanje lignitnega sloja, zajem in shranjevanje CO_2, podzemno uplinjanje premoga

1 Čiste premogovne tehnologije

V zadnjih letih se pomen premoga kot vira energije ponovno dviga zaradi razvoja tako imenovanih *čistih premogovnih tehnologij* (ang: Clean Coal Technologies – CCT). Premog še vedno zagotavlja 23% primarne energetske potrebe in približno 39% električne energije je pridobljene iz premoga [1]. Vendar zgorevanje premoga proizvede v svetovnem okviru tudi več milijard ton ogljikovega dioksida na leto, ki se sprošča v ozračje. Po srednjeročnem načrtu, ki predvideva obratovanje Premogovnika Velenje vsaj do leta 2045, se je Premogovnik odločil slediti svetovnim zahtevam za zmanjševanje emisij toplogrednih plinov in konec leta 2007 ustanovil projektno skupino Čiste premogovne tehnologije.

Osnovno načelo čistih premogovnih tehnologij je čistejša uporaba premoga z zmanjšanjem emisij ogljikovega dioksida in metana. Projekt čistih premogovnih tehnologij vključuje številna področja, kot so proizvodnja premoga, priprave odkopnih polj, transport premoga, nekonvencionalna proizvodnja premoga s podzemnim uplinjanjem premoga, dreniranje premogovnega plina iz jamskega zraka ter iz premogovnih slojev in proizvodnja električne energije na osnovi uplinjanja premoga. Nove čiste premogovne tehnologije bodo igrale v prihodnosti ključno vlogo pri zagotavljanju zadostnih količin proizvedene električne energije, tako v svetu kot tudi v EU in še posebej v Sloveniji.

Raziskovalna skupina bo razvijala nove tehnologije za čistejšo uporabo premoga. V ta namen bodo potekale tri različne skupine projektov:

- **Razplinjevanje lignitnega sloja (ang: Gas drainage**): Tehnologije razplinjevanja so znane po svetu za tanjše sloje premoga, za debele sloje premoga – kakor je v Velenju - pa še ni razvite tehnologije. Zajem premogovnih plinov iz premoških slojev se je izkazal kot učinkovita metoda za preprečevanje izbruhov plina iz premoga v premogovnikih. Razvoj tehnologije za razplinjevanje lignitnega sloja poteka v okviru mednarodnega projekta CoGasOUT.
- **Zajem in shranjevanje CO_2 (ang: Carbon capture and storage - CCS):** CCS je relativno nova metoda, ki temelji na zajemu CO_2 od »velikih onesnaževalcev okolja« kot so npr. termoelektrarne in nekatere kemične

tovarne. Po zajemu se CO_2 shrani v geosfero na način, da ne vstopi več v ozračje. CO_2 se lahko vtiska v globoke geološke formacije, v globoke predele oceanov v obliki mineralnih karbonatov, v izkoriščena naftna in plinska polja ter v premogovne sloje. V sklopu CCS poteka na Premogovniku Velenje projektna naloga z naslovom Metodologije fiksacije CO_2 na elektrofiltrski pepel, kjer preučujemo možnosti shranjevanja CO_2 z vezavo na elektrofiltrski pepel, ki nastaja pri sežigu premoga v Termoelektrarni Šoštanj. Projekt je v fazi začetnih raziskav in priprave laboratorijske opreme za nadaljnje preskuse.

- **Podzemno uplinjanje premoga - PUP (ang: Underground Coal Gasification - UCG):** PUP je nekonvencionalno izkoriščanje premoga z uporabo injekcijske in produkcijske vrtine s površja, kar omogoča sežig premoga v sintezni plin s pomočjo oksidantov (zrak ali kisik in para). Sežig premoga poteka pri visokih temperaturah (od 700 do 900 °C) in visokih pritiskih. Produkt uplinjanja premoga – sintezni plin- je zmes vodika, CO, CO_2 in v manjših količinah metana in H_2S. Sintezni plin se lahko uporablja kot energent za plinske turbine, za sintezo tekočih goriv ali za proizvajanje amoniaka in gnojil. Leta 2002 je bila na Premogovniku Velenje narejena študija izvedljivosti PUP, vendar ni bila dokončana. Študija iz leta 2002 se nadaljuje s predlogom projektne naloge za pilotni test možnosti podzemnega uplinjanja premoga v Velenju.

Raziskovalna skupina Čiste premogovne tehnologije sodeluje tudi na mednarodnem projektu CoGasOUT (Razvoj novih tehnologij za napoved in preprečevanje izbruhov plinov ter nenadzorovanih emisij v premogovnikih z debelimi in/ali strmimi sloji premoga), ki naj bi pripomogel k boljšemu odkopavanju premoga ter večji varnosti v rudnikih.

2 Projekt CoGasOUT

Premogovnik Velenje se je prijavil na mednarodni projekt CoGasOUT z glavnim namenom, da bi razvili nove tehnologije za predvidevanje in napovedovanje izbruhov plina in premoga v premogovnikih z debelimi in/ali strmimi sloji premoga. Premogovni sloj v velenjskem Premogovniku je debel v povprečju 160 m

in spada med debelejše sloje. V Premogovniku Velenje se je uveljavila velenjska odkopna metoda. Posebnost te metode je v postopku kontroliranega pridobivanja premoga iz nadkopnega dela odkopa s »točenjem« prek stropnikov v čelni transporter, kar omogoča zelo visoko zmogljivost odkopavanja ob izredni stopnji varnosti in veliki ekonomičnosti. Na dan proizvede Premogovnik Velenje do 20.000 ton premoga, kar letno znaša okoli 4 mio ton premoga.

S projektom CoGasOUT naj bi izboljšali razumevanje stanja napetosti in dinamiko tlakov plinov v premogovem sloju, ki lahko vodijo k izbruhom plina in premoga. Na odkopu se lahko sprožijo izbruhi plina zaradi previsokih koncentracij premogovnega plina v sloju premoga. Pri pripravah podzemnih prog pa se lahko sprožijo tako izbruhi plina kakor tudi izbruhi premoga. Rezultati projekta bodo doseženi z laboratorijskimi in terenskimi preiskavami.

V triletnem obdobju, kolikor je predvideno trajanje projekta, bo v Premogovniku Velenje ter pri ostalih partnerjih potekalo mnogo načrtnih akcij in eksperimentov, ki so mednarodno usklajevani ter usmerjeni k skupnim ciljem.

Projekt CoGasOUT se bo zaključil s pilotno študijo razplinjevanja plina iz sloja premoga. Rezultat projekta naj bi omogočal nadzor nad izpusti premogovnih plinov iz debelih slojev premoga. S tem se bodo lahko zmanjšali tudi stroški prezračevanja premogovnika, saj bodo z nadzorovanimi izpusti zmanjšane emisije plinov v jamskem zraku, kar bo zagotovilo tudi boljše varnostne razmere pri delu.

2.1 Raziskave v okviru projekta CoGasOUT

Od pričetka trajanja projekta v juliju lanskega leta je bil izpeljan program geotehničnih in plinskih meritev ter raziskav v jamskem okolju, obdelani so bili pridobljeni podatki ter jih povezani z dogodki, ko je zaradi odkopavanja prihajalo do povečanih volumnov premogovega plina za odkopa K.-50/B v jami Pesje ter K.-120/B v jami Preloge.

Zdaj poteka podoben obseg del na odkopih k. -50/C v jami Pesje in k. -130/A v jami Preloge. Na omenjenih odkopih potekajo tudi mikro-seizmične preiskave poljskega partnerja GIG ter priprave za izvedbo seizmične tomografije, ki jo bo izvajalo partnersko podjetje iz Nemčije K-UTEC. Rezultate teh preiskav bomo

lahko primerjali z rezultati seizmične tomografije z odkopa k. -110/B v jami Preloge, katere je K-UTEC izvedel za potrebe projekta EUREKA, ki je na Premogovniku Velenje potekal v letih od 2006 do 2008.

Izpeljana je bila večina nalog iz prvega delovnega paketa, kjer so bile aktivnosti usmerjene v zbiranje in vrednotenje obstoječih podatkov glede zračilnih, plinonosnih, geotehničnih ter proizvodnih parametrov in izvajanje nekaterih laboratorijskih eksperimentov s področja sorpcije.

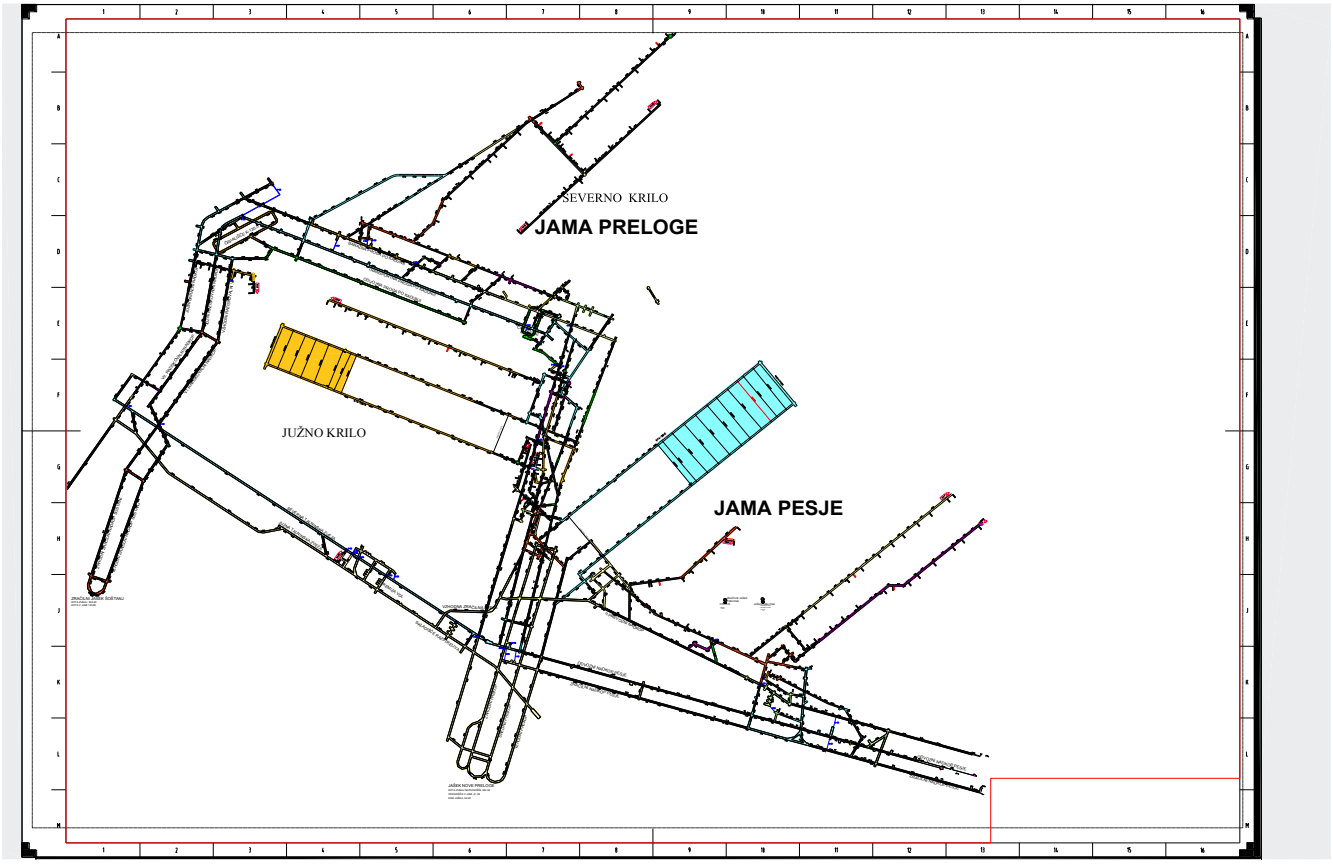

Slika 2-1: Shematski prikaz sistema rovov in odkopov v aktivnem delu Premogovnika Velenje.

Del delovnega paketa projekta CoGasOUT zajema spremljavo koncentracij premogovnih plinov v premogovnem sloju. V velenjskem premogovnem sloju sestavljata premogovni plin dva glavna predstavnika - ogljikov dioksid in metan s povprečno mešanico plinov približno CO_2:CH_4 ≥2:1.

Spremljava koncentracij plinov v premogovnem sloju poteka s pomočjo horizontalnih vrtin različnih dolžin. Poleg spremljave koncentracij plinov potekajo tudi meritve tlakov v tlačnih horizontalnih vrtinah. Z analizo teh podatkov bodo

lahko povezani pojavi izbruhov plina z napredkom odkopavanja premoga in s stanjem premogovega sloja.

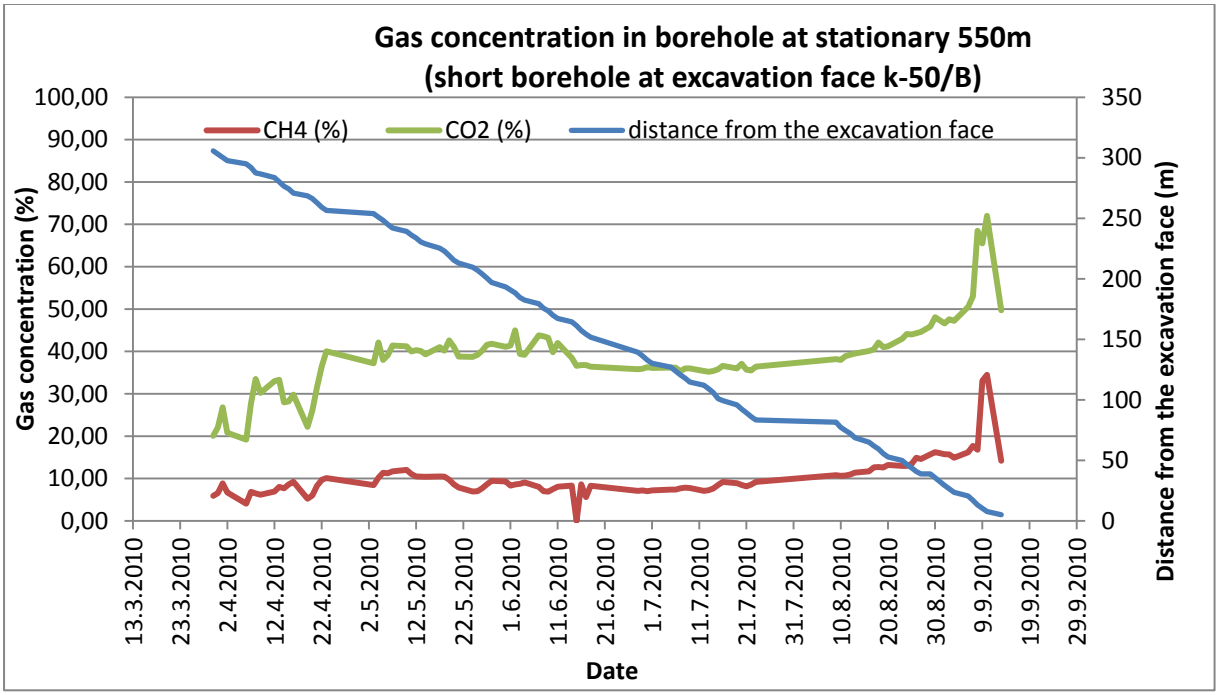

Slika 2-2: Rezultati spremljave koncentracij premogovnih plinov v horizontalni vrtini na območju Jame Pesje (k. -50/B)

Koncentracije CO_2 se spreminjajo od 18% do 98,8%, koncentracije metana od 1,1% do 100% in koncentracije tretjega plina - dušika se spreminjajo od 7,2% do 67,34%. Glavni vzroki za spreminjanje koncentracije so številni izvori premogovnega plina in različni fizikalno-kemični procesi med migracijo plina, kot so: difuzija, procesi adsorpcije in desorpcije [3].

Poleg merjenja koncentracij premogovega plina spremljamo tudi spreminjanje tlaka premogovnega plina v vrtini v odvisnosti od napredovanja odkopavanja premogovnega stebra. Tlak se spreminja zaradi migracij plinov, ki so posledica odkopavanja premoga. Odkopno čelo vpliva na samo hribino z napetostnim valom, ki potuje po premogovem sloju in tako ustvarja nove razpoke, skozi katere lahko plin migrira, tlak v vrtini pa zaradi tega razloga pada.

Za napoved in nadzor emisij plinov v premogovniku so bili testirani vzorci premoga s testi desorpcije – direktna metoda. Opravljeno je bilo 5 meritev, analiza podatkov je v toku.

3 Viri

[1] "Clean Coal" Technologies, Carbon Capture & Sequestration, http://www.world-nuclear.org/info/inf83.html, World Nuclear Association;

[2] S. Zavšek, L. Golob, J. Žula, Clean Coal Technologies at Velenje Coal Mine, Journal of Energy Technology Volume 3, (2010); P 41-52; Issue 3, August 2010;

[3] J. Pezdič, M. Markič, M. Letič, A. Popovič, S. Zavšek, 1999: Laboratory simulation of desorption – desorption processes on different lignite lithotypes from Velenje lignite mine, RMZ – Materials and Geoenviroment, Vol. 46, No. 3, 555-568;

[4] Research Programme of the Research Fund for Coal and Steel, Annual Report, March 2011;

[5] European Commission Research Directorate- general, Research Fund for Coal and Steel: Proposal overview submission form for Research, Pilot and Demonstration projects and Accompanying Measures for the promotion of knowledge gained (Project CoGasOUT);

[6] European Commission Research Directorate- general, Research Fund for Coal and Steel: Technical Annex Project CoGasOUT;

[7] A. Zapušek, G. Berčič, S. Zavšek, I. Veber, L. Golob, D. Konovšek: Underground Coal Gasification (UGC) – Velenje Coal Mine Experience, Journal of Energy Technology, Volume 1 (2008), P 1-10, Issue 1, October 2009;

[8] Kanduč, J. Pezdič: Origin and distribution of coalbed gases from the Velenje basin, Slovenia, Geochemical Journal, Vol. 39, 2005;

TEMPERATURNI IN VLAŽNOSTNI PROFILI V RAZLIČNIH GRADBENIH SKLOPIH PASIVNIH HIŠ

Jana Mlakar[1,2,3], **Janez Štrancar**[2,3]

[1]Eko produkt d.o.o., Ljubljana

[2]Odsek za fiziko trdne snovi, Inštitut Jožef Stefan, Ljubljana, Slovenija

[3] Mednarodna podiplomska šola Jožef Stefan, Ljubljana, Slovenija

jana@ekoprodukt.si

Povzetek. Gradbeni materiali in izvedba gradnje vplivajo na bivalne pogoje v hišah, ti pa vplivajo na ugodje in zdravje njihovih prebivalcev. Rezultati raziskav vpliva neustrezne temperature in vlažnosti na zdravje prebivalcev kažejo potrebo po ohranjanju primerne temperature in vlažnosti v bivalnem okolju. Slednje lahko dosežemo z izbiro ustreznih gradbenih materialov. V raziskavi smo želeli preveriti vpliv različnih gradbenih sklopov na časovni potek temperature in vlage v gradbenih sklopih. Merili smo temperaturo in vlago na različnih mestih v testnih objektih manjših dimenzij z gradbenimi sklopi pasivnih hiš, pri katerih so zmanjšane toplotne izgube, tako da preostalo potrebno toploto za ogrevanje prostorov pridobimo s pasivnim zajemom sončne energije, s toploto notranjih virov ali pridobimo iz ostalih obnovljivih virov energije. Rezultati so pokazali vpliv izbire gradbenih materialov na temperaturna in vlažnostna nihanja v gradbenih sklopih. Materiali na osnovi lesa uspešneje blažijo nihanja temperature in vlage, kar zagotavlja stabilnejše bivalne pogoje.

Ključne besede: temperaturni in vlažnostni profili, gradbeni sklopi, gradbeni materiali, pasivne hiše

1 Uvod

Bivalni pogoji v hišah močno vplivajo na ugodje in zdravje njihovih prebivalcev. Uporaba neustreznih gradbenih materialov in neustrezna izvedba gradnje lahko vodita do različnih bolezenskih stanj in trajnih poškodb organizma. Med najpomembnejše dejavnike vpliva spadata temperatura in relativna zračna vlažnost v bivalnih prostorih. Relativna vlažnost vpliva direktno na fiziološke funkcije organizma. Povezana je tako s simptomom bolnih hiš [1], s sezonskimi poslabšanji kožnih bolezni ter z razvojem simptomov astme in odziva na alergene [2],

izsuševanjem očesne sluznice in posledično vnetji oči, ter tudi z izsušitvijo sluznice nosu [3]. Indirektno relativna vlažnost vpliva na rast in razmnoževanje patogenih organizmov in adsorpcijo ter učinek različnih kemikalij. Številne študije patogenov, ki se prenašajo z zrakom, so pokazale, da je njihova infektivnost najmanjša pri relativni zračni vlažnosti med 40 in 70% [4]. Skupaj s povečano verjetnostjo preživetja in aktivnosti virusa gripe pri nižji zračni vlažnosti, nizka zračna vlažnost povečuje verjetnost okužbe z gripo, prehladi in drugimi tipičnimi okužbami dihal [3]. Spremembe temperature direktno vplivajo na sposobnost zraka za vpijanje vodne pare in tako na relativno vlažnost zraka. Indirektno pa vplivajo temperature na fiziologijo kože, ožilja, sluznic ter na imunski odziv. Po standardu 55-1992 ANSI/ASHERA velja, da je najbolj udobno območje med 20°C - 26 °C ter 30 - 60 % relativne vlažnosti. Opisani vplivi temperature in relativne vlažnosti jasno kažejo na potrebo po vzdrževanju optimalne vlažnosti in temperature zraka v prostoru [3]. Vlažilci zraka [5] in tradicionalni ogrevalni sistemi niso najprimernejša rešitev, saj ustvarjajo prevelike lokalne temperaturne in vlažnostne gradiente. Rešitev problema ni v iskanju aktivnih in sofisticiranih prezračevalnih sistemov, temveč v optimizaciji hiš v njihovi osnovi, torej izboru gradbenih materialov, ki ugodno vplivajo na bivalne pogoje, ter ustrezno izvedbo gradnje. V ta namen smo raziskali pasivni vpliv uporabe materialov z različno toplotno kapaciteto in toplotno prevodnostjo na temperaturna in vlažnostna nihanja pri spremenjenih pogojih objekta. Rezultati raziskav [6,7] so pokazali, da velike površine iz lesa ublažijo oscilacije notranje temperature v objektu ter povišajo relativno vlažnost.

2 Metode

Izdelali smo pomanjšane testne objekte, na katerih spremljamo oscilacije temperature v gradbenih slojih z različno sestavo sten in strehe. Trije pomanjšani testni objekti so enako orientirani in imajo senzorje v južni, zahodni in severni steni. Meritve beleži merilno nadzorni sistem z USB mikrokontrolerjem povezan na računalnik, ki zbira podatke. Temperaturo merijo senzorji LM 335, relativno zračno vlažnost senzorji HIH-4000 in solarni tok Silicon PIN Photodiode BPW34. Na testnih objektih zajemamo podatke vsake 3 minute na vseh 191 senzorjih v pomanjšanih testnih objektih. Zbrane podatke smo analizirali glede na različne sestave sten in strehe treh testnih objektov.

3 Rezultati

Spremembe temperature in relativne vlažnosti v gradbenih sklopih so odvisne od izbire gradbenih materialov. Primerjali smo jih v hiši izolirani s celulozno izolacijo (levo v slikah) ter v hiši izolirani s stekleno volno in stiroporjem (desno v slikah).

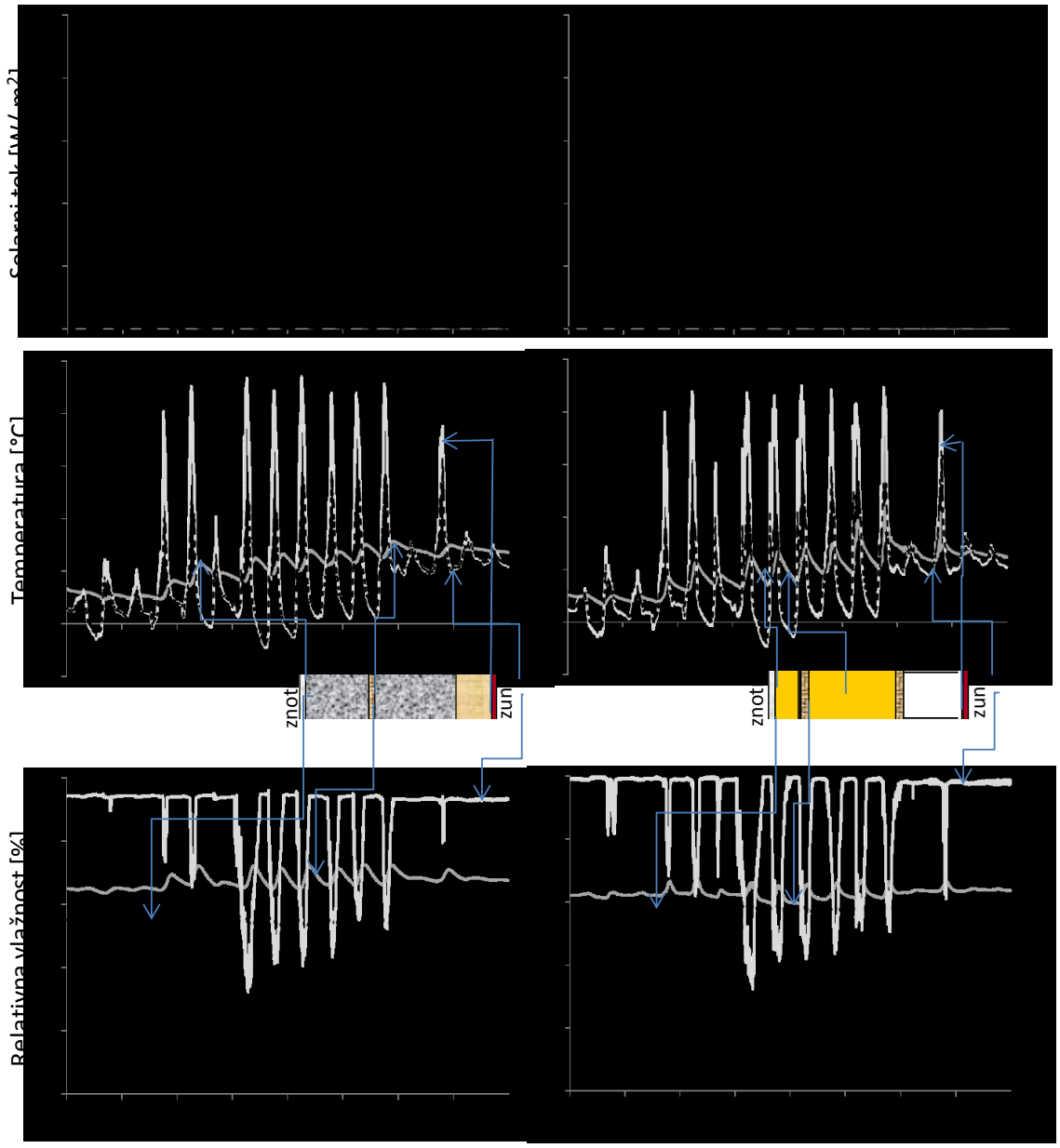

Slika 1: Solarni tok na južno fasado, temperature in relativne vlažnosti izmerjene v različnih delih (označeno s puščicami) južne stene dveh hišk z različno sestavo (leva hiša od znotraj navzven: mavčno kartonska plošča, celulozna izolacija, OSB/3 plošča, celulozna izolacija, leseno vlaknena plošča, fasadni sloj; desna hiša od znotraj navzven: mavčno kartonska plošča, steklena volna, parna zapora, OSB/3 plošča, steklena volna, OSB/3 plošča, polistiren, fasadni sloj). Obe hiši imata enake toplotne izgube.

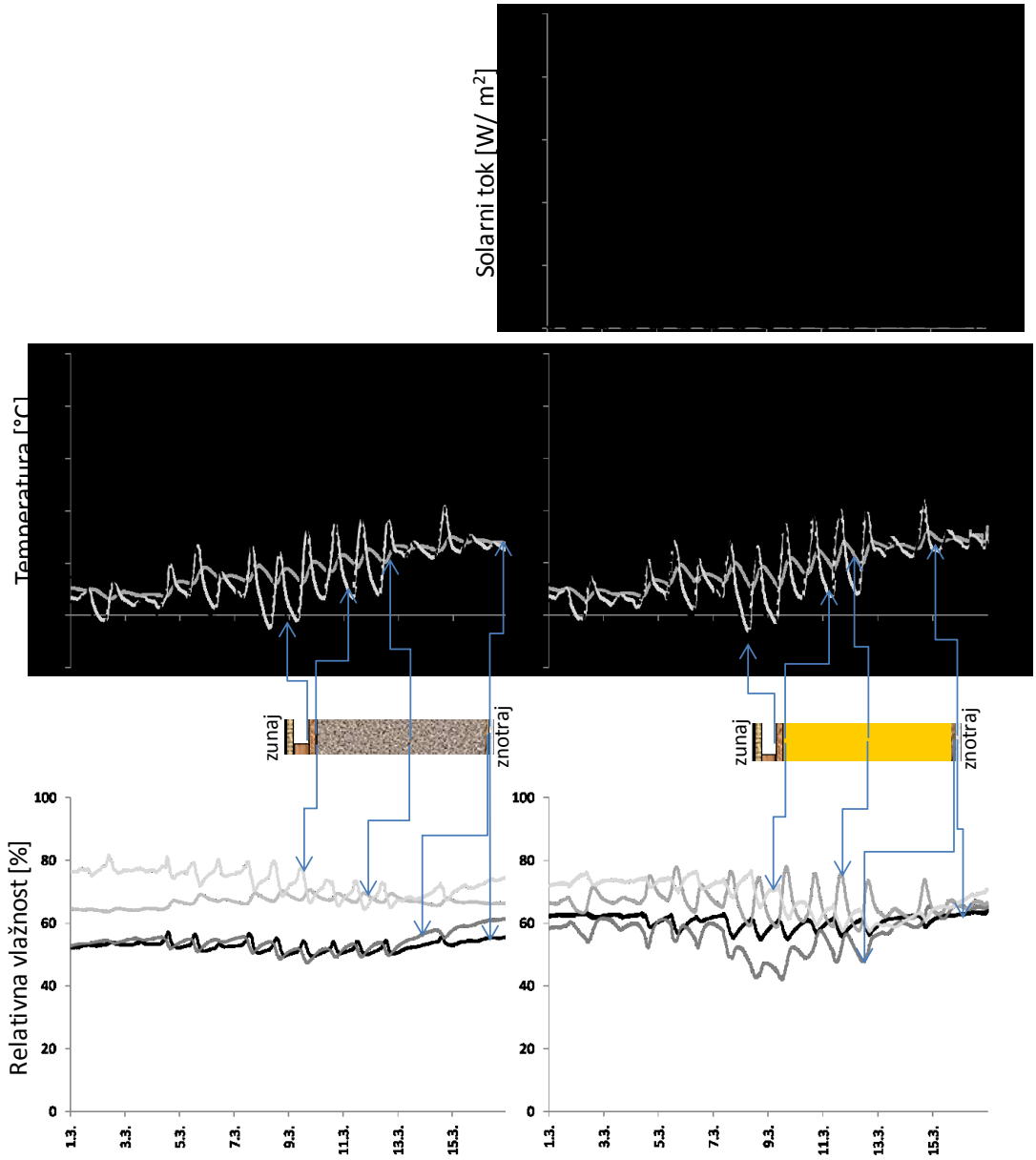

Slika 2: Solarni tok na fotodiodo (usmerjena proti jugu, 52°nad vodoravnico) na strehi, temperature in relativne vlažnosti izmerjene v različnih delih (označeno s puščicami) strehe dveh hišk z različno sestavo (leva hiša od znotraj navzven: mavčno kartonska plošča, parna ovira, celulozna izolacija, leseno vlaknena plošča; desna hiša od znotraj navzven: mavčno kartonska plošča, parna ovira; steklena volna, leseno vlaknena plošča).

Najprej lahko opazimo, da so temperature pod fasadnim slojem v največji meri odvisne od vpadnega sončnega toka na fasado, podobno tudi temperature pod mavčno kartonsko, zaradi energije, ki vstopi v hišo skozi okna. Zanimivi od materiala odvisni vzorci se pojavijo, ko primerjamo temperaturo pod fasadnim

slojem in temperaturo v sredini gradbenega sklopa (Slika 1). V hiši izolirani s celulozno izolacijo temperatura v sredini gradbenega sklopa ne sledi hitrim spremembam temperature pod fasadnim slojem, nasprotno je opaziti pri hiši izolirani s stekleno volno in polistirenom. Stena izolirana s celulozno izolacijo tako uspešno zamakne in zmanjša temperaturna nihanja v steni. Podobno je fazni zamik v sredini sklopa in manjša nihanja opaziti tudi v konstrukciji strehe hiše izolirane s celulozno izolacijo (Slika 2).

Gradbeni materiali blažijo tudi nihanja vlage. Večja so nihanja relativne vlažnosti v strehi hiše izolirane s stekleno volno in polistirenom v primerjavi s hišo izolirano s celulozno izolacijo, kljub enakim temperaturnim nihanjem, ki so rezultat sončne energije, ki vstopi skozi okna (Slika 2). V steni tega učinka ni opaziti, vendar verjetno tudi zaradi povsem drugačne sestave stene (zaporedja gradbenih materialov, Slika 1) in ne le razlike v izbiri gradbenih materialov.

4 Zaključek

Uporaba gradbenih materialov na osnovi lesa, ki igrajo vlogo začasnega ali stalnega blažilca nihanj temperature in vlage, vodi v bolj stabilne bivalne pogoje v stavbah.

Operacijo delno financira Evropska unija, Evropski socialni sklad.

Literatura:

[1]P. S. Burge. Sick building syndrome. *Occupational and Environmental Medicine,* 61:185-190, 2004

[2]M. Desrosiers, F. M. Baroody, D. Proud, L. M., Lichtenstein, A. Kagey-Sobotka, R.M. Naclerio. Treatment with hot, humid air reduces the nasal response to allergen challenge. *The Journal of Allergy and Clinical Immunology* 99, 1,1:77-86, 1997

[3]Y. Sunwoo, C. Chou, J. Takeshita , M. Murakami, Y. Tochihara Physiological and subjective responses to low relative humidity. *Journal of Physiological Anthropology* 25:7-14, 2006

[4]A. V. Arundel, E. M. Sterling, J. H. Biggin., T. D. Sterling. Indirect health effects of relative humidity in indoor environments. *Environmental Health Perspectives,* 65:351-361, 1986

[5]N. Hashiguchi, M. Hirakawa, Y. Tochihara, Y. Kaji, C. Karaki. Effects of setting up of humidifiers on thermal conditions and subjective responses of patients and staff in a hospital during winter. *Applied Ergonomics* 39:158-165, 2008

[6]S. Hameury in T Lundström. Contribution of indoor exposed massive wood to a good indoor climate: in situ measurement campaign. *Energy and Buildings* 36:281-292, 2004

[7]C. J. Simonson, M. Salonvaara, T. Ojanen. Improving indoor climate and comfort with wooden structures. *Building and Transport.* 431 VTT Publications, Technical Research Centre of Finland, ESPOO, ISBN 951-38-5847-22001

Za širši interes

Notranji bivalni pogoji močno vplivajo na udobje in zdravje njihovih prebivalcev. Uporaba neprimernih gradbenih materialov in neprimerna izvedba gradnje lahko povzročita bolezni in celo trajne poškodbe njihovih prebivalcev, zato je potrebno ohranjati temperaturo in vlago v optimalnem območju (20°C - 26 °C, 30 - 60 %), s čim manjšimi nihanji. Raziskave nakazujejo, da bivalno okolje v hišah lahko uravnamo z izborom ustreznih gradbenih materialov, ki znižajo nihanja temperature in vlage ter ju ohranjajo v optimalnem območju. Tako je o bivalnih pogojih potrebno razmišljati že pri načrtovanju pasivne hiše.

Z raziskavami v okviru projekta, ki ga delno financira Evropska unija, Evropski socialni sklad, želimo nakazati, kako uporaba pravilnih materialov prispeva k boljši kvaliteti bivanja v pasivnih hišah.

V ta namen smo izdelali testne objekte manjših dimenzij v pasivnem standardu z različnimi sestavami sten in strehe, v katerih spremljamo temperaturo in relativno vlažnost na različnih mestih. Temperaturo in vlago na različnih mestih v steni spremljamo tudi na delujočih hišah. Na tesnih objektih merimo kako različni gradbeni materiali, ki se razlikujejo v toplotni kapaciteti in toplotni prevodnosti (predvsem celulozna izolacija in leseno vlaknene plošče v primerjavi s stekleno volno in polistirenom) vplivajo na temperaturo in relativno vlažnost v pasivnih hišah. Z raziskavami želimo preveriti hipotezo, da večja toplotna kapaciteta materialov zmanjša temperaturna nihanja, da vgradnja različnih materialov na osnovi lesa še dodatno zmanjšuje oscilacije relativne vlažnosti v prostoru ter kako zmore ovoj hiš držati zračno vlago v območju med 40% in 60%.

Poleg tega v eni od delujočih hiš spremljamo delovanje vseh sistemov v hiši (ogrevanje, prezračevanje, dobitki sončne energije), s čimer lahko analiziramo celotno energijsko ravnovesje v hiši. Tako lahko opazujemo različne pojave v hiši ter z modeliranjem energijskega ravnovesja poiščemo preproste rešitve, ki preprečijo nezaželene pojave, npr. poletno pregrevanje hiše.

Rezultati raziskav bodo uporabni pri načrtovanju in optimizaciji pasivnih hiš. Z uporabo izsledkov raziskav bo mogoče načrtovati pasivne hiše, ki bodo omogočale še ugodnejše bivalne pogoje ter bodo hkrati manj obremenjevale okolje.

Validation of the analytical procedure for preparation of stable Cr(VI) and Cr(III) isotopic standard solutions from ^{50}Cr and ^{53}Cr enriched oxides

Breda Novotnik[1,2]

[1] Department of Environmental sciences, Jožef Stefan Institute, Ljubljana, Slovenia
[2] Jožef Stefan International Postgraduate School, Ljubljana, Slovenia
Supervisor: Assoc. Prof. Radmila Milačič

breda.novotnik@ijs.si

Abstract: Chromium is a common contaminant in the environment. The two most common oxidation states in the environment are Cr(III), which is an essential micronutrient and Cr(VI), which is toxic. Therefore, speciation analysis using enriched stable isotopes is of great importance. In this study, proper preparation of enriched stable isotopic spikes is presented, as well as the influence of oxidizing or reducing agents used in other studies for isotopic spike preparation.

Key words: chromium, speciation studies, preparation of stable isotopic spikes of Cr(VI) in Cr(III) from enriched oxides, FPLC-ICP-MS

1. INTRODUCTION

Chromium is a common contaminant in the environment because of the wide industrial use. Cr(VI) and Cr(III) are the oxidation states usually encountered in the environment. Cr(VI) is carcinogenic, whereas Cr(III) is an essential micronutrient, important in glucose and lipid metabolism. Because of different toxicology, bioavailability and essentiality of chromium, speciation studies are very important. In the past, stable isotopic spikes were prepared by the use of oxidizing and reducing agents such as hydrogen peroxide [1-3], which can, if present as a residue in isotopic spike solution, cause artefacts in speciation studies.

A new protocol for stable isotopic spike preparation is proposed and the influence of residual oxidizing and reducing agents in isotopic spikes is critically evaluated.

2. MATERIALS AND METHODS

2.1 Preparation of enriched stable isotope solutions using hydrochloric acid

Cr(III) stable isotope: Cr oxide was digested in nitric acid with microwave assisted digestion. After the digestion, nitric acid was evaporated and

hydrochloric acid was added. The solution was transferred into a glass tube and diluted with water.

Cr(VI) stable isotope: Cr oxide was melted together with sodium potassium carbonate and sodium hydroxide. To the melt hydrochloric acid was added. The clear solution was transferred into a glass flask and diluted with water.

For separation of Cr(III) and Cr(VI) FPLC Mono Q column coupled to ICP-MS was used.

To study the influence of oxidizing/reducing agents, hydrogen peroxide and ascorbic acid were added to the mixture of ^{53}Cr(III) and ^{50}Cr(VI) at pH 5, pH 7 and pH 12.

3. RESULTS

Speciation of ^{50}Cr(VI)) and ^{53}Cr(III) when prepared with hydrochloric is shown in Figure 1.

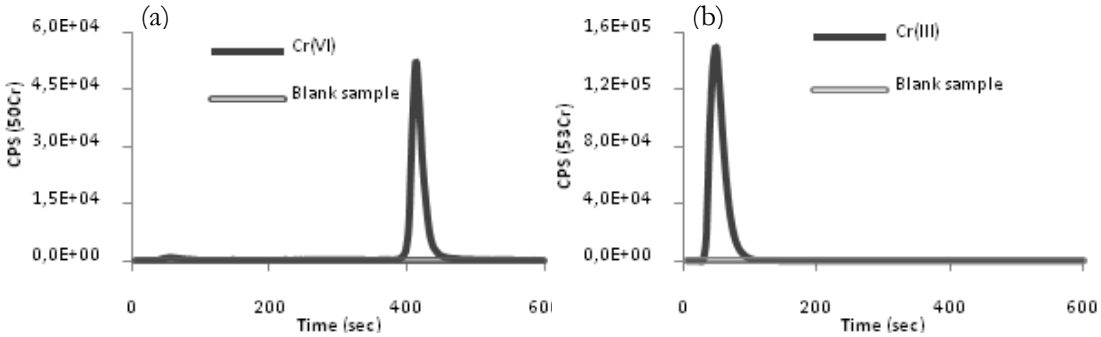

Figure 1: (a) Speciation of ^{50}Cr(VI) (10 ng mL^{-1}, pH 5) and (b) ^{53}Cr(III) (23 ng mL^{-1}, pH 5) by the FPLC-ICP-MS

Data from Figure 1 clearly demonstrate that stable isotopic spike solutions are pure.

In Figure 2 the effect of oxidizing and reducing agents (hydrogen peroxide or ascorbic acid) on double spikes of ^{50}Cr(VI) and ^{53}Cr(III) at pH 5, pH 7 and pH 12 is presented.

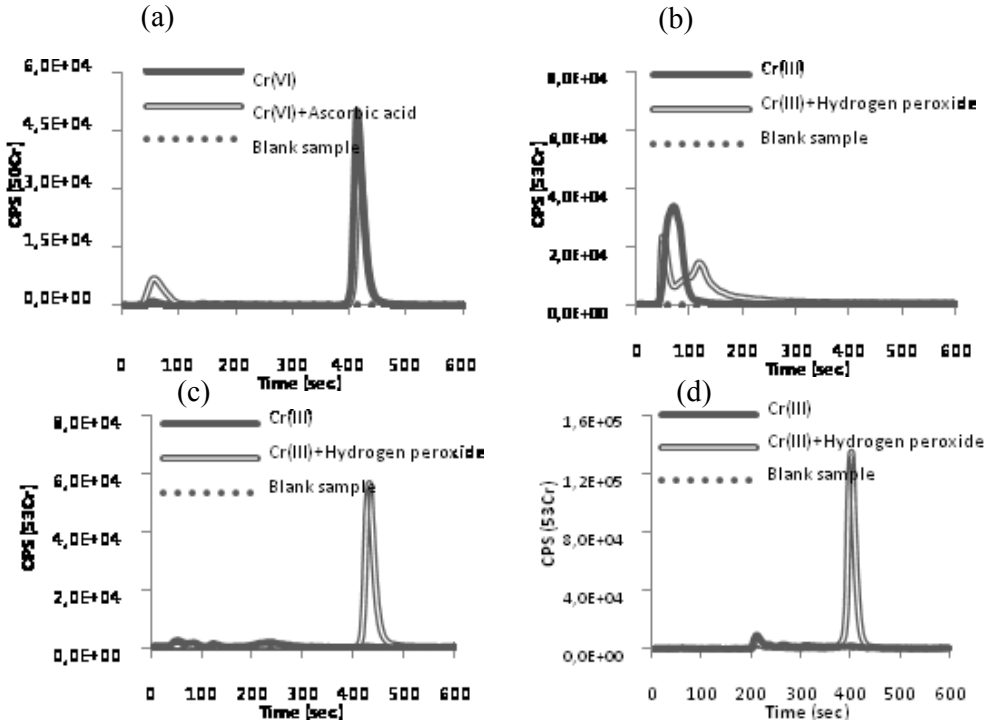

Figure 2: The influence of oxidising and reducing agents on speciation of Cr: (a) at pH 4, ^{50} Cr(VI)+ascorbic acid; (b) at pH 4, ^{53}Cr(III)+H_2O_2; (c) pH 7, ^{53}Cr(III)+H_2O_2; (d) pH 12, ^{53}Cr(III)+H_2O_2

Data from Figure 2 indicate that at pH 4 the presence of ascorbic acid can cause reduction of Cr(VI) (Figure 2a) and the presence of hydrogen peroxide can influence Cr(III) speciation (Figure 2b). Hydrogen peroxide causes moderate oxidation

of Cr(III) at neutral pH (Figure 2c), and complete oxidation at alkaline pH (Figure 2d). The results revealed that, if Cr enriched spiking solutions contain traces of oxidising and/or reducing agents, this could cause artefacts in Cr speciation in samples investigated and that adequate preparation of spiking solutions of Cr stable isotopes is of great importance.

References

1. H.M. Kingston, D. Huo, S. Chalk. Accuracy in species analysis: speciated isotope dilution mass spectrometry (SIDMS) exemplified by the evaluation of chromium species. *Spectrochimica Acta B*, 53: 299- 309, 1998.

2. H.M. Ma and P.A.Tanner. Speciated isotope dilution analysis of Cr(III) and Cr(VI) in water by ICP-DRC-MS. *Talanta*, 77:189-194, 2008.

3. K. Tirez, W. Brusten, A. Cluyts, J. Patyn, N. De Brucker. Determination of hexavalent chromium by species-specific isotope dilution mass spectrometry and ionchromatography—1,5-diphenylcarbazide spectrophotometry. *Journal of Analitical Atomic Spectrometry*, 18:922- 932, 2003.

For wider interest

Chromium is a metal that is present in the environment from antrophogenic and nonantrophogenic sources. Because of the wide industrial use, it is a common contaminant in the environment. Chromium has different properties according to its oxidation state. Cr(VI) is toxic and Cr(III) is an essential micronutrient. Because of these different species properties, speciation studies are necessary where not total chromium, but the concentrations of different oxidation states, are measured. Chromium stable isotopic spikes can be used as tracers of processes in the environment. In the past, these spikes were inadequately prepared, using oxidizing and reducing agents in the procedure. In our study, a protocol was developed for preparation of stable isotopic spikes without any oxidizing and reducing agents. It was experimentally proven that such isotopic solutions are pure and that the use of oxidizing and reducing agents, as reported in previous studies [1-3], can cause artefacts in samples investigated.

Razvoj analiznega postopka za določanje celotnih koncentracij kroma v morski vodi z ICP-MS

Tina Oblak[1], Radmila Milačič[1], Janez Ščančar[1]

[1] Odsek za znanosti o okolju, Inštitut Jožef Stefan, Ljubljana, Slovenija

Radmila.milacic@ijs.si (email of corresponding author)

Povzetek. Razvili smo analizni postopek, ki temelji na odstranitvi matrice morske vode z uporabo kelatno ionsko izmenjalne smole Chelex-100 in določitvi elementov z ICP-MS. Posebno pozornost smo posvetili kromu, ki se v vzorcih površinskih vod nahaja v dveh oksidacijskih stanjih. Trivalentna oblika kroma se veže na Chelex-100 smolo, šestvalentna, ki je prisotna v obliki negativnih anionov, pa se na smolo ne veže. Da bi zagotovili kvantitativno vezavo trivalentnega kroma v morski vodi na izmenjalec, smo vzorec najprej 5 krat redčili. Ker je v morski vodi poleg trivalentnega kroma prisoten tudi šestvalentni, smo vzorcu dodali dvovalentno železo, ki je šestvalentni krom reduciralo, celotni krom v trivalentni obliki pa se je nato vezal na kelatno smolo. Koncentracijo kroma smo določili z ICP-MS. Originalni, enostaven pristop, ki temelji na predhodni redukciji šestvalentnega kroma in redčenju vzorca morske vode pred postopkom ionske izmenjave, omogoča kvantitativno in zanesljivo določitev celotnega kroma v morski vodi z ICP-MS.

Ključne besede: krom, morska voda, Chelex-100, ICP-MS

1 Uvod

Zaradi intenzivne industrializacije in drugih človekovih aktivnosti prihaja do vnosa mnogih onesnaževalcev v okolje. Med zelo pogoste onesnaževalce spadajo kovine in med njimi tudi krom. Kovine se v vzorcih površinskih vod pojavljajo v sledovih, zato je pomembno izbrati tako instrumentalno analizno metodo, ki omogoča merjenje nizkih koncentracij in hkrati zagotavlja ustrezno točnost in natančnost meritev. Ena izmed vodilnih tehnik na tem področju je masna spektrometrija z induktivno sklopljeno plazmo (ICP-MS), ki omogoča hitro in multielementno analizo. Prednost te tehnike merjenja je tudi doseganje zelo nizkih mej zaznave.

Krom se v vzorcih iz okolja nahaja v dveh oksidacijskih stanjih: v trivalentni in šestvalentni obliki. V vodnih okoljih je pri pH < 4 trivalentni krom prisoten pretežno v kationski obliki kot Cr^{3+} koordiniran s šestimi molekulami vode. V istem območju pH je šestvalentni krom prisoten v obliki $Cr_2O_7^{2-}$ aniona. Šestvalentni krom je izredno toksičen, medtem ko je toksičnost trivalentnega kroma bistveno manjša, v nizkih koncentracijah je trivalentni krom esencialen element [1].

Vzorci morske vode imajo matrico z zelo kompleksno sestavo, poleg tega se kovine nahajajo le v sledovih. Zaradi visoke vsebnosti soli je direktno določanje kovin z ICP-MS nezanesljivo. Da bi zagotovili zanesljivo in kvantitativno določitev celotnih koncentracij kroma v morski vodi, smo razvili analizni postopek, ki temelji na odstranitvi matrice z uporabo kelatno ionsko izmenjevalne smole Chelex-100 in določitve elementov z ICP-MS. Posebno pozornost smo namenili kromu, ki ga do sedaj z omenjenim postopkom ni bilo mogoče kvantitativno določiti, saj se v vzorcih vod nahaja v dveh oksidacijskih stanjih. Trivalentna oblika kroma se veže na Chelex-100 smolo, šestvalentna, ki je prisotna v obliki negativnih anionov pa se na smolo ne veže. Chelex-100 namreč specifično veže katione kovin v dvovalentni in trivalentni obliki, razen zemljoalkalijskih, alkalijskih kovin in NH_4^+ ter negativno nabitih anionov, med njimi tudi $Cr_2O_7^{2-}$ in CrO_4^{2-}, ki prehajajo skozi kolono. Specifična vezava kovin na smolo omogoča odstranitev matrice vzorca (glavne sestavine morske vode: Na^+, K^+, Ca^{2+}, Mg^{2+}, Cl^-) in sočasno predkoncentracijo kovin, ki jih določamo.

2 Eksperimentalni del

Kelatno ionsko izmenjevalno smolo Chelex-100 (oblika Na^+) smo pretvorili v NH_4^+ obliko. Tako pripravljeno smolo smo napolnili v 1 mL kolono. Da bi zagotovili kvantitativno vezavo kroma v morski vodi na izmenjalec, smo vzorce najprej 5 krat redčili in nakisali s HNO_3 na pH 2. Ker je v morski vodi poleg trivalentnega kroma prisoten tudi šestvalentni, smo vzorcem dodali dvovalentno železo, ki je šestvalentni krom pri nizkem pH hitro reduciralo (2 uri) do trivalentnega kroma. Nato smo vzorcem dodali 0,2 mol L^{-1} HEPES s katerim smo dvignili na pH 4 ter pri pretoku 0,5 mL min^{-1} nanesli vzorce na kolono. Celotni

krom v trivalentni obliki, vezan na smolo, smo nato sprali z 5 mL 3 mol L^{-1} HNO_3 pri pretoku 0,5 mL min^{-1} in nato še z 5 mL vode pri pretoku 2 mL min^{-1}. Koncentracijo kroma smo določili z ICP-MS.

3 Rezultati in diskusija

Vzporedno z vzorci smo analizirali tudi certificiran referenčni material morske vode CASS-5 (Nearshore seawater for trace metals, National Research Council Canada, Ottawa, Ontario, Canada). Ker je koncentracija kroma v omenjenem referenčnem materialu blizu meje zaznave določitve kroma z ICP-MS, smo v vzorec referenčnega materiala dodali znano koncentracijo šestvalentnega kroma (1 ng mL^{-1}) in izračunali izkoristek med dejansko izmerjeno vrednostjo in teoretično izračunano vrednostjo. S tem smo preverili točnost analiznih postopkov, ki smo jih uporabili pri delu. Rezultate meritev prikazuje Tabela 1.

Tabela 1: Določitev izkoristka med dejansko izmerjeno vrednostjo kroma z ICP-MS in izračunano vrednostjo vsebnosti kroma v referenčnem materialu morske vode CASS-5. Rezultat je podan kot srednja vrednost treh določitev ± standardni odklon.

Element	Izmerjena koncentracija Cr (ng/mL)	Izračunana vrednost koncentracije Cr po dodatku 1 ng mL^{-1} v vzorec (ng/mL)	Izkoristek (%)
Cr	1,15±0,02	1,103±0,012	104

Iz rezultatov v Tabeli 1 je razvidno, da se izmerjena koncentracija kroma dobro ujema z certificirano vrednostjo, kar kaže na točnost analiznega postopka.

Določili smo tudi ponovljivost in obnovljivost analiznega postopka. Za določitev ponovljivosti, smo en realen vzorec morske vode naredili v šestih paralelkah in izmerili z ICP-MS. Z ICP-MS smo dobili dobro ponovljivost analiznega postopka (RSD 2,5 %). Za določitev obnovljivosti analiznega postopka pa smo isti realen vzorec morske vode po istem postopku analizirali čez nekaj dni prav tako v šestih

paralelkah. Tudi obnovljivost analiznega postopka z ICP-MS je bila dobra (RSD je 3,4 %).

Na osnovi razvitega analiznega postopka smo analizirali še štiri realne vzorce morske vode s slovenskega primorja: OOOF, OOOK, OOCZ in OODB2. Ker je koncentracija kroma v vzorcih morske vode blizu meje zaznave, smo v vzorce dodali znano nizko koncentracijo šestvalentnega kroma (1 ng mL^{-1}) in izračunali izkoristek med dejansko koncentracijo kroma v vzorcu in izmerjeno koncentracijo po dodatku 1 ng mL^{-1} kroma v vzorec. Rezultati so pokazali, da se izkoristki gibljejo med 102 % in 103 %, kar kaže na točnost analiznega postopka.

4 Zaključek

Na osnovi rezultatov lahko zaključimo, da enostaven pristop, ki temelji na predhodni redukciji šestvalentnega kroma in redčenju vzorcev morske vode pred postopkom kelatne ionske izmenjave, omogoča kvantitativno in zanesljivo določitev celotnega kroma v morski vodi z ICP-MS. Z večjim volumnom prečrpanega vzorca skozi kolono, lahko vzorec tudi koncentriramo. Poleg kroma lahko v morski vodi kvantitativno določimo tudi druge dvovalentne in trivalentne katione.

Literatura:

[1]S. A. Katz in H. Salem (eds). *The Biologiocal and Environmental Chemistry of Chromium*. VCH Publishers, Inc. New Your, 1994.

Za širši interes

Masna spektrometrija z induktivno sklopljeno plazmo (ICP-MS) je zaradi hitre, multielementne analize in doseganja nizkih mej zaznave ena izmed vodilnih tehnik s področja določanja koncentracij elementov. Elementi se v morski vodi pojavljajo v sledovih. Zaradi visoke vsebnosti soli je njihovo direktno določanje z ICP-MS nezanesljivo.

Razvili smo analizni postopek, ki temelji na odstranitvi matrice morske vode z uporabo kelatno ionsko izmenjalne smole Chelex-100 in določitvi elementov z ICP-MS. Posebno pozornost smo posvetili kromu, ki ga do sedaj z omenjenim postopkom ni bilo mogoče določiti, ker se nahaja v vzorcih vod v dveh oksidacijskih stanjih. Trivalentna oblika kroma se veže na Chelex-100 smolo, šestvalentna, ki je prisotna v obliki negativnih anionov pa se na smolo ne veže. Specifična vezava kovin na smolo omogoča odstranitev matrice vzorca (glavne sestavine morske vode: Na^+, K^+, Ca^{2+}, Mg^{2+}, Cl^-) in sočasno predkoncentracijo kovin, ki jih določamo. Ker je v morski vodi poleg trivalentnega kroma prisoten tudi šestvalentni, smo vzorcu dodali dvovalentno železo, ki je šestvalentni krom reduciralo, celotni krom v trivalentni obliki pa se je nato vezal na kelatno smolo. Razvit analizni postopek smo uspešno uporabili pri analizi celotnih koncentracij kroma v realnih vzorcih morskih vod.

Raziskave uporabnosti porcelanske črepinje pri pripravi glinič nega porcelana C-120

Helena Razpotnik[1,3], Ivan Lavrač[1], Janez Holc[2], Danjela Kuščer[2], mentor Marija Kosec[2]

[1] ETI Elektroelement d.d. Izlake, Slovenija

[2] Odsek za elektronsko keramiko, Inštitut Jožef Stefan, Ljubljana, Slovenija

[3] Mednarodna podiplomska šola Jožefa Stefana (Ekotehnologija, 2.leto)

helena.razpotnik@eti.si

Povzetek. Razvoj novih elektrotehničnih izdelkov ali samo izboljšanje obstoječih pogosto terja od vgrajenih materialov več kot opredeljuje standard. Pri glinič nih porcelanih se pojavljajo predvsem zahteve po višji mehanski trdnosti, enostavnejši izdelavi in ponovni uporabi odpadne porcelanske črepinje. Za izboljšanje mehanskih lastnosti glinič nega porcelana smo uporabili pristope z izboljšanjem mikrostrukture, kot so zmanjšanje količine velikih kremenovih zrn, zmanjšanje aglomeratov korunda ter na drugi strani zmanjšanje večjih področij taline in zmanjšanje skupkov por. V proizvodnji porcelanskih izdelkov nastaja odpad, imenovan porcelanska črepinja, ki ima enako sestavo kot osnovna masa in je kot tak primeren za uporabo v pripravi glinič nih porcelanov. Del surovin smo nadomestili s porcelansko črepinjo in izdelali glinič ni porcelan z ohranjenimi mehanskimi lastnostmi - izmerili smo enake upogibne trdnosti kot pri izboljšanem glinič nem porcelanu.

Keywords: Glinič ni porcelan, tehnološki odpadki, porcelanska črepinja, mehanska trdnost, mikrostruktura

Uvod

Porcelan predstavlja enega najbolj kompleksnih keramičnih materialov v vseh pogledih izdelave, od surovin, priprave, oblikovanja do kompleksnosti mikrostrukture in fazne sestave. Osnovne sestavine materiala za izdelavo porcelanskih izdelkov so naravne surovine. Vsebujejo 50% gline, ki ima vlogo veziva med ostalimi komponentami v surovem stanju, daje porcelanu plastičnost v prisotnosti vode in s tem možnost oblikovanja ter primerno trdnost izdelka po

sušenju, ki omogoča nadaljne delo; 25% talila, ki je nizko taljiva faza in reagira z ostalimi sestavinami ter znižuje temperaturo nastanka tekoče faze v sistemu, ter 25% polnila, ki je precej stabilna faza pri temperaturi sintranja in drži obliko izdelka med žganjem ter zmanjšuje krčenje in deformacijo telesa. Polnilo je lahko kremen ali korund, kjer se zahteva višje mehanske trdnosti. Navedeni deleži surovin so približni, praktične sestave so prilagojene zahtevanim karakteristikam posameznih materialov [1,2].

Elektrotehnični porcelan je silikatni material, ki je glede na karakteristike primeren za uporabo v elektrotehniki. To je material z visoko dielektrično trdnostjo in mehansko trdnostjo, dobro odpornostjo proti koroziji, staranju in kemikalijam, dobrimi izolacijskimi lastnostmi in dobro temperaturno odpornostjo. Pri izdelavi porcelana je ključnega pomena žganje, kjer poteka proces sintranja z zgoščevanjem v prisotnosti tekoče faze. Različni procesi, kot so taljenje, združevanje in rast por, prispevajo k zgoščevanju.. Ostali procesi, ki potekajo med žganjem, so razkroj glinenih mineralov, nastajanje steklaste faze, delno taljenje glinencev in kremena, glede na položaj evtektika, nastanek mulita in njegova rast. Stopnja zgoščevanja in mikrostruktura sta odvisni predvsem od mineraloške sestave surovin in dosežene stopnje ravnotežja. Lastnosti porcelana, kot so gostota, poroznost, mehanska trdnost, električne in termične lastnosti materialov, so odvisne od kemijske in mineraloške sestave, poleg tega pa tudi od razporeditve posameznih faz, njihove velikosti in oblike. Mikrostruktura gliničnega porcelana vključuje korundne ploščice, ki predstavljajo skelet porcelana, področja taline in kremenova zrna, ki izhajajo iz glinenih komponent in glinenca. Vključki zraka predstavljajo pore, ki so lahko različno razporejene, različnih oblik in velikosti.. Porcelan dobi pravo vrednost šele z optimizacijo mikrostrukture [3].

1.1 Reciklaža porcelanske črepinje

Zahteve okoljske zakonodaje povečujejo pritisk na podjetja, da izboljšajo kvaliteto procesov in produktov z vidika ekoloških zahtev. Proizvodnja tehnične keramike se tako sooča z dvema problemoma: naravne surovine so vse dražje ter odpadni material postaja vse večje stroškovno breme. Večja poraba naravnih surovin pomeni nevarnost izčrpanja neobnovljivih virov, v proizvodnji novih izdelkov nastaja vse več odpadkov, ki jih je čedalje težje odstranjevati. [4]

Nekateri odpadki so v osnovni sestavi podobni surovinam, ki se uporabljajo v proizvodnji keramike in vsebujejo ne samo materiale, ki so kompatibilni, pač pa tudi materiale, ki lahko pozitivno vplivajo na proces proizvodnje in karakteristike silikatne keramike celo izboljšajo. Tako odpadki v nekaterih primerih predstavljajo tudi tehnično prednost. [5]

Izboljšanje mehanskih lastnosti gliničnega porcelana s spremembo mikrostrukture ob uporabi porcelanske črepinje

Izhodišče raziskav je bila analiza referenčnega gliničnega porcelana, pri kateri smo pregledali mikrostrukture (SEM, Jeol 5800) in izmerili upogibno trdnost na napravi s tritočkovnim vpetjem (Netzsch 401/3). SEM analiza je pokazala, da je mikrostruktura precej nehomogena, prisotna so večja kremenova zrna, ki merijo do 50 μm in večja področja taline, ki tudi merijo do 50 μm. Obdana so s korundnimi zrni, ki so večkrat aglomerirana. Prisotnih je tudi veliko por, ki so posamezne ali združene v skupke, ki predstavljajo območja, velika tudi do 40 μm (slika 1).

Da bi izboljšali upogibno trdnost gliničnega porcelana, smo raziskave usmerili v izbolšanje homogenosti mikrostrukture in sicer :
- zmanjšanje prisotnosti velikih kremenovih zrn
- odpravo ali zmanjšanje skupkov in aglomeratov korundnih zrn
- zmanjšanje večjih področij taline
- zmanjšanje prisotnosti por, predvsem zmanjšanje skupkov por
- splošno izboljšanje homogenosti mikrostrukture.

Po izpopolnjenem postopku priprave smo izdelali izboljšani glinični porcelan, na katerem smo pri pregledu mikrostrukture ugotovili, da se je homogenost mikrostrukture izboljšala. Prisotna so še področja skupkov por, vendar jih je manj kot pri referenčnem gliničnem porcelanu. Kremenova zrna so manjša, do velikosti 20 μm, večja zrna, ki merijo do 40 μm, so izjeme. Korundna zrna so precej homogeno razporejena, večjih področij talin ni (slika 2).

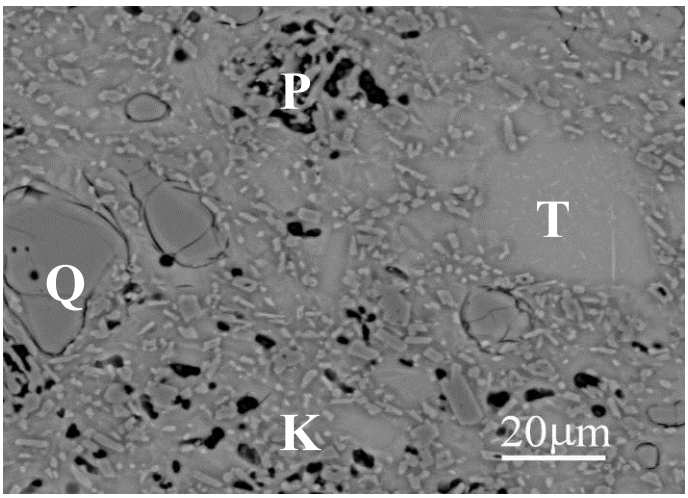

Slika 1 Mikrostruktura referenčnega gliničnega porcelana; Q – kremen, T – talina, K – korund, P - pora

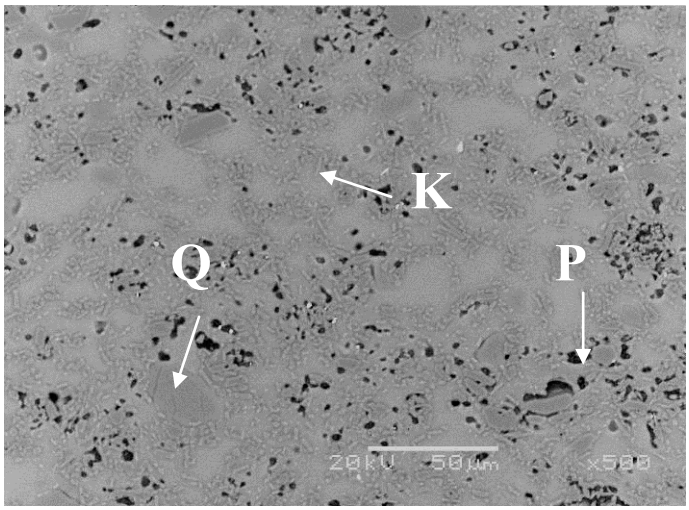

Slika 2 Mikrostruktura izboljšanega gliničnega porcelana ; Q – kremen, T – talina, K – korund, P - pora

Vzorcu izboljšanega gliničnega porcelana smo izmerili upogibno trdnost 133 +/- 7 MPa, kar pomeni glede na referenčni glinični porcelan, kjer smo izmerili upogibno trdnost 112 +/- 5 MPa, 18% zvišanje upogibne trdnosti.

V proizvodnji izdelkov iz gliničnega porcelana nastaja odpad, imenovan porcelanska črepinja, ki ima enako sestavo kot osnovna masa in je kot tak primeren za uporabo v pripravi gliničnih porcelanov. Del surovin smo nadomestili s porcelansko črepinjo, ki smo jo dodali v različnih deležih od 8 ut.% do 32 ut.%. Glinični porcelan z dodatkom porcelanske črepinje smo izdelali po originalno optimiziranem postopku.

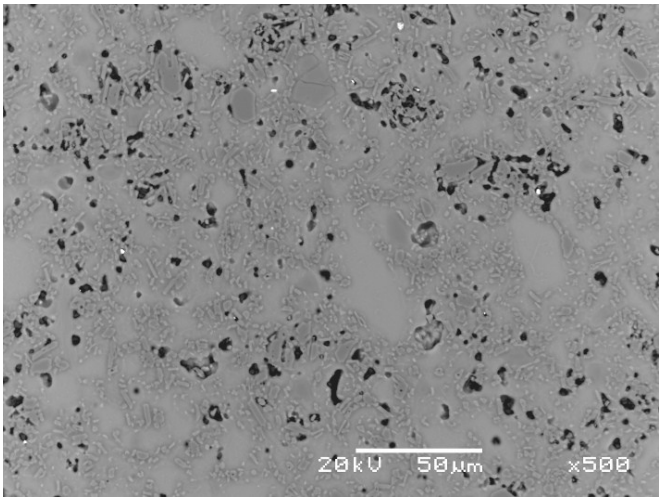

Slika 3 Mikrostruktura izboljšanega gliničnega porcelana z dodatkom 24 ut.% porcelanske črepinje.

Pri gliničnem porcelanu z različnimi količinami dodatka porcelanske črepinje se je upogibna trdnost le malo spreminjala. Pri gliničnem porcelanu brez porcelanske črepinje je bila upogibna trdnost 130 +/- 7 MPa, pri dodatku 8 ut.% porcelanske črepinje je bila 131 +/-5 MPa, pri 32 ut.% pa je bila 132 +/- 3 MPa. Mikrostruktura gliničnega porcelana z dodatkom porcelanske črepinje (slika 3) je primerljiva z mikrostrukturo izboljšanega gliničnega porcelana brez dodatka porcelanske črepinje (slika 2).

Izdelali smo glinični porcelan z dodatkom porcelanske črepinje z izboljšanimi mehanskimi lastnostmi, ki so posledica bolj homogene mikrostrukture. Z dodatkom porcelanske črepinje v območju od 8 do 32 ut.% se upogibna trdnost ni spremenila.

Literatura:

[1] J. Carty, M.; Senapati, W. U. Porcelan-Raw Materials, Processing, Phase Evolution, and Mechanical Behavior. *J.American Society*, 81 (1), 3-20

[2] Chiang, Y. M.; Birnie, D. P. III; Kingery, W. D. Physical ceramics, J. Wiley & Sons, New York, 522 p. (1997)

[3] Oberžan, M. High-alumina porcelain with improved mechanical and thermal properties, *Doctoral dissertation* (2009)

[4] Segadaes, A. M. Use of phase diagrams to guide ceramic production from wasts. *Advances in Applied Ceramics,* 105 (1) (2006)

[5] Hendrickson, C.; Horvath, A.; Joshi, S.; Lave, L. Economic Input-Output Models for Environmental Life-Cycle Assesment. *Env. Sci.&Tech. Policy Analysis,* 32, (7) (1998)

[6] Fassbinder, G. A new ceramic body concept for high strength high voltage insulators. *Journal of German Ceramic Society,* 79 (8) (2002)

Za širši interes

Novi elektrotehnični izdelki so podvrženi vse večjim obremenitvam, kar zahteva uporabo materialov z nadstandardnimi karakteristikami. Pri gliničnih porcelanih se pojavljajo predvsem zahteve po višji mehanski trdnosti, enostavnejši izdelavi in ponovni uporabi odpadnega žganega porcelana, tj. porcelanske črepinje.

Po natančni analizi mikrostrukture obstoječega gliničnega porcelana smo sklepali, da mehansko trdnost lahko izboljšamo z izboljšanjem homogenosti mikrostrukture. S spremenjeno pripravo smo izdelali glinični porcelan z izboljšano homogenostjo mikrostrukture. Mehanska trdnost gliničnega porcelana se je izboljšala. Izmerili smo 18% višjo upogibno trdnost kot pri referenčnem gliničnem porcelanu.

V proizvodnji porcelanskih izdelkov nastaja odpadek, ki izvira iz tehnološke obdelave. Odpadni žgani porcelan – porcelanska črepinja ima enako sestavo kot osnovna masa in je kot tak primeren za ponovno uporabo. Del surovin smo nadomestili s porcelansko črepinjo in izdelali glinični porcelan z ohranjenimi mehanskimi lasnostmi - izmerili smo enake upogibne trdnosti kot pri izboljšanem gliničnem porcelanu.

Poly[perfluorotitanate(IV)] Compounds. Synthesis, Characterization, Application

Igor Shlyapnikov[1,2], **Evgeny Goreshnik**[1], **Zoran Mazej**[1],

[1] Department of Inorganic Chemistry and Technology (K1), Jožef Stefan Institute, Ljubljana, Slovenia

[2] Jožef Stefan International Postgraduate School, Ljubljana, Slovenia

igor.shlyapnikov@yandex.ru

Supervisor : dr. Zoran Mazej

Abstract. Complex poly[perfluorotitanate(IV)] compounds attract much interest due to their stereoselective catalytic activity in organic synthesis and in reactions of olefin polymerisation. Unfortunately, the most effective application method of poly[perfluorotitanates] can't be achieved, because big gap in chemistry of these compounds exist: from the great variety of theoretically possible compounds with $[Ti_xF_{4x+y}]^{y-}$ (x,y ≥ 1) anions only few of them were synthesised. They are compounds including the following anions: $([TiF_5]^-)_n$, $[TiF_6]^{2-}$, $([Ti_2F_9]^-)_n$, $[Ti_2F_{10}]^{2-}$, $[Ti_2F_{11}]^{3-}$, $[Ti_4F_{18}]^{2-}$, $[Ti_4F_{19}]^{3-}$, $([Ti_7F_{30}]^{2-})_n$ and $([Ti_8F_{33}]^-)_n$. Moreover, no clear theoretical explanations of forces, leading to formation of different anions, exist.

The main challenges of this work are the synthesis of new phases with various poly[perfluorotitanate(IV)] anions and determination of their crystal structure by different physical methods of investigations, such as X-ray diffraction analysis (XRD), vibrational spectroscopy, etc. An attempt to give a theoretical explanation for the formation of different polyanions will be done.

Keywords: poly[perfluorotitanate(IV)] compounds, crystal structure, vibrational spectroscopy

1 Poly[perfluorotitanate(IV)] compounds

A great variety of poly[perfluorotitanate(IV)] compounds with octahedral coordination of titanium atom can theoretically exist. Some of such hypothetical fluorotitanate anions are presented in Table 1. Only compounds with the following anions (marked bold in Table 1): $([TiF_5]^-)_n$, $[TiF_6]^{2-}$, $([Ti_2F_9]^-)_n$, $[Ti_2F_{10}]^{2-}$, $[Ti_2F_{11}]^{3-}$, $[Ti_4F_{18}]^{2-}$, $[Ti_4F_{19}]^{3-}$, $([Ti_7F_{30}]^{2-})_n$ and $([Ti_8F_{33}]^-)_n$ were structurally characterised.

Table 1: Some hypothetical poly[perfluorotitanate(IV)] anions

$[TiF_5]^-$	**$[TiF_6]^{2-}$**		
$([TiF_5]^-)_n$	$([TiF_6]^{2-})_n$	$([TiF_7]^{3-})_n$	
$[Ti_2F_9]^-$	**$[Ti_2F_{10}]^{2-}$**	**$[Ti_2F_{11}]^{3-}$**	
$([Ti_2F_9]^-)_n$	$([Ti_2F_{10}]^{2-})_n$	$([Ti_2F_{11}]^{3-})_n$	
$[Ti_3F_{13}]^-$	$[Ti_3F_{14}]^{2-}$	$[Ti_3F_{15}]^{3-}$	$[Ti_3F_{16}]^{4-}$
$([Ti_3F_{13}]^-)_n$	$([Ti_3F_{14}]^{2-})_n$	$([Ti_3F_{15}]^{3-})_n$	$([Ti_3F_{16}]^{4-})_n$
$[Ti_4F_{17}]^-$	**$[Ti_4F_{18}]^{2-}$**	**$[Ti_4F_{19}]^{3-}$**	$[Ti_4F_{20}]^{4-}$
$([Ti_4F_{17}]^-)_n$	$([Ti_4F_{18}]^{2-})_n$	$([Ti_4F_{19}]^{3-})_n$	$([Ti_4F_{20}]^{4-})_n$
$[Ti_5F_{21}]^-$	$[Ti_5F_{22}]^{2-}$	$[Ti_5F_{23}]^{3-}$	$[Ti_5F_{24}]^{4-}$
$([Ti_5F_{21}]^-)_n$	$([Ti_5F_{22}]^{2-})_n$	$([Ti_5F_{23}]^{3-})_n$	$([Ti_5F_{24}]^{4-})_n$
$[Ti_6F_{25}]^-$	$[Ti_6F_{26}]^{2-}$	$[Ti_6F_{27}]^{3-}$	$[Ti_6F_{28}]^{4-}$
$([Ti_6F_{25}]^-)_n$	$([Ti_6F_{26}]^{2-})_n$	$([Ti_6F_{27}]^{3-})_n$	$([Ti_6F_{28}]^{4-})_n$
$[Ti_7F_{29}]^-$	$[Ti_7F_{30}]^{2-}$	$[Ti_7F_{31}]^{3-}$	$[Ti_7F_{32}]^{4-}$
$([Ti_7F_{29}]^-)_n$	**$([Ti_7F_{30}]^{2-})_n$**	$([Ti_7F_{31}]^{3-})_n$	$([Ti_7F_{32}]^{4})_n$
$[Ti_8F_{33}]^-$	$[Ti_8F_{34}]^{2-}$	$[Ti_8F_{35}]^{3-}$	$[Ti_8F_{36}]^{4-}$
$([Ti_8F_{33}]^-)_n$	$([Ti_8F_{34}]^{2-})_n$	$([Ti_8F_{35}]^{3-})_n$	$([Ti_8F_{36}]^{4-})_n$

In all perfluorotitanates Ti^{4+} ions are in an octahedral coordination of six F atoms, and polymeric ions are formed by sharing one or two fluorine atoms between two octahedra (shared apexes or edges – one or two bridging fluorine atoms, respectively). Sharing of three fluorine atoms is also possible (two octahedra share face – three bridging fluorine atoms), but crystal structures of those anions haven't been reported yet. In the solid state polyanions are found as discrete species, chains, double chains, columns or layers. Structures of known poly[perfluorotitanate(IV)] anions are presented in Figure 1.

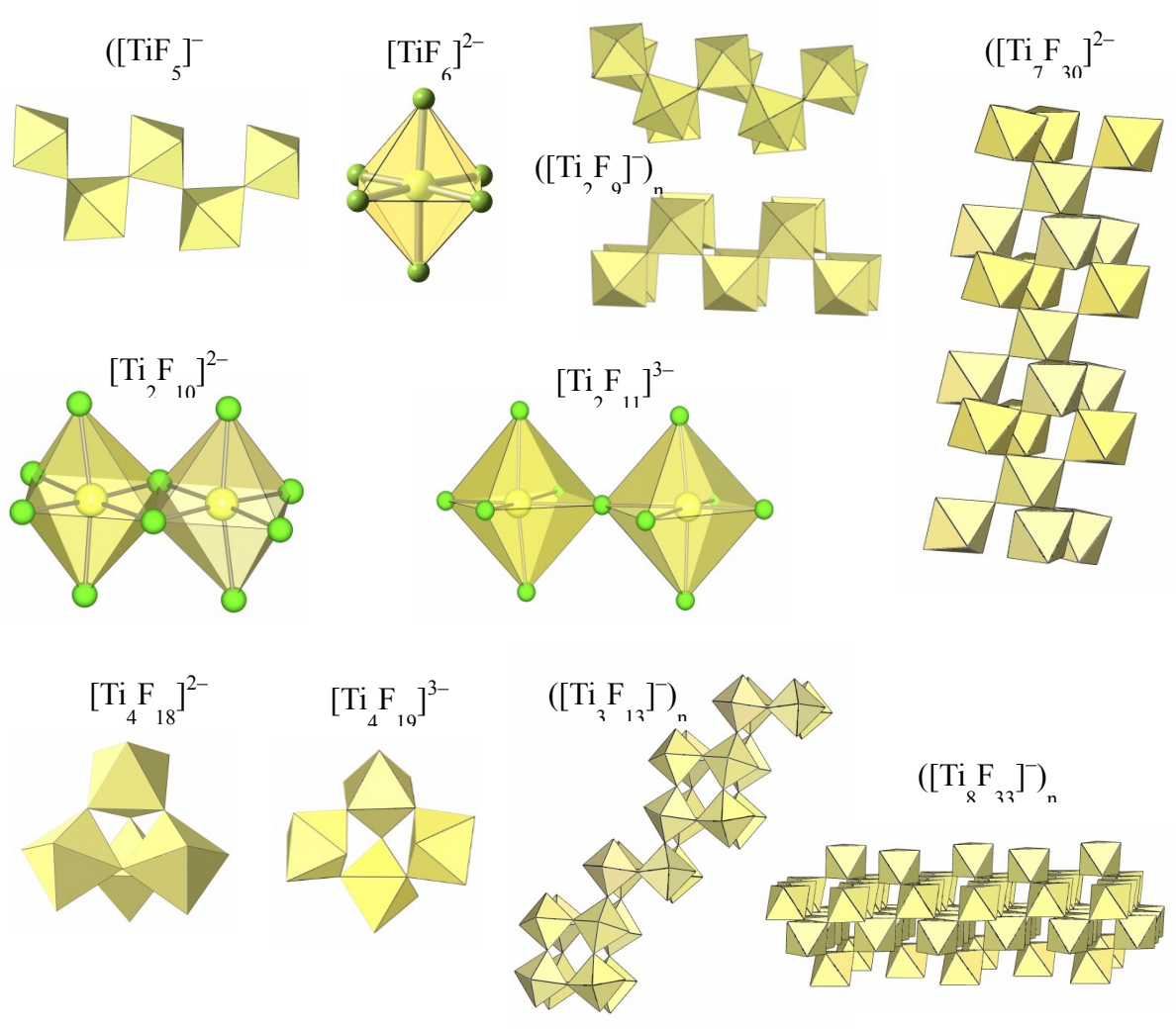

Figure 1: The known poly[perfluorotitanate(IV)] anions

Only one attempt to answer the question, why do different polyanions form in different systems, was made [1]. A reaction of dimerization

$$2[\text{cation}]^+[Ti_2F_9]^- \rightarrow [\text{cation}]^{2+}[Ti_4F_{18}]^{2-} \quad (1)$$

was considered by means of theoretical calculations, applying "volume-based" thermodynamic approach (VBT). On the basis of estimated ΔH^{298} and ΔG^{298} values of reaction 1 it was proposed, that monocations generally favour the formation of $[\text{cation}]^+[Ti_2F_9]$ (since $\Delta_{r1}H^{298}$ ($\approx\Delta_{r1}G^{298}$) is usually > 0), whereas dications favour $[\text{cation}]^{2+}[Ti_4F_{18}]$ (since $\Delta_{r1}H^{298}$ ($\approx\Delta_{r1}G^{298}$) < 0 and almost independent of the size of cation). It was also shown that the increase in the size of monocations favours the formation of $[Ti_2F_9]^-$ against $[Ti_4F_{18}]^{2-}$ ions, but small monocations with volume less than 0,019 nm^3 favour $[Ti_4F_{18}]^{2-}$ ions. Thus it is stated that previously reported compounds $[NF_4][Ti_2F_9]$ and $Cs[Ti_2F_9]$ [2] probably contain $[Ti_2F_9]^-$ anions, but

their presence was proved only by vibrational spectroscopy [2] and ^{19}F NMR spectroscopy [3].

Later it was shown that the assumption that only the size of cations influences the formation of $[Ti_2F_9]^-$ or $[Ti_4F_{18}]^{2-}$ anions was too simplified [4]. Reactions between TiF_4 and AF compounds with single-charged cations A^+ of various sizes in anhydrous HF were examined and crystal structures of obtained phases were determined. Finally, it was discovered that cations lager than Cs^+ (V = 0,01882 nm^3) always favour the formation of compounds with $[Ti_4F_{18}]^{2-}$ anions. The crystal structure determination of the product between CsF and $2TiF_4$ proved that the obtained product could be defined as $CsTi_2F_9$. However, instead of discrete $[Ti_2F_9]^-$ anions, polymeric anions $([Ti_2F_9]^-)_n$ consisting of infinite double chains are formed. Similar chains are also formed in the case of $H_3O[Ti_2F_9]$. It is assumed, that discrete anions $[Ti_2F_9]^-$ exist in aHF solution, but after removing the solvent it is energetically preferable that anions polymerize forming infinite double chains. On the other hand, dimeric anion $[Ti_4F_{18}]^{2-}$ is preferable in case of large cations because of better packing.

2 Synthesis of poly[perfluorotitanate(IV)] compounds

A main synthetic method for the preparation of new poly[perfluorotitanate(IV)] compounds is carrying out reactions between titanium tetrafluoride TiF_4 and various compounds acting as cations in anhydrous HF. Reaction vessels (length: 250 – 300 mm; i.d.: 15,5 mm; o.d.: 18,75 mm) made from tetrafluoroethylen-hexafluoropropylen (FEP; Polytetra GmbH, Mönchengladbach, Germany), sealed from the one side and equipped with Teflon valves from the other side, were used. All manipulations with volatile materials, such as aHF and F_2, are carried out in nickel-Teflon vacuum line and with non-volatile, such as TiF_4 – in a drybox (M. Braun) in an argon atmosphere.

The usual procedure for the synthesis is described in Figure 2. Isolated compounds are characterised by Raman spectroscopy (powder is sealed in a glass capillary to prevent reaction with moisture). Then, the obtained powder is recrystallized from aHF-solution in special doubled T-shaped reactor, consisting from two FEP tubes

with different diameter (18,75 and 6 mm). Solution from the wide arm of the reactor is decanted into the narrower arm and a temperature gradient is maintained. Obtained crystals are transferred in the dry box and then immersed into perfluorinated oil (perfluorodecalin) in order to prevent reaction with moisture and oxygen from the air outside the dry box.

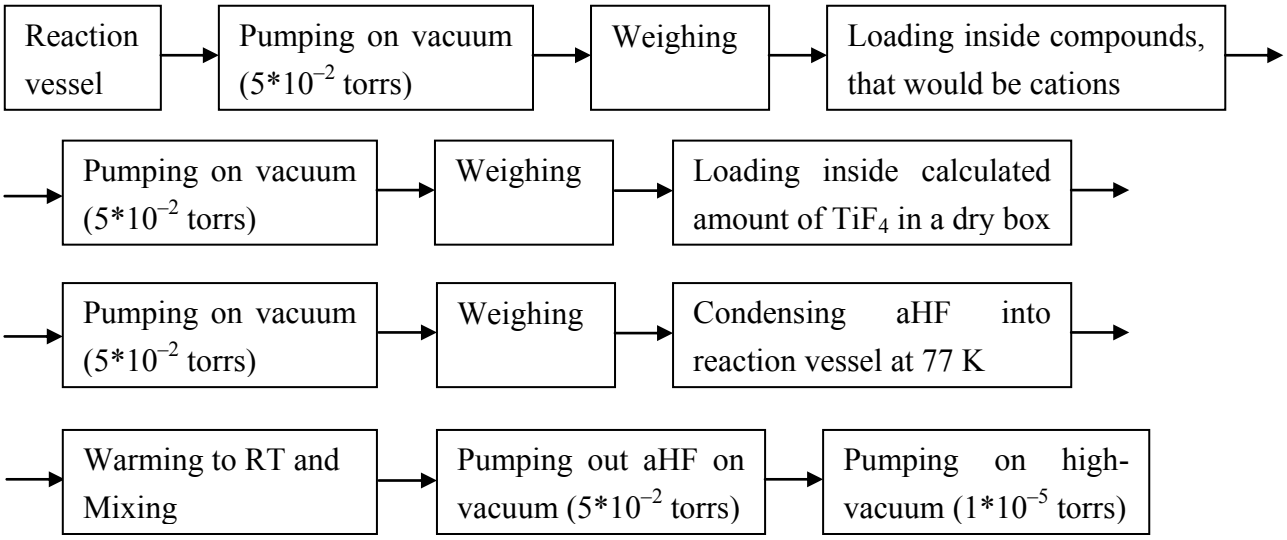

Figure 2: The usual procedure of the synthesis

3 Characterisation of poly[perfluorotitanate(IV)] compounds

The composition of the compound in solution and in the solid state could be different. The most reliable way to determine what kind of poly[perfluorotitanate(IV)] anions are presented in the isolated solids is to grow single crystals and to determine crystal structures using X-ray diffraction analysis. The main disadvantage of X-ray diffraction is that it is sometimes time-consuming and that it requires high professional skills.

Vibrational spectroscopy is a good fingerprint for identification of different poly[perfluorotitanate(IV)] compounds in the solid state. Many of fluorotitanate anions have different resolved vibration energies in the 600 – 800 cm^{-1} range. Mixtures of different phases could be easily detected.

The presence of $[Ti_xF_{4x+y}]^{y-}$ anions in different solutions (except aHF solutions) was confirmed only by ^{19}F NMR spectroscopy.

References:

[1]A. Decken, H. D. B. Jenkins, C. Knapp, G.B. Nikiforov, J. Passmore, J.M. Rautiainen. The autoionization of [TiF_4] by cation complexation with [15]crown-5 to give [TiF_2([15]crown-5)][Ti_4F_{18}] containing the tetrahedral [Ti_4F_{18}]$^{2-}$ ion. *Angew. Chem., Int. Ed.*, 44:7958-7961, 2005

[2]K.O. Christe, C.J. Schack. Synthesis and characterization of $(NF_4)_2TiF_6$ and of higher NF_4^+ and Cs^+ Poly(perfluorotitanate(IV)) salts. *Inorg. Chem.*, 16(2):353-359, 1977

[3]P.A.W. Dean. A^{19}F nuclear magnetic resonance study of polymeric fluoroanions of tin(IV) and titanium(IV). *Can. J. Chem.,* 51:4024-4030, 1973

[4]Z. Mazej, E. Goreshnik. Poly[perfluorotitanate(IV)] salts of $[H_3O]^+$, Cs^+, $[Me_4N]^+$ and $[Ph_4P]^+$ and about the existence of an isolated $[Ti_2F_9]^-$ anion in the solid state. *Inorg. Chem.*, 48:6918-6923, 2009

For wider interest

Fluorine and its compounds are strongly associated with high energies and very important properties: chemical stability and high reactivity, resistance to high-temperatures and decomposition with release of fluorine. Thus they could be successfully applied in various branches of science, technology and everyday life. For example, highly chemically inert material Teflon and highly reactive fluorinating agent MnF_4.

Nowadays, it became clear, that all industrial processes should be not only economically benefit, but also environmentally friendly. So, it is necessary to think about possibilities to increase yields of final products and to decrease amounts of by-products. For solving both, economic and environmental, problems applying and development of catalysts are the most promising ways.

This work is devoted to poly[perfluorotitanate(IV)] compounds, that contain poly[perfluorotitanate(IV)] anions with different structures. These substances are promising catalysts due to their selectivity to various processes that can take place in different industrial productions (pharmaceutical, waste treatment, etc).

Odstranjevanje ostankov zdravilnih učinkovin v pilotnih bioreaktorjih

Mojca Zupanc[1,2], Tina Kosjek[1], Boris Kompare[3], Željko Blažeka[4], Ester Heath[1,2] (MENTOR)

[1] Odsek za znanosti o okolju, Institut Jožef Stefan, Ljubljana, Slovenija

[2] Mednarodna podiplomska šola Jožefa Stefana, Ljubljana, Slovenija

[3]Fakulteta za gradbeništvo in geodezijo, Univerza v Ljubljani, Ljubljana, Slovenija

[4]Institut za ekološki inženiring d.o.o., Maribor, Slovenija

mojca.zupanc@ijs.si

Ostanki zdravilnih učinkovin so v okolju prisotni že od pričetka njihove uporabe, vendar se njihove potencialne nevarnosti zavedamo šele v zadnjem desetletju. Zdravilne učinkovine pridejo v okolje s humano in veterinarsko uporabo. Nizke koncentracije, v katerih se nahajajo v okolju (od ng L^{-1} do µg L^{-1}), lahko predstavljajo nevarnost za različne ekosisteme, predvsem pri kronični izpostavljenosti. V naši raziskavi smo preučevali odstranitev šestih zdravilnih učinkovin (diklofenak, naproksen, ketoprofen, ibuprofen, karbamazepin in klofibrinska kislina) z aktivnim blatom v pilotnih bioreaktorjih. Dokazali smo, da je odstranitev ibuprofena, ketoprofena in naproksena zadovoljiva (do 85%), medtem ko je razgradnja diklofenaka, karbamazepina in klofibrinske kisline nižja in nestabilna. Za zvišanje odstotka odstranitve izbranih spojin bomo biološke pilotne reaktorje sklopili z dodatnimi postopki čiščenja (UV, kavitacija, ozonacija in adsorpcija na aktivno oglje).

Ključne besede: Zdravilne učinkovine, diklofenak, naproksen, ketoprofen, ibuprofen, karbamazepin, klofibrinska kislina, pilotni bioreaktorji, odstranjevanje

1 Uvod

Ostanki zdravilnih učinkovin v okolju so šele v zadnjem desetletju pritegnili pozornost znanstvenikov in število raziskav o njihovem kroženju v okolju strmo

narašča [1], [2], [3]. Zdravilne učinkovine so po naravi farmakološko aktivne substance, katerih vpliv na ekosisteme je razmeroma nepreučen. Njihov glavni vir v okolju so (komunalne) odpadne vode, katerih izpusti, tudi po postopkih čiščenja, še vedno vsebujejo ostanke teh spojin. Zaradi kronične izpostavljenosti okoljskih organizmov in človeka lahko, kljub nizki okoljski koncentraciji (ng - μg L^{-1}), pričakujemo dolgodobne učinke, možno pa je tudi sinergistično delovanje [4].
Glavni cilji naše raziskave so na laboratorijskem nivoju poiskati uspešno kombinacijo biološkega in abiotskega (fotorazgradnja, ozonacija, kavitacija,…) čiščenja, ki bo zagotovila odstranitev izbranih spojin v čim večji meri. V okviru te predstavitve bomo prikazali rezultate odstranitve izbranih spojin biološkega čiščenja v pilotnih bioreaktorjih. V vzorcih vtokov in iztokov bioreaktorjev smo, poleg vsebnosti šestih zdravilnih učinkovin (diklofenak, naproksen, ketoprofen, ibuprofen, karbamazepin in klofibrinska kislina), merili tudi spremljajoče parametre (koncentracijo kisika, biomase, KPK-ja, nitratov, nitritov ter amonija), ki lahko vplivajo na postopke čiščenja odpadnih.

2 Pilotni bioreaktorji

Biološko razgradnjo izbranih zdravilnih učinkovin spremljamo v dveh paralelnih pilotnih bioreaktorjih (R1 in R2), v katere kontinuirano dodajamo hranilni medij in izbrane zdravilne učinkovine. Dnevno v vsak bioreaktor dodajamo sveže raztopljene hranilne snovi in zdravilne učinkovine. Hranilni medij je sestavljen tako, da združbi mikroorganizmov v bioreaktorju zagotavlja vse makro- in mikronutriente, ki jih potrebujejo za rast in razmnoževanje, zdravilne učinkovine pa dodajamo v okoljsko relevantnih koncentracijah (1 μg L^{-1}). Delovni volumen posameznega bioreaktorja je 4 L, vsak bioreaktor je razdeljen na tri predelke (Slika 1). V levi stranski predelek črpamo hranilni medij, iz katerega suspenzija tekočine in biomase preide v srednji predelek, ki ga prepihujemo s kisikom. S tem posnemamo delovanje aeracijskih bazenov v čistilnih napravah in zagotavljamo koncentracijo kisika nad 2 mg L^{-1}. Iz srednjega predelka suspenzija potuje v desni predelek, ki služi kot sekundarni usedalnik za biomaso. Iz njega z membranskimi črpalkami posedeno biomaso vračamo v prvi predelek, odvečna biomasa pa reaktor zapusti z odtokom. Zadrževalni čas spojin v bioreaktorju je 48 ur.

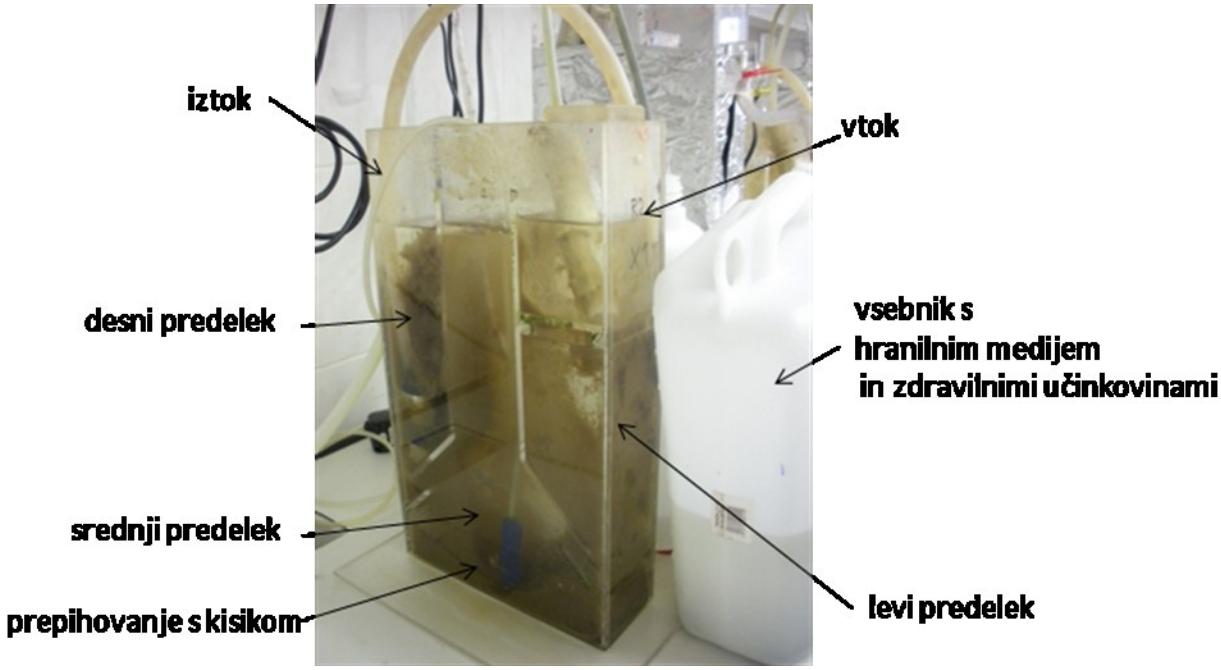

Slika 1: Pilotni bioreaktor

3 Kemijska analiza

Za določanje uspešnosti delovanja bioreaktorjev določamo vsebnost zdravilnih učinkovin v njihovih vtokih in iztokih in iz razlike določimo uspešnost njihove odstranitve. Pred analizo vzorce filtriramo, da odstranimo suspendirane delce. 200 mL filtriranega vzorca nakisamo na pH=2-3 ter dodamo interni standard. Vzorce nato ekstrahiramo na trdnem nosilcu (SPE). Ekstrakciji sledi elucija z etilacetatom. Po eluciji vzorce analiziramo s plinskim kromatografom sklopljenim z masno spektrometričnim detektorjem (GC-MS) in tako določimo vsebnost posameznih zdravilnih učinkovin v vtoku in iztoku obeh bioreaktorjev.

4 Rezultati in diskusija

Rezultati kemijske analize (Slika 2) kažejo povprečno 85%±9% odstranitev ibuprofena, 77%±10% odstranitev ketoprofena in 74%±7% odstranitev naproksena v obeh pilotnih bioreaktorjih. Meritve odstranitve karbamazepina, klofibrinske kisline in diklofenaka kažejo velika nihanja v rezultatih ter nižjo stopnjo odstranitve, kar je v skladu s strokovno literaturo. Slabša odstranitev izbranih spojin v prvih treh tednih vzorčenja kaže na to, da je združba

mikroorganizmov potrebovala čas, da se je na nove pogoje adaptirala (rezultati niso prikazani in zajeti v izračunih). Odstranitev zdravilnih učinkovin, s poudarkom na zvišanju odstranitve karbamazepina, klofibrinske kisline in diklofenaka, bomo v prihodnje poskusili povečati s sklopitvijo bioreaktorjev z novejšimi postopki čiščenja (UV, ozonacija in kavitacija).

Poleg odstranitve zdravilnih učinkovin smo v pilotnih bioreaktorjih merili tudi parametre, ki vplivajo na delovanje bioreaktorjev, kot npr. biomasa, kemijska potreba po kisiku, temperatura in koncentracija kisika. Rezultati so pokazali povprečno vsebnost biomase v R1 5,8 g L^{-1} in v R2 7,5 g L^{-1}. V stranskih prekatih reaktorja R2 smo določili nižjo vsebnost kisika (pod 2 mg L^{-1}), kar že omogoča rast anoksičnih mikroorganizmov. Ker je bila razgradnja naproksena, diklofenaka in karbamazepina v tem reaktorju višja, predvidevamo, da bi lahko anoksični mikroorganizmi v tem predelku bioreaktorja prispevali k višjemu odstotku odstranitve teh dveh spojin. Meritve amonija so pokazale, da se vsebnost amonija v R1 zniža iz 107 mg L^{-1} (vtok) na 5 mg L^{-1} (iztok), v R2 pa iz 106 mg L^{-1} (vtok) na 23 mg L^{-1} (iztok) . Ustrezno se povečata vsebnosti nitratov (R1: 8 - 71 mg L^{-1}, R2: 10 - 60 mg L^{-1}) in nitritov (R1: 0,5 - 2 mg L^{-1}; R2: 0,4 - 5 mg L^{-1}), kar potrjuje, da je potekal proces nitrifikacije.

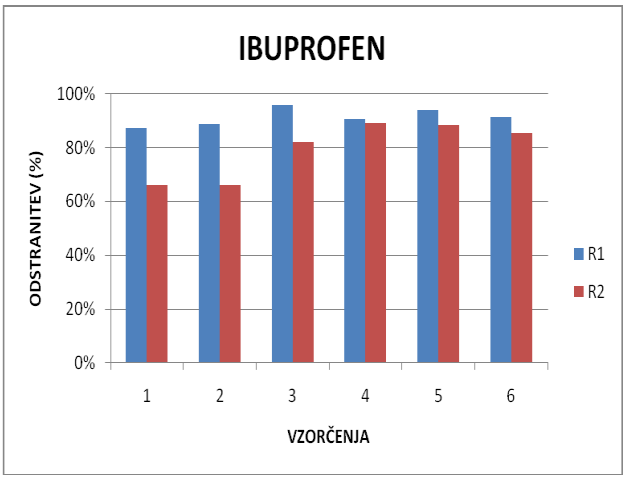

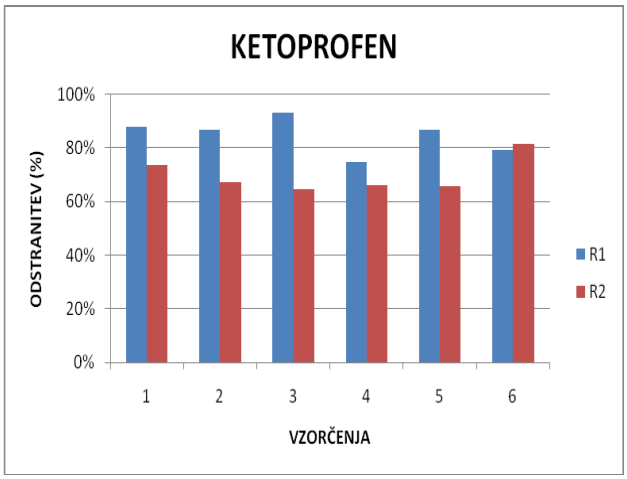

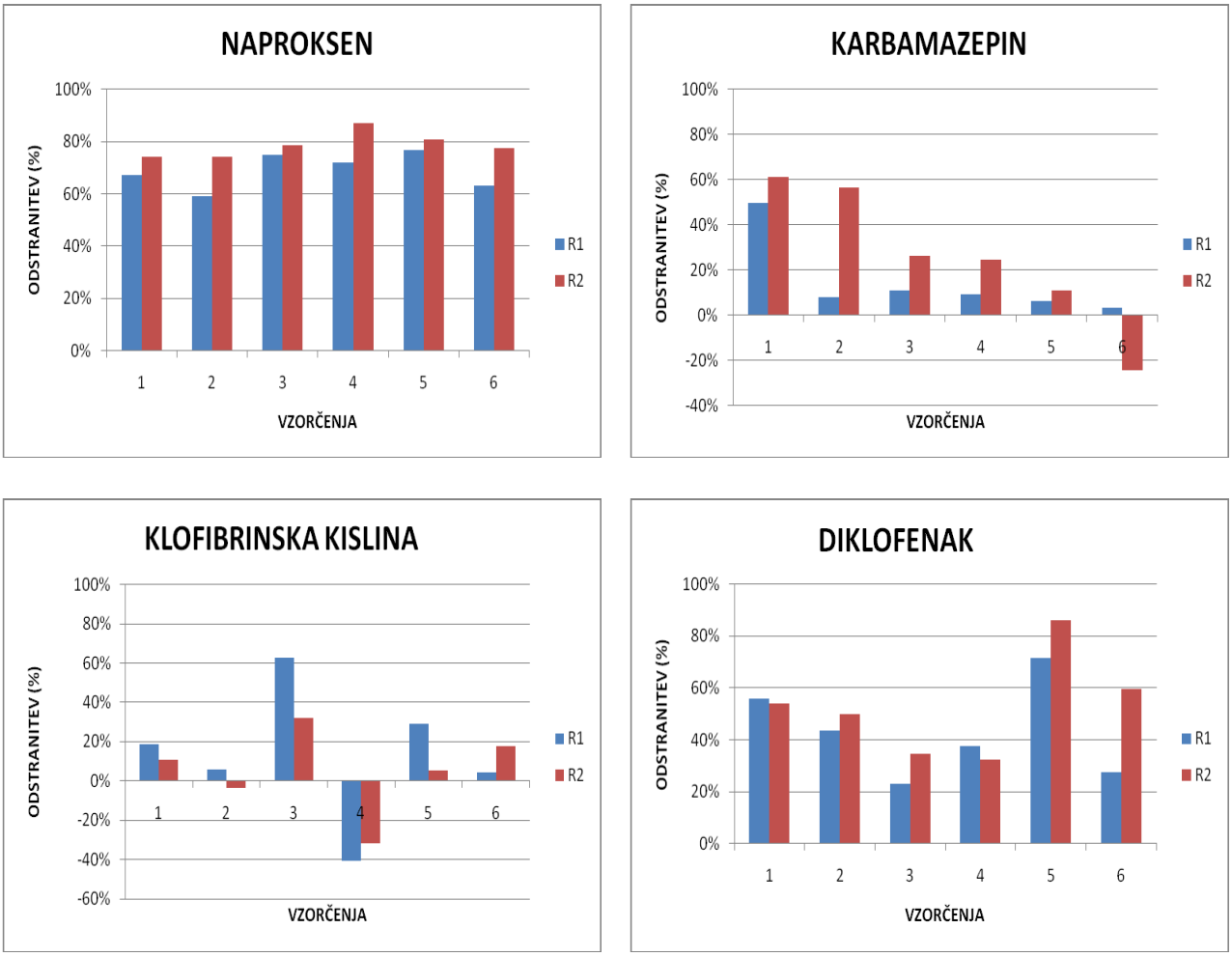

Slika 2: Rezultati odstranitve (%) izbranih zdravilnih učinkovin v pilotnih bioreaktorjih

(datumi vzorčenja: **1**=11.11.2010, **2**=25.11.2010, **3**=16.12.2010, **4**=20.1.2011, **5**=3.2.2011, **6**=24.3.2011)

5 Literatura

[1] Ternes T.A., Giger W., Joss A. Introduction. *In: Human Pharmaceuticals, Hormones and Fragrances: The challenge of micropollutants in urban water management*. Ternes T.A., Joss A., 2006

[2] Farre M., Perez S., Kantiani L., Barcelo D. Fate and toxicity of emerging pollutants, their metabolites and transformation products in the aquatic environment. *Trends in Analytical Chemistry*, 27 : 991-1007, 2008

[3] Kot-Wasik A., Debska J., Namiesnik J. Analytical techniques in studies of the environmental fate of pharmaceuticals and personal-care products. *Trends in Analytical Chemistry*, 26 : 557-568, 2007

[4] Halling-Sørensen B., Nors Nielsen S., Lanzky P.F:, Ingerslev F., Holten Lützhøft, Jørgensen.. Occurence, Fate and Effects of Pharmaceutical Substances in the Environment – A Review. *Chemosphere*, 36 : 357-393, 1998

Za širši interes

V Skupini za organsko analizo Odseka za znanosti o okolju se ukvarjamo s preučevanjem kroženja organskih onesnažil v okoljskih vzorcih. V zadnjem času namenjamo večjo pozornost ostankom zdravilnih učinkovin, kot so nesteroidni antirevmatiki (NSAID), estrogeni, antidepresivi, pomirjevala in citostatiki. Naše raziskovanje se običajno prične s preučevanjem odstranitve zdravilnih učinkovin v pilotnih bioreaktorjih, ki smo jih pognali pred petimi leti z aktivnim blatom iz Centralne čistilne naprave Domžale - Kamnik. Odstranitev zdravilnih učinkovin določamo z razliko njihove vsebnosti na vtoku in iztoku iz bioreaktorjev. V naše raziskave vključujemo vedno nove zdravilne učinkovine, ki zahtevajo vpeljavo in optimizacijo novih analiznih postopkov za njihovo določitev. Poleg izhodnih zdravilnih učinkovin sledimo tudi nastanku stabilnih razgradnih produktov. Cilj naših raziskav je mineralizacija, t.j. popolna odstranitev ostankov zdravilnih učinkovin, kar vključuje tako izhodne učinkovine kot njihove razgradne produkte. Za dosego tega cilja vzporedno z biološko razgradnjo preučujemo tudi novejše tehnologije čiščenja odpadnih vod, kot so npr. ozonacija, UV razgradnja ter kavitacija. Vzporedno s kemijsko analizo v naši skupini izvajamo tudi strupenostne teste (ekotoksičnost), kjer določamo strupenost posameznih zdravilnih učinkovin ter njihovih mešanic (izhodne zdravilne učinkovine, razgradni produkti, vtoki/iztoki iz bioloških reaktorjev). Celokupno uspešnost delovanja bioreaktorjev tako ocenimo na osnovi odstotka odstranitve izbranih učinkovin ter rezultatov strupenostnih testov.

Informacijske in komunikacijske tehnologije (Information and Communication Technologies)

Access Control in BitTorrent P2P Networks Using the Enhanced Closed Swarms Protocol

Vladimir Jovanovikj [1,2], **Dušan Gabrijelčič** [1], **Tomaž Klobučar** [1]

[1] Laboratory for Open Systems and Networks, Jožef Stefan Institute, Ljubljana, Slovenia

[2] Jožef Stefan International Postgraduate School, Ljubljana, Slovenia

vladimir@e5.ijs.si

Abstract. The future content delivery systems are predicted to be efficient, user-centric, low-cost and participatory systems, with social and collaborative connotation. The peer-to-peer (P2P) architectures, especially ones based on BitTorrent protocol, give a solid basis for provision of such future systems. However, current BitTorrent P2P networks lack flexible access control mechanisms. In this paper, an enhanced version of an existing access control mechanism for BitTorrent systems – the Closed Swarms protocol is presented, which provides a flexible access control mechanism and enables fine grained security policies specification and enforcement. The protocol fulfills a number of content providers' requirements and enables efficient, flexible and secure content delivery in future content delivery scenarios.

Keywords: access control, P2P, BitTorrent, flexible policy, Closed Swarms

1 Introduction

It is envisaged that in the future people will consume 3D content enriched with additional media types that will engage more of our senses. Moreover, they will have the ability to create virtual and personalized environments that will correctly simulate the real world. Future content delivery systems will have to provide efficient delivery of such high quality media content, with an excellent quality of service. Therefore, they are predicted to be personalized, low-cost, user-centric and participatory systems with social and collaborative connotation, suitable for large and small size content producers. Because of its characteristics (such as scalability and robustness) the peer-to-peer (P2P) architectures, especially ones based on BitTorrent protocol [1][2], give a solid basis for future provision of such systems.

The future P2P-based content delivery systems need to be secure and trusted in order to be widely accepted and used. The importance of security as well as the main security requirements for P2P networks has already been emphasized in [3]. Among them, access control is considered basic and standard security service, especially by content providers. The access control in the P2P-based content delivery systems is quite difficult to accomplish because of the basic properties of the system: the content consumers are directly involved in the process of content distribution; and the system tends towards full decentralization. Most of the current approaches for access control are centralized or they can be easily compromised. Although some approaches seem promising [4], they lack support for flexible and fine grained security policies.

The main goal of this paper is to present an enhanced version of an existing access control mechanism for BitTorrent P2P networks – the Closed Swarms protocol [4]. We believe that the enhanced protocol will provide a flexible access control mechanism for future P2P-based content delivery systems applicable in various scenarios. First, we describe the motivation for enhancing this protocol in Section 2. Then, we present the enhanced Closed Swarms protocol in Section 3. Finally, we conclude the paper and present our future work in Section 4.

2 Motivation

To motivate our work, we describe the following scenario. An international TV broadcaster (a content provider) wants to distribute live TV program to its clients (authorized users) using a P2P-based content delivery system, based on the BitTorrent protocol. The TV broadcaster wants to restrict its program's availability only in one country (e.g. only in Slovenia) because of the digital rights issues. Furthermore, it decides to deliver a service to clients under different conditions. Premium clients, for example, would receive higher content quality (e.g. HD video) for a certain amount of money, whereas basic clients would receive lower content quality (e.g. SD video) for free. This is beneficial from business perspective, as it can increase indirect earnings, and from technical perspective, since it can improve content delivery. Moreover, clients should be able to purchase certain service packages in which they will receive high content quality only during certain time periods, e.g., every day from 18 till 20 hours, during the most popular show.

Finally, the TV broadcaster aims at achieving fine grained load balancing and optimization of its program delivery process. This can be done by creating and maintaining a hierarchical structure of seeds in the live streaming swarm. The structure is formed by separation of the seeds into layers (levels) according to the priority assigned to them by the content provider (Fig. 1) and placing the seeds at strategic locations. The value of the priority defines the level of precedence a seed has among the other peers in the live streaming swarm (seeds and leeches) during the delivery. The structure will enable quick transport of the content from the content injector towards the lowest level of seeds, and consequently to the regular peers (clients).

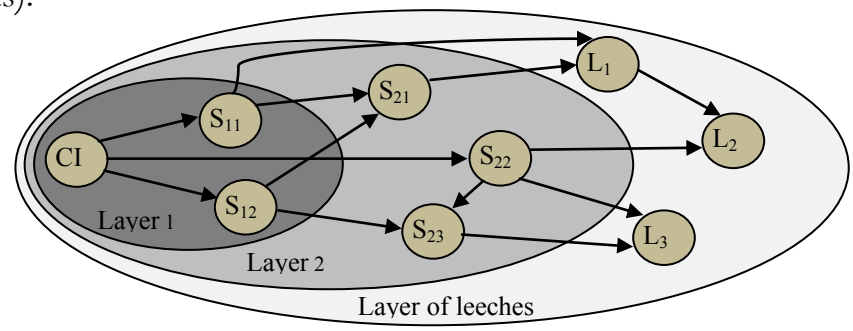

Figure 1: Hierarchical structure of a live streaming swarm: the content injector (CI) is not part of any layer; the layer 1 seeds (S) have greater priority than the layer 2 seeds; the leeches (L) are placed in one layer and do not have any priority.

3 The enhanced Closed Swarms protocol

The Closed Swarms (CS) protocol [4] is a distributed access control mechanism for BitTorrent P2P networks. The users can join the swarm after they have received an authorization credential (called Proof-of-Access) from the content provider. The CS protocol can be only applied under the same conditions for all users. Therefore, it is not fully applicable to our scenario, as distinction among several groups of users is needed. In order to make it applicable, we integrate a flexible authorization framework [5] to the protocol and provide proper policy enforcement.

The enhanced authorization credential of an arbitrary peer A is as follows:

$$SwarmID, K_S, K_A, ET, Rules_A, \{SwarmID, K_S, K_A, ET, Rules_A\}_{K_S^{-1}} \quad (1)$$

It contains information about: the specific swarm – its identifier (SwarmID) and public key (K_S); the credential holder, defined by its public key (K_A); and the expiry time of the credential (ET). Moreover, it contains a security policy (Rules) that specifies the conditions under which the credential holder is authorized by the

credential issuer to join the swarm and receive the requested service. In addition, the credential is digitally signed by the credential issuer, usually the content provider in correlation with a payment system, with the private key of the swarm (K_S^{-1}). The authorization credential is valid only when all the fields and the digital signature are correct.

Two peers, an initiator – peer A, and a swarm member – peer B, exchange their credentials in a challenge-response message exchange process:

$$A \rightarrow B : Version_A, SwarmID, Nonce_A \quad (2)$$

$$A \leftarrow B : Version_B, SwarmID, Nonce_B \quad (3)$$

$$A \rightarrow B : PoA_A, \mathrm{Req}Service_A, \{Nonce_A, Nonce_B, PoA_A, \mathrm{Req}Service_A\}_{K_A^{-1}} \quad (4)$$

$$A \leftarrow B : InfoID_B, Peers_B, \{Nonce_A, Nonce_B, InfoID_B, Peers_B\}_{K_B^{-1}} \quad (5)$$

$$A \leftarrow B : PoA_B, \mathrm{Req}Service_B, \{Nonce_A, Nonce_B, PoA_B, \mathrm{Req}Service_B\}_{K_B^{-1}} \quad (6)$$

$$A \rightarrow B : InfoID_A, Peers_A, \{Nonce_A, Nonce_B, InfoID_A, Peers_A\}_{K_A^{-1}} \quad (7)$$

First, they exchange (2, 3) the protocol version they support (Version), the identifier of the swarm they want to join/are part of and a randomly generated nonce (Nonce). Next, peer A sends (4) its credential (PoA) and specifies the service properties (ReqService) it wants to receive. If it is authorized to receive service with those properties and if peer B can provide the requested service, then peer B will enable upload to peer A; otherwise, it will terminate the communication. In both cases, it will first send an info message (5) in order to clarify the process outcome (InfoID) and to recommend other swarm members for contacting (Peers) to peer A. The process continues symmetrically, with peer B sending its credential. However, in this case peer A is never willing to terminate the communication and can just disable upload to B. In addition, the nonces ensure freshness while the digital signatures provide authentication of the messages. The process will be aborted after an invalid credential or incorrect swarm identifier, nonce or digital signature is sent.

The access control diagram of a request for service – message (4) is illustrated in Figure 2 (based on [6]). The Rules field is passed to the peer B's Access Control Decision Function (ADF), where the embodied polices are evaluated. On the other hand, the values from the ReqService field are assigned to specific environment variables and together with other environment variables are taken into account

during evaluation of the policies. The peer B's Access Control Enforcement Function (AEF) grants or denies the access to the requested service according to the evaluation of the specified policies.

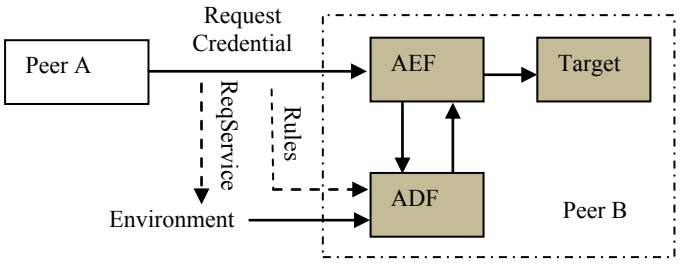

Figure 2: Access control diagram of the enhanced CS protocol (based on [6])

The specification and enforcement of flexible and fine grained policies provide distinction among several groups of users and fulfil the content provider's requirements from the described scenario above.

4 Conclusion and future work

In this paper we have presented the enhanced Closed Swarms protocol, a flexible access control mechanism for BitTorrent P2P networks that supports fine grained security policies specification and enforcement. The protocol fulfills a number of content providers' requirements and enables efficient and secure content delivery in future content delivery scenarios. Our future work includes integration of the proposed enhancements into the P2P-Next delivery platform (p2p-next.org) and their evaluation.

References:

[1]B. Cohen. BitTorrent protocol specification, www.bittorrent.org/beps/bep_0003.html, 2008

[2]J.J.D. Mol, A. Bakker, J.A. Pouwelse, D.H.J. Epema, H.J. Sips. The Design and Deployment of a BitTorrent Live Video Streaming Solution. In *11th IEEE International Symposium on Multimedia*, pp. 342-349. IEEE Computer Society, Los Alamitos, 2009

[3]ITU-T Recommendation X.1161: Data networks, open system communications and security, Framework for secure peer-to-peer communications, 2008

[4]N.T. Borch, I. Arntzen, K. Mitchell, D. Gabrijelčič. Access control to BitTorrent swarms using Closed Swarms. In *Proceedings of the 2010 ACM Workshop on Advanced Video Streaming Techniques for Peer-to-Peer Networks and Social Networking*, pp. 25-30. ACM, New York, 2010

[5]P. Chapin, C. Skalka, X.S. Wang. Authorization in trust management: Features and foundations. *ACM Computing Surveys*, Vol. 40, pp.1-48. ACM, New York, 2008

[6]ITU-T Recommendation X.812: Data networks, open system communications and security, Information technology – Open systems interconnection – Security frameworks for open systems: Access control framework, 1995

For wider interest

The vision for the future where people will consume high quality and large size media content (such as enriched 3D media content and virtual realities) and will produce most of the content, demands appropriate content delivery systems. These systems are predicted to be personalized, low-cost, user-centric and participatory, with social and collaborative connotation, suitable for large and small size content producers. Since peer-to-peer (P2P) architectures, especially ones based on BitTorrent protocol, have most of those properties, they are considered a good basis for provision of such content delivery systems. Indeed, BitTorrent P2P networks have already proved to be scalable, robust and efficient in delivery of audio and video data, and suitable for live streaming and social interaction between its users.

However, future P2P content delivery systems also need to be secure and trusted in order to be widely accepted and used. Access control is considered basic and standard security service, especially by content providers. In this paper we present a flexible access control mechanism that is able to fulfill a number of content providers' requirements, such as fine grained load balancing and optimization of the delivery process, restriction of the content delivery based on location, provision of different content quality and different business models.

Same as the BitTorrent P2P networks, the described mechanism is easy to deploy and do not require great infrastructure investments for it to function. The content provider will only need an additional software component that (in optional collaboration with a payment system) issues authorization credentials to its users. Therefore, it is suitable for professional content providers, as well as regular users that produce content.

Together with the described access control mechanism, P2P content delivery systems based on BitTorrent protocol promise to be flexible, efficient and secure systems, suitable for future content delivery.

Identifying Suspicious Behavior from Multiple Events

Bostjan Kaluza[1,2], **Gal Kaminka**[3], **Milind Tambe**[4]

[1] Department of Intelligent Systems, Jozef Stefan Institute, Ljubljana, Slovenia

[2] Jozef Stefan International Postgraduate School, Ljubljana, Slovenia

[3] Bar Ilan University, Ramat Gan, Israel

[4] Teamcore Research Group, University of Southern California, California

bostjan.kaluza@ijs.si

Abstract. Suspicious behavior detection becomes increasingly more challenging when agents are observed over a longer period of time. The detection system has to identify suspicious subjects from a collection of individual's events, where no single event is enough to decide whether his/her behavior is suspicious, but the combination of multiple events enables reasoning. We establish a probabilistic Bayesian framework for evaluating multiple events and show that the optimal evaluation is not possible in practice. We propose a naïve and a heuristic approach and test them on an airport domain. The heuristic approach achieves high performance resulting in high detection rate and low false-alarm ratio.

Keywords: suspicious behavior, Bayesian framework, scoring function, airport

1 Introduction

There are two approaches to detect suspicious behavior: suspicious detection models, which depend on suspicious behavior definitions, and anomaly detection models, which measure deviations from defined normal behavior. The basic unit of such analysis is *behavior trace* that provides characterized agent's actions over a period of time. However, given increasingly longer behavior traces it becomes inefficient to encapsulate the entire spectrum of either suspicious or normal behavior.

An important step in such analysis is therefore to utilize domain knowledge to identify interesting parts characterizing behavior trace. We denote them as *trigger*

events. Trigger events can present either positive or negative belief about the motivating goal and tend to be noisy – it is not clear if a person emitting suspicious events is indeed acting suspiciously. They also involve interactions of multiple agents making recognition under noise difficult. In many cases no single action or event is sufficient to reveal adversary intentions, but a collection of events enables the observer to infer the underlying intentions. The main question we are addressing is how to decide whether an event trace corresponds to behavior of a normal or a suspicious agent.

2 Detection Objectives

We leverage Bayesian framework for intrusion detection [1] for problem definition. *Event trace* $x^{(k)}$ is a sequence of k events $\boldsymbol{x}^{(k)}=(x_1,x_2,...,x_k)$ from a set of traces D. At each time step t an event x_t is generated by a hidden stochastic process H that is a mixture of two auxiliary stochastic processes, namely the normal process N and the suspicious process S. In real-world there can be many subprocesses contributing to each of them, i.e., many normal users with different behavior patterns, however, here we assume only a single N and a single S that capture all variability. Random variable $y_t=0$ if x_t is generated by N and $y_t=1$ if x_t is generated by S. The event x_t may depend on the current step t as well as on the pattern of events generated at time steps prior t. This allows that N and S are non-stationary, where their distribution depends both on actual time step t and events previously generated by both processes. The non-stationary nature might reflect that: (i) agent behavior depends on his/her prior actions; (ii) behavior changes over time (different population of agents); (iii) the nature of motivating goals changes over time; and (iv) the environment changes over time.

We assume a prior probability $\lambda=Pr\{S\}=Pr\{y=1\}$. In most cases λ is close to 0, since in real-world applications suspicious activities are sparse. The stochastic processes N and S induce measures $n(x_t)=Pr\{N(t)=x_t\}$ and $s(x_t)=Pr\{S(t)=x_t\}$, respectively. The objective of suspicious behavior detection is to identify those traces $\boldsymbol{x}^{(k)}$ that are likely to be suspicious activities, that is traces $\boldsymbol{x}$ for which

$$Pr\{S|H(t)=x_t, t=1,...,k\} > \tau \quad (1)$$

is above some threshold τ or is large relative to the probability for other traces.

3 Detectors

3.1 Bayes-Optimal Detector

Using Bayes theorem we can derive from Eq. (1)

$$Pr\{S|H(t) = x_t, t = 1, ..., k\} = \\ = \frac{\lambda \cdot Pr\{H(t) = x_t|S\}}{\lambda \cdot Pr\{H(t) = x_t|S\} + (1 - \lambda) \cdot Pr\{H(t) = x_t|N\}} \quad (2)$$

Note, that in order to compute $Pr\{H(t)=x_t, t=1,...,k|S\}$ one has to evaluate

$$s(x_1) \cdot s(x_2|x_1) \cdot ... \cdot (x_k|x_{k-1}, ..., x_1) \quad (3)$$

While some first terms can still be estimated, the estimation of latter terms including increasingly more history becomes intractable. In real-world applications we have no direct knowledge of values of the conditional probabilities, that is, we are unable to specify probability of an event given all possible combinations of history (the same applies for $Pr\{H(t)=x_t, t=1,...,k|N\}$). For this reason, we must approximate Bayes optimality in general. In particular, we will be concerned with estimating $Pr\{S|H(t)=x_t, t=1,...,k\}$ using approximate approaches.

3.2 Naïve Bayes Detector

A naive approach assumes that (i) events are independent and (ii) processes N and S are stationary, which means that the current event depends only on the current time step t and not on time steps prior t. Evaluation of the Eq. (2) is simplified using the naive assumption:

$$Pr\{S|H(t) = x_t, t = 1, ..., n\} = \\ \frac{\lambda \cdot \prod_{t=1}^{k} \hat{s}(x_t)}{\lambda \cdot \prod_{i=1}^{k} \hat{s}(x_t) + (1 - \lambda) \cdot \prod_{i=1}^{k} \hat{n}(x_t)} \quad (4)$$

We have to evaluate the probability that an event is generated by normal stationary process $n(x_t)$ and suspicious stationary process $s(x_t)$, which is tractable in terms of evaluation. Approaches for estimating $n(x_t)$ and $s(x_t)$ may include frequentist estimator, Hidden Markov Models, k-nearest neighbor, neural networks, etc. This paper does not explicitly address the problem of deciding whether an event is suspicious or not. In practice, the assumptions may over-simplify the model; however, we will use it as a baseline in our experiments.

3.3 Scoring Functions

The detection system can employ a *scoring function f* that interprets events to produce a score characterizing the overall suspicion that is to be contributed to the trace. Given a threshold value τ and a trace $\boldsymbol{x}^{(k)}$ we can classify as generated by a suspicious process if function value $f(\boldsymbol{x}^{(k)}) > \tau$.

A class of *well-behaved* functions consists of scoring functions for any $\boldsymbol{x}^{(k)}$, x_{k+1}

$$\begin{aligned} f(\mathbf{x}^{(k)}, x_{k+1}) &\geq f(\mathbf{x}^{(k)}) \qquad \textit{if } \Delta(x_{k+1}) = 1 \\ f(\mathbf{x}^{(k)}, x_{k+1}) &\leq f(\mathbf{x}^{(k)}) \qquad \textit{if } \Delta(x_{k+1}) = 0 \end{aligned} \tag{5}$$

where $\Delta(x_t)$ decides whether event is suspicious or not

$$\begin{aligned} \Delta(x_t) &= \begin{cases} 1; & \text{if } \tilde{s}(x_t) \geq \tilde{\tau} \\ 0; & \text{else} \end{cases}, \\ \tilde{s}(x_t) &= \frac{\lambda_\eta \cdot \hat{s}(x_t)}{\lambda_\eta \cdot \hat{s}(x_t) + (1 - \lambda_\eta) \cdot \hat{n}(x_t)}. \end{aligned} \tag{6}$$

The conditions imply that: (i) scoring function *f*'s evaluation increases when a new suspicious event is added to the trace and (ii) decreases when a normal event is added to the trace. The well-behaved scoring functions are motivated by the key observation that a suspicious event x_{k+1} ($\Delta(x_{k+1})=1$) is more likely to be generated by a suspicious process *S* than a normal process *N* regardless of the history $\boldsymbol{x}^{(k)}$. Given such assumptions the likelihood that a trace is emitted by a suspicious process as given by Eq. (2) is a well-behaved function.

The true likelihood function is difficult to obtain. Therefore, we defined the following well-behaved heuristic function to approximate it.

$$\begin{aligned} f_e(x_t, \mathbf{x}^{(t-1)}) &= a_t \cdot (f_e(\mathbf{x}^{(t-1)}) + b_t), \\ f_e(\mathbf{x}^{(0)}) &= 0, \\ b_t &= \beta \cdot \eta_s(\mathbf{x}^{(t)})^{\alpha(\tilde{s}(x_t) - \tilde{\tau})}, \\ a_t &= e^{-(\delta + \eta_n^*(\mathbf{x}^{(t)}))/(\gamma \cdot \eta_s(\mathbf{x}^{(t)}))} \end{aligned} \tag{7}$$

The b_t term models exponential increase in suspicion (according to the number of suspicious events η_s) with an exponential function using η_s as the base and likelihood that the event was generated by suspicious agent *s* as an argument. The parameters $\alpha>0$ and $\beta>0$ can be estimated from D_t. Additionally, the a_t term employs a *forgetting mechanism*, an exponential time decay function that discounts overall evaluation at time *t* in respect to agent's behavior prior *t*. Parameters $\gamma>0$ and $\delta>0$ are also estimated from D_t. The modified η^*_n presents *the time elapsed*

since the last event $s(x_i) > \tau$, that is, the number of normal events since the last suspicious event; the higher the number of normal events the faster the forgetting rate. Finally, we use a threshold value to decide whether a trace is generated by suspicious agent or not. The function f_e is a well-behaved function by definition.

4 Experimental Evaluation

To run proof-of-concept tests we first consider a simulated environment ESCAPES [3], a multi-agent simulator for airport evacuations with several types of agents exhibiting behaviors of regular travelers, authorities, and families. In cooperation with security officials we defined a basic scenario where a suspicious passenger goes from point *A* to point *B* while trying to avoid security personnel at the airport. A simulation is run with a given airport map, authority agents, regular passengers and a suspicious agent going from point *A* to *B*, outputting traces with 2D coordinates for all agents. We initialized the simulator with 100 agents including 10 authorities and a suspicious person with randomly chosen the initial and the final point. We ran 20 simulations, each consisting of 1500-3000 time steps. In total there were 2000 traces and 4316 interactions between authorities and passengers. We extracted two kinds of events: turns in absence of an authority and turns in presence of an authority. The first-type events were all considered as normal (detected with trajectory curvature), while the second-type events were either normal (e.g., passing by) or suspicious (e.g., avoiding in u-turns, changing direction, etc.). These were detected with Coupled Hidden Markov Models. The results were obtained with 10-fold-cross validation.

Table 1 compares three detectors: simple rule saying if there exists k suspicious events, mark this passenger as suspicious; Naïve Bayes detector; and scoring function. While simple rule and Naïve Bayes detector have high recall, precision is low (which means high false alarm rate). Scoring function, able to take into account history, achieves high precision with high recall outperforming other two approaches.

Detector	Recall	Precision	F-Measure
If exists k	70.00%	43.75%	53.85
Naïve Bayes	90.00%	40.91%	56.25
Scoring f_e	90.00%	90.00%	90.00

Table 1. Evaluation results comparing recall, precision and f-measure.

To get an estimate of how hard the problem of detecting suspicious passengers in real-world really is we can take the statistics [2] saying that officers across US required 98,805 passengers to undergo additional screenings, police questioned 9,854 of them and arrested 813. The final result was one arrested passenger per 100 inspected, which gives a precision of 1%.

References:

[1] Helman, P.; Liepins, G.; and Richards, W. 1992. Foundations of intrusion detection. In The IEEE Computer Security Foundations Workshop V.

[2] Kaye, K. 2009. TSA screening more than just carry-on bags. The Washington Post, Nov. 9.

[3] Tsai, J.; Kaminka, G.; Epstein, S.; Zilka, A.; Rika, I.; Wang, X.; Ogden, A.; Brown, M.; Fridman, N.; Taylor, M.; Bowring, E.; Marsella, S.; Tambe, M.; and Sheel, A. 2011. ESCAPES - Evacuation Simulation with Children, Authorities, Parents, Emotions, and Social comparison. In AAMAS- 2011.

For wider interest

Identification of suspicious activities arises in many domains where an adversary has a motivating goal and exhibits behavior that deviates from behavior of normal users. The goal is to augment traditional security measures by scrutinizing behavior of all subjects in the environment. This can be applied, for example, to detect a passenger at an airport who plans to smuggle drugs while keeping contacts with authorities at minimum, to detect a pirate vessel that plans to capture a transport vessel and therefore avoids security patrols, to identify a user that misuses access to the server, to catch a reckless driver, a shoplifter, etc.

We established a formal framework and show how to optimally detect suspicious behavior from a set of observed events, where no single event is sufficient to decide whether a person behaves suspiciously or not. Unfortunately, optimal detection is not feasible in practice because we cannot estimate all required parameters. We show two approximate methods (naïve and heuristic) and compare them on an airport domain. The heuristic approach achieves high performance, discovering almost all suspicious passengers with low false-alarm ratio.

Prepoznavanje ljudi na podlagi njihove hoje

Simon Kozina[1,2], **Matjaž Gams**[1,2]

[1] Odsek za inteligentne sisteme, Institut Jožef Stefan, Ljubljana, Slovenija

[2] Mednarodna podiplomska šola Jožefa Stefana, Ljubljana, Slovenija

simon.kozina@ijs.si (elektronski naslov odgovornega avtorja)

Povzetek. Prebivalstvo se stara in število starejših ljudi bo kmalu preraslo družbeno sposobnost za njihovo skrb pod sedanjimi pogoji. Na področju ambientalne inteligence so zato v razvoju novi pristopi. Ena izmed obetavnih rešitev so sistemi, ki nadzorujejo zdravje starejših ljudi in obveščajo zdravnike/svojce v primeru sprememb, ki bi jih lahko ogrožale. V sistemih, kjer je takšnih uporabnikov več, je pomembna tudi informacija o tem, kdo sistem trenutno uporablja. Da uporabniki ne bi sami skrbeli za določanje trenutnega uporabnika, smo razvili sistem, ki prepozna le-tega na podlagi njegove hoje. Algoritem strojnega učenja uporabljen pri testiranju, je bil algoritem naključnih gozdov. Testirali smo hojo 12 ljudi, katere je naš sistem prepoznal z 88.6% uspešnostjo.

Ključne besede: prepoznavanje hoje, strojno učenje, ambientalna inteligenca

1 Uvod

Prebivalstvo se stara. Razlog leži v dvigu življenjske dobe in zmanjševanju rodnosti. Odstotek ljudi starejših od 65 let naj bi se dvignil od 17.9% v letu 2007 na 53.5% v letu 2060 [1]. Število starejših ljudi bi tako preraslo družbeno sposobnost za njihovo skrb pod sedanjimi pogoji. Poskrbeti moramo, da bodo starejši ljudje lahko dlje živeli neodvisno, le z minimalno podporo aktivne populacije. To je glavni cilj mnogih projektov, me njimi tudi projekta Chiron [2].

Uporabniku lahko najbolje pomagamo, če imamo informacijo o tem, kdo v določenem trenutku tak sistem uporablja. Pri projektu Chiron vsaka oseba nosi dva pospeškomera, s katerima nadzorujemo njegove/njene aktivnosti. S pomočjo

podatkov iz teh senzorjev lahko uspešno napovemo, kdo trenutno uporablja senzorje oz. sistem.

2 Pregled področja

Raziskave na področju prepoznavanja ljudi na podlagi njihove hoje lahko razdelimo na dve skupini. Prva skupina raziskav temelji na prepoznavanju s pomočjo kamer, medtem ko druga skupina raziskav prepoznava hojo s pomočjo senzorskih naprav, pospeškomerov.

2.1 Prepoznavanje s pomočjo kamer

Sistemi, ki prepoznavajo hojo s pomočjo kamer, temeljijo na procesiranju slik in pridobivanju podatkov o hoji iz le-teh. Hayfron-Acquah in ostali [3] so prepoznavali hojo majhnega števila oseb. Pri prepoznavanju štirih oseb so dosegli 100% uspešnost, pri prepoznavanju šestih oseb pa 97% uspešnost. Lam in Lee [4] sta se lotila prepoznavanja 115 oseb s pomočjo 2128 sekvenc hoje. Uspešnost prepoznavanja je bila nekaj več kot 80%.

2.2 Prepoznavanje s pomočjo pospeškomerov

Prve raziskave na tem področju sta naredila Ailisto in ostali [5] ter Mäntyjävri in ostali [6]. Oboji so uporabili en pospeškomer pritrjen na bok človeka. Posneli so hojo 36 oseb in testirali uspešnost prepoznavanja, ki je znašala 85%.

3 Priprava podatkov za strojno učenje

Za prepoznavanje hoje ljudi je vsak od testnih ljudi imel na sebi pritrjena dva pospeškomera, enega na levem stegnu in drugega na prsih. Pospeškomer je naprava, ki meri spremembo pospeška v vseh treh straneh koordinatnega sistema. Pospeškomeri, katere smo uporabili za namene testiranja, so spremembo pospeškov zabeležil 10-krat na sekundo. Imamo torej tok podatkov, katere moramo pretvoriti v obliko primerno za strojno učenje. Podatke moramo smiselno razdeliti.

Pri poskusih, kjer se za potrebe strojnega učenja uporabljajo podatki iz pospeškomerov, se podatke običajno razdeli z drsečim oknom. Drseče okno združi

zaporedne podatke v fiksnem časovnem oknu. Podatki enega časovnega okna se nato uporabijo za računanje atributov in služijo kot učni oz. testni primer. Dolžina časovnega okna, katerega smo uporabili pri testiranju, je znašala 20 sekund. V naslednjem podpoglavju so opisani atributi, ki so bili uporabljeni pri stojnem učenju.

3.1 Računanje atributov

Podatke enega časovnega okna uporabimo za en učni oz. testni primer. Da bi lahko te podatke uporabili za stojno učenje, moramo izračunati atribute, s katerimi opišemo značilnosti posameznega časovnega okna. Kot omenjeno sta bila za pridobivanje podatkov uporabljena dva pospeškomera. Atributi so bili posebej izračunani za tok podatkov iz prvega in drugega pospeškomera. Izračunani atributi so bili naslednji:

- povprečna dolžina vektorja pospeškov znotraj časovnega okna,
- varianca povprečne dolžine vektorja,

$$\delta^2 = \frac{\sum_{i=1}^{N}(a_i - \bar{a})^2}{N} \tag{1}$$

  kjer je N število podatkov v enem časovnem oknu, a_i je povprečna dolžina i-tega vektorja in $\bar{a}$ pa povprečna dolžina vseh prejšnjih pospeškov,
- povprečna dolžina pospeškov v x, y in z koordinatnih smereh,
- maksimalni in minimalni pospeški v x, y in z koordinatnih smereh,
- razlika med maksimalnim in minimalnim pospeškom v x, y in z koordinatnih smereh,
- kot spremembe pospeška med maksimalnim in minimalnim pospeškom v enem časovnem oknu v x, y in z koordinatnih smereh. Definiran je kot:

$$\Omega = \arctan\left(\frac{a_{\max} - a_{\min}}{t_{a_{\max}} - t_{a_{\min}}}\right) \tag{2}$$

  kjer sta $a_{\max}$ in $a_{\min}$ maksimalni in minimalni pospešek v enem časovnem oknu, $t_{a_{\max}}$ in $t_{a_{\min}}$ pa časa izmerjena ob minimalnem in maksimalnem pospešku;

- orientacija pospeškomera. Predpostavljali smo, da je pospeškomer, ki je sestavljen iz vektorja pospeškov $a = [a_x, a_y, a_z]$, običajno obrnjen tako, da z koordinata kaže navzdol. Orientacija pospeškomera je takrat definirana kot:

$$\phi = \arccos\left(\frac{a_z}{\sqrt{a_x^2 + a_y^2 + a_z^2}}\right) \tag{3}$$

Izračunamo 18 atributov za posamezni tok podatkov iz vsakega pospeškomera, skupaj torej 36. Interakcija med pospeškomeroma je tudi pomembna informacija, za to izračunamo še en dodaten atribut, ki bo le-to tudi zabeležil – kot med povprečno dolžino vektorjev v enem časovnem oknu. Izračunan je na naslednji način:

$$\varphi = \arccos\left(\frac{\vec{a} \cdot \vec{b}}{\|\vec{a}\| \cdot \|\vec{b}\|}\right) \tag{4}$$

Vektorja $\vec{a}$ in $\vec{b}$ predstavljata povprečne dolžine vektorja pospeškov obeh pospeškomerov.

4 Rezultati

Testiranje je bilo opravljeno na 12 osebah (sedmih moških in petih ženskah). Vsaka oseba je hodila 16 minut, kar smo razdelili na 10 minut za učno množico, ostalih 6 minut hoje pa je bilo namenjeno testiranju. Kot je bilo izpostavljeno že zgoraj, smo podatke zajemali s pomočjo dveh pospeškomerov, ki sta bila pritrjena na prsih in na levem stegnu.

Za napovedovanje testnih primerov smo uporabili algoritem strojnega učenja – naključni gozdovi. Uporabili smo njegovo implementacijo v orodju za podatkovno rudarjenje Weka. Rezultati prepoznavanja hoje 12 oseb so navedeni v Tabeli 1. V prvem stolpcu in v prvi vrstici v tabeli so navedene zaporedne številke oseb, katere smo testirali. Na diagonali so tisti primeri, ki so napovedani pravilno, ostali primeri v vrstici pa so tisti, katere algoritem napove narobe.

Tabela 1 : Predstavitev rezultatov.

	1	2	3	4	5	6	7	8	9	10	11	12	Uspešnost [%]
1	19	0	0	0	0	0	0	0	0	0	0	0	100
2	0	21	0	0	0	0	1	0	0	0	0	0	95.5
3	0	0	16	0	0	0	0	0	0	0	0	1	94.1
4	0	0	0	19	0	0	0	0	0	0	2	0	90.5
5	0	0	0	0	21	0	0	0	1	0	1	0	91.3
6	0	0	0	0	0	21	0	0	0	0	0	0	100
7	0	0	0	1	0	6	17	0	0	0	2	0	65.4
8	0	0	0	0	0	0	0	23	0	0	0	0	100
9	0	0	0	0	0	0	0	1	20	0	0	1	90.9
10	1	0	0	0	0	1	0	0	0	9	1	0	75
11	0	1	0	0	1	0	0	0	0	1	10	0	76.9
12	1	0	0	0	0	0	0	1	0	0	1	7	70

Skupna uspešnost napovedovanja hoje s pomočjo pospeškomerov znaša 88.6%. Opazimo, da bi bil ta rezultat lahko boljši, saj so napovedi zadnjih treh oseb in osebe št. 7 zelo slabe. Problem je v premajhni učni množici za posamezno osebo, saj ugotavljamo, da imajo te osebe najmanjše število primerov tudi v testni množici.

5 Zaključek

V članku opisujemo problem prepoznavanja oseb na podlagi njihove hoje s pomočjo pospeškomerov. Hojo vsake osebe zajamemo z dvema pospeškomeroma, ki sta pritrjena na levo stegno in prsi. Podatke nato pretvorimo v obliko primerno za strojno učenje in izvedemo potrebne teste. Uspešnost testiranja je znašala 88.6%, kar bi lahko še izboljšali z novimi testiranji, ki bi vsebovali daljše intervale hoje vsake osebe.

Literatura:

[1]Eurostat. http://epp.eurostat.ec.europa.eu, 2011.

[2]Chiron. http://www.chiron-project.eu, 2011.

[3]J. B. Hayfron-Acquah, M. S. Nixon and J. N. Carter. Automatic gait recognition by symmetry analysis. *Pattern Recognition Letters*, vol. 24, pp. 272–277, 2003.

[4]T. H. W. Lam and R. S. T. Lee, A new representation for human gait recognition: Motion silhouettes image (MSI), in *International Conference on Biometrics*, pp. 612–618, 2006

[5]H. J. Ailisto, M. Lindholm, J. Mäntyjärvi, E. Vildjiounaite, and S.-M. Mäkelä, Identifying people from gait pattern with accelerometers. In *Proceedings of SPIE*, 2005.

[6]J. Mäntyjärvi, M. Lindholm, E. Vildjiounaite, S.-M. Mäkelä, and H. J. Ailisto, Identifying users of portable devices from gait pattern with accelerometers. *In IEEE International Conference on Acoustics, Speech, and Signal Processing*, March 2005.

Za širši interes

Osnovni cilji Odseka za inteligentne sisteme so raziskave računalniških osnov inteligence in razvoj naprednih aplikacij s področja inteligentnih informacijskih storitev, analize podatkov, inteligentnega preiskovanja spleta, podpore odločanja, inteligentnih agentov, medicine, ekologije, jezikovnih tehnologij, inteligentne proizvodnje in ekonomije. Podobno kot ta članek, so tudi druge raziskave usmerjene predvsem na delo, ki vključuje podatke iz merilcev pospeška, giroskopov in merilcev magnetnega polja. Trenutno zastavljeni cilji so uspešno prepoznavanje aktivnosti s čim manjšim številom senzorjev in računanje porabe energije pri človeku, kar bi kasneje združili v sistem za učinkovito upravljanje zdravja posameznika skozi celoten cikel oskrbe. Trenutno zaključujemo tudi projekt, kjer smo s sistemom, ki določa pozicijo človeka v prostoru, uspešno prepoznali padce, poleg tega pa je sistem prepoznaval tudi ostale aktivnosti, ki jih človek opravlja skozi dan.

IPSSC: Self-reparable systems on FPGA

Uroš Legat[1,2], Franc Novak[1,2]

[1] Computer systems department, Jožef Stefan Institute, Ljubljana, Slovenia

[2] Jozef Stefan International Postgraduate School, Ljubljana, Slovenia

uros.legat@ijs.si

Abstract. Highly reliable systems on Field Programmable Gate Arrays (FPGA) require error mitigation and recovery techniques to protect them from the errors caused by high energy radiation also known as Single Event Upsets (SEU). We developed a low area-overhead internal error recovery mechanism, which serves as a basis for more sophisticated self-reparable systems. We propose three different architectures of self-reparable systems which offer different levels of protection at the expense of different hardware overheads.

Keywords: self-reparable systems, FPGA, on-line testing

1 Introduction

Because of flexibility, cost, and easy design process Field Programmable Gate Arrays (FPGA) are increasingly used in industry, research, air or ground transport, banks, and all kinds of other applications.

Due to the increasing integration density, FPGA chips are getting more and more prone to faulty behavior caused by cosmic or artificial radiation. Such faults are modeled as Single Event Upsets (SEUs). Radiation is usually a major concern in space. The systems in avionics and at ground level are less exposed to the radiation because of the planetary atmospheric and magnetic radiation shield. However, experiments showed that with increased density of integrated circuits the neutron particles present in the atmosphere are also capable of producing SEUs. It is therefore imperative that FPGA based applications, where high reliability is required, include mechanisms that can easily and quickly detect and correct SEUs.

Many techniques have recently been developed to protect critical systems on SRAM FPGAs against SEUs [1]. At the design level of the FPGA, these techniques

are classified as SEU mitigation techniques, which prevent the SEU affecting the target design, and SEU recovery techniques that prevent the errors from accumulating inside the FPGA configuration memory.

On the basis of error recovery techniques from [2], we developed a small internal error recovery mechanism that constantly checks the configuration memory and corrects the error when it is detected. The salient feature of our internal scrubbing mechanism is that it requires the least reported hardware resources and is portable to different FPGAs. Using the internal recovery mechanism, we developed three different self-reparable systems' architectures.

2 Internal error recovery mechanism

The FPGA configuration memory determines the functionality of the FPGA and is organized in a network of configuration frames that are laid out on a device according to their frame address. The structure of the FPGA configuration is depictured in Fig. 1. More details about the FPGA configuration structure can be found in [3].

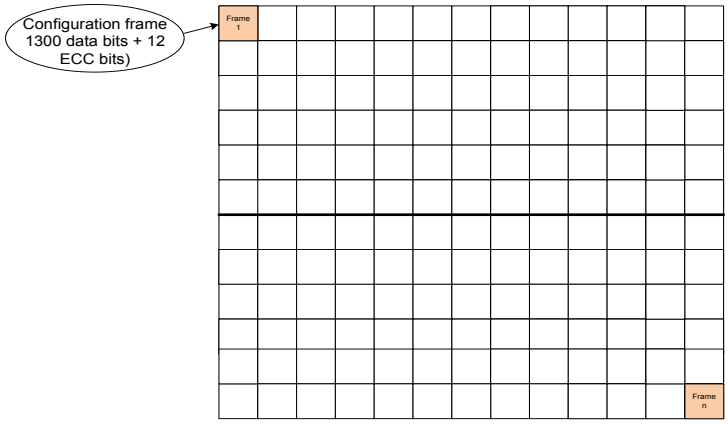

Figure 1: The FPGA configuration structure

A configuration frame is the smallest reconfigurable part of FPGA. The size of a frame in Virtex 4, and Virtex 5 FPGA, is 1312 bits. The frame has 1300 data bits and 12 Error Correcting Code (ECC) bits. These 12 ECC bits are pre-calculated and can be used to check the integrity of the data in a particular configuration frame. The internal recovery mechanism reads the FPGA configuration memory

frame by frame and checks if the data in every frame are consistent with the ECC bits. The following options may occur:

- In case of error-free frame, the error recovery mechanism starts reading the next configuration frame.
- In case of a single error, the error recovery mechanism determines the location of the erroneous bit inside the frame data and corrects it by partially reconfiguring the frame.
- In case of a double error, the configuration cannot be corrected by the internal recovery mechanism. The double error is reported. Further recovery procedure in this case will be explained in the next section.

The internal recovery mechanism was efficiently implemented in Virtex 4 and Virtex 5 FPGAs. A Finite State Machine (FSM) was used to control the error recovery process and an internal memory block RAM was used to buffer the data of one frame. Our implementation of the error recovery mechanism was compared to other reported implementations. The comparison of the occupied hardware resources for some known implementations is presented in Table.

Our recovery mechanism in Virtex 4 occupies 156 slices, 118 flip-flop registers, and 1 block RAM. The hardware design of the Virtex 5 recovery mechanism occupies merely 72 slices, 115 Flip-flop registers and 1 block RAM. For example, it occupies less than 1% of slices of the smallest Virtex 5 FPGA. Similar error recovery mechanism for Virtex 4 and 5 FPGA was implemented by Heiner et. al. [4], and Chapman [5] respectively. From the implementation results (Table 1) we can conclude that our implementation is the smallest.

	Virtex 4		Virtex 5	
	Our Mechanism	Heiner et.al. [4]	Our Mechanism	Chapman [5]
Slices	176	736	72	172
Flip-flops	118	680	115	321
Block RAM	1	2	1	1

Table: Hardware implementation comparison

3 Self-reparable systems

To protect reliable applications on Virtex 4 and Virtex 5, FPGAs different architectures of self-reparable systems are proposed. The self-reparable system

occupies a small portion of the FPGA configuration, while the rest of the configuration memory can be used for target design. The system detects and corrects soft errors in the FPGA configuration memory during the operation of the target application. The proposed architectures are the following:

- The most basic self-reparable system is shown in Fig 2. It contains only the internal error recovery mechanism which corrects faults in the configuration memory in concurrence with the target application. This self-reparable system fails if fault occurs in a critical bit inside the error recovery mechanism.

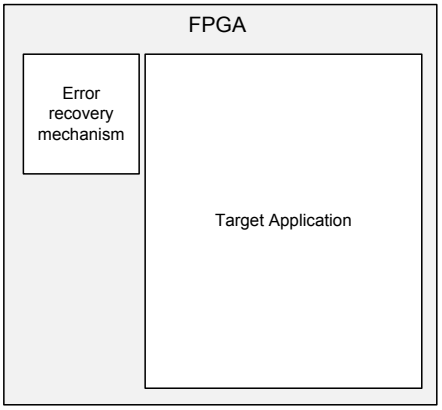

Figure 2: Self-reparable system with internal error recovery mechanism

- Fig. 3 shows the principle of a more advanced self-reparable system. This system has an external watchdog timer to monitor the internal error recovery mechanism. When the external watchdog timer detects the wrong operation of the internal error recovery mechanism, it recovers the mechanism from the external memory. This system recovers itself in a majority of cases. However, in some circumstances the external watchdog timer cannot detect the failure of the internal error recovery mechanism. In this case the self-reparable system fails.

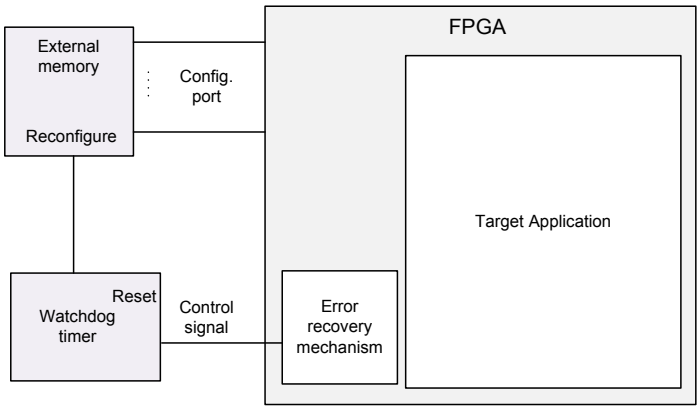

Figure 3: Self-reparable system with an external watchdog timer

- The third proposed self-reparable system architecture is depicted in Fig. 4. This system has an internal error recovery mechanism which is implemented by the Triple Modular Redundancy technique. This technique triplicates the original circuit. The outputs of the three modules of the circuit are connected to the majority voter which excludes the outputs of the faulty module. This self-reparable system fails if a fault occurs in the small voter circuit or in two modules at the same time. The system has a very small possibility of failure but takes three times more FPGA resources.

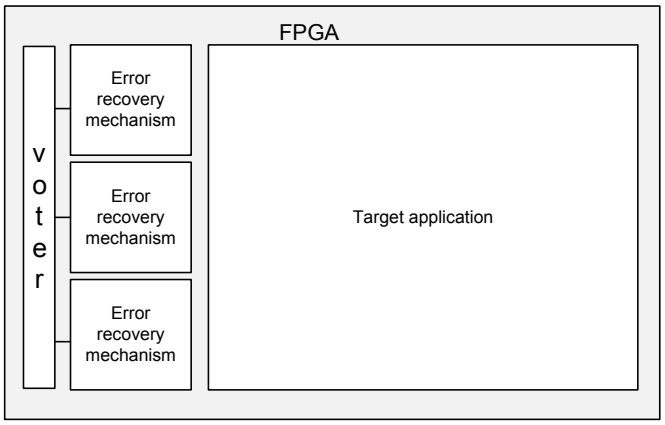

Figure 4: Self-reparable system with internal error recovery mechanism in TMR

4 Conclusion

We developed efficient self-reparable systems for SEU recovery. The systems are all based on a small error recovery circuit inside the FPGA. According to the desired level of protection, the system designer can decide between three architectures with different overheads. In future work, we intend to estimate the reliability of the proposed designs with extensive fault injection experiments.

References:

[1] Lima Kastensmidt F., Carro L., Reis R. *Fault-Tolerance Techniques for SRAM-Based FPGAs*, Springer, 2006.

[2] C. Carmichael, M. Caffrey, and A. Salazar. *Correcting single-event upsets through virtex partial configuration*, Xilinx Corporation, XAPP216 (vl.0), 2000.

[3] Xilinx. *Virtex-5 FPGA User Guide*, Xilinx Corporation, UG190 (v4,5), 2009.

[4] J. Heiner, N. Collins, M. Wirthlin. Fault Tolerant ICAP Controller for High-Reliable Internal Scrubbing. In *Proceedings of the IEEE Aerospace Conference*, 2008.

[5] K. Chapman. *SEU strategies for Virtex-5 Devices*, Xilinx Corporation, XAPP864 (v2.0), 2010.

For wider interest

Field Programmable Gate Arrays (FPGA) are programmable logic circuits that are increasingly used in industry, research, transport, banking systems, servers, and numerous other applications. FPGAs are also used in mission critical systems like aircraft and space exploration missions. Advantages of FPGAs to standard ASIC chips are fast prototyping, faster time to market, reconfigurability, lower costs in lower part numbers.

The functionality of the FPGA circuit is determined by configuration memory. FPGA can be reprogramed any number of times with different systems. FPGAs can be programmed with a simple logic function or a complete System on Chip (SOC) with microprocessors and other peripherals. Configuration memory of the FPGA comprises Static Random Access Memory (SRAM) cells which lose their content when they are powered off. When the device is powered on, it has to be reconfigured. Stand-alone applications have to have their configuration stored in external non-volatile memory.

The configuration memory of FPGA is vulnerable to high energy radiation which can cause a configuration bit inside the memory to flip and consequently alter the functionality of the circuit. These so called soft errors are very common in space where the radiation levels are high. But it has also been demonstrated that considerable risk of these soft errors exists in avionics and terrestrial applications. Therefore to protect the applications that require high level of reliability error recovery techniques have to be applied.

To protect the reliable and mission critical applications on FPGA, we propose three different architectures of self-reparable systems. The systems are all based on a small error recovery circuit inside the FPGA. According to the desired level of protection, the system designer can decide between these three architectures with different overheads.

Copula regression based ranking of non-linear decision options

Biljana Mileva-Boshkoska[1,2]
Marko Bohanec[1,2]

[1] Department of Knowledge Technologies, Jožef Stefan Institute, Ljubljana, Slovenia
[2] Jožef Stefan International Postgraduate School, Ljubljana, Slovenia
biljana.mileva@ijs.si, marko.bohanec@ijs.si

Abstract. In this paper we address the problem of ranking of qualitative decision making options. We start with the well developed Qualitative – Quantitative method that is used for ranking of qualitative options given with monotone of closely linear tabular valued functions. However, there are many cases when the linear approximation is not adequate. To overcome this problem, we extend the qualitative-quantitative method for ranking of a class of non-monotone options by introducing the concept of copula regression.

Keywords: multi criteria decision making, copula, qualitative-quantitative method

1 Introduction

If you have to choose one option from 57 varieties, making decisions becomes hard work [1]. To overcome this problem, over the past decades many multi-criteria decision methods (MCDM) have been developed as a support to the decision makers in the process of ranking and consequently choosing the best option from many. From the available MCDM, we focus on the qualitative decision methods, in particular the Qualitative-Quantitative method (QQ) [2], [3] which was developed as an upgrade of the DEX [4] and DEXi [5] methods. In QQ, each option is described with qualitative attributes and a qualitative class to which the option belongs. The main asset of QQ is that it manages to rank the qualitatively described monotone options which belong to the same class. The main disadvantage is that QQ in general fails to consistently rank the non-monotonic

options which belong to the same class. In this paper we present a copula based approach for overcoming this problem for a class of non-monotone options.

2 Methods used

We start from the QQ method that consists of three stages. In the first stage, the qualitative attributes of the options at hand are mapped into quantitative ones with attention to preserving the decision maker's preferences.

In the second stage QQ uses ordinary least square regression (OLSR) for ranking of options. The regression problem is a procedure in which we look for the expected value of the dependent variable Y, which is related in some functional format to the independent variables X_i. In OLSR model, Y has a linear relationship with the X_i:

$$Yi = \omega_0 + \omega_1 X_{1i} + \omega_2 X_{2i} + ... + \omega_k X_{ki} + \varepsilon_i \quad (1)$$

where ε_i is normal and independent, and the parameter estimates ω_i are obtained using the least squares algorithm. The QQ performs well if the relation between the dependent and intependant variables is linear. What if Y in non-linearly related to X_i and what if Y and X_i have any distribution? To solve these kinds of problems we modify the QQ method by replacing the OLSR with copula regression.

Copulas are functions that describe the joint distribution of random variables (r.v.). The joint distribution function is given by $H(x, y) = P[0 \le X \le x, 0 \le Y \le y]$, where P is a probability function. In 1946, Sklar proved that the joint distribution function of two r.v. is equal to the copula of their uniform distributions on the unit interval [0,1] [6]:

$$H(x, y) = C(F(x), G(y)) \quad (2)$$

where $u = F(x)$ and $v = G(y)$ are marginal distribution functions of the r.v. X and Y. One important class of copulas represents the Archimedean copulas which are constructed using the following relation [6]:

$$C(u, v) = \varphi^{[-1]}(\varphi(u) + \varphi(v)) \quad (3)$$

where $\varphi : [0,1]^2 \to [0, \infty]$ is called a generator function, and $\varphi^{[-1]}$ is pseudo-inverse of φ, meaning that $\varphi(0) < \infty$. In this paper, we focus on Clayton copula, which is a member of the Archimedian copulas, with generator function $\varphi(t) = \frac{t^{-\theta} - 1}{\theta}$ that leads to the following form of copula:

$$C_\theta(u,v) = [\max(u^{-\theta} + v^{-\theta} - 1), 0]^{-\frac{1}{\theta}} \quad (4)$$

In order to build multi-dimensional copulas that will provide the dependence among all the input and output variables, we use the fully nested Archimedian construction (FNAC) [7]. The basic element in the FNAC structure represents the bivariate copula. For example, to build a copula that consists of two input and one output variable, using the FNAC, first the distribution functions u_1 and u_2 of two variables are coupled, forming a Clayton copula $C_1(u_1, u_2)$ with parameter θ_1. In the next step C_1 is coupled with u_3 into $C_2(u_3, C_1)$ with parameter θ_2 leading to:

$$C(u_1, u_2, u_3) = C_2(u_3, C_1(u_2, u_1)) \quad (5)$$

Next we proceed with determining the value of the output, given the values of the input attributes using regression. For two r.v. X and Y, the regression curve is defined $y=E(Y|X=x)$, where y represents the conditional mean value of Y, as the most typical value of Y, for each value of $X=x$. An alternative to the mean values of Y are the quantiles q of Y leading to quantile regression. The q quantile for a r.v. is the value x such that the probability is $P[Y \le y | X = x] = q$. In order to perform quantile regression using copulas we need to find the conditional distribution of the output variable. For that reason we start by defining the density function using the relation:

$$P[Y \le y \mid X = x] = P[V \le G(y) \mid U = F(x)] = \frac{\partial C(u,v)}{\partial u} = q \quad (6)$$

Using the Clayton copula in (16), solving it for $q \in [0,1]$, and using the relations $u=F(x)$ and $v=G(y)$ we can find different quantile regression curves for the variable Y on X:leads to v:

$$y = G^{-1}[1 - (F^{-1}(x))^{-\theta} + (q(F^{-1}(x))^{1+\theta})^{-\frac{\theta}{1+\theta}}]^{-\frac{1}{\theta}} \quad (7)$$

In the example that follows, we will choose $q=1/2$ in order to perform median regression [8], thus finding the most probable value of the output. The obtained regression function is used for ordering the options in each class.

In the third stage, QQ normalizes the obtained regression values in the intervals $c \pm 0.5$, where c is the class where the option belongs to, thus preserving the class and the rank of options at the same time. The calculations obtained using Clayton copula, on which is applied the third stage of QQ, are named Clayton normalized, as shown in Table 1.

3 An example

In order to illustrate the method, we give the example in Table 1, in which options are given quantitatively. The first column in Table 1 is the option number, the second and the third columns are the two attributes, the fourth column is the class into which an option belongs to, and the last three columns are calculations of the ranks of options obtained with the Clayton copula, the Clayton copula normalised and the QQ methods.

Table 1: Example of MCDM problem solved with QQ, and Clayton copula methods

Opt. no.	Attribute 1	Attribute 2	Class	Clayton copula	Clayton normalized	QQ
1	4	1	1	2.05	0.50	1.16
2	2	3	1	2.48	1.40	1.25
3	3	4	1	2.53	1.50	0.75
4	4	2	2	2.50	2.50	1.79
5	1	4	2	2.05	1.50	2.21
6	2	2	3	2.45	3.50	3.14
7	1	4	3	2.05	2.50	2.86
8	1	1	4	1.76	3.50	4.33
9	3	1	4	2.04	3.88	3.97
10	2	2	4	2.45	4.42	4.00
11	2	3	4	2.48	4.46	3.85
12	3	3	4	2.51	4.50	3.67

Table 2: Example of QQ beaching the monotonicity property

Opt. no.	Attribute 1	Attribute 2	Class	Clayton copula	Clayton normalized	QQ
2	2	3	1	2.48	1.40	1.25
3	3	4	1	2.53	1.50	0.75

Looking in Table 1, we see that QQ breaches the monotonicity property on nine occasions, i.e., for the following option pairs (2, 3), (8, 9), (8, 10), (8, 11), (8, 12), (9, 12), (10, 11), (10, 12) and (11, 12). To explain the monotonicity, we give the example in

Table 2. From Table 2 we see that option 3 has bigger values for both attributes than option 2 hence we expect that QQ would provide better rank for the option number 3. Unlike QQ, which provides bigger rank for option 2 and consequently breaches the monotonicity property, the Clayton copula provides the correct rank.

Occasionally, we need to make comparison of an option with options that belong to different classes. Applying the final stage of the QQ method on the obtained results with Clayton copula allows ranking of the same option in different classes and therefore comparing it with different options. For example, the options 2 and 11 have the same values for the two attributes, however the option 2 is ranked and consequently compared to the other options in class 1, while option 11 is ranked and compared with options that belong to the class 4. Although these two equal options belong to different classes, the Clayton copula provides the same overall rank for both of them. In order to distinguish between the same two options which we classify in different classes, we apply the final stage of the QQ method, which we name normalization. Consequently, each of the options receives different class number (the point number) and the rank within the class (the decimal number). Options pairs (5, 7) and (6, 10) behave similarly.

4 Conclusion

In this paper we presented a copula based method for qualitative option ranking. The method uses elements of the QQ method; however it extends it so that it may be used for ranking of a class of qualitative non-monotonic options. The method is applied on an arbitrary example, and the results confirm that this method can be successfully used for a class of non-monotonic cases, for which QQ fails to provide consistent ranking.

References:

[1]The tyranny of choice: You choose, *The Economist,* 306, 53-54, 2010, http://www.economist.com/node/17723028

[2]M. Bohanec, B. Urh, V. Rajkovič. Evaluation of options by combined qualitative and quantitative methods, *Acta Psychologica* 80:67-89, 1992

[3]M. Bohanec. *Odločanje in modeli*, DMFA – Založništvo, Ljubljana, 2006.

[4]M. Bohanec, V. Rajkovič. DEX: An expert system shell for decision support, *Sistemica*, 1 145-157, 1990

[5]M. Bohanec. DEXi: Program for Multi-Attribute Decision Making, User's Manual, Version 3.03. IJS Report DP-10707, Jožef Stefan Institute, Ljubljana, 2011.

[6]R. B. Nelsen. *An Introduction to Copulas*, *2nd Edition*. Springer, 2006.

[7]D. Berg, K. Aas. Models for construction of multivariate dependence: A comparison study, *European Journal of Finance*, 15:639-659, 2009.

[8]N. Kolev, D. Paiva, "Copula-based regression models: A survey", *Journal of Statistical Planning and Inference,* 139 (2009) 3847-3856.

For wider interest

In everyday life people are faced with a variety of decision problems in selection of the best action from a set of possible alternatives (choices) based on a set of attributes (objectives or criteria). Humans have the upper limit capacity to group the large number of alternatives into five to nine classes. In order to overcome these shortcomings and additionally to perform a consistent overall alternative evaluation and ranking within a single class, we focus on developing of multi-criteria decision modelling methods. The decision modelling methods can be divided into two groups: quantitative and qualitative ones. Quantitative decision making methods are used when the objective is clearly defined. In these methods, it is possible to quantitatively measure the values of alternatives and their attributes. On the other hand, the qualitative decision making methods are applied in decision problems that are represented descriptively. Usually for such problems an explicit quantitative model does not exist. Qualitative problems are described based on the background knowledge of the experts. Consequently, it is difficult to define strict mathematical models for these problems. This results from insufficient data, imperfect knowledge about the problem or the numerous and loosely defined alternatives. Hence, we seek for decision methods that will be able to handle qualitative alternatives with various attribute inconsistencies, such as missing data, different data distributions, data sets, and data intervals.

Aligning business intelligence systems to end-user segments

Violeta Mirchevska[1,2], **Igor Korelič**[1]

[1] Result d.o.o., Ljubljana, Slovenia

[2] Jožef Stefan International Postgraduate School, Ljubljana, Slovenia

violeta.mircevska@result.si

Abstract. In this paper we present an approach for analysing end-user segments in business intelligence systems implicitly based on a data trace concerning history of user interaction with the system. The approach is part of a recommender system that provides content customized to the needs and preferences of the business intelligence system end-users.

Keywords: business intelligence systems, user segmentation, recommender systems

1 Introduction

Business intelligence systems are comprehensive systems which aim to accommodate all of the information needs of an organization. As stated by Luhn [1], one of the first authors to introduce the notion of business intelligence systems, the term *business* in business intelligence systems refers to "a collection of activities carried out for whatever purpose, be it science, technology, commerce, industry, law, government, defence, et cetera", whereas *intelligent system* refers to the underlying "facility serving the conduct of business (in the broad sense)". The notion of intelligence means that these systems perform advanced data processing activities in order to determine and disseminate interrelationships in business data in "such a way as to guide action towards a desired goal".

Business intelligence systems give users access to a variety of insights into the business data. These insights can significantly improve the quality of the

* Supervisor: Prof. Dr. Matjaž Gams

organization's decision-making, if only used in the right way. Considering the ever growing amount of business data and complexity of business decision making, the value that can be obtained by a business intelligence system is clear. However, practise shows that many business intelligence systems fail to fulfil users' needs. The most often stated reason for such failure is the lack of understanding of the end-users and, therefore, inability to align the business intelligence system to the needs of its end-user segments. Therefore, recommender system that will provide content in accordance with end-user needs and preferences is a necessity.

In this paper, we present an approach for determining end-user segments and their needs based on a data trace concerning history of user interaction, as part of a recommender system that provides content customized to the needs and preferences of business intelligence system end-users. An overview of the recommender system is presented in Section 2. The approach for determining end-user segments and their needs is described in Section 3. Section 4 presents an application of the approach to a real-life dataset.

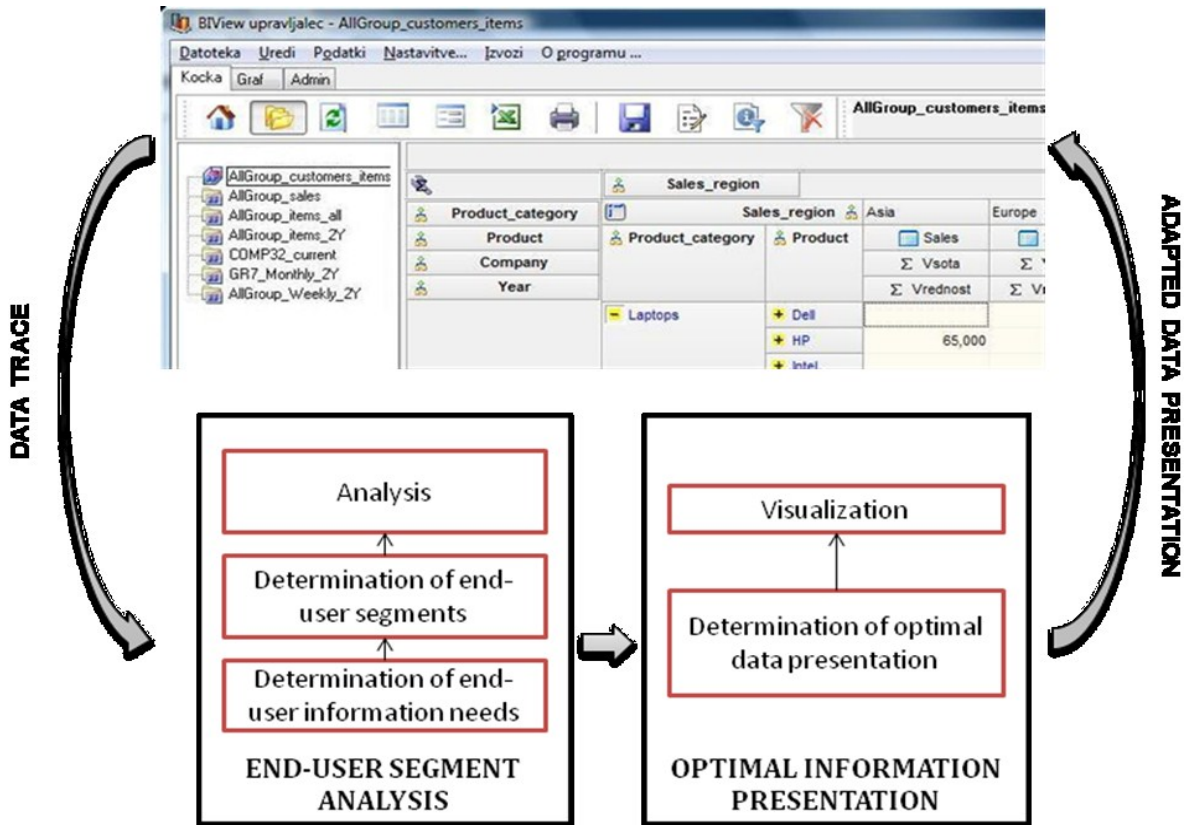

Figure 1 Methodology for recommending content to business intelligence system end-users based on their needs and preferences

2 Recommending content to business intelligence system end-users based on their needs and preferences

Figure 1 presents an overview of the methodology for recommending content to business intelligence system end-users based on their needs and preferences. The methodology can be divided in two parts: (1) determination of end-user segments and the needs of each identified segment, and (2) determination of optimal information presentation for each segment. In Section 3 we present the approach for determining end-user segments and their needs in detail. Korelič et al. [2] present the approach for determining optimal information presentation per end-user segment.

3 End-user segment analysis

The analysis of end-user segments can be divided into three steps: (1) determination of end-user profiles, (2) determination of end-user segments and (3) determination of the information needs of the users in each segment.

End-user profiles implicitly represent the information needs of end-users. End-user profile is a vector of the form P = (attr1, attr2, …, attrN), where each attribute represents the interest of the user for a particular piece of information. We estimate the interest of the user for a particular piece of information by the frequency of clicks the user makes of data views that contain that particular information.

Once the information needs of end-users are determined, the end-user segments are determined. Clustering algorithms [3] are used for this purpose. They divide data instances into natural groups. Each cluster represents one end-user segment.

The needs of each end-user segment are determined using the centroid of the cluster that represents the particular segment. The centroid of each cluster has the same vector form as the end-user profiles. The attributes in the centroid vector are used as a measure of the interest of the whole end-user segment for a particular piece of information.

4 Evaluation and results

We performed analysis of end-user segments on a data trace concerning sales-oriented decision-making. The data trace contains real-world interactions of 16 employees of one company with the application BIView [4] for a period of approximately two years. The data trace consists of records of the form R = (user, action, view, time) where *user* represents the user that interacted with BIView, action represents the action he/she performed, *view* represents the OLAP view that the user accessed and *time* represents the time when the action was performed.

Using the records in this data trace, the information needs of all 16 employees were represented by profiles of the form P = (detail level, time frame, time aggregation, view category), where

- *detail level* (DL) refers to the degree of interest in information at several detail levels: the company as a whole , individual branch offices or groups of branch offices
- *time frame* (TF) refers to the degree of interest in information at different time frames: current data or two year history
- *time aggregation* (TA) refers to the degree of interest in information of different time aggregations, such as weekly and monthly aggregation of data
- *view category* (VC) refers to the degree of interest in concrete view categories, such as sales per item, sales per product or sales as a whole

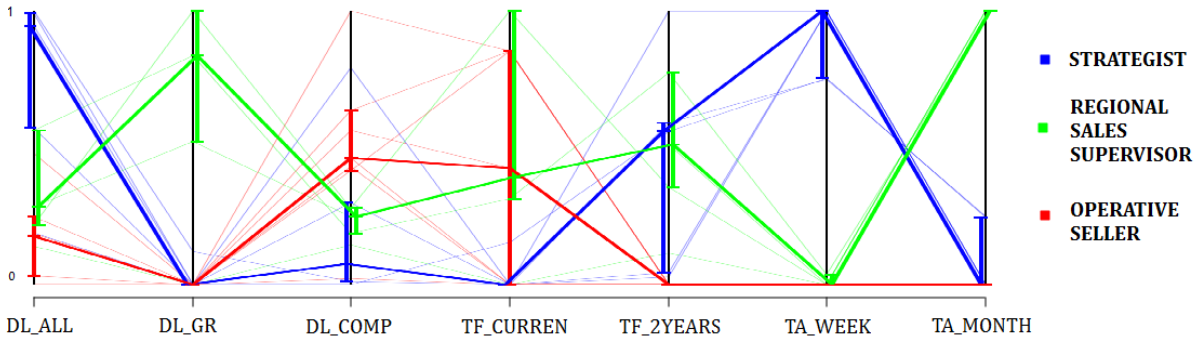

Figure 2 Determined end-user segments

The end-user profiles were input to a clustering algorithm by which three clusters were determined as presented in Figure 2.

Analyzing the centroids of each cluster, the following end-user segments were determined:

1. operative seller – deals with business at operational level with an own set of business partners and a subset of the organization articles with the aim to maximize profit,
2. regional sales supervisor – supervises sales of strategically important articles, interested in determination of potential deviations from business plans,
3. strategist – regulates products' life cycles, such as increase in sales, new product launches, withdrawal of articles on the market.

5 Conclusion

Business intelligence systems are comprehensive systems used by decision-makers at all levels for obtaining insight in the business data. Although their value is clear, practice shows that without proper adaptation of the presentation of information to the needs of the end-users, business intelligence systems may fall short in fulfilling users' expectations. In this paper we presented an approach for analysing end-users of business intelligence applications, as part of a recommender system that provides content customized to the needs and preferences of business intelligence system end-users. As user interactions with the business intelligence system are purposeful, data concerning such interactions contains information concerning end-user segments and their information needs. Using this data, end-user segments can be determined implicitly enabling recommendation of content suitable to end-user needs and preferences.

Acknowledgement

This work was partially financed by the European Union, European Social Fund.

References:

[1] H. P. Luhn. A Business Intelligence System. *IBM Journal*, October 1958

[2] I. Korelič, V. Rajkovič, M. K. Borštnar. Optimiyacija večrazsežnostnih podatkovnih modelov z uporabo metode večkriterijskega odločanja. *Zbornik konference Človek in organizacija*, March 2010

[3] I. H. Witten and E. Frank. *Data Mining: Practical machine learning tools and techniques, 2nd Edition*. Morgan Kaufmann, 2005.

[4] Result. BIView Business Intelligence Tool. Retrieved from www.biview.com. 2011

For wider interest

Business intelligence systems are comprehensive systems which aim to accommodate all of the information needs of an organization. As stated by Luhn (1958), one of the first authors to introduce the notion of business intelligence systems, the term *business* in business intelligence systems refers to "a collection of activities carried out for whatever purpose, be it science, technology, commerce, industry, law, government, defence, et cetera", whereas *intelligent system* refers to the underlying "facility serving the conduct of business (in the broad sense)". The notion of intelligence means that these systems perform advanced data processing activities in order to determine and disseminate interrelationships in business data in "such a way as to guide action towards a desired goal".

Although business intelligence systems provide valuable insights into business data, supporting decision-making at all levels, practice shows that without proper adaptation of the information presentation to the needs and preferences of the users these systems fall short in fulfilling users' expectations. The goal of this research is to develop a methodology that will present the right information to the right user at the right time in the business intelligence system.

The methodology for providing customized content to users is based on user segmentation, i.e. each user is assigned to a set of predefined segments based on his/her information needs and preferences. Although the information needs and preferences of the user can be obtained explicitly (e.g. by questionnaires), we aim at implicit determination of this data. As user interaction with the business intelligence system is purposeful, i.e. users perform actions in order to achieve concrete goals, we use data traces of past user interaction with the business intelligence system for determining end-users' needs and preferences. Based on the determined end-users' needs and preferences, user segments are determined by clustering. For each segment, we determine optimal data presentation using multi-criteria decision analysis.

Implementacija programa za evidentiranje in pomoč pri sestavljanju fragmentov stenskih poslikav

Miha Mlakar[1,2]**, Bogdan Filipič**[1,2] **(mentor)**

[1] Odsek za inteligentne sisteme, Institut »Jožef Stefan«, Ljubljana, Slovenija
[2] Mednarodna podiplomska šola Jožefa Stefana, Ljubljana, Slovenija
miha.mlakar@ijs.si, bogdan.filipic@ijs.si

Povzetek. Razvili smo program za evidentiranje in pomoč pri sestavljanju fragmentov stenskih poslikav za naročnika Restavratorski center. Za potrebe tega programa smo razvili algoritem za odstranjevanje ozadja iz slike fragmenta in vpeljali svojo diskretizacijo barv. S to diskretizacijo lahko sedaj uporabnik išče fregmente po barvah in njihovih deležih v fragmentih. Program se že uporablja in daje željene rezultate.

Ključne besede: stenska poslikava, fragmenti, evidentiranje, sestavljanje, Restavratorski center, algoritem

1 Uvod

Ob arheoloških izkopavanjih predstavlja velik izziv rekonstrukcija fresk, najdenih v obliki fragmentov. Naloga restavratorjev je zaradi različnih dejavnikov, kot je na primer slaba ohranjenost fresk, otežena. Sestavljanje v originalno stensko poslikavo je zahteven problem predvsem zaradi manjkajočih fragmentov ter preperelosti in ostalih poškodb fragmentov, s čimer se je izgubila pomembna informacija za sestavljanje. Posebej to velja za robove fragmentov, saj je težko ugotoviti, ali določena fragmenta sodita eden ob drugega, če so bili robovi poškodovani.

V preteklosti je v Restavratorskem centru, ki deluje v okviru Zavoda za varstvo kulturne dediščine Slovenije, Ljubljana prišlo do poskusa rekonstrukcije stenske poslikave iz fragmentov arheološkega najdišča »Turška mačka«, ki pa se je izkazal za prezapletenega. Gre za bogato arheološko najdišče iz časov rimskega mesta Celeia (slika 1). Fragmenti, ki so jih po izkopu prenesli v Restavratorski center, so različnih

barv in vsebujejo veliko vzorcev ter so relativno dobro ohranjeni. Restavratorski center se je zato za pomoč pri sestavljanju stenskih poslikav z omenjenega najdišča obrnil na Institut »Jožef Stefan«. Na podlagi pregleda obstoječega stanja smo skupaj z Restavratorskim centrom izbrali metodo za evidentiranje ter določili funkcije modula za pomoč pri sestavljanju fragmentov stenskih poslikav in nato razvili ustrezen računalniški program.

2 Opis problema

Do sedaj se je Restavratorski center problemov sestavljanja fragmentov stenskih poslikav loteval na bolj enostaven in manj sistematičen način. Tipičen postopek sestavljanja brez računalniške podpore je temeljil na tem, da so v posebej za to namenjen peskovnik postavili fragmente, ki so jih nato poskusili sestaviti. Peskovnik je primeren za sestavljanje zato, ker lahko kljub neravnemu ometu na hrbtni strani fragmentov dosežemo, da so lica fragmentov v isti ravnini. Poleg tega imajo fragmenti, zaradi različne debeline ometa, različno debelino in ker se v peskovniku lahko debelejše fragmente bolj vkoplje, imajo tako vsi fragmenti lice na isti višini. Tako postavljene fragmente se potem najlaže primerja in ugotovi njihovo sosednost v stenski poslikavi. Tak postopek je primeren za projekte, kjer fragmentov ni veliko. Pri projektu »Turška mačka« pa jih je preko 9000 in je zato tak način sestavljanja nemogoč.

3 Razvoj programa

3.1 Zasnova

Računalniški program, ki smo ga razvili za ta projekt je obsegal tri dele. Prvi je bil izdelava modula za evidentiranje fragmentov stenskih poslikav in za to namenjena podatkovna baza. Drugi del je bil implementitacija modula za pomoč pri sestavljanju fragmentov stenskih poslikav, ki bo podatke pridobil iz podatkovne baze predhodno evidentiranih fragmentov. Tretji del je vključeval implementacijo modula za posodabljanje podatkov v podatkovni bazi. S pomočjo teh modulov bo nato Restavratorki center poskusil rekonstruirati čim večji del stenske poslikave z omenjenega arheološkega najdišča.

Naloga modula za evidentiranje je bila sliko lica fragmenta obdelati, identificirati njene izbrane lastnosti in jo s pripadajočimi lastnostmi shraniti v podatkovno bazo. Sliko lica fragmenta je bilo za manjše fragmente mogoče dobiti z optičnim čitalnikom, za večje pa je bilo potrebno fotografiranje. Dobljeno sliko je bilo nato potrebno obdelati tako, da smo dobili točno obliko lica fragmenta, njegovo velikost in barve, ki jih fragment vsebuje. Za potrebe odstranjevanja ozadja in določanja barv lica fragmenta smo razvili algoritma, ki sta podrobno opisana v razdelkih 3.2 in 3.3.

Naloga modula za pomoč pri sestavljanju fragmentov (slika 1) je pomoč uporabniku pri sestavljanju originalne stenske poslikave. Modul v ta namen omogoča iskanje fragmentov po različnih kriterijih kot so velikost, identifikacijska številka, oznaka nahajališča fragmenta v skladišču, grafična predloga itn. Poleg iskanja modul omogoča premikanje, rotiranje, približevanje in združevanje fragmentov v skupine. Modul omogoča tudi različne vrste izpisov in podatkov o sestavljenih fragmentih, tiskanje postavitev fragmentov in prikaz števila in površine sestavljenih fragmentov.

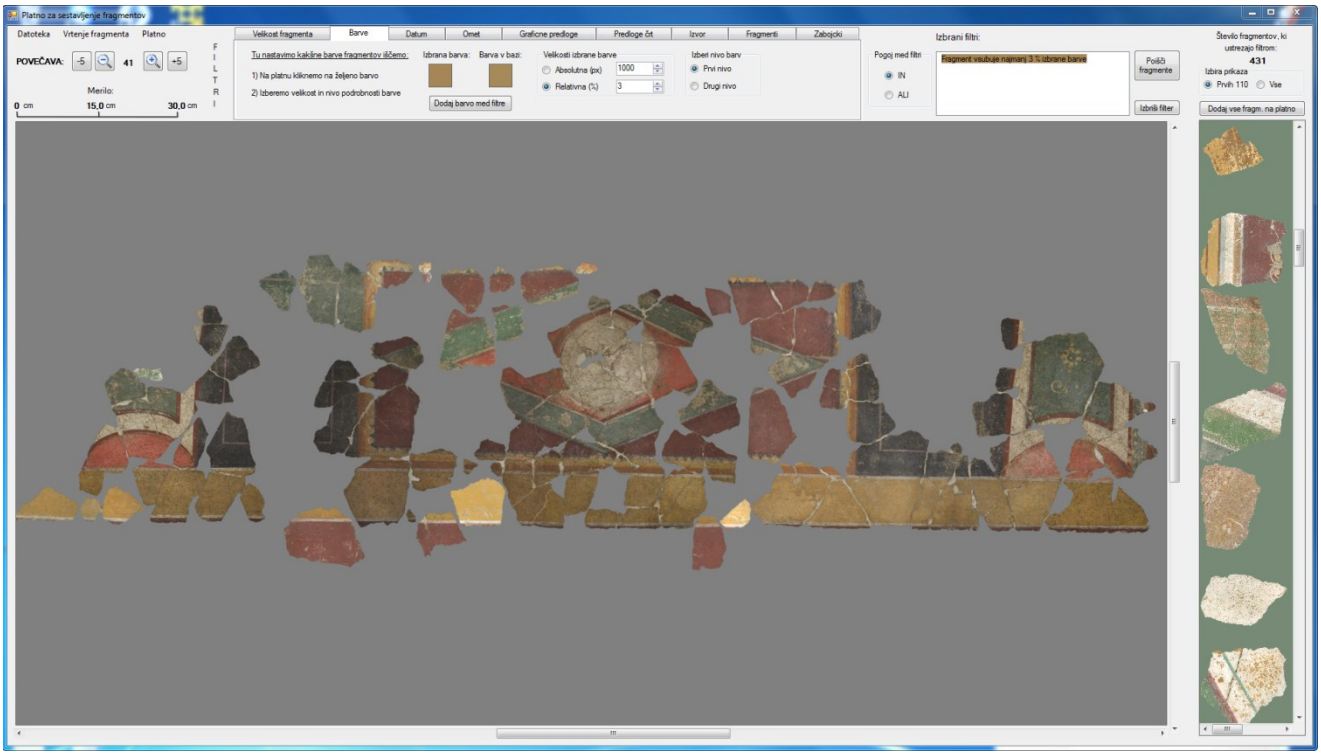

Slika 1: Računalniška podpora sestavljanja fragmentov stenskih poslikav

Tretji modul, ki smo ga razvili, je namenjen posodabljanju podatkov v podatkovni bazi in dodajanju značilnih grafičnih predlog ter značilnih črt, ki se pojavljajo na stenski poslikavi. S pomočjo teh predlog je mogoče enostavneje poiskati fragmente, ki pripadajo nekemu določenemu delu stenske poslikave.

3.2 Algoritem za odstranjevanje ozadja

Algoritmi za odstranjevanjevanje ozadja običajno temeljijo na metodi iskanja robov. Ta metoda na sliki išče prehode med barvami in tako določi, kje na sliki se nahaja rob. Na podlagi tako določenih robov je nato možno zaznati objekt na sliki in odstraniti ozadje tega objekta. V našem primeru odstranjujemo ozadje na slikah fragmentov, ki jih dobimo z optičnim čitalnikom ali digitalnim fotoaparatom. Ozadje je črno, vendar zaradi različne osvetlitve in manjših delcev barva ozadja ni enakomerna. Zato so se standardni algoritmi za odstranjevanja ozadja izkazali za neustrezne, saj ne odstranijo majhnih barvnih napak ozadja, ali pa odstranijo tudi dele fragmenta temne barve.

Zato smo naš algoritem zasnovali tako, da preverja razlike v barvah sosednjih točk (pikslov) in je relativno neobčutljiv na majhne barvne napake ozadja. Odpravo majhnih barvnih napak dosežemo tako, da namesto primerjave le dveh sosednjih pikslov obravnavamo pet pikslov v vrsti. Zanje nato izračunamo povprečno vrednost za vsako od treh barvnih komponent, ki sestavljajo piksel – rdečo, zeleno in modro. Ker vemo, da mora biti ozadje črno, lahko izračunamo odstopanja od črne barve. Na ta način se ob pravilni določitvi meje oziroma ugotovitvi, kdaj je odstopanje preveliko, da zelo zanesljivo določiti, kdaj naletimo na rob fragmenta in kdaj le na barvno napako ozadja.

3.3 Algoritem za določanje barv fragmenta

Ko je slika fragmenta obdelana tako, da je vidno le lice fragmenta, je potrebno ugotoviti barvno sestavo tega fragmenta. Fragmentom je potrebno določiti barve in njihovo intenzivnost zato, da je kasneje moč iskati skupine fragmentov istih barv. Za iskanje po barvah je bilo pomembno, da lahko iščemo točno določeno barvo, ali pa tudi barve, ki so blizu tej barvi. To pa zato, ker se pri iskanju določene barve

zaradi različne obledelosti fragmentov pogosto zgodi, da sta si dve barvi, ki sta bili prvotno enaki, sedaj le podobni. Zato je potrebno barvno lestvico diskretizirati. Prvi poskus diskretizacije barv z diskretizacijo zapisa barv z zapisom RGB (red, green, blue) se ni izkazal za primernega, saj za RGB lestvico ne velja, da je npr. svetlo modra blizu modri barvi. Zato barve diskretiziramo glede na lestvico HSB (hue, saturation, brightness oz. barvni odtenek, nasičenost, svetlost). Za vsak piksel lica fragmenta najprej preverimo njegovo svetlost in če je vrednost mejna, je piksel bel ali črn. Za ostale vrednosti svetlosti nato preverimo nasičenost. Nasičenost določa živost barve in če je ta dovolj nizka, to pomeni, da je piksel siv. Za ostale vrednosti piksle razdelimo glede na vrednost barvnega odtenka na pasove. Vsak pas nato razdelimo še na dva dela glede na vrednost nasičenosti in s tem dobimo svetlejši oziroma temnejši odtenek barve. Predpišemo dve širini pasu in s tem omogočimo dve stopnji natančnosti iskanja po določeni barvi. Diskretizacija barv, ki jo dobimo na ta način, se je izkazala za ustrezno pri iskanju fragmentov po barvi.

4 Zaključek

Za projekt sestavljanja fragmentov stenskih preslikav iz arheološkega najdišča »Turška mačka« smo razvili program za evidentiranje in pomoč pri sestavljanju fragmentov stenskih poslikav. Program je namenjen restavriranju fragmentov stenskih poslikav in je že v uporabi v Restavratorskem centru v Ljubljani. Trenutno so evidentirali in v podatkovno bazo shranili podatke skoraj 3000 fragmentov. Prvi odzivi uporabnikov so ugodni.

5 Literatura

[1] H. C. Leitao, J. Stolfi. A multiscale method for the reassembly of two-dimensional fragmented objects. IEEE Transactions on Pattern Analysis and Machine Intelligence, vol. 24, No. 9, pp. 1239 – 1251, Sept. 2002.

[2] T. Lindeberg. Edge detection and ridge detection with automatic scale selection, Int. J. of Computer Vision, vol 30, No. 2, 1998.

[3] Y. Lu. Interactive Reconstruction of Archaeological Fragments in a Collaborative Environment. COMP6720 Assignment, The Department of Computer Science, Faculty of Engineering and Information Technology, Australian National University, October, 2005.

Za širši interes

V prispevku opisujemo program za evidentiranje in pomoč pri sestavljanju fragmentov stenskih poslikav. Program je bil razvit za naročnika Restavratorski center iz Ljubljane, za pomoč pri sestavljanju fragmentov stenskih poslikav, ki so jih našli na najdišču »Turška mačka«. Gre za bogato arheološko najdišče iz časov rimskega mesta Celeia. Fragmentov, ki so sestavljali stensko poslikavo je več kot 9000 in so relativno dobro ohranjeni. Program omogoča detekcijo in zapis lastnosti posameznih fragmentov v za to namenjeno podatkovno bazo. Poleg tega nudi program tudi navidezno okolje za zlaganje fragmentov. To navidezno okolje nadomesti peskovnik, v katerem so do sedaj brez računalniške podpore sestavljali fragmente. V pomoč zlaganju je omogočeno iskanje po že evidentiranih fragmentih po različnih filtrih. Ti omogočajo iskanje po velikosti, barvi, grafičnih predlogah, značilnih črtah. Posebej za ta projekt smo razvili algoritem za odstranjevanje ozadja slike z licem fragmenta in svojo diskretizacijo barvne lestvice, ki omogoča dve natančnosti iskanja fragmentov po relativni vsebnosti določene barve. Program že aktivno uporabljajo za ta projekt in so po prvih odzivih z njegovim delovanjem zadovoljni.

Connecting Contiki enabled Versatile Sensor Nodes via ISM band radio

Zoltan Padrah, Carolina Fortuna

Supervisor: doc. dr. Mihael Mohorcic

Department of Communication Systems, Jožef Stefan Institute, Ljubljana, Slovenia
Jožef Stefan International Postgraduate School, Ljubljana, Slovenia

firstname.lastname@ijs.si

Abstract. In this demonstration, we show message exchange between Versatile Sensor Nodes (VSN) which run the Contiki operating system, and use the Texas Instruments CC1101 ISM band radio. We explain our port of the Contiki on VSN with emphasis on wireless communication. VSN is a modular sensor node platform featuring several communication interfaces. In the demonstration, we use the CC1101 radio to connect VSNs and RS232 to connect VSNs to PCs. The application used to illustrate the functioning of the system sends messages from a computer and displays them on the screen of all other computers attached to VSNs which received that message

Keywords: wireless sensor node, wireless communications, operating systems

1 Introduction

Wireless sensor networks are increasingly used to monitor certain phenomena or activities for longer time periods and/or in remote locations. Such networks are composed of wireless sensor nodes and sensors that are attached to them. These sensors measure various physical quantities which are transmitted via sensor nodes to the processing infrastructure.

Generally, such nodes consist of a microcontroller, a radio transceiver, power source, sensors, and in some cases external memory. The microcontroller runs the software of the sensor node and controls all the other components of the node. Usually it contains the CPU, embedded RAM and flash memory, and a large number of peripherals, including analog to digital and digital to analog converters.

The latter components are useful for retrieving the data from analog sensors. The radio transceiver is used for communication between the nodes. As sensor nodes are expected to operate autonomously for long periods of time, power efficiency is critical. Most common power sources are batteries and solar cells.

There are two main categories of software used on wireless sensor nodes: custom software and operating systems. The latter ones provide a set of hardware and application independent functionalities at the expense of the maximum theoretically achievable performance. As examples of most widely used operating systems for wireless sensor nodes are TinyOS and Contiki. Currently, there are several commercially available sensor nodes, but such nodes are often limited in their flexibility and reconfigurabily. Surveys in the domain of wireless sensor networks have shown that most wireless sensor nodes used today are highly application-specific [1].

In order to allow prototyping of a wide range of sensor applications, without developing each time a new node, we developed a fully reconfigurable sensor node platform called Versatile Sensor Node (VSN). We decided to port the Contiki OS on our hardware platform due to its advantages: small memory footprint, support for a wide range of network protocols, high portability, multi-tasking options, etc. To create the port, we implemented the architecture specific part of Contiki's clock module, developed appropriate communication drivers and integrated our source files into Contiki's build system.

This demonstration presents one of basic functionalities of a wireless sensor node, i.e. transmitting messages between nodes. Each node receives messages from a PC via a RS232 link, and transmits those messages through its CC1101 radio interface. When another node receives a message on the CC1101 radio interface, it sends the message via the RS232 link to the PC. Programs running on PCs send and display the messages involved in the communication.

In the rest of the paper, we describe VSN and the Contiki OS used in this application, we detail the port, and finally we conclude by summarizing the demonstration.

2 Versatile Sensor Node

The wireless sensor node presented in this demonstration has been designed to be a multipurpose sensor node platform: it can be easily adapted to many applications due to its modular design and the available expansion connectors[1]. The main module of the node is called the Versatile Sensor Core module (VSC) which hosts the microcontroller. The block diagram of this module is depicted in Figure 1.

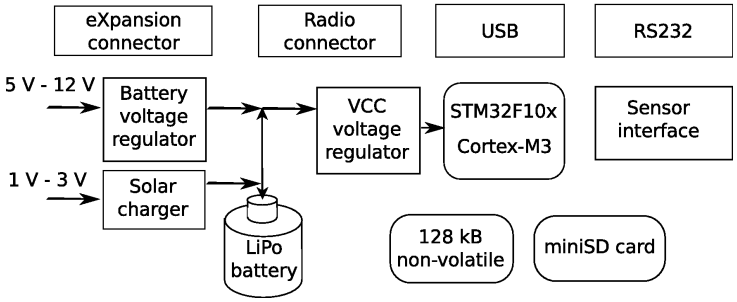

Figure 1: Versatile Sensor Node core module block diagram

The versatile sensor node employs a STM32F10x microcontroller, having a 32-bit ARM Cortex-M3 processor core. The microcontroller has 64 kB of RAM and 512 kB of flash memory, and supports a variety of interfaces: USB, RS232, UART, IrDA, SPI, I2C, 12 bit ADC, DAC.

The core module of the versatile sensor node has two expansion connectors: one designed for radio modules, and one for various other purposes. As radio expansion modules, sub-gigahertz and 2.4 GHz-band transceivers are available (i.e. using CC1101 and CC2500 radio chips), but alternatively external XBee or Bluetooth modules can be used as add-on boards to the radio transceiver modules. As examples of various expansion boards we mention the debugging and programming board, Ethernet to serial converter, WiFi to serial converter, protoboarding modules and the additional power supply module.

Software development for the versatile sensor node can be performed by using standard debug protocol (JTAG) and opensource tools (OpenOCD, CodeSourcery G++ lite and Eclipse). In this demonstration, we use the radio module with CC1101 chip from Texas Instruments, in the 868 MHz ISM band.

[1]A presentation about the VSN can be found online at http://videolectures.net/wsn2010_mihelin_vsn/

3 Porting Contiki Operating System To VSN

On the VSN platform we decided to use Contiki OS [2], which offers many services and functionalities to the applications running on it, two of which are particularly important for this demonstration. First, because the operating system supports multi-tasking, various functionalities can be separated to different tasks. For example, a radio driver can be separated from the main application. This simplifies the structure of the program. The other aspect is the large range of supported communication protocols, starting from a simple serial line driver, to various networking protocols such as uIP and TCP.

As we mentioned before, Contiki is highly portable. This portability is achieved by separating all the hardware dependent program code from the rest of the system. In order to support new hardware, just a set of interfaces have to be implemented[2]. Implementing the hardware-specific functions of the clock module and integrating the port with the Contiki's build system makes the base system functions (processes and basic timers) work. Input from the RS232 line is handled by a hardware-dependent code path feeding the generic serial-line module. Output to RS232 is implemented by defining the hardware-dependent functionality of a function (_write()), used by the C library of the compiler. Contiki has a dedicated interface for radio drivers. This interface provides functions for sending packets, signaling if a packet has been received, reading any received packet and turning the radio on and off. Our CC1101 driver implements such interface, so in the future it can be easily used with different communication stacks.

Figure 2: Illustration of the used communication stack

[2]See presentation about porting Contiki at http://www.sics.se/~adam/contiki-workshop-2007/workshop07porting.ppt

4 The Demonstration

The demo uses the CC1101 radio to connect VSNs and RS232 to connect VSNs to PCs. The application used to illustrate the functioning of the system sends messages from a computer and displays them on the screen of all other computers attached to VSNs that received that message. In this way we demonstrate the communication capabilities of our node and the working Contiki operating system port. The block diagram of the setup is depicted on Figure 2. The application that runs on the top of Contiki passes each message received on one communication channel (RS232 or radio) to the other communication channel.

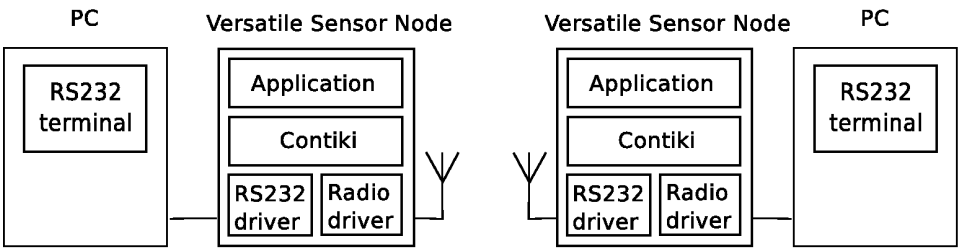

Figure 3: The demonstration setup

Figure 3 depicts the demonstration setup. The user interface of the chat application consists of a terminal emulator running on a PC. Initially only a prompt character(>) is displayed. Messages can be entered by using the keyboard of the PC, and they can be sent by pressing the Enter key. Each message will be sent to all the nodes in the transmission range of the radio. After a message is sent, a new prompt character should appear. Received messages appear on the terminal as new lines of text. However, because the application does not use a protocol that guarantees message delivery, it is possible that a message will be lost.

References

[1] J. Yick, B. Mukherjee, and D. Ghosal, "Wireless sensor network survey," *Computer Networks*, vol. 52, no. 12, pp. 2292 – 2330, 2008. [Online]. Available: http://www.sciencedirect.com/science/article/B6VRG-4S8TBBT-1/2/b242d2fd1f6d2cf5c6fce0a24c4cb029

[2] A. Dunkels, B. Gr ¨ onvall, and T. Voigt, "Contiki - a lightweight and flexible operating system for tiny networked sensors," in *Proceedings of the First IEEE Workshop on Embedded Networked Sensors (Emnets-I)*, Tampa, Florida, USA, Nov. 2004. [Online]. Available: http://www.sics.se/~adam/dunkels04contiki.pdf

For wider interest

Wireless sensor nodes are a type of hardware, typically incorporating three functions:

- measurement of physical quantities, by employing sensors
- performing simple processing
- communication with other sensor nodes, by using wireless technologies

Such nodes are typically deployed as a network, in order to gather measurement data from a given area.

The Versatile Sensor Node, developed by the collaboration of Jozef Stefan Institute and Isotel d.o.o., is a highly reusable sensor node. Its applications include:

- environmental monitoring and lightning control
- temperature monitoring in stables
- remote observation of sport-fishing conditions
- beehive local climate monitoring
- multispectral imaging and data harvesting over Unmanned Aerial Vehicle (UAV)

Currently we are preparing to use Versatile Sensor Nodes for monitoring the radio spectrum usage in an area. The gathered data could be used in research helping the creation of more efficient radio communication systems. For more information, visit SensorLab's web page: sensorlab.ijs.si.

Sprotno izbiranje podatkov

Dejan Petelin[1,2], **Juš Kocijan**[1,3] **(mentor)**

[1] Odsek za sisteme in vodenje, Inštitut Jožef Stefan, Ljubljana, Slovenija

[2] Mednarodna podiplomska šola Jožefa Stefana, Ljubljana, Slovenija

[3] Univerza v Novi Gorici, Nova Gorica, Slovenija

dejan.petelin@ijs.si

Povzetek. Sprotne meritve omogočajo, da imamo na voljo vse več podatkov, med katerimi je veliko podvojenih oziroma odvečnih. To pomeni, da navadno sistem lahko opišemo tudi z manjšim številom podatkov, zato je njihov izbor zelo pomemben. Za prikaz izbire podatkov smo uporabili modele na podlagi Gaussovih procesov, saj temeljijo na podatkih in so enostavni za uporabo. Poleg tega prikazujejo tudi podatek o zaupanju v napoved, ki je zelo uporaben pri določanju informativnosti novega vhodnega podatka. Predlagano metodo izbire podatkov za modeliranje smo preverili tudi na praktičnem primeru modeliranja procesa priprave plina.

Ključne besede: sprotno izbiranje podatkov, modeli na podlagi Gaussovih procesov, Gaussovi procesi.

1 Uvod

S hitrim razvojem tehnologije se povečuje tudi količina podatkov, ki jih želimo obdelati. Med temi podatki je lahko veliko podvojenih oziroma odvečnih podatkov. To pomeni, da lahko sistem opišemo tudi z manjšim številom podatkov kot jih imamo na voljo. Pri tem je zelo pomembna izbira pravih podatkov oziroma tistih, ki nosijo največ informacije. V veliko primerih se proces oziroma njegove zakonitosti s časom tudi spreminjajo, zato je izbiro podatkov oziroma model na podlagi uporabljenih podatkov potrebno sproti prilagajati. Pomembnost tega problema je izpostavljena v strokovni literaturi, na primer v [1].

Za prikaz sprotnega izbiranja podatkov smo uporabili modele na podlagi Gaussovih procesov ali krajše GP modele, ki temeljijo na merjenih podatkih in so

enostavni za uporabo. Njihova glavna prednost je dostopen podatek o zaupanju v napoved. Ta dodatni podatek je zelo uporaben pri ocenjevanju informativnosti oziroma novosti novega vhodnega podatka.

2 Modeli na podlagi Gaussovih procesov

Model na osnovi Gaussovih procesov je neparametrični model, kar pomeni, da neznanega sistema ne poskuša opisati s prilagajanjem parametrov (navadno velikega števila) baznih funkcij, ki sestavljajo model. GP model je sestavljen iz vhodno-izhodnih podatkov, ki opisujejo obnašanje opisovanega sistema, in kovariančne funkcije, ki pove v kakšni medsebojni odvisnosti so ti podatki oz. kakšne funkcije so verjetno uporabljene pri opisu sistema. Izhod modela je verjetnostna porazdelitev v obliki Gaussove porazdelitve, pri čemer je srednja vrednost najbolj verjetna vrednost izhoda, varianco pa lahko interpretiramo kot zaupanje v to napoved. Izražanje zaupanja v napoved je lastnost, ki GP model najbolj loči od ostalih metod za modeliranje. Poleg tega se GP model zelo dobro obnese pri primerih, kjer je malo podatkov, kar pomeni, da lahko opišemo področja, za katera je tipično pomanjkanje podatkov.

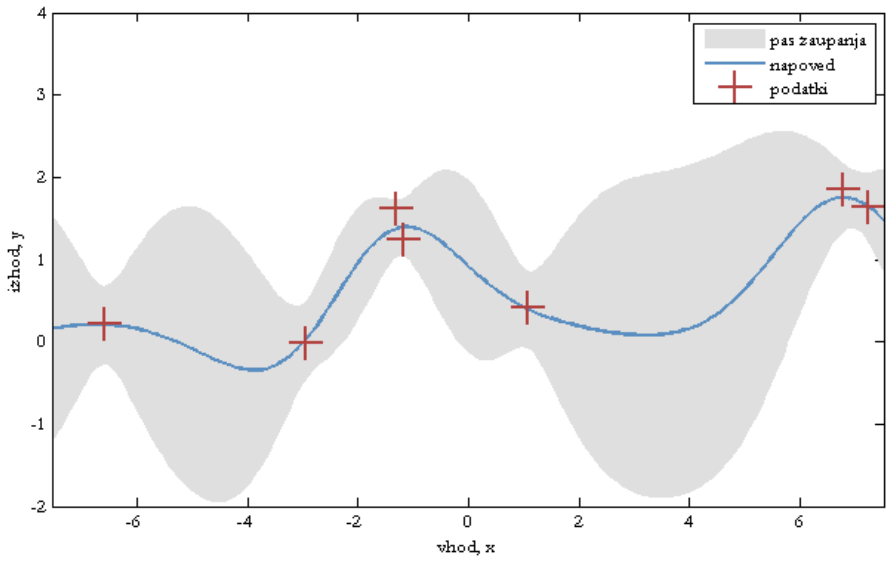

Slika 1: Napoved GP modelov: poleg srednje vrednosti (napovedi) dobimo tudi 95% pas zaupanja v napoved (sivi pas)

Kot smo že omenili, GP model temelji na podatkih, kar pomeni, da je potrebno določiti le kovariančno funkcijo, ki odraža korelacijo med vhodi. Kovariančna funkcija je lahko katerakoli funkcija, ki tvori semi-pozitivno definitno matriko. Z izbiro ustrezne kovariančne funkcije lahko enostavno vpeljemo naše predznanje o

sistemu. Če predznanja o sistemu nimamo, po navadi uporabljamo Gaussovo kovariančno funkcijo. Gaussova kovariančna funkcija je gladka, saj je neskončno mnogokrat odvedljiva, in stacionarna, kar pomeni, da je njena vrednost odvisna le od razdalje med vhodnima podatkoma. Poleg tega GP model omogoča tudi avtomatsko določanje ustreznosti (ang. automatic relevance determination - ARD) posamezne dimenzije vhodnih podatkov. Tako so nepomembne dimenzije oziroma regresorji vhodnih podatkov avtomatsko zanemarjeni [2].

Navadno ima kovariančna funkcija tudi določeno število parametrov, ki omogočajo dodatno prilagoditev podatkom GP modela. Imenujejo se hiperparametri, s čimer se poudari, da so to parametri neparametričnega modela. Za čim boljšo prilagoditev podatkom oziroma sistemu je potrebno vrednosti hiperparametrov optimizirati. Za to se najpogosteje uporablja metoda največje podobnosti (ang. maximum likelihood - ML).

Pogosto uporabljena metoda za optimizacijo hiperparametrov GP modela je metoda konjugiranih gradientov (angl. conjugate gradient), ki pa se izkaže za neučinkovit postopek v primeru večjega števila podatkov ali večjega števila hiperparametrov. V teh primerih se kot bolj učinkovite izkažejo stohastične metode, na primer evolucijski algoritmi [3], katerih končni rezultat ni odvisen od začetnih vrednosti, kot pri deterministčnih metodah, saj »naključno« iščejo vrednosti po celotnem prostoru.

3 Sprotna izbira podatkov

Izbrani podatki služijo kot učni podatki GP modela. Imenujemo jih množica izbranih podatkov ali krajše množica IP. Informativnost izbranih podatkov ocenjujemo preko kakovosti GP modela. Bolj kot je kakovosten GP model, bolj kakovostni so podatki.

Postopek sprotnega izbiranja podatkov z vsakim novim podatkom lahko opišemo z naslednjimi koraki. Najprej na podlagi trenutnega modela novemu vhodnemu podatku ocenimo porazdelitev izhoda. Če je razlika srednje vrednosti in dejanske vrednosti izhoda, torej napaka ocene, večja od določene, vnaprej izbrane meje, vhodni podatek dodamo v množico IP, saj zanj do sedaj nismo znali napovedati prave izhodne vrednosti. Torej se bomo z vključitvijo podatka v množico IP naučili

nekaj novega. Če je napaka manjša od določene meje, se o vključitvi vhodnega podatka v množico IP odločimo na podlagi ocenjene variance napovedi. V primeru velike variance vhodni podatek vključimo v množico IP, kajti model je sicer dobro ocenil izhodno vrednost, vendar očitno ni prepričan v to oceno. Najverjetneje zaradi pomanjkanja podatkov iz tega območja. Če pa je tudi varianca manjša od določene meje, podatka ne vključimo v množico IP, saj GP model že dovolj dobro oceni izhodno vrednost.

Velikost množice IP lahko tudi omejimo, saj navadno težko določimo ravno pravo mejo napake in variance, da bi dosegli tudi optimalno število podatkov glede na problem, s katerim se ukvarjamo. Kadar število podatkov v množici IP preseže določeno velikost, vsakemu podatku v množici IP z metodo ML ocenimo vrednost, ter nato najslabše ocenjenega odstranimo.

Po vsakem vključevanju novega podatka v množico IP se izvede še optimizacija hiperparametrov, s čimer se GP model prilagodi podatkom. Tako tudi omogočimo čim boljšo nadaljnjo izbiro podatkov. Podrobnejši opis celotnega postopka se nahaja v [4].

4 Primer

Za prikaz sprotnega izbiranja podatkov smo uporabili proces priprave plina, imenovan tudi ločevalnik plina in tekočine, ki se uporablja za proces kemijske nevtralizacije bazičnih odplak. Kvaliteta raztapljanja CO_2 v bazični odplaki in s tem učinkovitost nevtralizacije, je odvisna od tlaka plina. Zato tlak plina nastopa kot izhodni podatek procesa. Kot vhodni podatki nastopajo nivo vode v posodi, odprtost ventila in izhodni podatek (tlak) predhodne meritve. [5]

Na voljo smo imeli dve množici meritev: učno in testno. Vsaka množica vsebuje 14.520 meritev, ki so bile izmerjene med delovanjem procesa v procesnem laboratoriju Odseka za sisteme in vodenje na Institutu Jožef Stefan.

Metodo sprotnega izbiranja podatkov smo preverili tako, da smo najprej izbrali 1.000 podatkov iz učne množice, nato pa smo z dobljenim modelom iz izbranih

podatkov izvedli simulacijo z vhodnimi podatki iz testne množice. Na sliki 2 lahko vidimo, da je predlagana metoda uspešno izbrala najinformativnejše podatke, saj je rezultat simulacije glede na število izbranih podatkov zadosti dober.

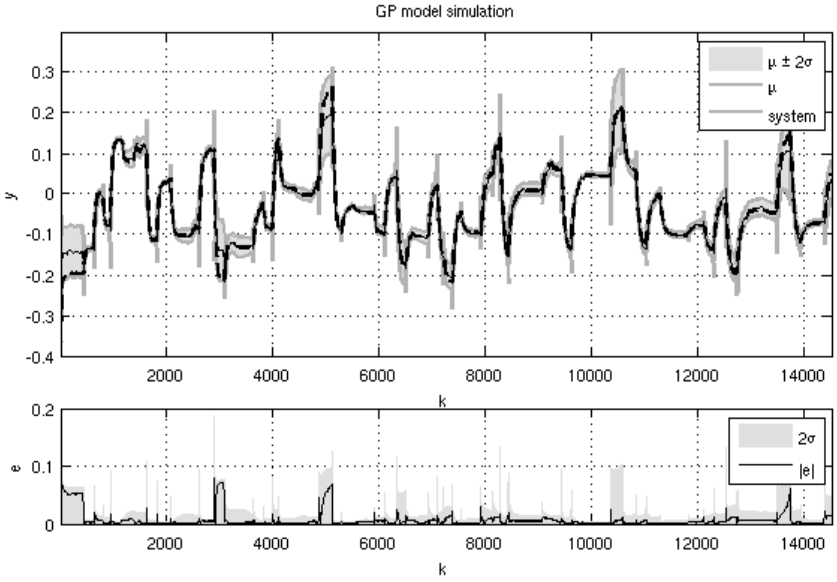

Slika 2: Rezultat simulacije in primerjava s testno množico meritev (zgornja slika) in prikaz napake s pasom zaupanja v napoved za rezultate simulacije (spodnja slika)

5 Zaključek

Za sprotno izbiranje podatkov smo predlagali metodo na podlagi GP modelov. Metodo izbiranja smo prikazali na praktičnem primeru modeliranja na podlagi meritev izmerjenih na procesu priprave plina, ki obsega 14.520 podatkov. Metoda se je izkazala za uspešno, saj je rezultat simulacije na podlagi izbranih 1.000 podatkov dober.

Literatura:

[1]L. Ljung. Perspectives on system identification. V *Proceedings of the 17th World Congress The International Federation of Automatic Control*, Seoul, Korea, 2008

[2]C. E. Rasmussen, C. K. I. Williams. *Gaussian processes for machine learning*. The MIT Press, 2006

[3]D. Petelin, J. Kocijan. Evolving Gaussian process models. V *EAIS 2011, IEEE Workshop on Evolving and Adaptive Intelligent Systems*, Paris, France, 2011

[4]D. Petelin, B Filipič, J. Kocijan. Optimization of Gaussian process models. V *Adaptive and natural computing algorithms. Part 2: 10th International Conference, ICAANGA 2011*, Ljubljana, Slovenia, 2011

[5]J. Kocijan, B. Likar. Gas-liquid separator modelling and simulation with Gaussian-process models, *Simulation Modelling Practice and Theory*, 2008, vol. 16, no. 18, str. 910-922

Za širši interes

S hitrim razvojem tehnologije se povečuje tudi količina podatkov, ki jih želimo obdelati. Med temi podatki je lahko veliko podvojenih oziroma odvečnih podatkov. To pomeni, da lahko sistem opišemo tudi z manjšim številom podatkov kot jih imamo na voljo. Pri tem pa je zelo pomembna izbira pravih podatkov oziroma podatkov, ki nosijo največ informacije. V veliko primerih se proces oziroma njegove zakonitosti s časom tudi spreminjajo, zato je izbiro podatkov oziroma model na podlagi uporabljenih podatkov potrebno sproti prilagajati

Za sprotno izbiranje podatkov predlagamo modele na podlagi Gaussovih procesov ali krajše GP modele, saj temeljijo na podatkih in so enostavni za uporabo. Njihova glavna prednost je dostopen podatek o zaupanju v napoved, ki jo podajajo. Ta dodatni podatek je zelo uporaben pri ocenjevanju informativnosti oziroma novosti novega vhodnega podatka.

Ker GP modeli temeljijo na podatkih, je izbiranje podatkov zelo enostavno, saj izbrani podatki služijo kot učni podatki GP modela. Imenujemo jih množica izbranih podatkov ali krajše množica IP. Tako lahko informativnost izbranih podatkov ocenjujemo preko kakovosti GP modela. Bolj kot je kakovosten GP model, bolj kakovostni so podatki.

Poleg izbiranja podatkov se z uporabo metode avtomatskega določanja ustreznosti in sprotno optimizacijo vrednosti hiperparametrov samodejno določa tudi pomembnost posameznih dimenzij vhodnih podatkov oziroma regresorjev. Nepomembni regresorji so tako s časom lahko tudi izključeni iz sprotnega izbiranja.

Pristop podatkovnega rudarjenja časovnih vrst za detekcijo zdravstvenih težav pri starejših

Bogdan Pogorelc[1,2,3]

[1] Institut Jožef Stefan, Odsek za inteligentne sisteme, Ljubljana, Slovenija

[2] Špica International d.o.o., Ljubljana, Slovenija

[3] Mednarodna podiplomska šola Jožefa Stefana, Ljubljana, Slovenija

bogdan.pogorelc@ijs.si

Povzetek. Članek predstavlja pristop podatkovnega rudarjenja časovnih vrst za detekcijo zdravstvenih težav in padcev pri starejših z namenom podaljševanja njihovega samostojnega življenja. Gibanje starejših je zajeto s sistemom za zajem gibanja in izhodne časovne vrste koordinat so modelirane s kombinacijo algoritmov k-najbližjih sosedov in dinamičnega ukrivljanja časa (DTW) z namenom prepoznave specifične zdravstvene težave ali padca. Pristop je splošen, ker za atribute uporablja vse izmerljive kote sklepov namesto specifičnih atributov za posamezne bolezni. Kljub temu doseže visoko klasifikacijsko točnost, podobno specifičnemu pristopu.

Ključne besede Zdravstvene težave, hoja, podatkovno rudarjenje, dinamično ukrivljanje časa.

1 Uvod

Po napovedih [1] naj bi do leta 2050 v razvitih državah živelo šestkrat toliko ljudi nad 80 let kot danes. Starejši navadno živijo izolirani od potomcev, zato v primeru bolezni ali poškodbe težko dobijo pravočasno pomoč. Namen te študije je razviti tehnologije, ki bi olajšale samostojno življenje starejših.

Predlagamo pristop podatkovnega rudarjenja k inteligentnemu in vseprisotnemu sistemu nadzora zdravja. Cilj pristopa je prepoznati nekaj najpogostejših in najpomembnejših bolezni starejših, ki so lahko razpoznane z opazovanjem in analizo karakteristik njihovega gibanja. Gre za dvostopenjski pristop; v prvi stopnji sistem klasificira aktivnosti uporabnika v pet razredov, vključno z dvema vrstama padcev. V drugi stopnji pa klasificira vzorce hoje v 5 različnih zdravstvenih stanj,

eno zdravo in štiri nezdrave. Gibanje uporabnika je zajeto s sistemom za zajem gibanja, ki sestoji iz značk pritrjenih na telo in senzorjev nameščenih v stanovanju. Izhodne časovne vrste koordinat so modelirane s predlaganim algoritmom, da bi razpoznali specifično zdravstveno težavo.

V sorodnem delu je zajem gibanja navadno narejen z inercialnimi senzorji [[2], [5]], s strojnim vidom in tudi s specifičnim senzorjem za merjenje kota upognjenosti sklepa [[3]] ali z elektromiografijo [[4]]. V naši študiji smo uporabili sistem (infrardeče) IR kamere z značkami pritrjenimi na telo. Ne naslavljamo samo razpoznave značilnih aktivnosti, kot je hoja, sedenje, ležanje, itn., kot je realizirano npr. v [[6], [8]], ampak tudi razpoznavamo zdravstvene težave. Z uporabo podobnega sistema za zajem podatkov so v [[7]] ločevali med hemiplegijo in diplegijo.

Bolj pogosti pristop iz sorodnega dela je zajem podatkov s sistemom za zajem gibanja in kasnejša ročna analiza podatkov[[3], [4], [9]]. Tak pristop ima pomanjkljivost v primerjavi z našim, da zahteva stalno pregledovanje strokovnjakov.

Študija [**Error! Reference source not found.**] ločuje me istimi petimi zdravstvenimi težavami kot v tem članku predstavljena študija, je pa zaradi 13 medicinsko definiranih atributov bolj specifična. V tem članku uporabljamo splošne atribute kotov med sklepi. Zato so enaki atributi in enake klasifikacijske metode uporabljene tako za i) razpoznavanje aktivnosti in ii) razpoznavanje zdravstvenih težav.

2 Materiali in metode

Ciljne aktivnosti in zdravstvene težave za detekcijo. Vse situacije, ki jih prepoznavamo, je predlagal sodelujoči medicinski strokovnjak na osnovi pogostosti nad 65 let starosti, medicinske pomembnosti in možnosti razpoznavanja iz gibanja. Predlagan sistem uporablja dvostopenjski sistem za razpoznavo pomembnih situacij. V prvem koraku razpoznava med petimi aktivnostmi: padec zaradi nesreče, padec zaradi bolezni, hoja, vstajanje/sedanje, uleganje/vstajanje. V drugem koraku razpoznane hoje iz prvega koraka klasificira kot: Parkinsonovo bolezen, hemiplegijo, bolečine v hrbtu, bolečine v nogah ali normalno hojo. Oba koraka sta

izvedena z metodo k-najbližjih sosedov in dinamičnim ukrivljanjem časa (dynamic time warping oz. DTW) za mero podobnosti.

Atributi za podatkovno rudarjenje. Meritve sestavljajo pozicije koordinat v x,y,z za 12 značk nošenih na ramenih, komolcih, zapestjih, kolkih, kolenih in gležnjih, zajete s sistemom za zajem gibanja Smart z 10Hz. Primeren prikaz uporabnikovega gibanja je bil pomemben del naše študije. Gibanje mora biti predstavljeno z enostavnimi in splošnimi atributi, da bo klasifikator s temi atributi delal dobro tudi na drugačnih gibanjih, saj zajamemo le majhen del vseh možnih gibanj. Ob upoštevanju navedenega smo zasnovali atribute kot kote med sosednjimi deli telesa:

- kot levega in desnega ramena glede na zgornji del trupa v trenutku *t*,
- kot levega in desnega kolka glede na spodnji del trupa,
- kot med spodnjim in zgornjim delom trupa,
- levi in desni komolčni ter levi in desni kolenski kot.

Koti med deli telesa, ki rotirajo v več kot eno smer, so izraženi s kvaternioni.

Dinamično ukrivljanje časa. Dinamično ukrivljanje časa (DTW) poravna 2 časovni vrsti na način, da minimizira neko mero. Optimalna poravnava je dobljena s preslikavo več zaporednih vrednosti ene časovne vrste v eno vrednost druge časovne vrste in tako je lahko DTW računan tudi na časovnih vrstah različnih dolžin. V nasprotju z Evklidsko razdaljo, DTW lahko najde podobnosti med vzorcema dveh časovnih vrst tudi če ta vzorca nista časovno poravnana ali pa sta vzorca različnih dolžin.

DTW algoritem, ki je navadno opisan v literaturi, je uporabljen le za poravnavo univariantnih časovnih vrst. Delo, predstavljeno tukaj, pa poravnava multivariantne časovne vrste. Najprej je vsaka točka zajete časovne vrste pretvorjena v prostor kotnih atributov, kjer bo izvedena klasifikacija.

Imamo testno meritev, ki jo želimo poravnati z učno meritvijo (kjer je bil klasifikator naučen), najprej izračunamo matriko lokalnih razdalj *d(i,j)*, v kateri vsak element *(i,j)* predstavlja lokalno razdaljo med *j*-to časovno točko učne in *i*-to časovno točko testne meritve. Naj bo L_{jf} element generičnega atributnega vektorja glede na učno meritev in T_{if} naj bo element atributnega vektorja, relativno na novo testno meritev za razpoznavo, kjer je $1 \le f \le N$ upoštevani atribut. Za definicijo

lokalne razdalje je bila uporabljena Evklidska razdalja, definirana kot $d(i,j)=\sum_{f=1}^{N}\left(L_{jf}-T_{if}\right)$. Na osnovi matrike lokalnih razdalj je zgrajena matrika globalnih razdalj *D*. Končni izhod algoritma je vrednost minimalne globalne razdalje za celotno poravnavo DTW in je najdena v zadnji vrstici in stolpcu, $D(R_j,C_j)$.

3 Eksperimenti in rezultati

Uporabili smo 256 meritev zdravih posameznikov in posameznikov z določenimi zdravstvenimi težavami, pri čemer je bil vsak posameznik 4-5 krat posnet z različnimi hitrostmi izvajanja aktivnosti. Klasifikacijski proces upošteva eno vhodno testno časovno vrsto, ki jo primerja z vsemi ostalimi, da najde minimalno globalno razdaljo za vsako poravnavo in sklepa, da je vhodna meritev istega razreda kot učna meritev, ki ima najmanjšo razdaljo do te vhodne meritve. Metoda "izpusti enega" (leave one out) za 5-najbližjih sosedov da klasifikacijsko točnost 97.5 % za aktivnosti/padce in 97.6 % za zdravstvena stanja.

4 Zaključek

Članek predstavlja splošni pristop k detekciji zdravstvenih težav in padcev za namen podaljšanja samostojnega življenja starejših. Je splošen, ker ne uporablja specifičnih atributov, ampak splošen pristop iz kombinacije DTW in k-najbližjih sosedov. Dobimo klasifikacijsko točnost 97.5 % za aktivnosti/padce in 97.6 % za zdravstvena stanja. Kljub temu, da je metoda splošna in lahko razpozna tudi nove vrste gibanj, dosega visoke klasifikacijske točnosti, podobne pristopom s specifičnimi atributi iz literature.

Zahvala

Operacije, ki so pripeljale do tega članka, je delno sofinancirala Evropska Unija, Evropski socialni sklad. Avtor članka se zahvaljuje mentorju prof dr. Matjažu Gamsu za pomoč.

Literatura:

[1]Toyne S., Ageing: Europe's growing problem, BBC News.
[2]Strle D., Kempe V., "MEMS-based inertial systems", MIDEM 37(2007)4, 199-209.

[3]Ribarič S., Rozman J., "Sensors for measurement of tremor type joint movements", MIDEM 37(2007)2, 98-104.
[4]Trontelj J., et al., "Safety margin at mammalian neuromuscular junction – an example of the significance of fine time measurements in neurobiology", MIDEM 38(2008)3, 155-160.
[5]Bourke A.K et al., An optimum accelerometer configuration and simple algorithm for accurately detecting falls. In Proc. BioMed 2006 (2006), 156–160.
[6]Confidence Project. http://www.confidence-eu.org.
[7]H. Lakany, Extracting a diagnostic gait signature. Patt. recognition 41(2008), 1627–1637.
[8]Luštrek, M., and Kaluža, B. Fall detection and activity recognition with machine learning. Informatica 33, 2 (2009).
[9]Moore ST, et al., Long-term monitoring of gait in Parkinson's disease, Gait Posture (2006).
[10] Bogdan Pogorelc, Matjaž Gams: Learning Abnormal Gait Patterns of Elderly from Motion Capture System, UDM on ECAI 2010, 57-61.

Za širši interes

Po napovedih naj bi do leta 2050 v razvitih državah živelo šestkrat toliko ljudi nad 80 let kot danes. Starejši navadno živijo izolirani od potomcev, zato v primeru bolezni ali poškodbe težko dobijo pravočasno pomoč. Namen te študije je razviti tehnologije, ki bi olajšale samostojno življenje starejših. Članek predstavlja pristop k razvoju sistema za detekcijo zdravstvenih težav in padcev pri starejših z namenom podaljševanja njihovega samostojnega življenja. Če je zaznan padec ali zdravstvena težava, sistem avtomatsko obvesti medicinsko službo. Gibanje starejših je zajeto s sistemom za zajem gibanja in celoten sistem je naučen, da prepoznava specifične zdravstvene težave ali padce. Pristop je splošen, ker za atribute uporablja vse izmerljive kote sklepov namesto specifičnih atributov za posamezne bolezni. Kljub temu dobro prepoznava zdravstvene težave, podobno kot specifični pristopi iz literature.

Process-aware Information Resource Delivery

Tadej Štajner[1,2] **Dunja Mladenić**[1,2]**, Marko Grobelnik**[1]

[1] Artificial Intelligence Laboratory, Jožef Stefan Institute, Ljubljana, Slovenia

[2] Jožef Stefan International Postgraduate School, Ljubljana, Slovenia

Supervisor: prof. dr. Dunja Mladenić

tadej.stajner@ijs.si (email of corresponding author)

Abstract. This paper proposes a framework and an implementation for pro-active information resource delivery, based on knowledge process modeling and process mining. We focus on providing a light-weight implementation and deployment scenario resulting in a desktop application that presents a ranked list of information resources, such as documents, web sites or e-mail messages, that are considered to be most relevant at that point in time.

Keywords: Knowledge process modeling, Information delivery, Process mining

1 Introduction

We introduce the scenario of knowledge workers, professionals in enterprises whose job is based on accessing various resources, such as web pages, documents and e-mail messages. That scenario includes sales people, engineers, scientists and many other professions. We propose a prototype for process-based prediction and its implementation. The premise of this work is that we can learn about a model from patterns of events within the usage these patterns, which we refer to as the knowledge process model, and use the learned model in a way that would streamline the workflow by suggesting information resources to the user before he needs to retrieve them [1]. For the purpose of this paper, we use the term knowledge process model, which corresponds to a set of patterns that describe how a knowledge worker is using various information resources. We capture these events in an on-line fashion through workspace instrumentation and logging infrastructure. For example, the events consist of accesses of search engines and

web sites, documents on the desktop and usage of e-mail. We use the resulting event stream both to learn knowledge process models from usage patterns, as well as to react with suggestions for information resources given live data, which we distil to contain three basic components: text, social network, and time. We then suggest the top most relevant information resources in an on-line fashion using the knowledge process model learned from users' behaviour.

2 Related Work

As presented in Holz et al. [3], approaches for information delivery mainly vary in two dimensions: process support and information delivery, meaning that some information delivery approaches work on top processes ranging from ad-hoc to strictly-structured, and having from light- to heavy-weight information delivery mechanisms. In our domain, having light-weight modeling is important to simplify deployment and adaptation. Our design goal is to maximize information delivery performance while learning from usage logs alone.

3 Knowledge process model framework

In our experience, process mining requires well-defined nondivisible actions as its input - which is a requirement which may not be easily satisfied in some domains, such as most knowledge work [2]. The data that we are dealing with are natural examples of the TNT (text, network, time) framework [4]: the data points are events carrying temporal information, content and a social network component. We decompose the information delivery problem in knowledge processes into a framework with three separate sub-problems, each solvable with multiple approaches. We partition the log of events into sessions, which represent instances of knowledge process executions. This model can be extended by also encoding information from neighbouring events. The sequential addition to the simple vector space event model enables event representations that capture some session information, resulting in a **session vector space model**, which takes into account the positioning, but only the fact that a step has been executed in the same session within a scope, regardless of order.

However, as process models still map from a space of action-to-action transitions to conditional probabilities, we still need to map sequences of documents into sequences of actions that can give us a higher level of abstraction than literal

events. For that purpose, we cluster the events into k clusters where k is the desired granularity of actions. Using these clusters, we train a centroid classifier that classifies events into actions. Given these sequences of actions, we train the process model that will be used to estimate probabilities of future actions, conditioned by the last couple of observed actions. When suggesting new information resources, we use the process model to evaluate each candidate resource's probability of appearing given the observed events. Smoothing of the process model is necessary because of the sparseness of data, for which we employ Laplace smoothing by adding one to each action count.

4 Implementation

We have implemented a prototype of just-in-time information resource delivery that fits into the desktop environment of knowledge workers, rendered as a ranked list of information objects, as shown in Figure 1. We use the following semantic properties as features for individual events: bag-of-words of document content, social roles of participants (inside vs. outside of organization, manager, developer, researcher, private vs. multiple people, single vs. multiple organizations) and event metadata (type of event, type of media).

Since we don't expect the process model alone to produce a good ranking by itself, we run it in combination with a baseline: for that purpose we have chosen the similarity between the most recently accessed information resources and the candidate resource. We merge the two rankings by multiplying the similarity with a probability coefficient of the candidate. This is done in order to see whether having a process model can be approximated by just biasing the ranking towards resources, more similar to the last accessed resource. The intuition behind this using the context model

is when a knowledge worker is working in a context, we assume that the resources, belonging to a context, tend to be similar to one another. We combine the following criteria for ranking:

- The probability of the candidate information resource di?? given the history: $P(d_i | d_{hist\ 0}..., d_{hist\ j})$;
- The similarity of the candidate information resource to the most recently observed information resource: $sim(d_i,d_{hist\ j})$;

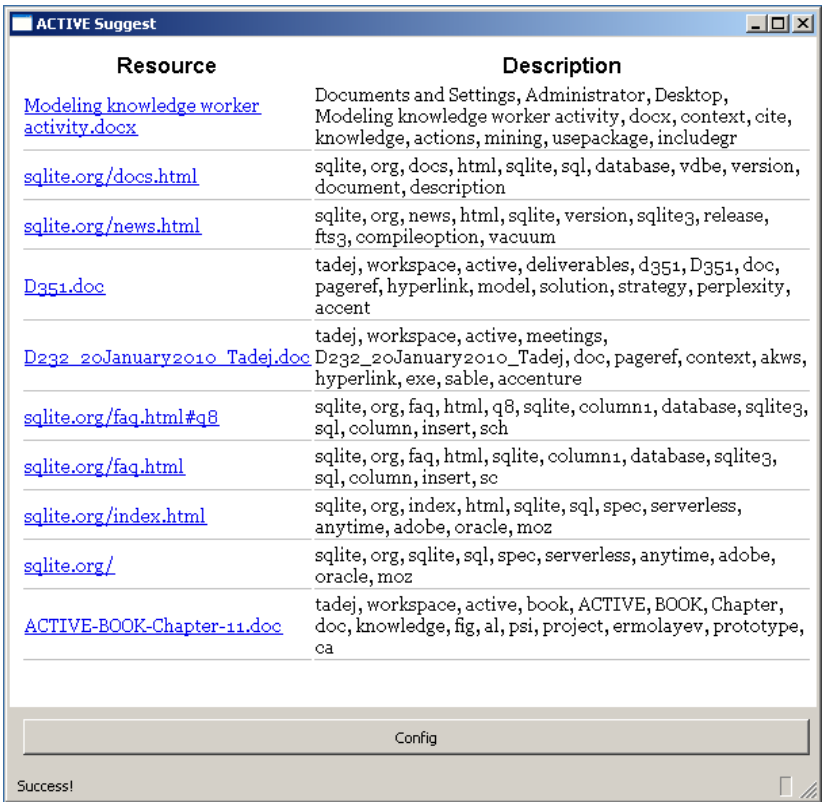

Figure 1: Examples of recommendation

5 Evaluation

In our experiments, we have performed evaluation by constructing combinations of models with one set of data and evaluating them with another subset using ten-fold cross-validation to account for generalization error. We evaluated various knowledge process model configurations by measuring how high they rank the actual events in the test set. In other words, we are measuring how well the system predicts the actual workflow. We have evaluated on the knowledge worker logs, training a model on one subset and testing predictions on the remainder Since the TNT events have no predefined actions, we use the vector space event models – IDF and *SessionIDF*. They all use the TFIDF weighing scheme for features, but differ in the way that the features are generated: whereas IDF contains only the features from a particular event, *SessionIDF* contains also the neighbouring events. Since dimensionality of event features is an issue, we experiment by compressing with a *Clustered* model.. For process models, we experimented on either using an identity transform which assumes uniform processes as a baseline (None) or a bigram Markov model with Laplace smoothing.

Event Model	Action Model	Process Model	Reciprocal rank	Percentage in top 20
IDF	Clustered:10	None	0.0794	0.2697
IDF	Clustered:10	Laplace	**0.1076**	**0.3485**
IDF	Clustered:30	None	0.0853	0.3081
IDF	Clustered:30	Laplace	0.0797	0.2490
SessionIDF	Clustered:10	None	0.0756	0.2807
SessionIDF	Clustered:10	Laplace	0.0701	0.2384
SessionIDF	Clustered:30	None	0.0832	0.3013
SessionIDF	Clustered:30	Laplace	0.0874	0.3051

Table 1: Results of evaluation

Results in Table 1 show the following: the best performing configuration is the one with plain TF-IDF features of events, defining a clustered action model with few distinct clusters as actions and a process model with Laplace smoothing. All in all, we are able to place the correct information resource in the top-20 list roughly on over one third of occasions.

6 Conclusion

To summarize, many of the issues in process mining lie in transforming the input data into well-defined actions. We have discovered that encoding the dependency patterns in the feature vectors show significant improvement from the baseline, but encoding the dependencies on the level of actions works even better. For our future work, the clustering-based action definition will include using a complex graph data representation. We will also experiment in applying this model in other specific knowledge worker domains, focusing on supporting multiple knowledge workers with personalized models.

References:

[1] Gomez-Perez, J., Grobelnik, M., Ruiz, C., Tilly, M., Warren, P.: *Using task context to achieve effective information delivery*. In: Proceedings of the 1st Workshop on Context, Information and Ontologies. ACM (2009)

[2] Štajner, T., Mladenić, D., Grobelnik, M.: *Exploring Contexts and Actions in Knowledge Processes*: Proceedings of the 2nd Workshop on Context, Information and Ontologies (2010)

[3] Holz, H. Maus, H. , Bernardi, A., Rostanin, O.: *From lightweight, proactive information delivery to business process-oriented knowledge management*. Journal of Universal Knowledege Management, vol. 2, 101--127 (2005)

[4] Grobelnik, M., Mladenić, D., Ferlež, J.: *Probabilistic Temporal Process Model for Knowledge Processes: Handling a Stream of Linked Text*. Proceedings of SiKDD 2009 (Conference on Data Mining and Data Warehouses), 2009.

For wider interest

The research presented in this this article aims to find novel ways to apply machine learning methods to problems that knowledge workers are facing nowadays with information overload and constant context switching.

Knowledge workers can be roughly defined as professionals which use knowledge resources in their day-to-day tasks. In practice, they may be sales people pitching products, consultants preparing projects, engineers implementing the latest technology or even scientists doing their research. What they all have in common is that their efficiency is largely conditioned on how much effort does it take to access existing knowledge resources, such as e-mail conversations, project proposals, technical documentation and so on.

The aim of this work is developing a model in the knowledge worker domain that can be conductive to applying machine learning techniques and actually design and implement the algorithms that could enable them to be more productive in their workflows by automatically learning about these workflows.

Academically, the problem is challenging because the data representation needs to be rich enough to model the interesting dependencies between events, and the algorithms fast enough to handle the rich complex graph representation in a way that can be delivered in an on-line fashion to users. There are two hard problems: just-in-time information retrieval and underneath, complex graph clustering. For end users, these approaches can make their productivity significantly higher by having them focused on the task at hand instead of being stuck looking for files in deep hierarchies of folders.

Modeliranje večagentnih sistemov

Aleš Tavčar[1,2], **Damjan Kužnar**[1], **Matjaž Gams**[1,2] (mentor)

[1] Odsek za Inteligentne sisteme, Institut "Jozef Stefan", Ljubljana, Slovenija

[2] Mednarodna podiplomska šola Jožefa Stefana, Ljubljana, Slovenija

ales.tavcar@ijs.si, damjan.kuznar@ijs.si, matjaz.gams@ijs.si

Povzetek. V tem delu obravnavamo postopke za analize podatkov z namenom zaznavanja tipičnega obnašanja posameznikov in več-agentnih sistemov. Na ta način lahko odkrivamo in napovedujemo kompleksnejše strategije, ki jih posamezniki izvajajo za doseganje določenih ciljev. Pri tem pa je pomembno upoštevati tudi kognitivno in čustveno stanje opazovanih ljudi, saj le-to lahko pomembno vpliva na njihove akcije.

Ključne besede: več-agentni sistemi, analiza podatkov, analiza obnašanja kognitivna stanja

1 Uvod

Modeliranje obnašanja posameznikov ali več-agentnega sistema se tesno navezuje na nalogo: Kako naj le z zunanjim opazovanjem množice posameznikov uspešno analiziramo njihovo obnašanje, to obnašanje modeliramo in zgrajeni model nato uporabimo za vodenje skupine inteligentnih agentov. Taka analiza je zelo zahtevna, saj mora upoštevati kompleksne predstavitve stanj in asinhronost delovanja agentov. Učenje modelov na osnovnih numeričnih podatkih ima določene pomanjkljivosti. Tako zgrajeni modeli so uporabni, kadar želimo opisati probleme predstavljene s prostorom stanj, vendar so nezmožni opisovanja sprememb tega prostora, ki se zgodijo v zaporednih časovnih korakih. Poleg tega je večina algoritmov strojnega učenja precej občutljiva na šum in nekonsistentnost v vhodnih podatkih.

V tem prispevku sta predstavljeni dve glavni funkcionalnosti modelirnega algoritma. Prva je gradnja strateških vzorcev iz sledi agentnega obnašanja. Druga je učenje simbolnih pravil, ki te grafične vzorce opisujejo. Algoritem je tako sposoben odkrivanja strateškega agentnega obnašanja in gradnje ustreznih simbolnih pravil,

kar uporabnikom omogoča boljše razumevanje in preučevanje najdenih strateških konceptov.
Metoda je nadgradnja algoritma MASDA [1], ki je bil razvit na Odseku za inteligentne sisteme IJS. Za razliko od osnovnega algoritma, predstavljena metoda omogoča upoštevanje kognitivnega stanja agentov. Ta dejavnik je izjemno pomemben pri modeliranju obnašanja ljudi, saj kognitivno in čustveno stanje pomembno vplivata na motive, na podlagi katerih ljudje izbirajo akcije v določenih situacijah.

Z analizo vedenja se je ukvarjalo veliko avtorjev [2,3,4], vendar so pri analizi povečini uporabljali knjižnice vzorcev obnašanja in njihove metode poskušajo najti ujemanja med opazovanji več-agentnega sistema in vnaprej danimi vzorci. V tem prispevku predstavljena metoda ne potrebuje takšnega domenskega znanja, saj uspešno zgradi vzorce le na podlagi opazovanj, brez vnaprej danih knjižnic.

2 Grafična analiza

V tem poglavju so predstavljeni domena in učni podatki, ki jih uporabljamo pri analizi, gradnja grafičnega modela in uporaba abstrakcije z namenom pridobitve splošnejših akcij.

2.1 Učni podatki

Za potrebe začetnega testiranja nove metode smo razvili enostavno več-agentno simulacijo, kjer nastopata dve asimetrični skupini agentov: mirovne sile in civilisti. Agresivni civilisti želijo z metanjem kamenja v mirovnike vzpodbuditi izgrede, naloga slednjih pa je lovljenje agresivnih civilistov in s tem ohranjati red. Civilistom so pripisana tudi kognitivna stanja, ki se s časom spreminjajo. Tako lahko v začetku miren civilist, glede na dogajanje, postane agresiven in se pridruži konfliktu. Podobno lahko napadalnega civilista prevzame strah in se umakne v varno področje.

Med potekom simulacije se premiki, akcije in stanja agentov zapisujejo v tekstovne datoteke, ki se nato uporabljajo pri analizi. Naloga je najti tipične vzorce napada obeh skupin in zgraditi pravila, ki te vzorce opisujejo.

2.2 Gradnja Akcijskega grafa

Akcijski graf je usmerjen graf, kjer vozlišča predstavljajo stanje agenta ob začetku akcije, povezave pa izvršene akcije. Vozlišči a in b sta povezani, če neka akcija spremeni stanje agenta predstavljeno z vozliščem a v stanje agenta predstavljeno z vozliščem b. Pozicija vozlišč v prostoru je izračunana iz pozicij agentov v domenskem prostoru. Slika 1 prikazuje akcijski graf zgrajen iz podatkov pridobljenih z večkratnim poganjanjem simulacije.

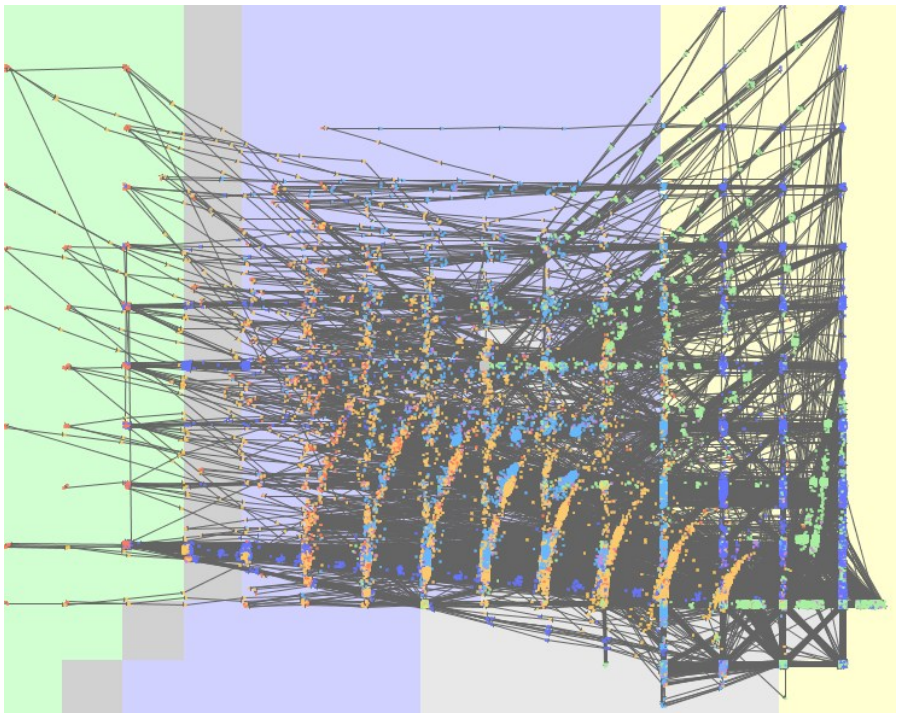

Slika 1: Akcijski graf

Take kompleksne akcijske grafe z velikim številom vozlišč je težko predstaviti na razločen in človeku razumljiv način. Zato potrebujemo postopek, ki bi zmanjšal število vozlišč, obenem pa ohranjal pomembne akcijske koncepte. To dosežemo s hierarhičnim združevanjem vozlišč grafa. Z združitvijo dveh bližnjih vozlišč dobimo novo vozlišče, ki predstavlja bolj splošen akcijski koncept.

2.3 Gradnja Abstraktnega akcijskega grafa

Rezultat hierarhičnega združevanja je Abstrakten akcijski graf (AAG). To je akcijski graf, kjer vozlišča grafa lahko vsebujejo več agentnih akcij. Pričakovano je, da abstraktni graf opisuje obnašanje agentov na bolj splošen način kot osnovni akcijski graf. Takšen graf se doseže s ponavljajočim združevanjem podobnih vozlišč, dokler

ni najmanjša razdalja med vozlišči večja od nekega praga. Razdalja med vozlišči je definirana kot linearna kombinacija štirih spremenljivk: povprečne oddaljenosti med pozicijami agentov v domenskem prostoru, razdalje med vrednostmi vozlišč a in b v ontologiji agentnih vlog, ontologije agentnih akcij in ontologije kognitivnih stanj agentov. Ontologije so edino domensko znanje, ki ga algoritem potrebuje in opisujejo lastnosti domene. Ontologija agentnih akcij opisuje akcije, ki jih lahko agenti izvedejo. Uporabljene ontologije so v obliki drevesnih struktur, kjer vozlišča na višjih nivojih opisujejo bolj splošne koncepte. Primer abstraktnega akcijskega grafa je prikazan na sliki 2. Vidimo lahko, da je tak graf veliko bolj pregleden in razumljiv, saj vsebuje bolj splošne akcijske koncepte.

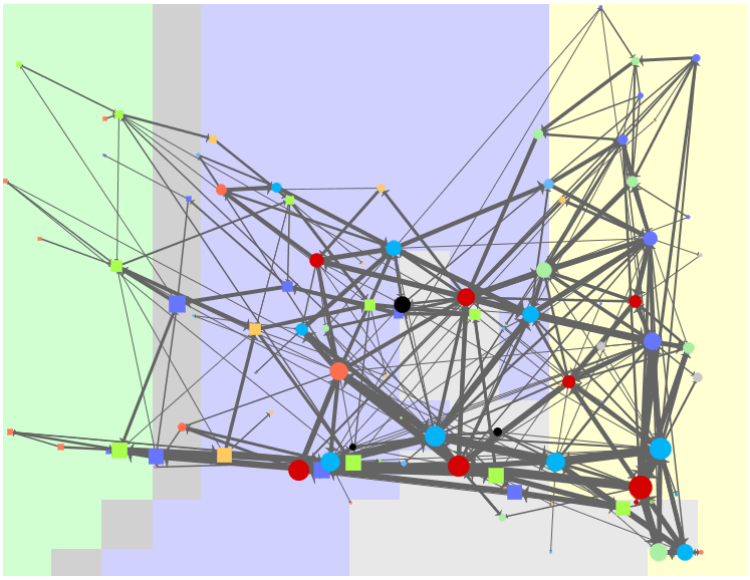

Slika 2: Abstraktni akcijski graf stopnje 100

Naslednji korak v algoritmu je detekcija pomembnih in pogostih akcijskih sekvenc znotraj grafa. Tako dobimo množico sekvenc različnih dolžin in zadnji korak je gradnja pravil, ki dobljene sekvence simbolno opisujejo.

3 Gradnja opisnih pravil

Za vsak akcijski koncept znotraj sekvence se definira nov dvorazredni učni primer, kjer pozitivni učni razred predstavlja ciljni akcijski koncept. Poleg tega je potrebno določiti tudi učne primere. Algoritem to izvede na naslednji način. Za pozitivne učne primere algoritem vzame le instance, ki se končajo v želenem ciljnem akcijskem konceptu. Negativni primeri pa so vse ostale instance, ki se zaključijo v nekem drugem akcijskem konceptu. Ko algoritem določi pozitivne in učne primere

ter ustrezne učne podatke, se lahko požene algoritem za indukcijo pravil, npr. SLIPPER [5].

Na sliki 3 lahko vidimo en primer grafičnega vzorca civilista, ki ga je našel algoritem. Vsaki povezavi se pripiše tudi pravilo, ki ga SLIPPER inducira. Pravilo pravi: Če se civilist nahaja v področju, kjer so kamni in je jezen, potem bo izvedel neko napadalno akcijo. »Offensive« je abstrakten koncept iz ontologije agentnih akcij in vsebuje več različnih akcij, ki pa so vse napadalne narave.

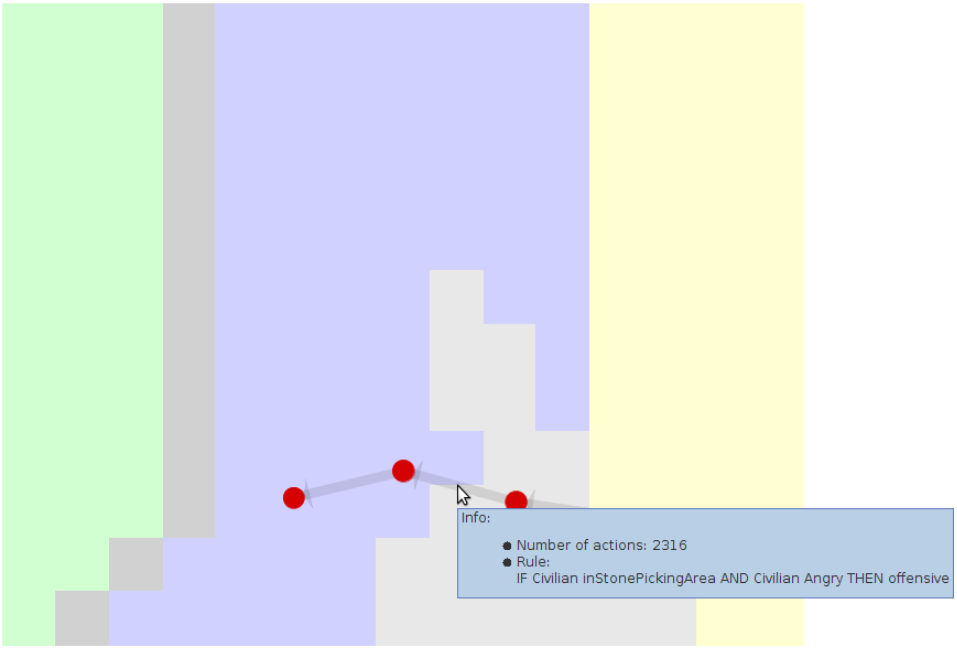

Slika 3: Primer grafičnega in simbolnega opisa akcijske sekvence

Glede na to, da je simulacija, ki smo jo uporabili za pridobivanje učnih podatkov, zelo enostavna, so zgrajena pravila precej dobra in informativna. Naslednji korak je preizkusiti algoritem na novi, bolj kompleksni domeni.

Literatura:

[1] A. Bežek et al.. Multi-agent strategic modeling in a robotic soccer domain. AAMAS 2006, 457-464, 2006

[2] Y. Horman, G. A. Kaminka. Removing Statistical Biases in Unsupervised Sequence Learning. In *Proceedings of Intelligent Data Analysis (IDA), 2005*

[3] J. A. Iglesias, et al.. Classifying Efficiently the Behaviour of a Soccer Team. Intelligent Autonomous Systems, *2008*

[4] G. A. Kaminka et al. Learning the Sequential Coordinated Behaviour of Teams from Observations, Proceedings of the RoboCup-2002 Symposioum, 2002

[5] W. W. Cohen et al. A Simple, Fast and Effective Rule Learner. In *Proceedings of the Sixth National Conference on Artificial Intelligence, 335-342, 1999*

Za širši interes

V tej raziskavi preučujemo analizo vedenja skupine agentov (tj. računalniško vodenih avatarjev) z namenom detekcije skupne strategije, ki jo izvajajo. Metoda ni uporabna le za analizo obnašanja skupin računalniško vodenih agentov, ampak tudi posameznikov in skupine ljudi, saj poskuša med delovanjem upoštevati tudi kognitivno stanje posameznikov v skupinah. Na primer, neka oseba se pod stresom v določeni situaciji odziva na popolnoma drugačen način, kot če je popolnoma sproščena.

Metoda ima širok spekter uporabe. Lahko se jo aplicira na večino problemov, ki jih lahko predstavimo z več-agentnim sistemom. Od analize obnašanja uporabnikov v računalniški mreži, navad uporabnikov določenega programskega paketa, pa vse do analize interakcij uporabnikov socialnih omrežij.
Metoda se lahko uporabi tudi pri problemih, kjer imamo opravka s šumnimi podatki, saj postopek abstrakcije poskrbi za neke vrste glajenje podatkov in s tem zmanjša vpliv šuma na rezultate.

Rezultat algoritma je množica vzorcev in pravil, ki opisujejo značilno obnašanje uporabnikov. Ta pravila omogočajo boljše razumevanje in preučevanje dogajanja v opazovanem sistemu.
Algoritem smo preizkusili na simulaciji, ki je bila razvita v ta namen in je na kratko opisana v prispevku. Kljub preprostosti same simulacije metoda uspe najti v podatkih pomembne vzorce in uspešno zgradi smiselna pravila.

WSN Testbeds for Lighting Control and Environmental Monitoring

Matevz Vučnik[1], **Carolina Fortuna**[1], **Maria Porcius**[1], **Mihael Mohorčič**[1,2]

[1] Department of Communication Systems, Jožef Stefan Institute, Ljubljana, Slovenia

[2] Jožef Stefan International Postgraduate School, Ljubljana, Slovenia

firstname.lastname@ijs.si

Abstract. This paper introduces a set of outdoor wireless sensor network (WSN) testbeds deployed for demonstrations and trials in the areas of lighting control and environmental monitoring. The largest testbed deployed for lighting control currently consists of 15 sensor nodes attached to public light poles that control the LED lights and measure temperature, humidity, pressure, luminance and battery voltage. Other testbeds in the area of environmental monitoring deployed or under development cover specific applications for hyperthermia detection in stables, remote observation of sport-fishing conditions, beehive local climate conditions monitoring, and multispectral imaging and data harvesting using Unmanned Aerial Vehicle (UAV). The paper focuses on two out of the three functional blocks: the network of sensors and the middleware. The testbeds are based on Versatile Sensor Node (VSN) which is a fully modular WSN platform featuring a custom power supply solution for the constraints of the environment. The data are gathered, processed, stored and exposed by the middleware which is designed to separate meta-data from the data in order to allow efficient use of semantic and data mining technologies.

Keywords: Middleware, sensor node, testbed, VSN

1 Introduction

Sensor deployments gained popularity in recent years, especially in the environmental sciences. Sensors are typically connected via radio into wireless sensor networks (WSN) generating large amount of data which are then analyzed and used by scientists and public communities. Several research testbeds based on sensors exist already. However, most of them are indoor and their size is relatively

small, except for TWIST from TU Berlin, which supports 204 mostly Tmote Sky nodes. Outdoor testbeds are less common due to higher deployment and maintenance costs. In the Swiss Experiment, several research groups from areas such as environmental monitoring and computer science, collaborate for deploying and maintaining monitoring stations in the Swiss Alps. The deployment consists of over 4000 sensor streams, however the testbed is mostly manually maintained by several groups. CitySense is an outdoor testbed with 100 wireless sensors deployed across the city of Cambridge, MA. Each sensor node consists of an embedded PC with 802.11a/b/g interface. The Copenhagen Wheel project seems to be one of the few mobile outdoor sensing experiments in which sensor nodes are embedded into the bicycles' wheels [1].

Our largest testbed that we are developing currently consists of 15 sensor nodes mounted on the public light poles in the Gorica region of Slovenia. The testbed is planned to grow to 100 nodes by late 2011 and subsequently up to several hundred nodes. Such testbeds provide valuable insight into actual problems of deployment and scalability of sensor network solutions, as well as testing of some specific implementations.

For building the testbed, we identified three main functional blocks, these being (1) the network of sensors, (2) middleware and (3) data/application. In the following section of the demonstration we address the first two components, explain their role, our approach and development plans. In the last section we describe other tesbeds we are currently working on.

2 Testbed Architecture

1.1 The Network of Sensors

One of the aims of testbed deployments is to investigate heterogeneous sensor networks by integrating several types of sensor nodes. The nodes can be integrated at various levels of abstraction: network level by using the same wireless communication standard and compatible routing protocols, and data level by connecting to the same middleware. Another equally important aim is to use custom hardware that we can reconfigure and have full control over it so that applications and mash-ups can be prototyped easily.

In the testbeds, we are using a VSN platform which has a modular base and can be quickly adapted to various applications. It has a powerful 32 bit microcontroller with ARM Cortex-M3 low-power high performance core. The actual microcontroller is STM32F103 with maximum clock frequency of 72 MHz, 64 kB of RAM and 512 kB of flash memory. There is an additional 128 kB of fast FRAM and the possibility to use miniSD cards to store larger amounts of data. VSN supports digital interfaces such as I2C, SPI, UART, IrDA, RS232, USB and analog interfaces, 12 bit ADC and DAC.

The node has various options of power supply including mains, batteries and solar cell, and for energy saving it supports three low-power states, i.e. sleep, stop and standby, plus additional low-power state deep hibernation which consumes below 7μA.

The radio used in current testbed configurations is XBee-PRO which works in the ISM 868 MHz frequency band. This radio has indoor or urban range of 550 m and the range of 40 km in ideal line-of-sight conditions with dipole antenna. The network topology in multiple sensor node deployments is a star, based on a polling protocol which collects the measurements from the sensors in predefined intervals.

1.2 The Middleware

The middleware consists of several components and it is designed to be scalable. It consists of a database, a triple store and a data mining toolkit. The database schema (see Fig. 1) is designed to be minimalistic and separates the meta-data stores from the measurements store. The meta-data stores contain the necessary meta-data about the stores with additional meta-data such as unit of measurement, sensitivity, measured phenomena, sampling frequency, etc. stored in the triple store using RDF representation. The data store contains the raw measurements which are processed, enriched and indexed using JSI analytic tools. In this way, our system is able to detect trends, correlate them and possibly explain their cause.

The running implementation of the middleware consists of an HTTP server which periodically receives the sensor measurements and multiplexes it to all the registered listeners. Currently, we have three listeners: the MySql database, the JSI Sense and GSN. JSI Sense is a tool that combines existing libraries [2] with the necessary extensions for handling streaming data and composed event detection.

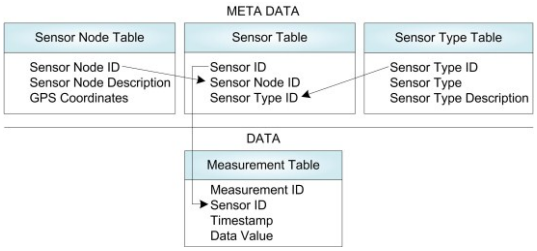

Figure 1: Database schema

GSN is a middleware which supports flexible integration and discovery of sensor networks and sensor data, and enables fast deployment and addition of new platforms. GSN's central concept is the virtual sensor abstraction which enables the user to specify XML-based description of sensors or of entire sensor nodes [3]. For the processing of the input data streams, GSN uses wrappers which adjust the data received from the data source into the standard GSN data model.

2 Testbeds

VSN's modularity and flexibility regarding supported communication interfaces, sensors, actuators, and possibilities to combine different energy sources allows its usage in a large set of applications. In the following, we briefly describe several examples that prove the applicability of above described testbed architecture [4], [5].

- **Public lighting control and local climate monitoring**
  Our largest sensor network testbed is deployed on the public light poles in the region of Gorica. The nodes consist of the sensors that measure temperature, humidity, pressure, luminance and battery voltage. There are two luminance sensors on some of the nodes to increase the accuracy of the measurements. Based on luminance measurements the dimming of the light is controlled.
- **Hyperthermia detection in stables**
  The goal is to measure temperature and humidity inside and outside stables in order to detect the danger of hyperthermia at cows and issue an early warning.
- **Remote observation of sport-fishing conditions**
  By using WSN technology information on water level, picture of a fishing spot and water, and air temperature can be provided.

- **Beehive local climate conditions**

  The purpose of this testbed is to monitor climate conditions inside (temperature and humidity) and outside (temperature, humidity, air preassure, wind direction and speed) of the beehives. Through bee counting sensor, presence of pesticides in the vicinity can be detected. For the test purposes, sound monitoring is also possible.

- **Multispectral imaging and data harvesting over Unmanned Aerial Vehicle (UAV)**

  Data harvesting over large areas where deployed WSNs have no Internet connection can be a very time consuming and expensive task. Our solution uses Unmanned Aerial Vehicles (UAV) equipped with a gateway sensor node. In addition, UAV is used to collect multispectral images with a Tetracam ADC camera.

Figure 2 summarizes hardware aspects of the testbeds we described above, illustrating VSN's versatility in terms of topology and used sensors, power supply and communications interfaces.

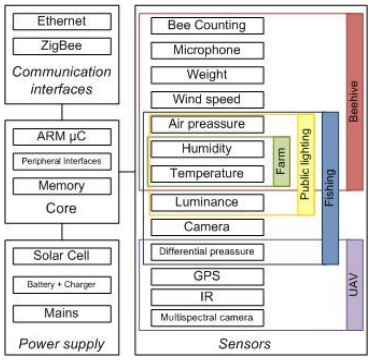

Figure 2: VSN Modularity as used in testbeds

References:

[1]N. Savage, Cycling through data, In *Communications of the ACM*, Vol 53, No. 9, September 2010

[2]B. Fortuna, C. Fortuna, D. Mladenić, Real-time News Recommender System, ECML/PKDD, Barcelona, Spain, September 2010.

[3]H. Jeung, et al. Effective Metadata Management in Federated Sensor Networks. In *Proc. IEEE International Conference on Sensor Networks, Ubiquitous, and Trustworthy Computing (SUTC '10),* 2010.

[4]M. Smolnikar, C. Fortuna, M. Vučnik, M. Mihelin, M. Mohorčič, Postavitev senzorskega omrežja na infrastrukturi javne razsvetljave, 25. delavnica o telekomunikacijah VITEL - Internet Stvari, 12. - 13. april 2011, Brdo pri Kranju.

[5]K. Alič, M. Kastelic, D. Škrabl, M. Smolnikar, T. Javornik, M. Mohorčič, Uporaba vsestranskega senzorskega vozlišča za podporo okoljskim aplikacijam, 25. delavnica o telekomunikacijah VITEL - Internet Stvari, 12. - 13. april 2011, Brdo pri Kranju.

For wider interest

Wireless sensor networks have a big potential in many different fields. We described in this paper some applications mainly focusing on environmental monitoring.

Wireless sensor networks are supposed to be low-power so that they can operate using batteries and optionally solar power. The networks consist of sensor nodes which are small embedded computers incorporating measuring capabilities and communication interface and are able to interoperate by each other.

In all our testbeds, we are using a sensor node developed at the Department of Communication Systems, Jožef Stefan Institute in collaboration with Isotel d.o.o. It is called the Versatile Sensor Node because it is a highly reusable sensor node as we show in this paper. It is suitable for a large variety of applications with varying constraints.

We are building and adapting embedded and server side software too in such way that we can efficiently scale VSN deployments, accommodate heterogeneous sensors, collect data and meta-data, process them in real time and support high added value applications. Sensor networks are interesting especially because they leverage integration of the physical and virtual (i.e. Web) worlds. In the future, we can expect wireless sensor nodes all around us generating high amounts of data which are then processed with advanced algorithms extracting knowledge out of these data and then sending the commands to the actuators depending on the situation.

Nanoznanosti in nanotehnologije (Nanosciences and Nanotechnologies)

Dielectric investigations of a new class of relaxor polymer

Andreja Eršte[1,2], Vid Bobnar[1], Xian-Zhong Chen[3], Cheng-Liang Jia[3], Qun-Dong Shen[3]

[1] Condensed Matter Physics Department, Jožef Stefan Institute, Ljubljana, Slovenia

[2] Jožef Stefan International Postgraduate School, Ljubljana, Slovenia

[3] Department of Polymer Science and Engineering and Key Laboratory of Mesoscopic Chemistry of MOE, School of Chemistry and Chemical Engineering, Nanjing University, Nanjing, China

andreja.erste@ijs.si (email of corresponding author)

Abstract. Relaxor polymers based on poly(vinylidene fluoride-trifluoroethylene) are attracting considerable attention due to fast response speeds, giant electrostriction, high electric energy density and large electrocaloric effect. Until now, detailed dielectric analysis of relaxor polymers was complicated due to the fact that two similar dynamics take place in the same temperature range; in a new class of relaxor polymer, the reduced poly(vinylidene fluoride-trifluoroethylene) copolymer, relaxor dynamics in the crystalline part can be separated from the glassy processes in the amorphous matrix. Our investigations revealed that (i) relaxor dielectric dynamics (linear and nonlinear) is almost identical to that observed in inorganic systems and reminiscent of the dynamic behaviour observed in various spin glasses; (ii) even low bias voltage effectively blocks the ac electrical conductivity of the studied copolymer; and, more generally, (iii) that nonlinear dielectric susceptibility dominantly influences the dielectric dynamics of relaxors in dc bias electric fields.

Keywords: relaxor, polymer, dielectric spectroscopy

Relaxor polymers based on the poly(vinylidene fluoride-trifluoroethylene) P(VDF-TrFE) are of great interest for a broad range of applications, as they exhibit fast response speeds, giant electrostriction, high electric energy density and large electrocaloric effect. Analysis of dielectric processes in relaxor P(VDF-TrFE)-based systems (electron-irradiated copolymer and terpolymers) has revealed dynamics

similar to the one observed in inorganic relaxors and a broad dielectric relaxor peak, where for a relaxor polymer very high dielectric constant of ~40 was obtained near room temperature. Dielectric analysis of relaxor polymers has been incomplete until now, i.e., data interpretation was complicated by the fact that two similar dynamic processes, relaxor behavior in the crystalline part of the system and glass-to-rubber transition in the amorphous matrix, take place in the same temperature range and thus superimpose in the detected response.

In order to investigate both processes separately, we performed high-resolution dielectric measurements of a new class of relaxor polymer, synthesized via reductive dechlorination from the P(VDF-TrFE-CTFE) system [1]. Here, in the reduced P(VDF-TrFE) copolymer, the relaxor peaks take place at much higher temperatures than in the previously reported relaxor polymers and, concomitantly, relaxor and glassy dynamics can be studied separately. Measurements of the temperature and frequency-dependent linear and third-order nonlinear dielectric

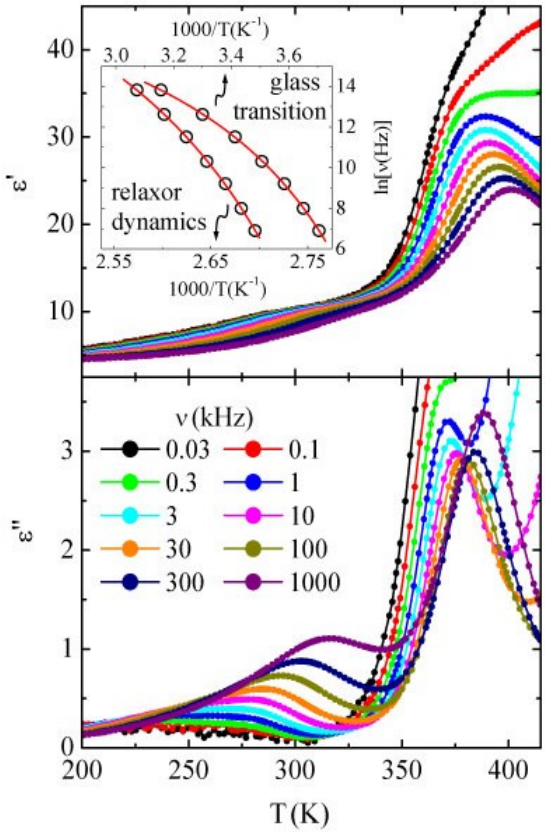

Figure 1: Temperature dependence of the real, ε', and the imaginary, ε'', parts of the complex linear dielectric constant. Inset shows the Vogel-Fulcher dependence of the characteristic relaxation times for the relaxor dynamics and glassy transition.

response in the temperature range of 175 K – 420 K and in the frequency range of 30 Hz – 1 MHz have been performed, and the influence of dc bias field has been studied.

Figure 1 shows two dispersive dielectric anomalies, relaxor (350–400 K) and glassy (275–335 K) in the temperature dependence of the real, ε', and imaginary, ε'', parts of the complex linear dielectric constant. Characteristic relaxation frequencies, determined from peaks in $\varepsilon''(T)$, for both processes follow the Vogel-Fulcher law (inset to Figure 1), a dependence, which is typical for relaxor (and glassy) systems. Furthermore, in temperature region, where the relaxor dynamics dominates the dielectric response, the temperature dependence of the dielectric nonlinearity $a_3=\varepsilon_3 / \varepsilon_o^3 \varepsilon^4$ reveals a typical relaxor paraelectric-to-glass crossover (Figure 2).

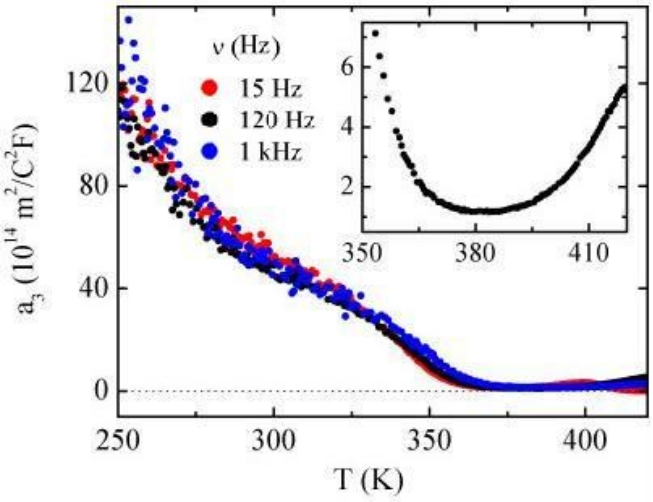

Figure 2: Temperature dependence of the dielectric nonlinearity a_3. Inset shows a paraelectric-to-glass transition in the temperature region where relaxor dynamics dominates the dielectric response.

In dc bias electric field, for the relaxor contribution both, ε' and ε'', decrease and the peaks occur at lower temperatures, however, there is almost no influence of the field on the glassy processes in the amorphous matrix. The data in Figure 3 depict changes in relaxor dynamic processes due to a dc bias electric field. A strong decreasing of the Vogel-Fulcher freezing temperature T_o suggests a negative nonlinear dielectric contribution [2]. This conclusion is confirmed by a similar analysis performed in the relaxor PLZT ceramics, where it is known that the nonlinear dielectric response increases the static polarization [3].

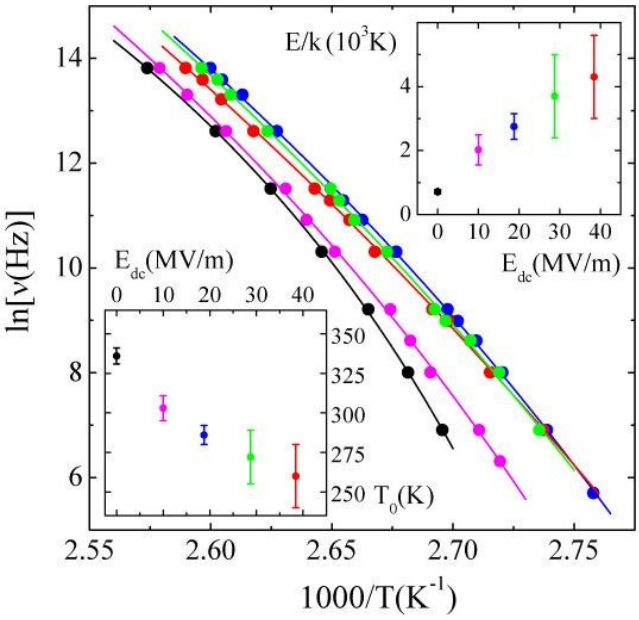

Figure 3: The Vogel-Fulcher dependence of the characteristic relaxation time for the relaxor dynamics in dc bias electric fields. Insets show the field dependence of the activation energy (upper inset) and Vogel-Fulcher temperature (lower inset).

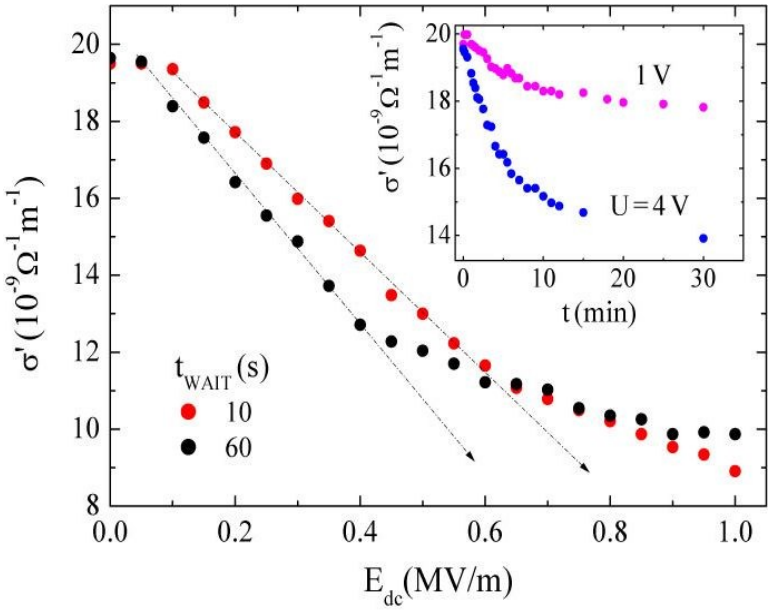

Figure 4: The electrical conductivity (at 110 Hz) as a function of the dc bias electric field, detected with two different field change rates - the waiting time between two subsequent points was either 10 s or 60 s. The arrows point towards anticipated ac conductivity blocking field. Inset shows the time-decreasing of the ac conductivity under applied bias voltages of 1 V and 4 V, corresponding to the dc bias fields of 0.05 MV/m and 0.2 MV/m, respectively.

Finally, experimental data reveal that the ac electrical conductivity decreases in dc bias electric fields (Figure 4); the conductivity remains low after removal of the bias, however, it can be restored by applying ac voltage of the same level as previously applied dc bias. This indicates that charge carriers, being responsible for the ac electrical conductivity, migrate in a dc bias field and pin, mainly at the electrode-sample interface, while the ac electric field unpins them and restores the conductivity. Similar space charge blocking effect has already been found in various ionic conductors [4] and thin ceramic films [5]. This is throughout a dynamic process, thus determination of any blocking field (as indicated by arrows in Figure 4) is strongly influenced by the measurement rate. The inset to Figure 4 shows that even very low bias voltages in few minutes effectively block the ac electrical conductivity of the reduced P(VDF-TrFE) system.

In summary, dielectric investigations of a new class of relaxor polymer revealed:

(i) dielectric dynamics (linear and nonlinear) in relaxor polymers is almost identical to that observed in classical inorganic systems and, furthermore, reminiscent of the behavior observed in various spin glasses;

(ii) even low bias voltage effectively blocks the ac electrical conductivity of the studied copolymer;

and, more generally, that

(iii) nonlinear dielectric susceptibility dominantly influences the dielectric dynamics of relaxors in dc bias electric fields.

References:

[1] A. Eršte, C. Filipič, A. Levstik, V. Bobnar, X.-Z. Chen, C.-L. Jia, Q.-D. Shen. Contributions of distinctive dynamic processes to dielectric response of a relaxorlike reduced poly(vinylidene fluoride-trifluoroethylene) copolymer. *Physical Review B*, 81(21): 214103, 2010.

[2] R. Pirc and R. Blinc. Nonlinear Magnetoelectric Effect in Magnetically Disordered Relaxor Ferroelectrics. *Ferroelectrics*, 400(1): 387-394, 2010.

[3] V. Bobnar, A. Eršte, X.-Z. Chen, C.-L. Jia, Q.-D. Shen. Influence of dc bias electric field on Vogel-Fulcher dynamics in relaxor ferroelectrics. *Physical Review B*, 83(13): 132105, 2011.

[4] M. E. Lines. Interfacial polarization effects in ionic conductors. *Physical Review B*, 19(2): 1189-1195, 1979.

[5] X. Chen, A. I. Kingon and O. Auciello. AC conductivity and dielectric properties of sol-gel PZT thin films for ferroelectric memory applications. In *Proceedings of the 8th IEEE International Symposium on Applications of Ferroelectrics*, Greenville, South Carolina, USA, 1992.

For wider interest

Relaxor polymers are of great interest for a broad range of applications (e.g., actuators, sonars and artificial muscles) as they exhibit giant electromechanical response, which is several orders of magnitude larger than in classical piezoelectric ceramics. The input electric energy that can be converted into strain energy during electromechanical application is directly proportional to the dielectric constant of the electroactive material. The dielectric investigations thus play a key role in optimization of these systems: In order to induce the desired strain with lower external electric fields it is namely necessary to develop systems with high values of the dielectric constant.

Disordered ferroelectric polymers exhibit typical relaxor properties. These systems are composed of crystalline regions embedded in an amorphous matrix. This complicates the interpretation of the dielectric results: The relaxor dynamics in the crystalline regions and the glassy transition in the amorphous matrix occur in the same temperature range and thus superimpose in the detected response.

In order to investigate both processes separately, we performed high-resolution dielectric measurements of a new class of relaxor polymer, synthesized via reductive dechlorination from the P(VDF-TrFE-CTFE) system. Here, in the reduced P(VDF-TrFE) copolymer, the relaxor and glassy dynamics can be studied separately, as the relaxor peaks take place at much higher temperatures (80–130°C) than in the previously reported relaxor polymers. Our investigations revealed that (i) dielectric dynamics (linear and nonlinear) in relaxor polymers indeed is almost identical to that observed in classical relaxor systems and, furthermore, reminiscent of the dynamic behaviour observed in various spin glasses; (ii) even low bias voltage effectively blocks the ac electrical conductivity of the studied copolymer; and, more generally, that (iii) nonlinear dielectric susceptibility dominantly influences the dielectric dynamics of relaxors in dc bias electric fields.

Increasing of the dielectric constant represents a major challenge in the development of electromechanical applications, in which the input electric energy that can be converted to strain energy is directly proportional to the dielectric constant of the electroactive material. In order to further the optimization of relaxor VDF-TrFE-based polymers, detailed dielectric investigations were performed in a new class of relaxor polymer, the reduced P(VDF-TrFE) copolymer, and the results have been published in Physical Review B 81, 214103 (2010), and, just recently (April 22, 2011), in Physical Review B 83, 132105 (2011).

Single nanoparticle detection in live cell by fluorescence microscpectroscopy

Maja Garvas[1,2] **, Polona Umek**[1]**, Janez Štrancar**[1,2]

[1] Condensed Matter Physics, Jožef Stefan Institute, Ljubljana, Slovenia

[2] Jožef Stefan International Postgraduate School, Ljubljana, Slovenia

Supervisor: Assoc. Prof. Dr. Janez Štrancar

maja.garvas@ijs.si

Abstract. Recently, the number of different applications of nanomaterials has dramatically increased, especially in the fields of chemical, food, cosmetic and electronic industries, as well as in environmental technology and medicine. Although they bring many new functionalities, their exact impact on human health and the environment is still not predictable. Their characteristics, such as size, surface charge, and functionalization, play a crucial role in particle-cell interactions. Despite the aggregation of nanoparticles in solution, they can actually be identified inside the cell. To prove they are able to penetrate the cell membrane and become located within the cell, a new tool has been developed - fluorescence microspectroscopy (FMS). The application of FMS allowed the spectral-based identification of nanoparticles within the cells, even the single one, with size under optical resolution.

Keywords: single nanoparticle detection, titanium nanoparticles, nanoparticle uptake, fluorescence microspectroscopy (spectral imaging), cancer cells

1 Introduction

Large production of various kinds of nanomaterials can have an important impact on our daily lives and our environment, which need to be unravelled despite many new opportunities in different industries as well as in medicine for purposes of diagnosis, imaging and drug delivery. The real (negative) effects of nanomaterials are not yet known and safety issues are still under scientific investigations [1-7]. Most of the studies are biophysicochemically oriented, trying to evaluate the effect of size, shape, composition and surface charge of nanoparticles on biological

samples [4,5,7]. It seems however, that observing mechanisms of nanoparticles passage through cell membrane into the live cell in real time is much more demanding, especially if we want to obtain information about a single nanoparticle with its size significantly under the resolutions of optical methods. Until recently, knowledge about uptakes into the cells has been gained through experiments on fixed samples (electron microscopy) or by indirect fluorescence experiments on fixed or live cells such as temperature experiments or cytoskeleton disruption [8].

To provide new insight into the nanoparticle uptake, we built a system which allows us to detect fluorescently marked nanoparticles within the cells despite the fact that they cannot be spatially recognized by optical microscopy. Instead, the identification is done via detecting fluorescence emission spectra in every voxel of the image with the ability of monitoring the processes in real time in live cell samples. The system combines confocal fluorescence microscopy with fluorescence spectroscopy within one system, fluorescent microspectrometer (FMS) [9].

2 Materials and methods

2.1 Nanoparticle synthesis and functionalization

Titanate nanostructures have been prepared from anatase form of TiO_2 under hydrothermal conditions. According to TEM analysis, the size of nanotubes in one dimension was between 6-11 nm and in other was up to 500 nm. TEM and EDS analysis were done afterwards. To detect single nanoparticle in live cell with fluorescence microspectroscopy, surface functionalization with florophore molecule of titanium nanoparticle (TiNT) was done in two-steps. Firstly, 3-(2-aminoethylamino)propylmethyldimethoxysilan (APMS) was attached to titanium nanotubes (through hydroxyl groups on the surface). Secondly, fluorophore Alexa 488 SDP ester was attached to TiNT – APMS complex. FTIR, zeta potential measurements and HAADF-STEM microscopy with EELS spectroscopy were used to characterize fluorescently labeled nanomaterial and confirm the APMS and fluorophores binding on the nanoparticles.

2.2 Confocal fluorescence microspectroscopy system

The system we used is in detail described in ref. [9], but shortly, the confocal FMS system is built on an inverted microscope. The confocal unit houses a spinning disk, excitation, dichroic and emission filters. As an excitation source, a high power xenon arc lamp is used which provides flexibility with respect to the wavelength of excitation light. All electronic microscope functions, as well as camera control, shutters, stage, and focus, are controlled using home-built software. The microspectroscopic images are taken successively at different wavelengths, i.e. as a wavelength stack. The liquid crystal filter is tunable in the range from 400 to 720 nm, with the bandwidth of around 10 nm. The last component in the system is a highly sensitive EMCCD camera with a very high quantum efficiency, which is needed mainly because of the light intensity losses due to spinning disk and LCTF.

2.3 Spectra acquisition and analysis

For spectra acquisition and analysis, a home-built program has been developed which controls the recording of images at different wavelengths and their analysis in order to extract fluorescence emission spectra. A spectrally contrasted image is generated for a fast and intuitive visual inspection of the acquired data from the obtained spectra. Every point of the image is color-coded according to its spectral properties: the wavelength of maximal intensity λmax is coded with hue, and the level of brightness corresponds to the intensity at λmax [9].

2.4 Interaction of cancer cells with fluorescently labeled nanoparticles

Cultures of human breast adenocarcinoma cell line MCF-7 cells were used in fluorescence microspectroscopy experiments to define the interaction of living cancer cells with nanoparticles.

3 Results and discussion

Our focus was oriented into detection of a single nanoparticle when interacting with cells. For nanomaterial, titanate nanoparticles were chosen as a class of materials with wide range of applications due to UV absorption, disinfection, tumor cell killing. Firstly, functionalization of the nanoparticles was checked including attachment of APMS linker to nanoparticle surface following the methods

published elsewhere [10,11]. In first step, the reaction was monitored by infrared spectroscopy which shows successful bonding of APMS linker to the surface. Zeta potential measurements also show surface changes relative to the original material. HAADF-STEM microscopy with EELS spectroscopy furthermore supported these results. In next step, covalent binding of different fluorescent molecules was targeted, but unfortunately the outcome was not stable, due to pH changes in the environment and various cell processes that forced the fluorophore to quickly dissociate from nanomaterials. Successfully binding was however achieved by an ester fluorophore molecule, Alexa 488 SDP, which is less prone to pH changes and does not bleach significantly. We optimized purification process but we still cannot avoid aggregation problem at pH under 10, which appears in all biological samples. To discriminate between unbound fluorescent molecules and labelled single nanoparticles thus avoiding misinterpretation of the results FMS system was used. On the contrary to normal fluorescence imaging, FMS can detect small shift in fluorescence emission spectra, which proves binding of a fluorophore to a linker and allows discrimination between free probe and single labelled nanoparticles, which both have no geometrical contrast due to their size (less then optical resolution). Our FMS results show that nanoparticles in the cells have maximum position at 523 nm and coincide with results obtained with spectrophotometer where free Alexa dye had emission maximum at 526 nm, and one attached to titanium nanotubes at 523 nm (figure 1C). Together with the lack of geometrical contrast of the nanoparticles signal within the cells, and plenty of spectrally identified signal within the cells, this confirms the presence of single or at least very small aggregates of nanoparticles within the cells unravelled by the FMS system.

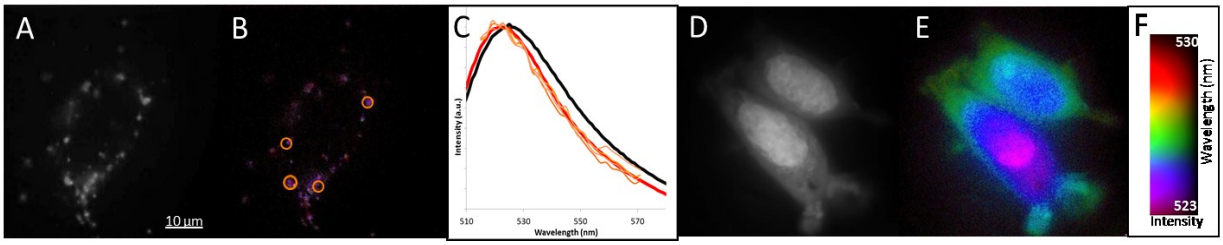

Figure 1: Interaction of titanium nanoparticles with living cells. Cells incubated *in vitro* with fluorescently labeled TiNT for one day (A,B). From the intensity image we cannot discriminate between unbound fluorescent molecules and labelled single nanoparticles(A),but spectrally contrasted image (λmax) can detect small shift in fluorescence emission spectra, which proves binding of a fluorophore to a linker(B). FMS spectra taken from different region of an image (orange circle) coincide with results taken by spectrofotometer, where red line

presents signal of labelled nanoparticles and the black signal of free dye(C). Cell incubated *in vitro* with fluorescently labelled TiNT for one day, before imaging for cell localization, cell probe (acridine orange) was added (D, E). From fluorescence intensity contrasted images it is not possible to determine localization of nanoparticles due to overlap of fluorescent emission spectra of the nanoparticles and the cell probe (D). Spectrally contrasted image shows the distribution of the cell probe - acridine orange (blue/green) and labelled nanoparticles - Alexa (violet/pink) (E). The wavelength of maximal intensity λmax is coded with hue, and the level of brightness corresponds to the intensity at λmax (F – color legend). Emission wavelength maximum is colored according to the legend (F) from 523 – 530 nm in both images (B, E). Nanoparticles are coded with violet/pink corresponding to maximum emission wavelength of around 523 nm, acridine orange is coded with blue/green correspondiing to λmax around 526 nm (B, E).

4 Conclusions

An important step was done in nanomaterial functionalization to increase the stability of the label binding to the nanoparticles. The application of FMS allowed the spectral-based identification of nanoparticles within the cells. From the colour coding according to maximum emission wavelength (λmax) it is possible to distinguish distribution of fluorescently labelled nanoparticles relative to acridine orange even though the difference of λmax is only about 3 to 4 nanometers. Moreover, from the emission spectra maximum of fluorescently labelled nanotubes at around (λmax = 523 nm) we can conclude that all of the probe remains bound on nanoparticles during the experiment, since unbound probe emits at around λmax = 526 nm. Further work will focus on reducing the problem of aggregation, increasing the purification and stability, and optimizing the fluorophores in terms of higher environmental sensitivity, high quantum yield and efficiency.

References:

[1]A. Nel, T. Xia, L. Mandler, N. Li. Toxic potential of materials at the nanolevel. *Science,* 311:622, 2006

[2]A. Magrez, L. Horvath, R. Smajda, V. Salicio, N. Pasquier, L. Forro, B. Schwaller.Cellular toxicity of TiO_2-based nanofilaments. *ACS Nano,* 3:2274, 2009

[3]H. F. Krug, P. Wick. Nanotoxicology: An interdisciplinary challenge. *Angew. Chem. Int. Ed.*, 50:1260-1278, 2011

[4]A. E. Nel, L. Madler, D. Velegol, T. Xia, E. M. Hoek, P. Somasundaran, F. Klaessig, V. Castranova, M. Thompson. Understanding biophysicochemical interactions at the nano-bio interface. *Nature materials,* 8:543-557, 2009

[5]A. Verma, O. Uzun, Y. Hu, Y. Hu, H. Han, N. Watson, S. Chen, D. J. Irvine, F. Stellacci. Surface-structure-regulated cell-membrane penetration by monolayer-protected nanoparticles. *Nature materials*, 7:588-595, 2008

[6]R. R. Arvizo, O. R. Miranda, M. A. Thompson, C. M. Pabelick, R. Bhattacharjeva, J. D. Robertson, V. M. Rotello, Y. S. Prakash, P. Mukherjee. Effect of nanoparticle surface charge at the plasma membrane and beyond. *Nano Lett*. 10:2543-2548, 2010

[7]V. Mailander, K. Landfester. Interaction of nanoparticles with cells. *Biomacromolecules*, 10:2379, 2009

[8]J. Rejman, V. Oberle, I. S. Zuhorn, D. Hoekstra. Size dependent internalization of particles via the pathway of caltrin-and caveolae- mediated endocytosis. *Biochem. J*., 377:159-169, 2004

[9]Z. Arsov, I. Urbančič, M. Garvas, D. Biglino, A. Ljubetič, T. Koklič, J. Štrancar. Fluorescence microscopy as a toll to study mechanism of nanoparticle delivery into living cancer cells. *Biomed. Opt. Express*, 2011:submitted

[10]E. Ukaji, T. Furusawa, M. Sato, N. Suzuki. The effect of surface modification with silane coupling agent on suppressing the photo-catalytic activity of fine TiO_2 particles as inorganic UV filter. *Appl.Surf. Sci*., 245:563-569, 2007

[11]G. Tan, L. Zhang, C. Ning, X. Liu, J. Liao. Preparation and characterization of APTES films on modifiied? titanium by SAMs. *Thin Solid Films*, 2011, doi:10.1016/j.tsf.2011.01.068

For wider interest

Single nanoparticle detection in live cell by fluorescence microscpectroscopy

The number of different applications of nanomaterials is dramatically increasing, especially in the fields of chemical, food, cosmetic and electronic industries, as well as in environmental technology and medicine. Although nanotechnology brings success in many fields, exact impact of used material on human health and the environment is still not known. Nanomaterial characteristics, such as size, surface charge, chemical composition, play a role when particles and human cells meet. They influence strongly how particles pass the membrane or attach to it, pass nucleus or even parts of tissues and organs like human skin, lungs, gastrointestinal tract. Despite nanoparticle property - aggregation of nanoparticles, they can actually be identified inside the cell. This is a strong reason to further investigate nanoparticle-cell interaction.

To provide new insight into the nanoparticle uptake, we built the system which allows us to detect fluorescently marked nanoparticles within the cells despite they cannot be spatially recognized under optical microscope (due to small size, which is under optical resolution). Instead, the identification is done by detecting fluorescence emission spectra at every point of the image with the ability of monitoring the processes in real time in live cell samples. The system combines confocal fluorescence microscopy with fluorescence spectroscopy within one system, fluorescent microspectrometer (FMS).

Processing of High-quality $KTaO_3$ Ceramics

Sebastjan Glinšek[1,3], Barbara Malič[1,3], Elena Tchernychova[1], Cene Filipič[2], Marija Kosec[1,3]

[1]Electronic Ceramics Department, Jožef Stefan Institute, Ljubljana, Slovenia

[2]Condensed Matter Physics, Jožef Stefan Institute, Ljubljana, Slovenia

[3]Jožef Stefan International Postgraduate School, Ljubljana, Slovenia

sebastjan.glinsek@ijs.si

Abstract. $KTaO_3$ powder was prepared by heating the mechanochemically activated K_2CO_3-Ta_2O_5 powder mixture at 800 °C. A second heating at the same temperature was employed to improve the homogeneity of the powders. Phase-pure perovskite ceramics, with relative densities of 95 %, were obtained by hot-pressing the powder compacts at 1250 °C. The low-temperature dielectric permittivity value is ~4000, and is comparable to the value reported for the single-crystals.

Keywords: $KTaO_3$, ceramics, processing, mechanochemical activation

1 Introduction

Incipient ferroelectrics are materials whose dielectric permittivity ε' continuously increases with decreasing temperature. As quantum fluctuations prevent dipole ordering at low temperatures they do not experience a paraelectric–ferroelectric phase transition. Therefore they have a high dielectric permittivity and at the same time low dielectric losses $tan\delta$, especially at cryogenic temperatures. They are of special interest for microwave components which are integrated into modern wireless devices.[1]

$KTaO_3$ is one of the prototype incipient ferroelectrics with well-known properties in its single-crystal form. On the other hand, reports on $KTaO_3$ ceramics are very limited. This is due to difficulties encountered during the processing, such as the hygroscopic nature of the starting compounds, losses of potassium oxide upon heating, and insufficient densification during the sintering.[2,3]

In this paper we report on preparation of highly dense $KTaO_3$ ceramics. Mechanochemical activation of the starting K_2CO_3-Ta_2O_5 powder mixture was

implemented in the solid-state synthesis. After the calcination, the homogeneity of the powders was followed using electron microscopy. Structural and chemical heterogeneities were revealed in the powders after one calcination step. The homogeneity of the powder was improved by repeating the calcination. Pressure-assisted sintering, i.e. hot-pressing, was employed to promote densification of the ceramics. Phase-pure ceramics, prepared from the double-calcined powders, exhibit dielectric properties comparable to single-crystals.

2 Experimental

K_2CO_3 (99+ %, Sigma-Aldrich) and Ta_2O_5 (99 %, Alfa Aesar) were used as the starting compounds for the synthesis. Mechanochemical activation of the starting mixture was performed for 10 h in a planetary mill using a WC-Co milling vial and balls.

The activated mixture was pressed into pellets and heated once or twice at 800 °C for 4 h. After each calcination step the powder was milled at 175 min^{-1} for 4 h in acetone using a polyethylene vial and yttria-stabilized zirconia milling balls. For the pressure-assisted sintering the powder compacts were packed in coarse MgO powder in an alumina die and hot-pressed at 1250 °C for 2 h. The heating and cooling rates for both, calcination and sintering, were 5 K/min.

The powders were investigated with field emission scanning electron microscope (FE-SEM) Supra 35 VP (Carl Zeiss) and transmission electron microscope (TEM) JEM-2010F (JEOL). For microstructural analysis of the ceramic samples an FE-SEM instrument JSM-7600F (JEOL) was used.

The complex dielectric permittivity $\varepsilon^*(\omega, T)$ of the ceramics was measured in the frequency range from 1 Hz to 1 MHz using a Novocontrol Alpha High Resolution Dielectric Analyzer (Novocontrol Technologies) with the amplitude of the probing AC electric field of 1 V/mm. The dielectric response was measured in the temperature range from 300 K to 5 K with cooling rate of 1 K/min.

Further details of processing and characterization methods can be found in Ref [4,5].

3 Results

According to the X-ray diffraction (XRD) analysis single- and double-calcined powders are single-phased perovskites. As evident from FE-SEM micrographs in Figure 1, both powders consist of cuboidal particles with sizes ranging from ~100

nm to ~500 nm. A further TEM analysis of the powders after one calcination (left inset of the Figure 1) revealed presence of the nanoparticles with sizes 5 nm – 20 nm attached to larger particles. These nanoparticles are crystalline as well as amorphous and their chemical composition varies significantly. [4] No such heterogeneities were revealed in the $KTaO_3$ powders after the second calcination (right inset of the Figure 1). These powders with improved homogeneity were used for preparation of the ceramics.

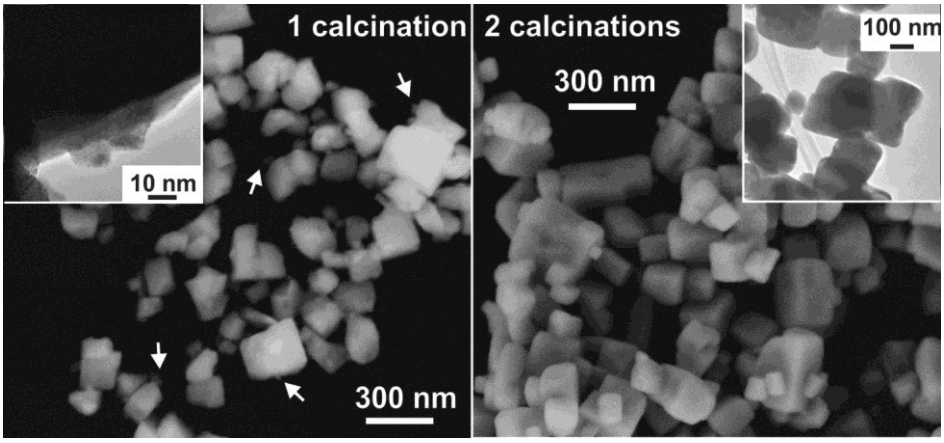

Figure 1: FE-SEM micrographs of the powders after one and two calcinations at 800 °C for 4 h. Detailed TEM micrographs are shown in the insets.

After hot-pressing the powder compacts at 1250 °C the perovskite $KTaO_3$ ceramics have relative densities of ~95 %. A bimodal grain size distribution is observed in the FE-SEM micrographs (Figure 2). Larger grains can exceed 3 μm in size, between the smaller grains are situated inside the porous regions. The average grain size is in the order of 1 μm.

A comparison of the temperature dependence of the dielectric permittivity ε' of the $KTaO_3$ ceramic and single-crystal is shown in Figure 3. In the case of the ceramic, the permittivity increases from 240 at room temperature to ~4000 below 10 K. The Barret formula, distinctive for incipient ferroelectrics, was used to fit the experimental data:

$$\varepsilon'(T) = C * \left(T_S - \coth\left(\frac{T_S}{T}\right) - T_0\right)^{-1}.$$

The obtained values of the fitted parameters C, T_S, and T_0 are 5.9x10^4, 25, and 11, respectively. Very similar parameters were reported for the high-quality single-crystal, which has only slightly higher low temperature permittivity, i.e. ~4500.[6]

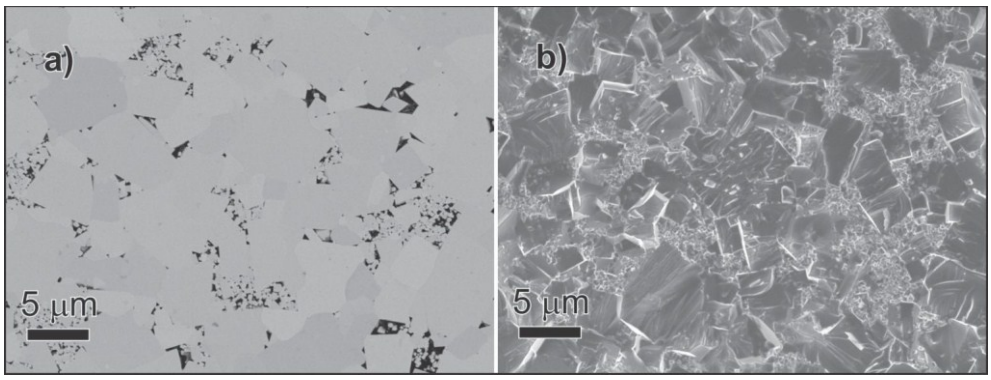

Figure 2 : FE-SEM micrographs of the a) polished and b) fractured surfaces of the $KTaO_3$ ceramics obtained by back-scattered and secondary electrons imaging modes, respectively.

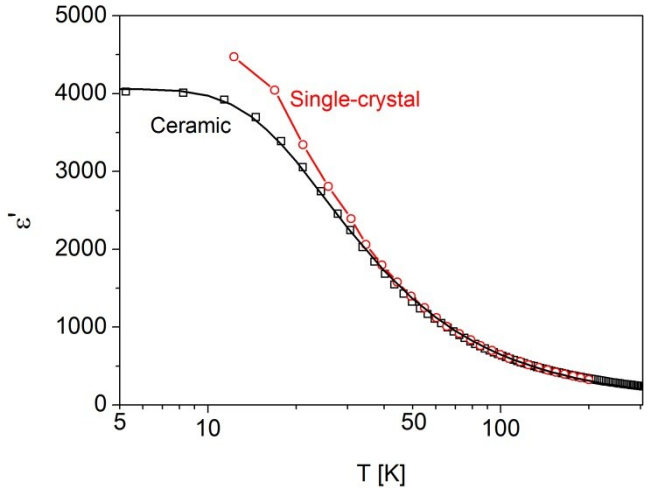

Figure 3: Temperature dependence of the dielectric permittivity ε' of the $KTaO_3$ ceramic measured at 100 kHz and single-crystal calculated from the hyper-Rayleigh spectra.[6] The line through the experimental points of the ceramic is fit to the Barret formula, while in the case of the single-crystal it is guide to the eye only.

Three frequency dispersion regions can be observed in the loss-spectrum of the $KTaO_3$ ceramic shown in Figure 4. All of them follow the Arrhenius law, with their characteristic activation energies E_A 84 meV, 225 meV, and 370 meV. The first one is typically reported for the $KTaO_3$ single-crystals and is related to an intrinsic lattice defect or unavoidable impurity. The origin of the second dispersion region is presently unclear, while the third one originates from the Co^{2+} impurity.[5]

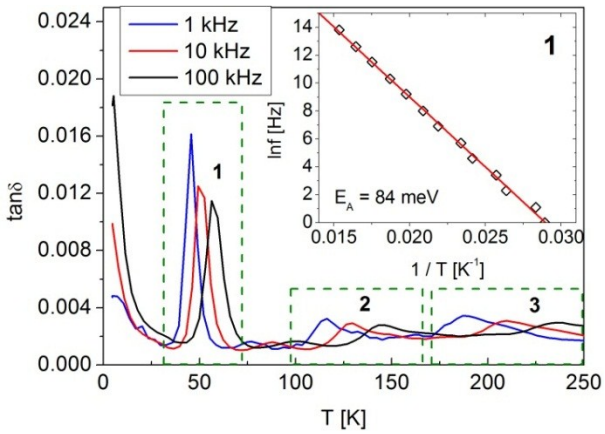

Figure 4: Temperature dependence of dielectric losses *tanδ* of the $KTaO_3$ ceramics measured at several frequencies. Different frequency dispersion regions are marked with numbers. The Arrhenius plot from the dispersion region 1 is shown in the inset. E_A…activation energy.

4 Conclusions

Processing of high-quality $KTaO_3$ ceramics using a combination of mechanochemical activation of the starting powder mixtures and conventional solid-state synthesis has been presented. The perovskite $KTaO_3$ powder was obtained after calcination at 800 °C, however, local heterogeneities were revealed by electron microscopy. The key step in the processing is the second calcination during which the homogeneity is improved.

The phase-pure ceramics with relative densities of 95 % were obtained by hot-pressing the double-calcined powder compacts at 1250 °C. The high homogeneity of the ceramics is reflected by excellent dielectric properties. The low-temperature value of dielectric permittivity, measured at 100 kHz, is 4000, and is very close to the single-crystal value, 4500.

References:

[1] S. Gevorgian. *Ferroelectrics in Microwave Devices, Circuits and Systems; Physics, Modeling, Fabrication and Measurements*. Springer, 2009.

[2] G. A. Samara. The relaxational properties of compositionally disordered ABO_3 perovskites. *Journal of Physics-Condensed Matter,* 15: R367–411, 2003.

[3] A. K. Axelsson et al. Synthesis, Sintering, and Microwave Dielectric Properties of $KTaO_3$ Ceramics. *Journal of the American Ceramic Society,* 92: 1773–1778, 2009.

[4] E. Tchernychova et al., Combined Analytical Transmission Electron Microscopy Approach to Reliable Composition Evaluation of $KTaO_3$. *Journal of the American Ceramic Society,* DOI: 10.1111/j.1551-2916.2010.04288.x, 2010.

[5] S. Glinšek et al. $KTaO_3$ Ceramics Prepared by the Mechanochemically Activated Solid-State Synthesis *Journal of the American Ceramic Society,* DOI: 10.1111/j.1551-2916.2010.04254.x, 2010.

[6] H. Vogt. Hyper-Rayleigh Scattering from the Bulk of Nominally Pure $KTaO_3$. *Physical Review B*, 41: 1030–1034, 1990.

For wider interest

The progress of modern wireless communication technology is very fast and the market is quickly expanding. Near-future microwave devices should be highly adaptable, have higher information densities, increased speed of data transfer and have reduced size as well as costs. A strong market demand for electronically tunable capacitors, i.e. varactors, including those based on ferroelectrics, therefore exists.

The ferroelectric material should have a large enough tunability, defined as the ratio between the dielectric permittivity ε' at zero applied DC electric field to the permittivity at some selected field, which is directly correlated to the high permittivity value. At the same time the material should have low dielectric losses $tan\delta$ at operating frequencies (microwave range). In order to avoid losses and hysteresis arising from the domain wall motions, ferroelectrics are preferably used in their paraelectric phase. When considering dielectric losses, single-crystals are the most obvious choice for the applications; on the other hand, ceramics are the cost-efficient alternative. In recent years a lot of research activities have focused on ferroelectric thin films due to miniaturization of electronic components, easier integration and much lower tuning voltages compared to bulk materials.

Our research involves a broad field of preparation and characterization of the ceramics and thin films of incipient ferroelectric $KTaO_3$, as well as its solid solution with ferroelectric $KNbO_3$. We are preparing the ceramics by solid-state synthesis and thin films by chemical solution deposition. Our aim is to establish the correlation between the dielectric properties and the synthesis conditions. Further on, we want to evaluate the influence of grain boundaries on the dielectric permittivity ε' value and the influence of the strain on dielectric properties in $KTaO_3$ polycrystalline films. The knowledge of these correlations will result in improved functional properties of the ceramics and thin films.

This work has been supported by the Slovenian Research Agency (young researcher program, contract number: 10000-07-3100068).

Priprava stolpičastih struktur $CoFe_2O_4$ pod vplivom magnetnega polja

Petra Jenuš[1,2], Darja Lisjak[1] , Darko Makovec[1], Miha Drofenik[1,3]

[1] Odsek za sintezo materialov, Inštitut Jožef Stefan, Ljubljana, Slovenija

[2] Mednarodna podiplomska šola Jožef Stefan, Ljubljana, Slovenija

[3] Fakulteta za kemijo in kemijsko tehnologijo, Maribor, Slovenija

petra.jenus@ijs.si ,darko.makovec@ijs.si(mentor)

Povzetek. V tem delu smo pripravili stolpiče kobaltovega ferita pod vplivom magnetnega polja iz stabilnih suspenzij nanodelcev kobaltovega ferita stabiliziranih s citronsko kislino oziroma z dodecilbenzen sulfonsko kislino v vodi oz. 1-butanolu. Delce smo sintetizirali s soobarjanjem in hidrotermalno sintezo. Sintetizirane nanodelce smo analizirali s presevnim elektronskim mikroskopom in z energijsko disperzijsko spektroskopijo. Delce smo iz suspenzij nanesli na korundno podlago in jih posušili v magnetnem polju. Morfologijo nastalih nanosov smo opazovali z vrstičnim elektronskim mikroskopom. Stolpiči, nastali pod vplivom magnetnega polja, so osnova za nadaljnjo pripravo magneto-električnih nanokompozitov.

Ključne besede: kobaltov ferit, soobarjanje, hidrotermalna sinteza, magneto-električni nanokompoziti

1 Uvod

V preteklem desetletju je zanimanje za magneto-električne (ME) materiale zaradi njihovih zanimivih fizikalnih lastnosti in široke uporabnosti na področju senzorjev, shranjevanja podatkov itn., nenehno naraščalo. Takšni materiali lahko izražajo spontano dielektrično polarizacijo kot odgovor na izpostavitev zunanjemu magnetnemu polju, ali inducirano magnetizacijo kot odgovor na vpliv zunanjega električnega polja. Ker so naravni enofazni magneto-elektriki redki in ker je njihov ME odziv šibek, ali ker se ME odziv pojavi pri temperaturah, ki so prenizke za uporabo v informacijski tehnologiji, so se raziskave na področju nanokompozitnih materialov, ki izražajo hkrati feroelektričnost in fero/ferimagnetnost, zelo povečale

[1]. ME nanokompozite lahko, glede na stik med obema fazama, razdelimo na tri skupine: 0-3 (Slika 1a) , 2-2 (Slika 1b) in 1-3 (Slika 1c) tip.

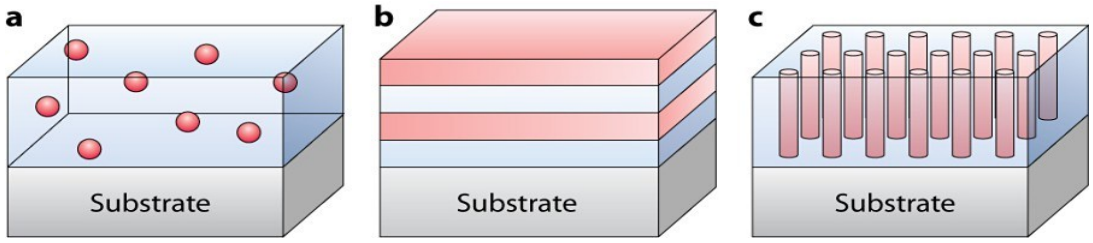

Slika 1: Shematska predstavitev treh tipov ME kompozitov [2].

Na sliki 1(a) je t.i. 0-3 tip, kjer so magnetni nanodelci umeščeni v feroelektrično matrico; (b) 2-2 izmenjujoči se nanosi fero/ferimagnetnega in feroelektičnega materiala; (c) 1-3 navpične heterostrukture, kjer so stolpiči magnetnega materiala umeščeni v feroelektrično matrico (ali obratno) [2].
Pri 1-3 tipu ME nanokompozitov je stična površina med obema fazama največja. Pomembnost le-te se odraža v velikem sklopitvenem učinku (angl. coupling effect), ki je posledica elastičnih interakcij na površini vzdolž navpične osi ter interakcij na stiku nanos/podlaga [3].
Zaradi posebnih lastnosti 1-3 ME nanokompozitov je bil namen tega dela priprava magnetnih stolpičastih struktur, ki bi pomenile osnovo za kasnejši nanos ter pripravo ME nanokompozitov.

2 Eksperimentalni del

2.1 Materiali

$Fe(NO_3)_3 \times 12\ H_2O$ (98 + %, Alfa Aesar); $Co(NO_3)_2 \times 6\ H_2O$ (98 + %, Alfa Aesar); TMAH (tetrametil amonijev hidroksid, 25 % w/w, aq. soln., Alfa Aesar); Citronska kislina (99 + %, Alfa Aesar); Amoniakalna raztopina (25 % for analysis, Merck); NaOH (98 %, Alfa Aesar); DBSA (dodecilbenzil sulfonska kislina, 96 + %, Alfa Aesar).

2.2 Sinteza $CoFe_2O_4$ – soobarjanje (vzorec A)

Pripravili smo vodno raztopine železovih (Fe^{3+}) in kobaltovih ionov (Co^{2+}). Tetrametil amonijev hidroksid - TMAH (n(TMAH) = 3 n (Fe^{3+}) + 2 n (Co^{2+}) smo ob mešanju segreli na 70 °C. Po kapljicah smo dodali raztopino ionov in presežen TMAH (pH > 12,5) ter nastalo suspenzijo mešali še 30 minut pri nespremenjeni

temperaturi 70 °C. Pri soobarjanju je nastala oborina črne barve, nastale delci, ki so kazali magnetne lastnosti, smo spirali z etanolom. Spranim delcem smo dodali destilirano vodo in citronsko kislino (γ = 0,5 g/ml), zaradi česar se je pH znižal na 2,4. Potrebno ga je bilo zvišati 5,2 z amoniakalno raztopino. Zatem smo nastalo suspenzijo mešali pri temperaturi 80 °C 90 minut, jo ohladili in uravnali pH na 10,1. V suspenziji je bilo 2,7 ut.% delcev $CoFe_2O_4$, kar smo določili z žaroizgubo pri 110 °C.

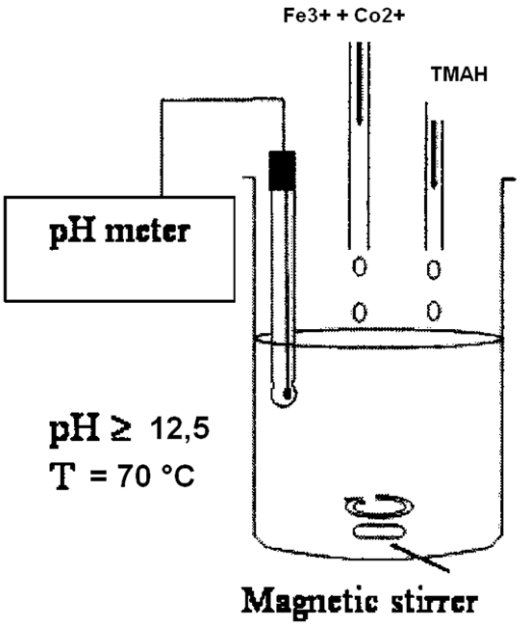

Slika 2: Soobarjanje v vodni raztopini

2.3 Sinteza $CoFe_2O_4$ – hidrotermalna sinteza (vzorec B)

K vodni raztopini ionov Fe^{3+} in Co^{2+} (molsko razmerje Fe : Co je 2 : 1) smo med mešanjem dodali vodno raztopino NaOH (m_{NaOH} = 4,6 g) in v časovnem intervalu 30 minut še dodecilbenzil sulfonsko kislino (DBSA). Suspenzijo smo prelili v teflonski lonček, ki smo ga namestili v avtoklav. Avtoklav smo postavili v peč na temperaturo 120 °C za 2 uri. Nastala oborina je bila črna barve, sintetizirani delci so izkazovali magnetne lastnosti. Po sintezi smo delce sprali in dispergirali v 1-butanolu. Stabilna suspenzija vsebuje 1,3 ut.% delcev kobaltovega ferita, kar smo določili z žaroizgubo pri 80 °C.

2.4 Priprava stolpičastih struktur

Obe stabilni suspenziji $CoFe_2O_4$ smo nanesli na podlago Al_2O_3 in nanosa pod vplivom magnetnega polja (B = 0,7 T) posušili pri sobni temperaturi. Nanašanje

smo ponovili trikrat (enkraten nanos je 10 kapljic), pred vsakim naslednjim nanosom smo organski del odstranili s segrevanjem s korakom 0,5°/min do temperature 460°C, pri kateri je bil zadrževalni čas 2 uri.

2.5 Karakterizacija

Velikost in kristaliničnost nanodelcev kobaltovega ferita smo določili s presevnim elektronskim mikroskopom (TEM). Njihovo kemijsko sestavo smo določili z energijsko disperzijsko spektroskopijo (EDS). Morfologijo nanosov smo opazovali z vrstičnim elektronskim mikroskopom (SEM), magnetne lastnosti nanosov smo izmerili z magnetometrom z vibrirajočim vzorcem (VSM).

3 Rezultati in diskusija

3.1 Karakterizacija delcev kobaltovega ferita

Karakterizacijo delcev smo opravili s TEM. Delci sintetizirani s soobarjanjem so bili sferične oblike s povprečno velikostjo 10 nm. Po hidrotermalni sintezi so nastali delci kubične oblike, kar nakazuje na večjo stopnjo kristaliničnosti nastalega kobaltovega ferita, in s povprečno velikostjo 15 nm. Pripadajoča elektronska difrakcija je pokazala, da imajo oboji delci spinelno strukturo. Njhova sestava določena z EDS je v obeh primerih pokazala, da je at.% Co : Fe = 1 : 2

3.2 Karakterizacija nanosov

3.2.1 SEM analiza

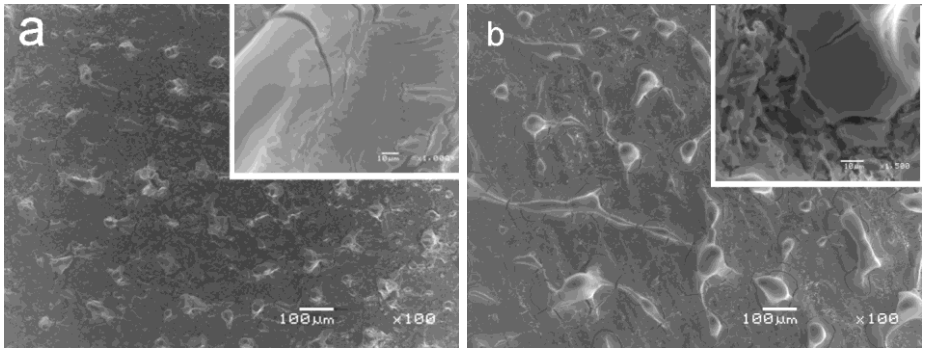

Slika 3: SEM slika stolpičastih struktur $CoFe_2O_4$ (gledano od zgoraj), vzorec A (a) in vzorec B (b). Povečana izseka prikazujeta pogled od strani.

Slika 3. prikazuje morfologijo nastalih nanosov kobaltovega ferita pod vplivom magnetnega polja. Slika 3.a prikazuje navpične heterostrukture pripravljene iz vzorca A. Slika 3.b prikazuje nastale strukture $CoFe_2O_4$, kjer smo za nanos uporabili stabilno suspenzijo vzorca B. Razdalje med nastalimi stolpiči se ne razlikujejo veliko glede na vrsto suspenzije (povprečna razdalja med dvema sosednjima stolpičema znaša med 100 in 200 μm). Nastale strukture se razlikujejo po obliki, saj je nastalo pri vzorcu A več samostojnih stolpičev, kot pri vzorcu B, kjer so stolpiči med seboj povezani z mostovi. Velikost nastalih stolpičev je v obeh primerih podobna in doseže vrednosti do nekaj milimetrov (2-3 mm). Mikroanaliza EDS je pokazala, da prostor med stolpiči sestavljata le Al in O, iz česar sklepamo, da je možno pri uporabljenih pogojih delce $CoFe_2O_4$ usmerjeno nanesti v stolpiče.

Za nadaljnjo uporabo in pripravo ME nanokompozitov so uporabnejši samostojni stolpiči, saj se s takšno obliko zagotovi večja stična površina med ferimagnetom in feroelektrikom.

3.2.2 Magnetne meritve

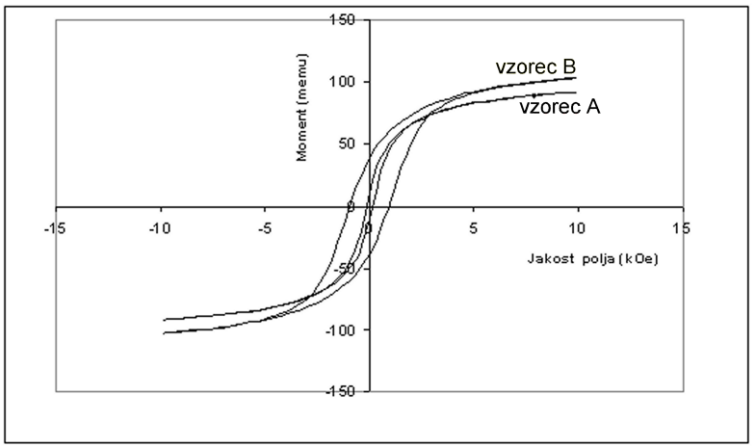

Slika 4: Magnetna histereza merjena pri sobni temperaturi za nanosa pripravljena iz vzorcev A in B.

Slika 4 prikazuje histerezni zanki za nanosa iz vodne (vzorec A) in butanolne suspenzije $CoFe_2O_4$ (vzorec B). Koercitivnost, H_c = 940,72 Oe, je pri nanosu iz butanolne suspenzije, kjer so bili delci $CoFe_2O_4$ sintetizirani s hidrotermalno

sintezo, precej višja kot pri nanosu delcev iz vodne suspenzije, sintetiziranih s soobarjanjem, ki so izkazali koercitivnost, H_c = 141,16 Oe. Razliko lahko pripišemo razliki v velikosti delcev in večji stopnji kristaliničnosti pri delcih sintetiziranih po hidrotermalnem postopku (vzorec B) kot pri delcih sintetiziranih s soobarjanjem (vzorec A) (glej del 3.1).

4 Zaključek

Pripravili smo stolpičaste strukture kobaltovega ferita pod vplivom magnetnega polja. Nanose smo pripravili iz stabilnih suspenzij nanodelcev kobaltovega ferita stabiliziranih s citronsko kislino v vodi oziroma z dodecilbenzil sulfonsko kislino v 1-butanolu. Rezultati so pokazali, da po sušenju pri sobni temperaturi pod vplivom magnetnega polja in odstranitvi organske faze nastanejo stolpičaste strukture kobaltovega ferita. Nastale vertikalne strukture bomo v nadaljevanju uporabili kot eno izmed faz v magneto-električnih nanokompozitih.

Literatura:

[1] F. Zavaliche, H. Zheng, L. Mohaddes-Ardabili, S. Y. Yang, Q. Zhan, P. Shafer, E. Reilly, R. Chopdekar, Y. Jia, P. Wright, D. G. Schlom, Y. Suzuki and R. Ramesh Electric Field-Induced Magnetization Switching in Epitaxial Columnar Nanostructures, Nano Lett., **2005**, 5, 1793-1793

[2] Y. Wang, J. Hu, Y. Lin, C.-W. Nan, Multiferroic magnetoelectric composite nanostructures, *NGP Asia Mater.*, 2010, **2**(2), 61-68

[3] X. Y. Lu, B. Wang, Y. Zheng, E. Ryba, Phenomenological theory of 1-3 type multiferroic composite thin film: thickness effect, *J. Phys. D: Appl. Phys.*, 2009, **42**, 015309

Za širši interes

Raziskave na Odseku za sintezo materialov so usmerjene v razvoj naprednih oksidnih materialov, ki izkazujejo uporabne elektromagnetne lastnosti. Namen raziskav je pridobiti znanje o kemiji materialov, kar omogoča načrtovanje novih materialov z želenimi lastnostmi.

Pridobljeno znanje o kontrolirani sintezi osnovnih materialov nadgrajujemo z znanjem o prilagajanju njihovih kemijskih lastnosti za sintezo sestavljenih in/ali večfunkcionalnih materialov. Na odseku tako raziskujemo materiale za uporabo v elektroniki, telekomunikacijah, medicini, tehniki, ekologiji.

Večfunkcionalni materiali

Obvladovanje površinskih lastnosti nanodelcev nam omogoča pripravo nanokompozitov, ki kombinirajo različne uporabne lastnosti materialov, ki jih vsebujejo. Predvsem gre za kombinacijo ferimagnetnih materialov in dielektrikov (magnetodielektrikov) ali feromagnetnih in feroelektričnih materialov (kompozitnih multiferoikov). V okviru razvoja novih magnetooptičnih materialov študiramo mehanizme kristalizacije magnetnih delcev v različnih optično prozornih matricah ter vpliv magnetnih lastnosti delcev in zunanjega magnetnega polja na optične lastnosti. Ti sestavljeni materiali so osnova naprednih magnetooptičnih senzorjev. S prevlečenjem magnetnih nanodelcev z nanodelci TiO2 sintetiziramo magnetno odzivne fotokatalitske nanokompozitne delce, ki se uporabljajo za čiščenje onesnaženih voda in plinov.

Synthesis and characterisation of nano-TiO_2 particles with different techniques

Matic Krivec[1,2], **Ricardo A. Segundo**[3], **Rita R. N. Marques**[3], **Goran Dražić**[1,2]

[1] Department of nanostructured materials, Jožef Stefan Institute, Ljubljana, Slovenia

[2] Jožef Stefan International Postgraduate School, Ljubljana, Slovenia

[3] FEUP-Faculdade de Engenharia da Universidade do Porto, Porto, Portugal

matic.kriveck@ijs.si

Abstract. Anatase and rutile TiO_2 particles were successfully prepared from two different precursors (Ti(IV)isopropoxide and peroxotitanium complex) by sol-gel and hydrothermal methods. Samples were doped with urea and K_2SO_4 and the particles were characterized by X-ray diffraction (XRD), UV-Vis spectrophotometry, Transmission Electron Microscopy (TEM) and photocatalytic experiments. The results show the formation of rutile particles at low temperature with the peroxotitanium complex as a precursor. These particles exhibit high photocatalytic activity in comparison to the traditionally prepared rutile particles.

Keywords: TiO_2, anatase, rutile, XRD, TEM, photocatalysis.

1 Introduction

Nowadays, remediation of different hazardous wastes, contaminated grounds and air has attracted attention all over the world. In order to overcome this problem, extensive research is being conducted to develop new analytical, biochemical and physicochemical methods for the characterization and elimination of hazardous chemicals from air, soil and water [1].

Semiconductor photocatalysis is a physicochemical method, which is supplementary to the conventional approaches. Semiconductors are sensitive for light-reduced redox processes due to their electronic structure, which has a filled valence band and an empty conduction band. When a photon with appropriate energy reaches the semiconductor, an electron is promoted to the conduction band leaving a hole behind in the valence band. Photogenerated free electrons and holes

are excellent reducing and oxidizing agents and they directly or indirectly (hydroxyl radicals, superoxide ions) remediate various contaminations such as alkanes, aliphatic carboxylic acids, dyes, simple aromatics, halogenated alkanes, pesticides [1].

Semiconductor photocatalysis is primary focused on TiO_2 which has been successfully applied to a variety of problems of environmental interest for water and air purification [1]. It can be found in three crystal modifications: anatase, rutile and brookite. Photocatalysis has been extensively investigated on the first two structures; anatase is active in UV-A spectrum while rutile has smaller band gap and it can be activated by visible light. Solar energy contains only small amounts of UV light (approximately 5 %), therefore rutile should have bigger photocatalytic activity in the solar spectrum, which is not the case. Anatase has better photocatalytic properties than rutile due to several factors. The first one is lower surface hydroxylation rate of rutile particles: they are usually obtained at higher calcination temperatures (above 600 °C), where most of surface hydroxyl groups are removed from the surface. The substrates cannot get into contact with the photocatalyst and initiate the reaction. The second is lower specific surface area, which is due to the larger rutile particles in comparison to anatase particles. The third is the recombination probability: rutile has a smaller band gap than anatase and therefore a higher recombination probability [2].

Doping of materials or introducing point defects to the crystal structure of the material is one of the possibilities for visible-light-induced photocatalysis. Two types of TiO_2 doping are frequently used: doping with metal impurities (Fe, Al, Sn, Ce, Nb …) and doping with non-metal elements (N, C, S, B, P, F). The second type (anion doped system) has become the most attractive in the recent years [3]. These observations suggested that doping led to the formation of midgap states above the valence band. In this case, visible light can excite electrons from the midgaps, although the electron excitation is still more probable with UV light [4].

Another way of producing visible-light-induced photocatalysts is to improve photocatalytic properties of rutile particles. The traditional preparation method consists of a high-temperature calcination step, which leads to agglomeration of nanocrystalline particles with low surface area and smaller surface hydroxylation rate. Fabrication of rutile nanoparticles at low temperatures is an option, which can

ensure better characteristics of the rutile phase. A relatively new and fast method of rutile nanoparticle preparation is by using a peroxotitanium complex [5].

2 Experimental

2.1 Samples preparation

Ti(IV)isopropoxide was used as a starting agent for the synthesis of TiO_2 particles in two procedures. The first one started with the addition of deionized water. The pH was adjusted to 2,5 with nitric acid and the sol-gel was put under reflux conditions for 24 h. Urea and K_2SO_4 were added as the dopants of N and S atoms. The whole solution was put into autoclave at 150 °C for 48 h. Some samples were additionally calcinated at different temperatures.

The second procedure started with the synthesis of peroxotitanium complex with the addition of hydrogen peroxide to Ti(IV)isopropoxide. The pH of the solution was below 1 and the solution was stirred under reflux conditions for 24 h. The continuation of the procedure was the same as in the first procedure.

2.2 Characterization

The phases of TiO_2 powders were identified by X-ray diffraction (XRD) which was conducted on a X`Pert PRO MPD diffractometer (PANalytical, The Netherlands).The average particle size of the sample was calculated from Scherrer`s equation. The UV-Vis absorption spectra for energy band-gaps calculations were obtained with the Jasco V-560 spectrophotometer (Jasco, USA). The morphology of the particles was observed with a transmission electron microscope Jeol 2010F (TEM; Jeol, Japan). Characterization of photocatalytic activity of the samples was conducted inside a SolarBox 1500 apparatus (CO.FO.ME.GRA. Srl, Italy) with light which simulates the outdoor exposure.

3 Results and discussion

The results from XRD measurements revealed the presence of the pure anatase phase after the hydrothermal synthesis from Ti(IV)isopropoxide precursor without additional calcination step. The average particles size of anatase particles was around 10 nm and up to 30 nm after the calcination process. Rutile particles with

70 nm size were seen after being calcinated at 800 °C for 3 h, although this was not the case in the S-doped sample. The sol-gel synthesis of TiO_2 particles with the use of peroxotitanium complex and without doping has shown the formation of rutile particles, which is rather surprising, because they are normally obtained after a high-temperature calcination process of the anatase phase. The addition of urea and K_2SO_4 destabilized the rutile formation route, which led to the formation of anatase particles (Table 1).

The band gap calculations are consistent with those in the literature. The band gap values of anatase phase vary between 3,18 eV to 3,27 eV. The only exception is the sample prepared from a sol-gel synthesis with the peroxotitanium complex and with S-doping, where the band gap was very low (2,49 eV). Band gaps of rutile particles are lower than those of anatase and they are around 3,07 eV (Table 1).

TEM micrographs of TiO_2 particles show different structures of anatase and rutile particles. Rutile particles were easily synthesized by a sol-gel method at low temperatures and without calcination. Particles became more homogeneous after the hydrothermal treatment. High resolution images of anatase and rutile did not reveal any incorporation of dopants into the crystal structure of the nanoparticles (Fig. 1).

Photocatalytic activity was measured with the oxidation of caffeine after different irradiation times inside a SolarBox apparatus. The best photocatalytic activity (78 % conversion) was measured with the HT_isopropoxide_Sdoped_800 sample. Rutile particles synthesized from a peroxotitanium precursor at low temperature had also a very high photocatalytic activity (73 % conversion). Rutile particles synthesized by the conventional calcination method (HT_isopropoxide_Ndoped_800) did not show any photocatalytic activity (Table 2).

4 Conclusion

In this paper, we described two different paths of TiO_2 synthesis from Ti(IV)isopropoxide and peroxotitanium complex as a precursor. Based on the results, the doping of N and S elements was not successful as the elements did not incorporate into the crystal structure of TiO_2 particles. We managed to synthesize rutile particles at low temperature, which improved their photocatalytic activity. In

the future, photocatalytic activity of the particles will be measured on the visible-light illumination.

Table 1: Average particles sizes of TiO_2 particles and their energy band gap values (A-anatase, R-rutile).

Sample	Particle size (nm)	Band gap (eV)
SG_isopropoxide_300	A: 7	*n.m.
SG_isopropoxide_600	A: 14	*n.m.
SG_isopropoxide_Ndoped_300	A: 8	*n.m.
SG_isopropoxide_Ndoped_600	A: 20	*n.m.
SG_isopropoxide_Sdoped_300	A: 4	*n.m.
SG_isopropoxide_Sdoped_600	A: 14	*n.m.
SG_peroxotitanium	R: 46	3,07
SG_peroxotitanium_Sdoped	A: 12	2,49
HT_isopropoxide	A: 9	*n.m.
HT_isopropoxide_800	A: 22 and R: 74	*n.m.
HT_isopropoxide_Ndoped	A: 9	3,23
HT_isopropoxide_Ndoped_300	A: 9	3,21
HT_isopropoxide_Ndoped_500	A: 11	3,19
HT_isopropoxide_Ndoped_800	R: 74	*n.m.
HT_isopropoxide_Sdoped	A: 7	3,18
HT_isopropoxide_Sdoped_300	A: 7	3,2
HT_isopropoxide_Sdoped_500	A: 8	3,23
HT_isopropoxide_Sdoped_800	A: 33	3,27
HT_peroxotitanium	R: 39	3,07
HT_peroxotitanium_Sdoped	A: 12	3,25
HT_peroxotitanium_Ndoped	A: 17	3,26
Degussa P25	A and R: 21	3,33

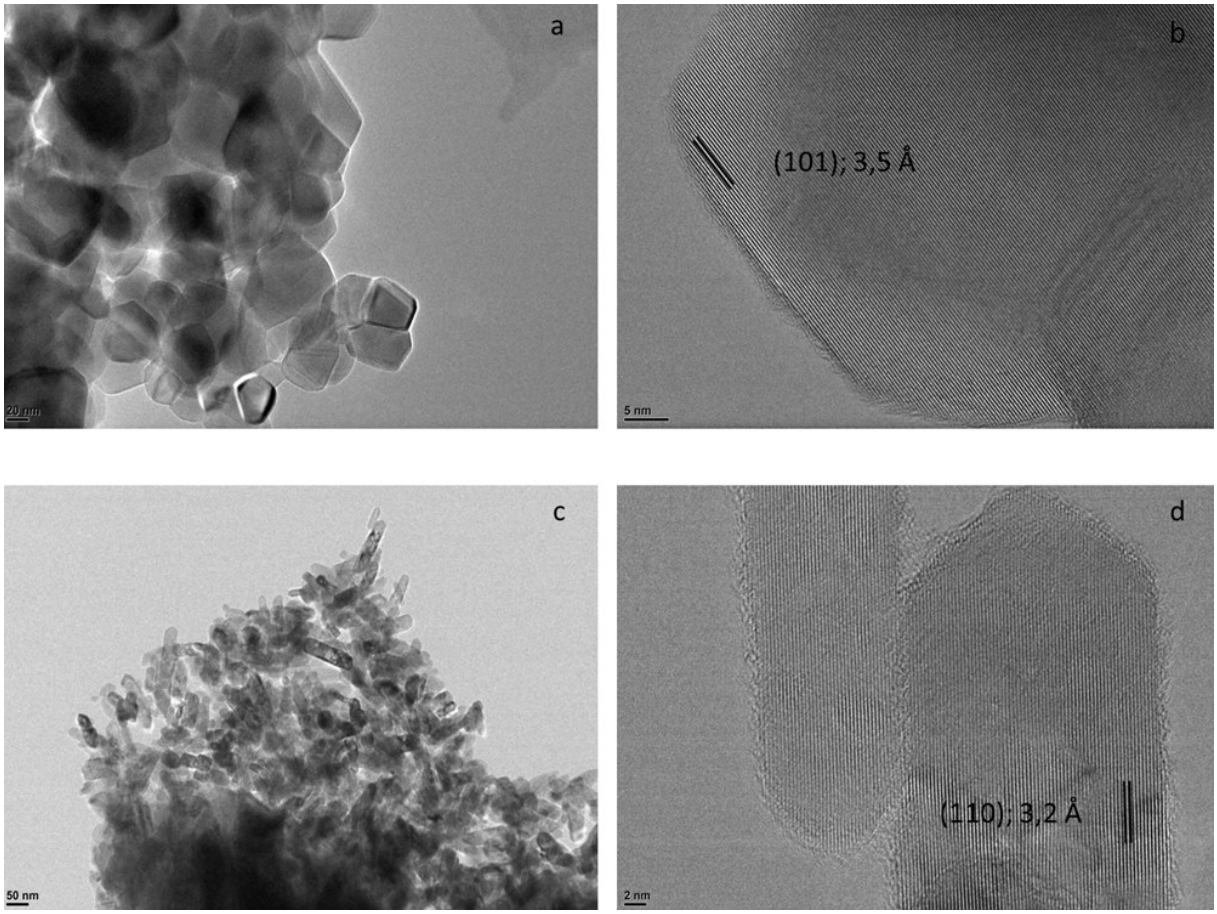

Figure 1: TEM images of anatase (a, b) and rutile (c, d) particles prepared by different techniques: (a) and (b) HT_isopropoxide; (c) and (d) HT_peroxotitanium.

Table 2: Photocatalytic conversion of caffeine with different TiO_2 samples after 120 minute irradiation time.

	Crystal phase	Photocatalytic coefficient	Conversion (t = 120 min)
HT_isopropoxide_Ndoped	anatase	7,5E-03	0,67
HT_isopropoxide_Ndoped_500	anatase	2,7E-03	0,47
HT_isopropoxide_Ndoped_800	rutile	0	0
HT_isopropoxide_Sdoped	anatase	1,3E-03	0,12
HT_isopropoxide_Sdoped_800	anatase	1,1E-02	0,78
SG_peroxotitanium	rutile	6,0E-04	0,09
SG_peroxotitanium_Sdoped	anatase	6,4E-03	0,49
HT_peroxotitanium	rutile	4,4E-03	0,73
HT_peroxotitanium_Ndoped	anatase	7,7E-03	0,64
HT_peroxotitanium_Sdoped	anatase	7,1E-03	0,67
Degussa P25	anatase + rutile	3,2E-02	1

References:

[1]M. R. Hoffmann, S. T. Martin, W. Choi and D. W. Bahnemann. *Environmental Applications of Semiconductor Photocatalysis.* Chemical Reviews, 95: 69-96, 1995.

[2]A. Sclafani, J. M. Herrmann. *Comparison of the Photoelectronic and Photocatalytic Activities of Various Anatase and Rutile Forms of Titania in Pure Liquid Organic Phases and in Aqueous Solutions.* Journal of Physical Chemistry, 100: 13655-13661, 1996.

[3]D. Devilliers. *Semiconductor Photocatalysis: Still an Active Research Area despite Barriers to Commercialization.* Energeia, 17, 2006.

[4]A. Fujishima, X. Zhang, D.A. Tryk. *TiO_2 photocatalysis and related surface phenomena.* Surface Science Reports, 63: 515-582, 2008.

[5]Y. Zhang, L. Wu, Q. Zeng, J. Zhi. *Synthesis and characterization of rutile TiO_2 nano-ellipsoid by water-soluble peroxotitanium complex precursor.* Materials Chemistry and Physics, 121: 235-240, 2010.

For wider interest

Photocatalytic reaction with TiO_2 has become a well-known procedure for the remediation of different pollutants; the process is efficient, environmental-friendly and relatively cheap. The main requirement of this process is to ensure the illumination of TiO_2 with a proper energy source (UV light). While the solar spectrum contains only small amount of UV light (5 %) which is even smaller when the weather is cloudy, it is important to shift the photocatalytic activity towards the visible spectrum. In our research work, we will try to improve the photocatalytic activity and we will try to produce a very sensitive photocatalyst, which would efficiently oxidize different pollutants on the solar spectrum. Furthermore, our aim is to strongly attach the photocatalyst to some substrate to prevent the TiO_2 pollution. We would like to produce a microreactor with the TiO_2 coating on the inner surface of the reactor. The advantages of reactions at micro level favor the idea of TiO_2 implantation into microreactors; high surface-to-ratio area, higher heat and mass transfer, higher spatial illumination homogeneity and better light penetration through the entire reactor are just a few of several properties that make this procedure interesting in designing micro-cleaning devices. Moreover, the scale-up of this cleaning device can be easily done with parallel binding, without any restrictions in immobilization in comparison with the large-scale reactors.

Enhancing the materials for new generation of piezoelectric devices

Nikola Novak[1,2] and **Zdravko Kutnjak**[1]

[1] Department of Condensed Matter, Jožef Stefan Institute, Ljubljana, Slovenia

[2] Jožef Stefan International Postgraduate School, Ljubljana, Slovenia

nikola.novak@ijs.si

Abstract. Piezoelectric elements are commonly used in smart electronic systems as sensors, actuators and motors or in the field of ultrasound imaging and telecommunication. The broad spectrum of technological possibilities to use the piezoelectric effect makes the materials with piezoelectric properties very interesting. Especially development and improvement of this material has attracted considerable attention in last few decades. In this paper we show the piezoelectric response of ferroelectric relaxor $PMN_{(1-x)}$-PT_x [100] single crystal with concentration near morphotropic phase boundary, x=0.26. The critical behaviour of piezoelectric coefficient near the liquid-vapour type critical point is discussed. This was presented as a new driving mechanism for the enhancement of the piezoelectric response of relaxor materials [1, 2].

Keywords: critical point, relaxor ferroelectric, piezoelectricity.

1 Introduction

Piezoelectricity is a property of a material to transform mechanical signals into electric signals and vice versa. This property is used in many applications like sensors, actuators, ultrasonic devices, telecommunications and devices that we use in everyday life like microphone, speakers, lighter and toys. In the quest to make these devices increasingly smaller and more efficient the enhancement of the piezoelectric response is of great importance. Therefore, two approaches to resolve this issue are usually considered. In the first approach, one tries to find a new material that exhibits a large piezoelectric response. In the second approach, we try to understand mechanisms that are responsible for the enhancement of the piezoelectric response. The latter approach would allow the possibility of synthesizing better piezoelectric materials.

Ferroelectric relaxor $(Pb(Mg_{1/3}Nb_{2/3})O_3)_{(1-x)}$-$(PbTiO_3)_x$ $PMN_{(1-x)}$-PT_x is one of the most studied systems due to the large piezoelectric response which can be observed near the rhombohedral to tetragonal phase transition known as morphotropic phase boundary [1, 3, 4]. It was for a long time accepted that the polarization rotation mechanism which was detected with different experimental methods is responsible for enhanced piezoelectric coefficient near the morphotropic phase boundary [5, 6, 7]. This was reasonable due to the presence of the intermediate monoclinic phase sequence, i.e., monoclinic B (M_B) – orthorhombic (O) – monoclinic C (M_C) which represents the polarization path between rhombohedral (R) and tetragonal (T) phase in PMN-PT systems. Recently, a new approach was presented on PMN-PT system that explains the enhancement of piezoelectric response by taking into account the influence of the electric field. It was experimentally shown that if we apply sufficiently high electric field, $E \geq E_{cp}$, the ferroelectric to paraelectric transition line in E-T-x phase diagram end in the so called liquid-vapour type of critical point [1]. In the proximity of the critical point the critical behaviour of piezoelectric coefficient is observed. The criticality of piezoelectric coefficient is in agreement with recently theoretically confirmed divergence of the piezoelectric and dielectric susceptibility tensor at the critical point [2, 3, 8].

Here, we report the results of dielectric and piezoelectric measurements of $PMN_{(1-x)}$-PT_x single crystal with the PT concentration near the cubic (C)-tetragonal-rhombohedral (C-T-R) triple point, x=0.26. We investigate the temperature behaviour of the piezoelectric coefficient of the $PMN_{0.74}$-$PT_{0.26}$ single crystal poled along [100] direction at various temperatures and electric fields.

2 Experiments and discussion

The complex dielectric constant as a function of temperature and electrical field was measured in a frequency range between 20 Hz and 1 MHz by using a HP4282 Precision LCR Meter. Dielectric measurements show typical relaxor dispersion of ε peak with anomalous behaviour around 370 K at sufficiently high electric field (Fig.

1) [9]. According to the previous reports in PMN-PT systems [1, 8] the dielectric anomaly is related to monoclinic phase sequence [10-11].

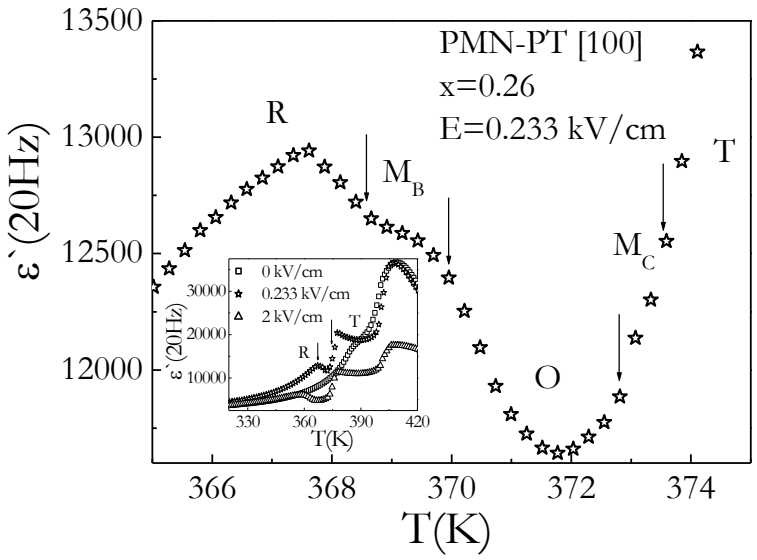

Figure 1: Intermediate monoclinic phase sequence observed in the dielectric response of $PMN_{0.74}$-$PT_{0.26}$ single crystal in [100] direction.

The influence of the electric field on monoclinic phase sequence (inset to Fig. 1) shows that these transitions get suppressed and smeared out at higher electrical fields. Similar behaviour was reported for pure PMN [111] and [100] as for PMN-PT systems for concentration $x \leq 0.30$ [1, 8, 12].

The temperature dependency of the piezoelectric coefficient of the $PMN_{0.74}$-$PT_{0.26}$ single crystal poled along [100] direction at various temperatures and electric fields was studied by the dielectric resonant method. We scanned the sample which acts like a piezoelectric bar resonator with frequency signal between 100 kHz and 1 MHz. From the obtained data the complex piezoelectric constant was calculated [13]. Figure 2 shows the piezoelectric coefficient d_{31} as a function of temperature of $PMN_{0.74}$-$PT_{0.26}$ single crystal poled along [100] direction at electric field 0.934 kV/cm.

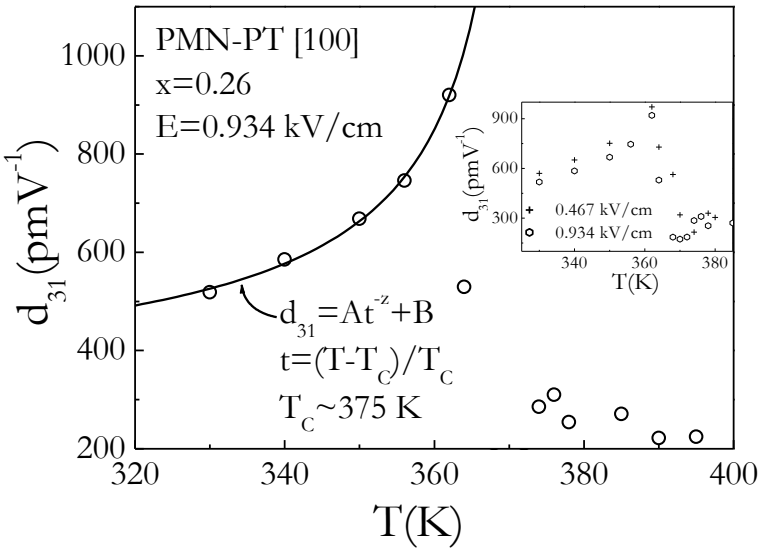

Figure 2: Solid line represents a fit to the power law ansatz of temperature dependent piezoelectric coefficient at E=0.934 kV/cm. The inset shows temperature dependence of the d_{31} at E=0.467 kV/cm and 0.934 kV/cm.

We observed a peak in the rhombohedral phase which is much smaller than that reported for electric fields applied along [111] and [110] axes [8]. This is due to the fact that the direction of the electric field is further away from the [111] polar axis direction. Nevertheless, it is interesting that the piezoelectric coefficient peak was observed below monoclinic phase sequence and not in the temperature range of monoclinic phase sequence as we would expect due to the polarization rotation. It was shown with simple power law ansatz that observed critical dependence of the d_{31} is actually related to critical behaviour of the phase transitions above the monoclinic phase sequence. This suggests that the monoclinic phase sequence is actually responsible for prior cut off of the critical dependence of d_{31} and not for enhancement of d_{31}. With increasing electrical field the cut off temperature and peak values of d_{31} are decreasing. This is due to the shifting downwards of M_B-R phase transition temperature and increasing of M_C-T phase transition temperature with increasing electric field [8].

3 Conclusion

The studies of ferroelectric relaxor PMN-PT systems show that the improvement of the piezoelectric response can be achieved in two steps. In the first step, the

system has to be engineered in such a way that it is brought to the vicinity of the critical point where the piezoelectric tensor diverges due to the divergence of the dielectric susceptibility [1, 2, 8]. In the second step, we have to take into account the influence of monoclinic phase sequence. Temperature dependence of the piezoelectric response at various electric fields of $PMN_{0.74}$-$PT_{0.26}$ single crystal poled along [100] direction and all previously reported studies on PMN-PT [111] and [110] axis [8] show cut off of d_{31} in the temperature range of monoclinic phase sequence. This suggests that the piezoelectric response could be even larger if it would be possible to create a material without or at least with very narrow temperature range of intermediate monoclinic phase sequence between the R-T transition.

References:

[1] Z. Kutnjak, J. Petzelt, R. Blinc. The giant electromechanical response in ferroelectric relaxors as a critical phenomenon. *Nature,* 441:956-959, 2006

[2] M. Porta, T. Lookman, A. Saxena. Effects of criticality and disorder on piezoelectric properties of ferroelectrics. *Journal of Physics: Condensed Matter,* 22:345902, 2010

[3] E. V. Colla, N. K. Yushin, D. Viehland. Dielectric properties of $PMN_{(1-x)}$-PT_x single crystals for various electrical and thermal histories. *Journal of Applied Physics,* 83:3298-3304, 1998

[4] G. Xu, D. Viehland, J. F. Li, P. M. Gehring, G. Shirane. Evidence of decoupled lattice distortion and ferroelectric polarization in the relaxor system PMN-xPT. *Physical Review B,* 58:212410, 2003

[5] M. Davis, D. Damjanović, N. Setter. Electric-field-, temperature-, and stress-induced phase transitions in relaxor ferroelectric single crystals. *Physical Review B,* 73:014115, 2006

[6] D. Viehland, J. Powers. Effect of uniaxial stress on the electromechanical properties of $0.7Pb(Mg_{1/3}Nb_{2/3}O_3)$-$0.3PbTiO_3$ crystals and ceramics. *Journal of Applied Physics,* 89:1820-1825, 2001

[7] D. Damjanović. Comments on Origins of Enhanced Piezoelectric Properties in Ferroelectrics. *IEEE Transastion on Ultrasonics, Ferroelectrics, and Frequency Control.* 56:1574-1585, 2009

[8] Z. Kutnjak, R. Blinc, Y. Ishibashi. Electric field induced critical points and polarization rotations in relaxor ferroelectrics. *Physical Review B,* 76:104102, 2007

[9] L. E. Cross. Relaxor ferroelectrics. *Ferroelectric,* 76:241-267, 1987

[10] D. E. Cox, B. Noheda, G. Shirane, Y. Uesu, K. Fujishiro, Y. Yamada. Universal phase diagram for high-piezoelectric perovskite systems. *Applied Physics Letters,* 79:400-402, 2001

[11] L. Yu, D.-Y. Jeong, Z.-Y. Cheng, Q. M. Zhang, H.-S. Luo, Z.-W. Yin, D. Viehland. Phase transitional behavior and piezoelectric properties of the orthorhombic phase of $Pb(Mg_{1/3}Nb_{2/3}O_3)$-$PbTiO_3$ single crystals. *Applied Physics Letters,* 78:3109-3111, 2001

[12] X. Zhao, W. Qu, X. Tan, A. A. Bokov, Z.-G. Ye. Electric field-induced phase transitions in (111)-, (110)-, and (100)-oriented $Pb(Mg_{1/3}Nb_{2/3})O_3$ single crystals. *Physical Review B,* 75:104106, 2007

[13] D. Damjanović. An equivalent electric circuit of a piezoelectric bar resonator with a large piezoelectric phase angle. *Ferroelectrics,* 110:129-135, 1990

For wider interest

Piezoelectricity is a property of materials to transform electric energy to mechanical work and vice versa. This is very useful in many applications, for instant in smart electronic systems as sensors, actuators and motors or in the field of ultrasound imaging and telecommunication. The broad spectrum of technological possibilities to use the piezoelectric effect makes piezoelectric materials very interesting. In the last few decades, development and improvement of these materials have attracted considerable attention. One way to improve the piezoelectric response is to understand the basic principles which are responsible for enhancement of piezoelectric coefficient. For a long time the enhancement of piezoelectric response was attributed to morphotropic phase boundary and a polarization rotation mechanism. Recently, a new way to enhance the piezoelectric response was shown in which the influence of the electric field is taken into account. Specifically, by applying a sufficiently high electric field the system is brought to the proximity of liquid-vapour type critical point where maximum of the piezoelectric coefficient can be observed. It was theoretically shown that the enhancement of the piezoelectric coefficient is directly related to the divergence of the dielectric susceptibility tensor at critical point. Our investigation of piezoelectric response in the ferroelectric relaxor PMN-PT system close to the morphotropic phase boundary show that the enhancement of the piezoelectric coefficient is not predominantly related to the polarization rotation within the monoclinic phase sequence as previously thought. In contrast, it was observed that at the onset of the monoclinic phase sequence the critical piezoelectric response is greatly reduced.
Our studies reveal two new possibilities of improvement of piezoelectric response. One is to bring the system in the vicinity of critical point and another is to synthesise materials without or at least with very narrow temperature range of monoclinic phase sequence close to the morphotropic phase boundary.

Magnetne lastnosti nanodelcev Ba heksaferita ($BaFe_{12}O_{19}$) sintetiziranih s hidrotermalno sintezo

Darinka Primc[1,2], Miha Drofenik[1,3], Darja Lisjak[1], Darko Makovec[1]

[1] Odsek za sintezo materialov, Inštitut Jožef Stefan, Ljubljana, Slovenija

[2] Mednarodna podiplomska šola Jožef Stefan, Ljubljana, Slovenija

[3] Fakulteta za kemijo in kemijsko tehnologijo, Maribor, Slovenija

darinka.primc@ijs.si

Mentor: doc. dr. Darja Lisjak

Izvleček. V prispevku opisujemo uspešno pripravo magnetnih tekočin na osnovi nanodelcev Ba heksaferita sintetiziranih s hidrotermalno sintezo. Raziskali smo vpliv adsorpcije oleinske kisline na površino nanodelcev med hidrotermalno sintezo. Pokazali smo, da adsorbirana oleinska kislin na površini nanodelcev popolnoma blokira proces sekundarne rekristalizacije. Morfologijo in velikost delcev smo zasledovali z presevno elektronsko mikroskopijo (TEM) medtem ko smo z magnetometrom z vibrajočim vzorcem (VSM) določili magnetne lastnosti sintetiziranih produktov.

Keywords: Ba heksaferit, hidrotermalna sinteza, nanodelci, magnetne lastnosti

1 Uvod

Magnetne tekočine so stabilne koloidne suspenzije magnetnih nanodelcev. Uporabljajo se v tehnične namene, kot so tesnenje, prenos toplote in dušenje vibracij. V medicini se magnetne tekočine uporabljajo za povečevanje kontrasta pri slikanju s tehniko NMR, medtem ko se testirajo za ciljano dostavljanje zdravilnih učinkovin in kot mediatorji pri zdravljenju raka z magnetno hipertermijo.[1] Magnetne tekočine lahko služijo tudi za pripravo magnetnih nanosov in kot prekurzorji pri sintezi nanokompozitov. [1]

Za pripravo magnetnih tekočin so potrebni nanodelci, ki izkazujejo superparamagnetne lastnosti. V superparamagnetnih nanodelcih pride zaradi termične energije do spontane relaksacije magnetnih momentov. Medtem ko se večji, feromagnetni delci zaradi magnetnih interakcij med seboj močno aglomerirajo, pa je možno pripraviti stabilno suspenzijo superparamagnetnih

nanodelcev. Z adsorpcijo surfaktanta na nanodelce zagotovimo odbojne sile med njimi in preprečimo njihovo aglomeracijo.[1,2]

Danes se za pripravo magnetnih tekočin uporabljajo predvsem nanodelce različnih spinelnih feritov (npr. Fe_3O_4, γ-Fe_2O_3, $CoFe_2O_4$, $NiFe_2O_4$). Zaradi posebnih intrinzičnih lastnosti, ki jih izkazujejo magnetni materiali iz družine heksagonalnih feritov ($BaFe_{12}O_{19}$, $SrFe_{12}O_{19}$), pa bi bila zanimiva tudi priprava magnetnih tekočin na osnovi nanodelcev Ba-heksaferita. [2]

Problem priprave magnetnih tekočin na osnovi heksaferitov je v sintezi majhnih delcev z ozko porazdelitvijo velikosti. V nasprotju z spinelnimi feriti, ki jih lahko enostavno sintetiziramo že pri sobni temperaturi, so za kristalizacijo heksaferitov običajno potrebne visoke temperature, okoli 700 °C, ki vodijo do tvorbe velikih delcev.

V tem delu smo nanodelce Ba heksaferita sintetizirali s hidrotermalno sintezo, ki jo je razvil Drofenik s sodelavci.[3,4] Raziskovali smo vpliv reakcijske temperature in dodatka oleinske kisline med hidrotermalno sintezo na velikost in morfologijo sintetiziranih nanodelcev.

2. Eksperimentalni del

2.1. Sinteza nanodelcev

Nanodelce smo sintetizirali z uporabo hidotermalne sinteze. Izhodne spojine Ba nitrat ($Ba(NO_3)_2$, 3,95 mmol) in železov nitrat ($Fe(NO_3)_3.9H_20$, 20,85 mmol), smo raztopili v deionizirani vodi (400 ml) in z dodatkom NaOH (1,07 mmol) oborili zmes tetrahidroksoferatov $[Fe(OH)_4]^-$ in barijevega hidroksida $Ba(OH)_2$. Zmes smo hidrotermalno obdelovali pri različnih temperaturah in reakcijskih časih. Sintetizirane nanodelce smo spirali z destilirano vodo in razrečeno dušikovo kislino, ki raztaplja z barijem bogate faze, ki nastajajo med sintezo kot posledica prebitka barija.

2.2. Priprava magnetnih tekočin

Nanodelce Ba hexaferita smo sintetizirali tudi tako da smo v suspezijo oborjenih hidroksidov dodajali oleinsko kislino (1,5 g oleinske kisline računano na g sintetiziranih delcev). Po sintezi smo hidrofobne delce oborili z znižanjem pH vrednosti z dodatkom HNO_3 pod 5 in delce večkrat sprali z acetonom.

Hidrofobne delce smo nato suspendirali v nepolarnem nosilnem mediju: dekanu. Suspenzija po centrifugiranju je stabilna magnetna tekočina. Na ta način smo pripravili relativno koncentrirane magnetne tekočine.

2.3. Karakterizacija

Nanodelce smo karakterizirali z uporabo presevnega elektronskega mikroskopa (TEM, JEOL 2010 F, JEOL 2100) in rentgensko praškovno difrakcijo (XRD, PANalytical X' Pert PRO). Velikost delcev smo določili iz TEM posnetkov in z uporabo Sherrerjeve metode, ki temelji na širitvi rentgenskih uklonov na XRD. Pri tem smo uporabili računalniški program Diffrac^{plus} TOPAS^{TM}. Magnetne lastnosti smo določili na magnetometru s tresočim vzorcem (Lake Shore VSM)

3. Rezultati in diskusija

V prvem delu eksperimentov smo raziskovali vpliv reakcijske temperature na velikost in morfologijo delcev sintetiziranih s hidrotermalno sintezo in določili območje reakcijskih pogojev, pri katerih pride do enakomerne rasti delcev.

Na sliki 1a je prikazan TEM posnetek Ba heksaferitnih nanodelcev sintetiziranih pri temperaturi 150 °C. Iz slike je razvidno da so delci pretežno okrogle oblike. Podrobnejša TEM analiza je pokazala da so delci v obliki tankih okroglih ploščic, premera okoli 10 in debeline 3 nm. Na posameznih področjih (označeno s krogom na sliki 1a) so delci orientirani pravokotno na podlago. Delci se med seboj združujejo v aglomerate. Elektronska difrakcija (slika 1 (a)) ustreza strukturi Ba heksaferita, medtem ko je EDS analiza pokazala sestavo z razmerjem med Ba in Fe blizu 1 : 12, kar dokazuje, da je med hidrotremalno sintezo res nastal Ba heksaferit.

V primeru zvišanja reakcijske temperature hidrotermalne sinteze na 180 °C se v vzorcu poleg majhnih 10 nm delcev pojavijo tudi velike heksagonalne ploščice vidne na sliki 1b. Heksagonalne ploščice nastanejo kot posledica procesa sekundarne rekristalizacije (Ostwaldove pogrobitve), ki nastopi, ko se porabi ves reaktant in nadaljnja rast delcev poteka lahko le z mehanizmom sekundarne rekristalizacije, pri čemer nastajajo veliki delci, ki rastejo na račun manjših.[3,4] Nastanek velikih delcev predstavlja problem pri pripravi stabilnih suspenzij saj zaradi svoje magnetne narave povzročijo aglomeracijo delcev.

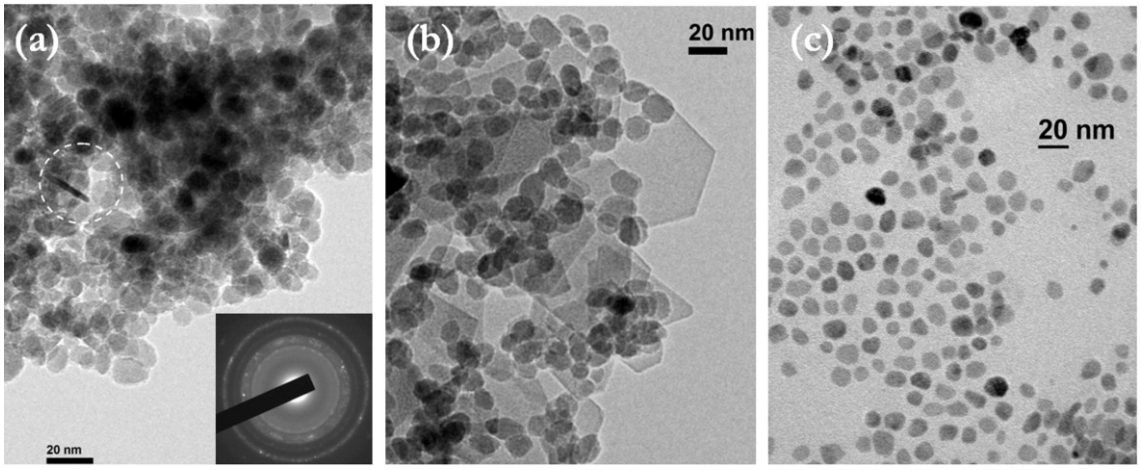

Slika 1: TEM posnetek delcev Ba heksaferita sintetiziranih pri temperaturi 150 °C (M-150) (a), pri temperaturi 180 °C (M-200) (b) in pri temperaturi 200 °C v prisotnosti oleinske kisline (OA-200) (c). Delci Ba heksaferita na sliki (c) so bili na TEM mrežico nanešeni v obliki stabilne suspenzije v dekanu.

V nadaljevanju smo poskušali blokirati pretirano rast delcev Ba heksaferita z dodatkom surfaktanta. V ta namen smo v reakcijsko zmes dodajali oleinsko kislino. Slednja se uporablja tudi kot dispergant pri pripravi magnetnih tekočin.
Na sliki 1c je prikazan TEM posnetek barijevega heksaferita sintetiziranega s segrevanjem do 200 °C (OA-200) ob prisotnosti oleinske kisline. Kljub visoki temperaturi v vzorcu ni bilo velikih ploščatih delcev, ki bi nastali kot posledica Ostwaldove pogrobitve. Med hidrotermalno sintezo Ba heksaferita očitno pride do adsorbcije oleatnega iona na površino delcev, kar zavira njihovo rast.
TEM analiza vzorca (slika 1c) tudi pokaže, da delci po sušenju na podlagi niso v direktnem kontaktu. Tanek ovoj oleinske kisline na površini omogoča steričen odboj in preprečuje da bi nanodelci prišli v direktni kontakt in se tako aglomerirali. Taki delci so zato primerni za pripravo magnetnih tekočin.[4]

Spremembe v velikosti in morfologiji nanodelcev v sintetiziranih produktih se odražajo tudi v magentnih lastnostih. Slika 2 prikazuje magnetno histerezo vzorca (OA-200), sintetiziranega pri temperature 200 °C v prisotnosti oleinske kisline. Nasičena magnezitacija vzorca OA-200, ki vsebuje le majhne nanodelce veliksoti 10 nm, izkazuje relativno nizke vrednosti magnetizacije izmerjene v polju 1T. Te znašajo okoli 1.5 emu/g, kar je precej nižje od magnetizacije grobozrnatega Ba

heksaferita kjer slednja znaša 67 emu/g. Znižanje magnetizacije gre predvsem na račun zmanjšanja velikosti delcev, kar je v največji meri poledica nepopolne koordinacije površinskih atomov. Hkrati nizka koercitivnost vzorca OA-200 kaže na to, da je večina delcev najverjetneje v superparamagnetnem stanju.[4]

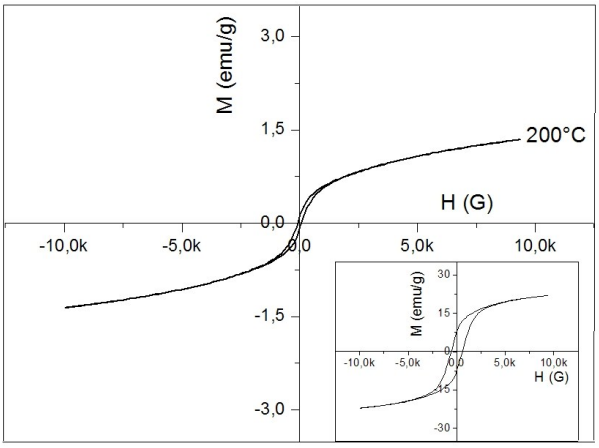

Slika 2: Magnetne histereze za vzorce Ba heksaferita sintetizirane pri temepraturi 200 °C (OA-200) v prisotnosti oleinske kisline in Ba heksaferitni nanodelci sintetizirani pri 160 °C (M-180) brez dodatka surfaktanta (vstavljeno v sliko).

Bistveno višje vrednosti magnetizacije smo izmerili v primeru vzorca M-180. Nasičena magnetizacija, izmerjena v polju 1T, znaša 20.5 emu/g. Razlog za znatno povečanje magnetizacije je v veliki vsebnosti heksagonalni ploščic, kar se kaže tudi v večji vrednosti koercitivnosti, ki v tem primeru znaša okoli 400 Oe.

4. Zaključek

S hidrotermalno sintezo smo sintetizirali delce Ba heksaferita, primerne za pripravo magnetnih tekočin. Določili smo območje reakcijskih parametrov, pri katerih še ne pride do pretirane rasti delcev. Ba heksaferitne nanodelce z ozko porazdelitvijo velikosti je možno sintetizirati le v ozkem temperaturnem območju. Da bi to območje razširili smo raziskali vpliv dodatka oleinske kisline. Nanodelci sintetizirani v prisotnosti oleinske kisline so bili hidrofobni, kar je omogočalo njihovo dispergiranje v nepolarnem mediju in tako pripravo relativno koncentriranih stabilnih suspenzij. Nanodelci zaradi svoje majhne velikosti in posledično nepopolne koordinacije površinskih atomov izkazujejo nizke vrednosti magnetizacije, okoli 1 emu/g.

Literatura:

[1] Q. A. Pankhurst, J. Connolly, S. K. Jones, J. Dobson, *J. Phys. D: Appl. Phys.*, 36, R167, 2003.
[2] R.E. Rosenwieg, *Ferrohydrodynamics* (Cambridge: Cambridge University Press) 1985.
[3] M. Drofenik, M. Kristl, A. Žnidaršič, D. Hanžel, D. Lisjak, *J. Am. Ceram. Soc*, 90, 2057, 2007
[4] D. Primc, D. Lisjak, D. Makovec, M. Drofenik, *Nanotechnology*, 20, 315605, 2009.

Za širši interes

Raziskave na Odseku za sintezo materialov so usmerjene v razvoj naprednih oksidnih materialov, ki izkazujejo uporabne elektromagnetne lastnosti. Namen raziskav je pridobiti znanje o kemiji materialov, kar omogoča načrtovanje novih materialov z želenimi lastnostmi.
Pridobljeno znanje o kontrolirani sintezi osnovnih materialov nadgrajujemo z znanjem o prilagajanju njihovih kemijskih lastnosti za sintezo sestavljenih in/ali večfunkcionalnih materialov. Na odseku tako raziskujemo materiale za uporabo v elektroniki, telekomunikacijah, medicini, tehniki, ekologiji.

Večfunkcionalni materiali
Obvladovanje površinskih lastnosti nanodelcev nam omogoča pripravo nanokompozitov, ki kombinirajo različne uporabne lastnosti vsebovanih materialov. Predvsem gre za kombinacijo ferimagnetnih materialov in dielektrikov (magnetodielektrikov) ali feromagnetnih in feroelektričnih materialov (kompozitnih multiferoikov). V okviru razvoja novih magnetooptičnih materialov študiramo mehanizme kristalizacije magnetnih delcev v različnih optično prozornih matricah ter vpliv magnetnih lastnosti delcev in zunanjega magnetnega polja na optične lastnosti. Ti sestavljeni materiali so osnova naprednih magnetooptičnih senzorjev. S prevlečenjem magnetnih nanodelcev z nanodelci TiO_2 sintetiziramo magnetno odzivne fotokatalitske nanokompozitne delce, ki se uporabljajo za čiščenje onesnaženih voda in plinov.

IPSSC: Using a movable active element to control the density of neutral oxygen atoms in a plasma afterglow chamber

Gregor Primc[1,2], **Miran Mozetič**[1,2]

[1] Department of Surface Engineering and Optoelectronics, Jožef Stefan Institute, Ljubljana, Slovenia

[2] Jožef Stefan International Postgraduate School, Ljubljana, Slovenia

gregor.primc@ijs.si (email of corresponding author)

gregor.primc@ijs.si (email of mentor)

Abstract. Systematic measurements of neutral oxygen atoms under various conditions and at the presence of a special active element (recombinator) were performed in weak ionized oxygen plasma. The density was measured using a fiber optic catalytic probe. It has been found that the density of neutral oxygen atoms depends not only on the pressure of the inlet oxygen gas and exciting power, but also mostly on the presence and the position of the recombinator. The measured densities of neutral oxygen atoms are of the order of 10^{21} particles per m^{-3} is a characteristic value in glass discharge chambers. Such orders of neutral oxygen atom density suffice for the treatment of organic materials. The problem with organic materials is that interaction with oxygen atoms heats the material. Therefore, it is often necessary to decrease the atom density as soon as possible to prevent heating of the material. As described in this paper, this is possible by using a movable recombinator, which enables us to select the appropriate atom density without having to change the discharge parameters.

Keywords: weak ionized plasma, oxygen, neutral atoms, catalytic probe, and density measurement

1 Introduction

Nowadays, different material treatments increasingly performed by the use of weakly ionized highly dissociated gaseous plasma. Material plasma treatment features excellent quality, stability, and above all ecological integrity. Different technologies often use oxygen, nitrogen or hydrogen plasma, especially as an alternative to environmentally unfriendly wet chemical treatments [1]. Plasma is

mainly used for surface cleaning, organic material activation [2], selective etching of polymer composites [3], cold ashing [4] of biological samples, in modern medical applications for sterilization of sensitive materials [5], and lately also for nanomaterial synthesis.

When treating different materials, it is very important to know the density of plasma particles in the vicinity of a treated sample, as method and treatment intensity highly depend on particle flux density on the surface of the sample. Furthermore, diverse gradients of concentration may appear in the processing chamber, so the position of the sample is very important. Frequently, the treated sample represents a strong sink for plasma particles, so that particle flux density on the surface of the sample is dependent on dimensional and material properties of the sample. Therefore it is most important to know the exact neutral atom density and to be able to actively regulate it during treatment, independently of discharge parameters.

2 Experiment

All measurements were performed at "Jožef Stefan" Institute in the plasma laboratory at the Department of Surface Engineering and Optoelectronics. A plasma reactor was used to create oxygen plasma by radiofrequency discharge. The idea was to use a special active element (recombinator) that can be moved horizontally in the chamber (Fig. 1). The recombinator was used to actively change the density of neutral oxygen atoms. A nickel-plated fiber-optic catalytic probe at a fixed position was used to measure changes in neutral oxygen atom densities at different powers and pressures applied, and most importantly at different recombinator positions. A copper rod was used as a recombinator.

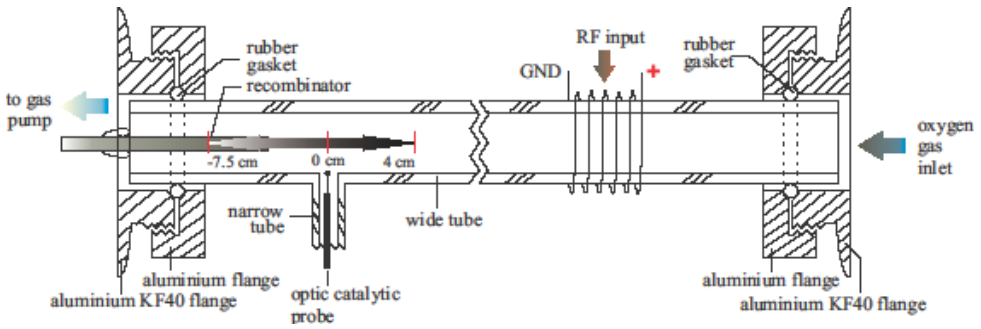

Figure 1.: Schematic of plasma system.

3 Results and conclusions

The calculated densities are of the order of 10^{21} particles per m^{-3} which is a characteristic value in glass discharge chambers. Such orders of density suffice for organic material treatment. The problem with organic materials is that interaction with oxygen atoms heats the material. Therefore it is often necessary to decrease the atom density as soon as possible. As it is described in this paper, this is possible by using a movable recombinator which enables a selection of the appropriate atom density without having to change the discharge parameters. [6]

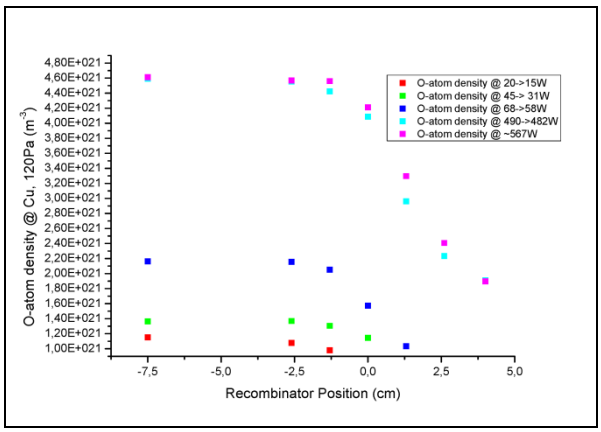

Figure 2.: Densities of neutral oxygen atoms at a pressure of 120 Pa.

Figure 2 shows that recombinator did its function perfectly, namely to decrease the neutral atom density independently of the discharge parameters. That was also the goal of the experiment – to quantitatively demonstrate that we may change the atom density in any part of the discharge tube by moving the recombinator.

References:

[1]A. Drenik, M. Mozetič, A. Vesel, U. Cvelbar. Environmentally friendly plasma-based surface engineering technologies. *Journal of Physics: Conference Series,* 207:012009, 2010.

[2]A. Vesel, I. Junkar, J. Kovač and M. Mozetič. Activation of PTFE foil by treatment in oxygen and nitrogen plasma. In *MIDEM proceedings of 43th International Conference on Microelectronics, Devices and Materials and the Workshop on Electronic Testing 2007*, Bled, Slovenia, 2007.

[3]U. Cvelbar, M. Mozetič and M. Klanjšek Gunde. Selective oxygen plasma etching of coatings. *IEEE trans. plasma sci.*, 33(2):236-237, 2005.

[4]M. Mozetič. Cold ashing with oxygen plasma. In *Proceedings of the 7th European Vacuum Conference and 3rd European Topical Conference on Hard Coatings 2001*, Madrid, Spain, 2001.

[5]A. Vesel and M. Mozetič. Plazemska sterilizacija. *Vakuumist,* 23(4):9-14, 2003.

[6]G. Primc and Z. Kregar. Controlling of O atom density by a movable recombinator. In *Proceedings of 3rd International Conference on Advanced Plasma Technologies 2010,* Bohinj, Slovenia, 2010.

For wider interest

Although nowadays plasma is used in many applications, the behaviour of the particles and inter-particle interactions are still not fully understood.

The Department of Surface Engineering and Optoelectronics at Jožef Stefan Institute is focused on basic and applied research of low pressure gaseous plasmas and interactions between plasma radicals and solid surfaces. Research includes studies of gaseous discharges, coupling between plasma and discharge generator, plasma characterization, the interaction of charged and neutral particles with solid surfaces, and the analysis of plasma-modified materials.

This basic research is the foundation for applied research in the field of environmentally friendly technologies. These technologies include plasma discharge cleaning, selective plasma etching, cold ashing of bio-materials, sterilization of sensitive medical materials, and the synthesis of nanomaterials.

The aim of this research is to build software driven control system that will allow us to sustain and to dynamically change the density of neutral atoms. In order to support this idea, we have to monitor and control the discharge parameters and movable recombinators, and simultaneously measure the density of plasma particles. Discharge parameters are output power and coupling of the generator, vacuum degree and gas flow, features of the plasma chamber, and the specific properties of treated sample.

For monitoring the density of plasma particles, we will use catalytic probes, electric (Langmuir) probes, optical emission spectroscopy and mass spectroscopy methods. The final goal of the research is to develop a plasma reactor with a stable and arbitrary neutral atom density, which will allow for an effective and controlled processing of materials.

Liquid Crystal Elastomers, Electrocalorics, and new Soft Magnetoelectrics: Materials for Advanced Technologies

Brigita Rožič[1,2], Zdravko Kutnjak[1,*], George Cordoyiannis[10], Boštjan Zalar[1], Slobodan Žumer[1,6], Simon Krause[7], Heino Finkelmann[7], Barbara Malič[3], Alja Kupec[3], Janez Holc[3], Marija Kosec[3], Raša Pirc[4], Robert Blinc[1], Marko Jagodič[8,10], Sašo Gyergyek[5], Miha Drofenik[5], Samo Kralj[9], Gojmir Lahajnar[1], Zvonko Jagličić[8]

[1] Condensed Matter Physics Department, Jožef Stefan Institute, Ljubljana, Slovenia

[2] Jožef Stefan International Postgraduate School, Ljubljana, Slovenia

[3] Electronic Ceramics Department, [4] Department of Theoretical Physics, [5] Materials Synthesis Department, Jožef Stefan Institute, Ljubljana, Slovenia

[6] Department of Physics, University of Ljubljana, Ljubljana, Slovenia

[7] Institut für Makromolekulare Chemie, Freiburg, Germany

[8] Institute of Mathematics, Physics and Mechanics, Ljubljana, Slovenia

[9] Department of Physics, University of Maribor, Maribor, Slovenia

[10] EN-FIST Centre of Excellence, Ljubljana, Slovenia

Brigita.Rozic@ijs.si ; * supervisor

Abstract. In recent years, a pronounced interest in materials that are perspective for applications in everyday life has started to grow. Our interest has been focused on different conversion of energies in such advanced materials. We have studied a giant conversion of thermal to mechanical energy, i.e., thermomechanical effect in nematic liquid crystal elastomers [1-3], a giant conversion of electrical to thermal energy, i.e., electrocaloric effect in PLZT thin films [4], and an electric control of magnetization, i.e., magnetoelectric effect, in soft multiferroics such as mixtures of SCE9 ferroelectric liquid crystal and magnetic nanoparticles [7-9].

Keywords: Liquid crystal elastomers, electrocalorics, magnetoelectrics, magnetic nanoparticles, ferroelectric liquid crystals

1 Introduction

Liquid crystal elastomers (LCEs), i.e., materials that combine the properties of liquid crystals and elastomers are one of the so called smart materials, which are very promising for many applications such as artificial muscles. The most interesting and potentially most attractive feature for use of LCEs is the thermomechanical effect, which means that LCEs spontaneously stretch or shrink due to the temperature change in the vicinity of a phase transition from an isotropic to a nematic (I-N) phase (Fig. 1). So far the nature of this transition was not clear and generally it was thought that the LCEs are supercritical. We tested an existence of the critical point in LCEs, i.e., whether LCEs could exhibit also a first order and a continuous I-N transition besides a supercritical one. Here, we will demonstrate how to control the thermomechanical response from on-off or discontinuous to continuous one via changing the nature of the I-N transition.

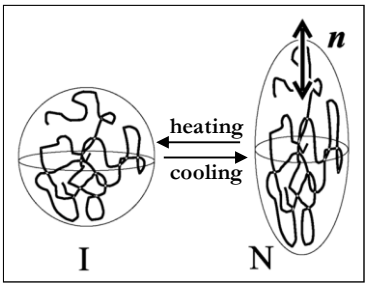

Figure 1: LCEs spontaneously stretch/shrink due to the temperature changes.

Electrocalorics are materials that show an interesting phenomenon, i.e., electrocaloric effect (ECE). ECE is a conversion of electrical energy to heat and vice versa. It generates great interest due to its broad range of applications in new generation heating and cooling devices which could be more energetically efficient and environmentally friendly. The background of the ECE is not yet fully understood [5], but an idea of its explanation lies in a change of entropy, due to the applied electric field induced changes of the polar states in a dielectric material. An adiabatically applied bias electric field results in an increase of a material temperature and adiabatically removal of the field causes a cooling of the material (Fig 2). The electrocaloric effect has been known for long time but it was not interesting and useful for commercial applications, due to its small magnitude in previously known materials. An interest in electrocalorics was renewed recently by

the first predictions of a giant ECE in some organic and inorganic materials. These predictions were based on indirect measurements of the electric polarization as a function of temperature and an electric field [5,6]. We will present direct measurements of the electrocaloric effect in PLZT thin films.

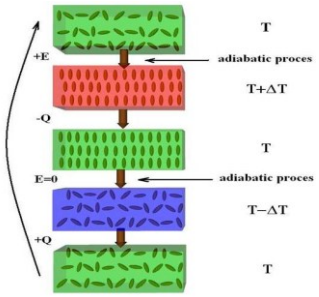

Figure 2: Schematic representation of the electrocaloric cycle.

Magnetoelectrics have become recently a very attractive research topic due to their properties, i.e., in such materials it would be possible to control the magnetic properties via electrical ones, and vice versa, and also due to their potential, for example in the information storage industry [7]. It is known that mixtures of nanoparticles (NPs) and other conventional materials could exhibit special behaviour not found in the individual components [8]. Such conventional materials which we are interested in are liquid crystals (LCs). It has been shown that the spontaneous onset of liquid crystal ordering could be a way to obtain very well aligned NPs. We experimentally analysed mixture of maghemite magnetic NPs and ferroelectric liquid crystal SCE9 in the vicinity of the ferroelectric smectic C* phase. We will present measurements of the impact of the electric field on the magnetic susceptibility via SQUID susceptometer.

2 Experiments and Discussion

All experiments were made by using the high-resolution calorimeter allowing precise measurements [1-3]. In the case of magnetoelectric, also the SQUID susceptometer was used.

Study of the paranematic-nematic phase transition was performed on liquid crystal side-chain and main-chain elastomers with various crosslink density, oriented by applying different external mechanical stress fields, and crosslinked at different

curing temperature during the sample preparation. It was shown that increasing the density of crosslinkers results in decrease of the latent heat. The external stress also reduces latent heat and drives the transition toward smeared supercritical behaviour, and reduced crosslinking temperature results in a much sharper first order I-N transition with significant latent heat [1-3].

We made direct electrocaloric measurements on 450 nm 8/65/35 PLZT thin films covered with gold electrode (Fig.3). For temperature measurements, a small thermistor was used. Fast internal thermal response times, in order of few tens of milliseconds, allow application of the simple zero-dimensional model. The ECE temperature change ΔT_{EC} was measured as function of electric field change near room temperature. It was observed that a magnitude of the ECE in these materials exceed 30 K. The temperature dependence of the ΔT_{EC} reveals that the maximum of ECE is obtained at the ferroelectric phase transition [4].

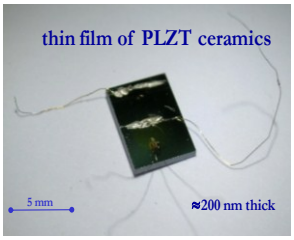

Figure 3: Thin film of 8/65/35 PLZT ceramics.

In case of soft magnetoelectrics, we experimentally investigated the mixtures of a SCE9 liquid crystal and maghemite ($\gamma - Fe_2O_3$) nanoparticles (NPs) (Fig. 4). We prepared mixtures of concentration $x = 14\%$. Preparation details of NPs, LC-NPs mixtures and samples for measurements are described elsewhere [9].

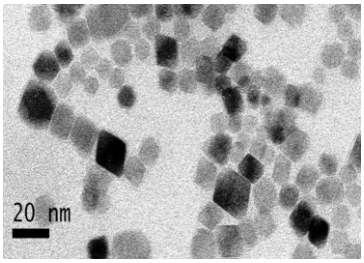

Figure 4: TEM image of our magnetic nanoparticles.

As a result the anomaly in the excess magnetization Δm was observed at the SmA to SmC* phase transitions. This demonstrates the coupling between the LC director field and the magnetization of NPs [9].

3 Conclusions

It has been shown that the LCEs critical behaviour could be controlled by crosslinking concentration, external field, and crosslinking temperature.

In case of electrocaloric effect, we can conclude that our direct measurements confirm existence of the giant electrocaloric effect in 8/65/35 PLZT thin films.

Our calorimetry and magnetic susceptibility measurements demonstrate the possible indirect coupling between the magnetic and ferroelectric order. Due to this, the mixtures of ferroelectric LC and magnetic NPs are candidates for soft indirect magnetoelectrics.

References:

[1]A. Lebar, Z. Kutnjak, S. Žumer, H. Finkelmann, A. Sanchez-Ferrer, B. Zalar. Evidence of Supercritical Behavior in Liquid Crystal Elastomers. *Phys. Rev. Lett.*, 94:197801, 2005.

[2]G. Cordoyiannis, A. Lebar, B. Rožič, B. Zalar, Z. Kutnjak, S. Žumer, F. Brömmel, S. Krause, H. Finkelmann. Controling the Critical Behavior of Paranematic to Nematic transition in Main-Chain Liquid Single Crystal Elastomers. *Macromolecules,* 42: 2069-2073, 2009.

[3] B. Rožič, S. Krause, H. Finkelmann, G. Cordoyiannis, and Z. Kutnjak. Controlling the thermomechanical response of liquid-crystalline elastomers by influencing their critical behavior. *Appl. Phys. Rev. Lett.,* 96: 111901, 2010.

[4]S. G. Lu, B. Rožič, Q. M. Zhang, Z. Kutnjak, X. Li, E. Furman, L. J. Gorny, M. Lin, B. Malič, M. Kosec, R. Blinc, R. Pirc. Organic and inorganic relaxor ferroelectrics with giant electrocaloric effect. *Appl. Phys. Lett.,* 97: 162904, 2010.

[5]A. S. Mischenko, Q. Zhang, J. F. Scott, R. W. Whatmore, N. D. Mathur. Giant Electrocaloric Effect in Thin-Film $PbZr_{0.95}Ti_{0.05}O_3$. *Science*, 311: 1270-1271, 2006.

[6]B. Neese, B. Chu, S.-G. Lu, Y. Wang, E. Furman, Q. M. Zhang. Large electrocaloric effect in ferroelectric polymers near room temperature. *Science,* 321: 821-823, 2008.

[7]W. Erenstein, N. D. Mathur and J. Scott. Multiferroic and Magnetoelectric Materials. *Nature,* 442: 05023, 2006.

[8]A. Balazs, T. Emrick, and T. P. Russell. Nanoparticle polymer composites: Where two small words meet. *Science,* 314: 1107-1110, 2006.

[9] B. Rožič, M. Jagodič, S. Gyergyek, M. Drofenik, S. Kralj, G. lahajnar, Z. Jagličić, Z. Kutnjak. Orientational order-magnetization coupling in mixtures of magnetic nanoparticles and the ferroelectric liquid crystal. *Ferroelectrics,* 410: 37-41, 2011.

For wider interest

All our studied materials mentioned above (liquid crystal elastomers, electrocalorics and soft magnetoelectrics) are very promising for various applications.

Liquid crystal elastomers, i.e., materials with combined properties of elastomers (rubbers) and liquid crystals, are novel advanced materials exhibiting giant thermomechanical response, which is very important for the new generation of sensors, actuators, and artificial muscles. Study of the nature of I-N transition and its control will allow also control of thermomechanical response which can be tailored to specific application demand.

Studies of electrocalorics, i.e., materials that exhibit a temperature change under an applied/removed electric field at adiabatic conditions, are very important for development of electrocaloric elements which will play a crucial rule in novel environmentally friendly cooling/heating devices with practically no moving parts and better energy efficiency. Possible applications include household refrigerators, heat pumps, devices for cooling computer chips, applications in microrobotics, sensors, actuators, etc.

Magnetoelectrics are materials that exhibit simultaneously ferroelectric and ferromagnetic properties, and in such materials it would be possible to control the magnetic properties via electrical ones, and vice versa. These materials attract considerable scientific attention because of their widespread applications as actuators, transducers, and memory devices. Development and discovery of new magnetoelectric materials is of great importance for such applications. Our development of new soft magnetoelectrics has proved for the first time that soft materials can also exhibit magnetoelectricity, which could open new possibilities in application of magnetoelectric materials. So, magnetoelectrics are expected to revolutionize computers. Such memory elements would permit an electric write operation combined with a magnetic read, eliminating the need for the destructive read in present-day ferromagnetic RAMs, thus making possible fatigue-free memories.

Innovative Approach to Synthesis of $Pb(Mg_{1/3}Nb_{2/3})O_3$ Based Materials using Colloidal Interactions

Gregor Trefalt[1,2], Barbara Malič[1], Bosiljka Tadić[3], Janez Holc[1], Danjela Kuščer[1], Marija Kosec[1]

[1] Electronic Ceramics Department, Jožef Stefan Institute, Ljubljana, Slovenia

[2] Jožef Stefan International Postgraduate School, Ljubljana, Slovenia

[3] Department of Theoretical Physics, Jožef Stefan Institute, Ljubljana, Slovenia

gregor.trefalt@ijs.si

Abstract. A new approach to the synthesis of $Pb(Mg_{1/3}Nb_{2/3})O_3$ (PMN) based materials is presented. By manipulating the colloidal interactions, the designed self-assembled aggregates are formed, which enable the synthesis of PMN based materials in a single-annealing step. Furthermore the as prepared ceramics are sintered at 200 K lower temperatures compared to conventionally used methods and exhibit excellent electrical properties.

Keywords: PMN, synthesis, self-assembly, simulations, ceramics

1 Introduction

Lead magnesium niobate $Pb(Mg_{1/3}Nb_{2/3})O_3$ (PMN) and its solid solution with lead titanate $xPb(Mg_{1/3}Nb_{2/3})O_3$-$(1-x)PbTiO_3$ (PMN-PT) belong to the group of relaxor ferroelectric materials and are the most studied materials of this group. They are known for large electrostrictive (strain ~0.1%) as well as large dielectric properties (ε_r ~ 15 000) at room temperature and are therefore used in actuator and high-dielectric-permittivity applications [1-4]. PMN based ceramics are usually prepared via solid-state synthesis. The general approach in the solid-state synthesis is to choose reactant compounds, typically inorganic compounds, composed of elements that are needed to make a particular multi-metal oxide. After mixing and heating at elevated temperatures the reaction starts at the contact of reactant powder particles and proceeds via diffusion. Therefore the starting compounds must consist of small particles and they have to be mixed homogenously to get fast reactions and homogenous product. This is true for two component systems, however not always

true, if we have more than two components. In a two component system a typical reaction is as follows A + B → AB. With reducing particle size and by homogenous mixing of A and B particles, the contact area between the A and B particles is increased, which is beneficial for the solid-state reaction. In the systems with more than two components multiple reactions may occur and all are not always wanted. A typical example of such problem is the PMN synthesis. This material is difficult to prepare in a pure perovskite form, due to the preferential reaction between lead and niobium oxide yielding secondary $Pb_xNb_yO_z$ pyrochlore phases. Therefore the final product is composed of a mixture of pyrochlore and perovskite PMN or PMN-PT phases. Pyrochlores are known to deteriorate dielectric properties of the PMN and PMN-PT ceramics. Therefore the pyrochlore phases should be avoided during the synthesis to produce high-quality electronic ceramics.

2 Idea

The columbite method is usually used for the preparation of pyrochlore-free materials. In this method the synthesis is composed of two steps, first the $MgNb_2O_6$ (columbite) is synthesized, and in the second reaction, the columbite reacts with PbO or PbO + TiO_2 to form the perovskite PMN or PMN-PT [5]. First step is needed to prevent the reaction between PbO and Nb_2O_5 to pyrochlore.

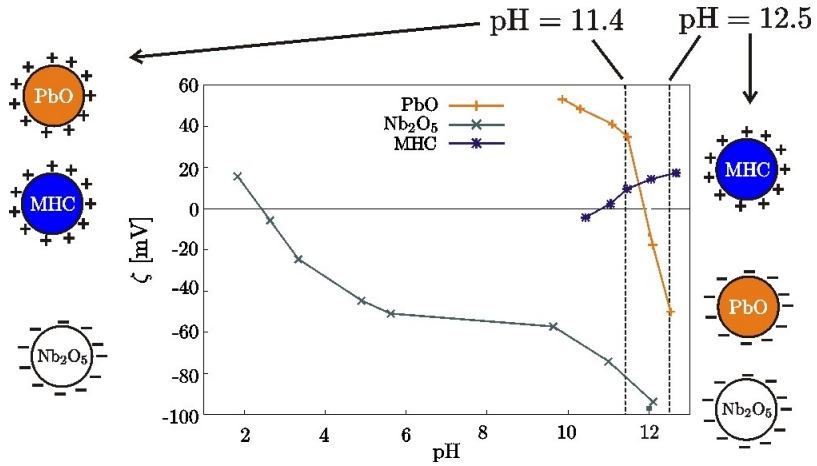

Figure 1: Zeta-potential measurements of the starting components as a function of pH. The dotted lines represent the pH values used for the synthesis of PMN.

In order to simplify the reaction to one-step method, we have to avoid the reaction between lead and niobium oxide in the reaction mixture of the starting compounds;

PbO, Nb_2O_5, $4MgCO_3 \cdot Mg(OH)_2 \cdot 4H_2O$ (MHC), and TiO_2. Our idea was to prevent contacts between PbO and Nb_2O_5 particles in the reaction mixture, and hence to slow down the reaction to the pyrochlore phase. This could be achieved by the directed self-assembly of the reactant particles in the suspensions. By changing the pH of the suspension, the zeta-potential of the particles is changing (see Fig. 1), and hence the interactions between the particles are changing. Therefore at different pH conditions aggregates with different type of contacts between particles should form. This was further investigated with the use of numerical modelling.

3 Simulation Study of Aggregate Formation

The Monte Carlo simulation method was used for modelling the aggregate formation in the suspension containing reactant particles for the PMN synthesis: PbO, Nb_2O_5, MHC. The method and the results are explained in detail in Ref. [6]; here the results are just briefly summarized. In Figure 2 the spatial distributions of reagent particles are shown for the suspensions with pH 11.4 and pH 12.5.

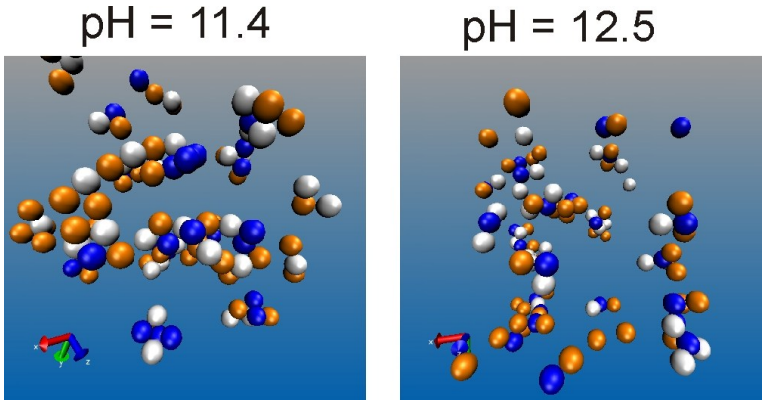

Figure 2: Snapshot of the formed aggregates in suspensions of PbO, Nb_2O_5 and MHC particles at pH 11.4 (left), and 12.5 (right). PbO – orange, Nb_2O_5 – white, MHC – blue.

At pH 11.4, a large population of aggregates with contacts between PbO and Nb_2O_5 is observed, whereas at pH 12.5, no such aggregates are formed. At lower pH, the charge of PbO and Nb_2O_5 is opposite and the two types of particles are attracted and form aggregates. At pH 12.5, PbO and Nb_2O_5 are both negatively charged, while MHC is positively charged, this situation leads to aggregates where MHC particles are effectively separating PbO and Nb_2O_5 particles. From the simulation results we can conclude that at the pH 12.5, the separation of PbO and

Nb_2O_5 should slow down the reaction to pyrochlores and therefore the conditions should be more favourable for synthesizing pyrochlore-free PMN.

4 Experimental Results

The starting powders for PMN and 0.65PMN-0.35PT synthesis, PbO, Nb_2O_5, MHC, and in the case of PMN-PT also TiO_2, were mixed in aqueous suspensions at pH 11.4 in the first case and at pH 12.5 in the second case. The suspensions were dried after milling and calcined at 900 °C for 5 h. The calcined powders were pressed to pellets and sintered as low as 950 °C. Then the electrical properties of the ceramics were measured. More detailed information on experimental procedures can be found in Ref. [7].

Based on the simulation results we have expected that the dried suspension of the starting compounds, prepared at pH 11.4, would react to the mixture of the perovskite and secondary pyrochlore phase after heating at 900 °C. On the contrary, the powder mixture, prepared at pH 12.5, should react to pure perovskite after the calcination at 900 °C. The XRD patterns of both calcined samples in the case of PMN synthesis confirm the simulation results. In addition to the perovskite phase also 5 mass% of secondary pyrochlore phase is detected in the pH 11.4 sample, while the pH 12.5 sample contains only the perovskite PMN phase. After sintering at 950 °C the pH 12.5 ceramic sample reaches 95 % of theoretical density (TD), while the pH 11.4 reaches only 85 % of TD.

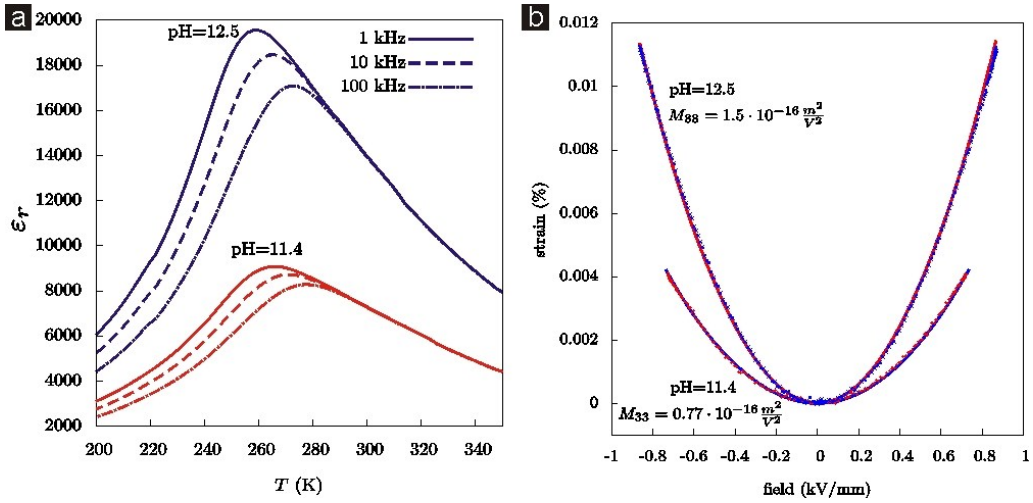

Figure 4: Electrical properties of the PMN ceramics prepared at pH 11.4 (red) and pH 12.5 (blue). a) Dielectric constant vs. temperature. b) Electrostrictive properties: strain vs. electric field.

Additionally the dielectric and electrostrictive properties were measured for both samples (see Figure 4). The pH 12.5 sample exhibits approx. two times higher dielectric constant in the measured temperature range as well as two times higher electrostriction coefficient M_{33} in comparison to the pH 11.4 sample. Clearly, the dielectric and electrostrictive properties of the pH 11.4 sample are deteriorated, due to the presence of the secondary pyrochlore phase and low density.

The same synthesis approach was tested on 0.65PMN-0.35PT system; here additionally TiO_2 particles are added into the reaction mixture. Again, the sample prepared at pH 11.4 and heated at 850 °C, contains in addition to the perovskite also a secondary pyrochlore phase, whereas in the pH 12.5 sample calcined at the same temperature, only the perovskite phase is detected. To further compare the two samples, ferroelectric and piezoelectric properties of the samples sintered at 950 °C were measured, see Figure 5.

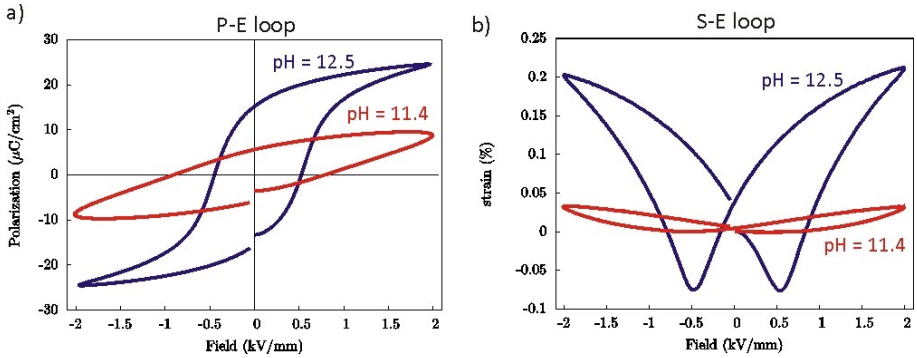

Figure 5: Electrical properties of the 0.65PMN-0.35PT ceramics prepared at pH 11.4 (red) and pH 12.5 (blue). a) Polarization vs. electric field. b) Strain vs. electric field.

The properties of the ceramics prepared from the pH 12.5 suspension are superior in comparison to the pH 11.4 sample also in the case of the PMN-PT synthesis.

5 Summary

By applying our new synthesis approach the phase-pure PMN and PMN-PT powders and high quality ceramics were prepared from simple materials in only one milling, one calcination, and one sintering step. We suppose that the presented approach is general and could be implemented for the synthesis of other complex perovskite materials.

References:

[1]G. H. Heartling. "Feroelectric ceramics: History and Technology". *J. Am. Ceram. Soc.*, 82(4):2341-2359, 1999.

[2]N. Setter. "Piezoelectric materials in devices", pages 1-27. EPFL, Lausanne, Switzerland, 2002.

[3]T. R. Shrout and A. Halliyal. "Preparation of Lead-Based Ferroelectric Relaxors for Capacitors". *Am. Ceram. Soc. Bull.*, 66(4):704-711, 1987.

[4]H. Uršič et al., "A large-displacement 65Pb($Mg_{1/3}Nb_{2/3}$)O_3-35PbTiO_3/Pt bimorph actuator prepared by screen printing. *Sens. Actuators, B.*, 133(2):699-704, 2008.

[5]S. L. Swartz and T. R. Shrout. "Fabrication of perovskite lead magnesium niobate". *Mat. Res. Bull.*, 17(10):1245-1250, 1982.

[6]G. Trefalt et al., "Formation of colloidal assemblies in suspensions for Pb($Mg_{1/3}Nb_{2/3}$)O_3 synthesis: Monte Carlo simulation study". *Soft Matter*, DOI: 10.1039/c1sm05228d.

[7]G. Trefalt et al., "Synthesis of Pb($Mg_{1/3}Nb_{2/3}$)O_3 by Self-Assembled Colloidal Aggregates". *J. Am. Ceram. Soc.*, 2011, DOI: 10.1111/j.1551-2916.2011.04443.x.

For wider interest

PMN and PMN-PT relaxor-ferroelectric materials are widely studied because their electrical properties (e.g. dielectric permittivity, electrostriction, piezoelectricity, ferroelectricity) enable their use in capacitor, actuator and sensor applications. Some of their typical applications are in actuators for precise positioning (piezo stages), sensors for force and pressure, ultrasonic transducers (medical imaging), and energy harvesting devices. It is hard to produce good quality ceramics from these materials, due to the formation of secondary pyrochlore phases during the synthesis. This work presents a new and simple approach to the synthesis of these materials with only one calcination step. This method has a potential to lower the production costs of these materials. A further advantage of this method is the use of environmentally friendly aqueous media and simple starting materials as well as simple and efficient processing techniques. Moreover, the method presented in this work is to our knowledge a new approach in the field of solid-state chemistry of complex multi-metal oxides. We supose that our approach of solid-state synthesis with designed heterogeneity could be used generally for the synthesis of materials with a complex chemical composition, which are of high technological importance.

This work was supported by Slovenian Research Agency, Grant No. PR-02485 and P2-105.

Organizator

V sodelovanju z

Sponzorji

Seznam sodelujočih podjetij

- Akrapovič, d.d.
- BSH hišni aparati, d.o.o.
- Cosylab, d.d.
- Datalab Tehnologije, d.d.
- Domel, d.d.
- ETI Elektroelementi, d.d.
- Gorenje, d.d.
- Hyb, d.o.o.
- Juteks, d.d.
- Kolektor Group, d.o.o.
- Mediato International, d.o.o.
- Premogovnik Velenje, d.d.
- Talum, d.d.
- Telekom Slovenije, d.d.
- Trimo, d.d.
- Salonit Anhovo, d.o.o.
- Zemanta, d.o.o.